UNITED STATES DEPARTMENT OF COMMERCE

Alexander B. Trowbridge, *Secretary* • NATIONAL BUREAU OF STANDARDS • A. V. Astin, *Director*

Calculation of the Properties of Vacancies and Interstitials

Proceedings of a Conference
Shenandoah National Park, Va.
May 1-5, 1966

Supported in part by the
Advanced Research Projects Agency

National Bureau of Standards Miscellaneous Publication 287
Issued November 17, 1966

For sale by the Superintendent of Documents, U.S. Government Printing Office, Washington, D.C. 20402
Price $2.50

Abstract

This is the Proceedings of a Conference on the Calculation of the Properties of Vacancies and Interstitials, Skyland, Virginia, USA, held on May 1–4, 1966. The Conference dealt with the theory and techniques of calculation of the properties of point defects in metallic and nonmetallic crystals. The contributed and invited papers divided about evenly among three major topics: (1) static-lattice calculations of the energies and configurations of simple vacancies and interstitials in, mainly, metals and ionic crystals; (2) electronic states at and near point defects in metals, rare gas solids, and insulators (*f*-centers, electron traps); and (3) vibrational states at point defects. The report of a panel discussion on each topic is also included. The emphasis is on the theory of the properties of isolated, simple defects rather than on the statistical properties of defect assemblies. The Conference attempted to examine the point defect theory and calculations critically, from the standpoint of general theory, rather than simply compare results with experiment.

Key Words: Calculations, electronic states, energies of formation, energies of motion, interstitials, point defects, theory, vacancies, vibrational states.

Library of Congress Catalog Card Number: 67-60032

Foreword

The Institute for Materials Research of the National Bureau of Standards has as a major responsibility the task of ensuring that basic, urgently needed data on the properties of materials are available to meet the requirements of the Nations' scientists and engineers. Data in this sense is a rather broad term. Not only does it imply experimentally measured numbers, but it also includes theoretical data, such as the calculated properties of point defects in crystals, which formed the subject of this Conference.

In an immediate sense, this responsibility is met in part through measurements done in Institute laboratories, in part through compilation and publication of critically evaluated data gathered from the literature. It is also necessary for the Institute to take a long-range view, to look further ahead, and to try to help in stimulating fields from which data of the future will come. The Conference on the Calculation of the Properties of Vacancies and Interstitials was part of that long-range effort. The field is a rapidly growing one, containing diverse elements, related to each other in subject and often in method, but being pursued to some extent independently. No conference bringing together these diverse elements had previously been held on this topic. Thus it appeared that the present Conference could perform an important function in providing an opportunity for a critical examination of the whole field, and a forum for interchange of ideas and discussion of problems at a most opportune time for such an interchange.

The Institute presents these Proceedings of the Conference in order to make the results available to a wider audience. The Institute would like to express appreciation to the participants, whose time, energy, and thought are embodied in these Proceedings, and to the Advanced Research Projects Agency, whose sponsorship made the Conference possible.

Gordon K. Teal
Director,
Institute for Materials Research

Introduction

The Conference on the Calculation of the Properties of Vacancies and Interstitials was held at Skyland, on the Skyline Drive in the Shenandoah National Park, Virginia, on May 1–4, 1966. It brought together approximately 70 scientists from the United States, Great Britain, Japan, West Germany, France, Italy, and the Netherlands, to discuss theoretical problems concerning isolated point defects in crystalline solids.

Prior to this conference, the theory and calculation of the properties of point defects had not been the sole topic of such a gathering. The field, however, had become an important one, and seemed ready to benefit by the concentrated discussions a conference of this kind makes possible. Several apparently unrelated currents of research bearing on this topic have developed in recent years, and it appeared desirable to try to bring their practitioners together.

Essentially static-lattice calculations for metals and nonmetals have been quite successful in obtaining estimates of defect formation energies, and to a lesser extent, migration energies as well. These calculations have passed the initial rough-approximation state, and rather sophisticated problems involving interatomic potentials, electron redistributions, and atomic configurations about the defects are now being attacked. Calculations of electronic states in the vicinity of a point defect are also making progress. Those working on color centers in ionic crystals are struggling to find ways of dealing with polarization effects and with problems presented by the overlap of the defect wave function with the neighboring ions. The problem in metals is the collective electron one in the presence of a sizable perturbation in the periodic crystal potential. Rather similar methods are being developed to handle vibrational and electronic states induced by the presence of point defects in otherwise periodic lattices; in both cases scattering theory is proving to be of great value.

These three general topics, static-lattice energies and configurations, electronic states, and vibrational states, formed the program of the conference. The object was to try to assess and compare the reliability of calculations of these properties from a theoretical point of view; not simply to compare the results with experiment, but to examine the calculations critically, from general theory. The conference concentrated on the theory of isolated defects rather than of statistical properties of assemblies of defects, so that topics like radiation damage or diffusion do not appear as such.

As the Table of Contents shows, the conference program was actually subdivided into three sections corresponding to these three topics. Within each section, contributed papers on current research plus several invited talks were presented. Then a panel discussion was held on the topic at hand, in which an attempt was made to summarize and comment upon what the contributed papers and their discussion had revealed. It was hoped in this way to provide some synthesis, some overview, of the topic.

These proceedings consist of the contributed papers, arranged by topic, and followed by a report on the panel discussion on the topic. These reports were prepared by the several panel chairmen, and each of course bears the stamp of its author's approach to the problem presented. We believe this use of panels to have been an interesting experiment in communication among scientists, and hope these reports will provide guidance and stimulation to others involved in similar experiments.

All conferences require a good deal of work on the part of many people. The editor would like to take this opportunity to call attention to the indispensable efforts of those whose work made the conference possible. The brunt was borne by R. E. Howard (Institute for Materials Research, NBS) and R. F. Wood (Oak Ridge National Laboratory), and important contributions were made by A. B. Lidiard (United Kingdom Atomic Energy Research Establishment, Harwell), C. McCombie (Reading University), A. Seeger (Max Planck Institut fur Metallforschung, Stuttgart), G. Vineyard (Brookhaven National Laboratory), and J. A. Krumhansl (Cornell University). Messrs Lidiard, McCombie, and Krumhansl served as panel chairmen as well.

Contents

Page

Foreword iii
Introduction v

I. Energies and Configurations

Interatomic Potentials and Defect Calculations in Ionic Crystals* 1
M. P. Tosi

The Energy of Formation of Schottky Defects in Ionic Crystals 7
I. M. Boswarva and A. B. Lidiard

Recent Calculations Concerning Point Defects in Alkali Halides 11
G. J. Dienes, R. D. Hatcher, R. Smolchowski, and W. D. Wilson

Energy of Formation of Vacancy Pairs in KCl 15
K. Tharmalingam

Vacancies and Monovalent Cation Impurities in the Alkali Halides 17
M. Doyama and M. P. Tosi

Born–Model Defect Energies for CaF_2 19
A. D. Franklin

Lattice Distortion Around Defects 21
T. Kurosawa

Calculation of Lattice Distortion Around Point Defects by Lattice Statics 23
H. Kanzaki

Calculation of Migration Energies of an Interstitial in Germanium and Silicon 27
R. R. Hasiguti

Calculation of The Physical Properties of Defects in Crystals by Approximate Self-Consistent-Field Methods 31
E. B. Moore, Jr.

Interatomic Potentials for Defect Calculations in Metals* 35
H. B. Huntington

Calculations for Defects in an F.C.C. Lattice 39
R. A. Johnson

Atomistic Calculations of Interstitials in F.C.C. Metals 43
M. Doyama and R. M. J. Cotterill

Morse Potential Calculations of Vacancy and Vacancy-Type Defect Properties in F.C.C. Metals 47
R. M. J. Cotterill and M. Doyama

A Two-Body Central-Force Interatomic Potential for Anharmonic Solids 53
R. Chang and L. J. Graham

A Re-examination of the Born-Mayer Potential for Ion-Core Interactions in Copper 55
S. S. Jaswal and L. A. Girifalco

The Interactions Between Point Defects 59
J. S. Koehler

The Energies and Configurations of Point Defects in Solids: Report of The Panel I Discussion 61
A. B. Lidiard

II. Electronic States

Vacancies, Phonons, and Dielectric Screening in Close-Packed Metals* 69
N. H. March and B. Oli

Calculations on Point Defects in Metals Allowing for Realistic Fermi Surfaces and Scattering Mechanisms 75
A. Seeger and E. Mann

Electrical Resistivity of Impurities and Vacancies in Aluminum 97
Y. Fukai

Structure Factor Approach to Energies of Migration 99
H. B. Huntington and M. D. Feit

Perturbed Bloch Functions Obtained From Koster-Slater Perturbation Theory 101
B. Mozer

Residual Resistivities of Dilute Aluminum Alloys 109
F. J. Blatt and H. R. Fankhauser

Point Imperfections in Solid Rare Gases 111
A. Gold

The Use and Misuse of Models in The Calculation of Energy Levels in Insulators 115
W. B. Fowler

Methods for Calculation of The Electronic Structure of Defects in Insulators 119
U. Öpik and R. F. Wood

A Model to Treat Lattice Distortions and The F-Center Electron Consistently 123
H. S. Bennett

T-Matrix Theory of Localized Electronic States Due to a Vacancy With Application to Diamond 127
K. H. Bennemann

Energy Levels Associated With Isolated Vacancies in Silicon 131
J. Callaway and A. J. Hughes

Electron Trapping as a Function of Normal Modes 133
A. M. Lemos

Electronic Properties of Point Defects in Solids. Report of the Panel II Discussion 135
J. A. Krumhansl

III. Vibrational States

Phase Shift Analysis of The Scattering of Lattice Vibrations by Localized Perturbations 141
G. Toulouse and J. Friedel

Influence of Defects on Elastic Constants 151
W. Ludwig

A Calculation of Force-Constant Changes for the *U* Center 157
R. F. Wood and R. L. Gilbert

Local Modes and Resonance Scattering of Lattice Waves Due to Point Defects: Optical and Thermal Properties of Imperfect Crystals 161
G. Benedek and G. F. Nardelli

Comment of The Paper of G. Benedek and G. F. Nardelli 179
Wm. M. Hartmann

One-Phonon Infrared Absorption in a Rare Gas Crystal Induced by Rare Gas Defects 181
Wm. M. Hartmann

Vibrations in Molecular Lattices 185
K. Dettmann and W. Ludwig

The Use of Morphic Effects for The Study of Vibrational and Optical Properties of Impurity Atoms in Crystals 189
A. A. Maradudin, S. Ganesan, and E. Burstein

The Vibrational Properties of Point Defects in Solids. Report of The Panel III Discussion 195
C. W. McCombie

*Invited Paper.

I. Energies and Configurations

Interatomic Potentials and Defect Calculations in Ionic Crystals*

M. P. Tosi

Argonne National Laboratory, Argonne, Ill. 60440

Lattice calculations of point defect properties in crystals started in 1938 with the classical work of Mott and Littleton [1][1] on the energies of formation and migration of a vacancy in alkali halide crystals. A defect is a rather severe disturbance of a crystal lattice: it disrupts the equilibrium conditions of the perfect crystal, causing atomic displacements to new positions where the net force on each atom vanishes, and produces rearrangements in the electron distribution. The theory describes the billiard-ball part of the problem by means of empirical interatomic potentials, and takes care of the electron redistribution in ionic crystals by the dipolar approximation, introducing appropriate ionic polarizabilities. The scheme is basically analogous to that adopted in lattice dynamics calculations and is justified to the extent that the cohesive properties and the dielectric properties of the perfect crystal can be understood on the basis of such concepts.

According to the analysis of the dielectric properties of ionic crystals given by Szigeti [2], the polarization mechanisms of an ion in a crystal include the electron-shell response to an electric field, as well as mutual distortions of the electron shells of neighboring ions accompanying relative displacements of the nuclei. The work of Eshelby [3] and Kanzaki [4], on the other hand, shows that the lattice distortion has long range character even in the absence of electric fields. The long range distortion and polarization around a charged point defect in an ionic crystal have generally been described by means of quasi-continuum solutions appropriate to a dielectric in a nearly uniform electric field and to an elastic medium, with an atomistic treatment of the immediate neighborhood of the defect. In this approximation, the relevance of the polarization mechanism of Szigeti and of the long range elastic relaxation in the vacancy formation problem in the alkali halides have been investigated by Kurosawa [5] and by Brauer [6] and Fumi and Tosi [7], respectively: a unified discussion of these effects is being given by Boswarva and Lidiard [8]. An atomistic treatment of a crystallite containing a vacancy has been given recently by Scholz [9]. The approach is being extended to other solids, such as the alkaline-earth halides [10], which seem to conform closely to the ideal ionic model[11].

A considerable body of theoretical [12,13] and experimental [14] evidence is available to show that the electron distribution of an ion is distorted in passing from the free ion state into the crystal, even in a crystal formed from closed-shell ions. A characteristic deformation is a "loosening" and a "tightening" of the outer electron shells of the positive and of the negative ions, respectively, that quantum mechanical calculations show to be partly due to the Madelung potential [13]. Such distortions give rise to many-body contributions to the binding in the alkali halides, although noncentral terms in the crystal energy appear to be of minor importance [12]. While the use of a pair-wise central potential in the ionic model is an approximation, some of the features of the real crystal which are a consequence of many-body effects are included empirically in the potential through the determination of its parameters from experimental data. This applies, in particular, to the ionic radii [15,16]. The additional electron rearrangements which take place around a defect have often dipolar character, to a first approximation, and are accounted for separately in the model.

The standard description of the short-range interactions in the ionic model is by means of an exponentially decaying repulsive term extended to second neighbors and supplemented by a van der Waals attractive term. The van der Waals coefficients available in the literature on ionic crystals have generally been estimated by the procedure developed by Mayer [17] in the early thirties, which is based on an analysis of optical absorption data for a few alkali halides involving an assignment of the absorption in different energy regions to the different ions. A recent reexamination of this analysis by Lynch [18] points out that the absorption regions of the positive and of the negative ions are in effect overlapping to some extent in the alkali halides and intermixed in silver chloride, and that the analysis is also affected by uncertainties in the effective field correction. As is well known, the

*Based on work performed under the auspices of the U.S. Atomic Energy Commission.

[1] Figures in brackets indicate the literature references at the end of this paper.

model yields very close agreement of the cohesive energy with experiment, in the alkali halides as well as in calcium fluoride; on the contrary, the Mayer values for the van der Waals energy in the silver halides are insufficient to account for the observed binding, and sizable increases in these values, or possibly some covalent binding, are indicated [19].

The accompanying tables present a numerical illustration of effects of the potential on the basic energy parameters of the vacancies in sodium chloride and potassium chloride, for which the experimental values are fairly well established. The effects are analogous in the two salts, though more dramatic in sodium chloride. Table 1 reports the values of the first and second derivative of the first neighbor interaction energy, at the equilibrium interionic distance in the perfect crystal, for the various potentials. Quite independently of the detailed functional form of the short range potential, these provide a measure of its "hardness" in the first neighbor bond over a limited range of interionic distance. The energies reported in table 2 (the lattice energy E_L, the energies of formation of a positive-ion and a negative-ion vacancy, the Schottky defect energy $E_s = E_f^+ + E_f^- - E_L$, and the energies of vacancy migration for a positive and a negative ion along the face diagonal) have been evaluated in the ionic model with a consistent description of the crystal polarization based on the Mott-Littleton model [20].

The values given in the first column have been obtained with the Born-Mayer form of the short range potential, which includes the van der Waals interactions and the second neighbor repulsive interactions, with the parameters obtained recently by Tosi and Fumi [16]. In the second column we give the results obtained by using a single exponential repulsion between first neighbors fitted to the same data. A partial cancellation between the repulsive and the van der Waals interactions of second neighbor pairs, and the small radius differences in the TF potential combine to reduce the net effects of the second neighbor interactions on the defect energies. The two potentials yield results in essential agreement and in fair agreement with experiment. The SE values for the Schottky defect energy are in close agreement with the early results of Mott and Littleton [1], but the migration barriers are higher than their values of about 0.5 eV for NaCl.

Historically, the parameters in the Born-Mayer form have passed through several stages of refinement. Many defect calculations have been based on the values reported originally by Born and Mayer [21], who adopted the Goldschmidt values of the ionic radii and fitted the compressibility of the alkali halides on the average. This potential yields rather erratic results for the vacancy formation and motion energies, and this has in fact been a motivation for the latest steps in its refinement [15,16]. These defect energies are reported here, in the columns labeled BM, as an illustration of the sensitivity of defect energy calculations to the potential parameters. Clearly, the hardness of the first neighbor interactions is seriously underestimated, especially in sodium chloride; and this reflects itself into exceedingly low values for the formation energy of the negative ion vacancy and for the Schottky defect energy [22,23] as well as for the migration energy of the positive ion [23]. The overestimate of the chlorine-chlorine repulsion implied by the use of Goldschmidt radii and the large dipoles carried by the negative ions combine to keep the relaxation around a positive ion vacancy within reasonable bounds, giving reasonable values for E_f^+, [22] whereas the not unreasonable values for E_m^- are largely a consequence of a cancellation of

TABLE 1. *"Hardness" parameters of the various potentials* [a]

		TF	SE	BM	FT	WTF
NaCl	$-\varphi'(r_0)$	0.81	0.77	0.57	0.79	0.87
	$\varphi''(r_0)$	2.59	2.69	1.65	2.34	2.74
KCl	$-\varphi'(r_0)$	0.63	0.62	0.57	0.63	0.75
	$\varphi''(r_0)$	1.95	2.00	1.69	1.94	2.22

[a] The units are 10^{-4} dynes for $\varphi'(r_0)$ and 10^4 dynes/cm for $\varphi''(r_0)$.

TABLE 2. *Effects of the short-range potential in defect energy calculations* (eV)*

	NaCl						KCl					
	TF	SE	BM	FT	WTF	Experiment	TF	SE	BM	FT	WTF	Experiment
E_L	8.06	8.09	8.06	8.01	7.81	[a]8.07	7.34	7.28	7.29	7.33	7.01	[a]7.35
E_f^+	4.70	4.78	4.78	4.60	4.65	.....	4.50	4.51	4.52	4.49	4.37	.....
E_f^-	5.30	5.25	4.59	5.19	4.97	.....	4.84	4.72	4.58	4.85	4.58	.....
E_s	1.94	1.94	1.31	1.78	1.81	[b]2.12±0.06	2.00	1.95	1.81	2.01	1.94	[d]2.22−2.31
E_m^+	0.85	0.90	0.30	0.70	0.92	[b]0.80±0.02	0.85	0.86	0.67	0.83	0.96	[d]0.59−0.84
E_m^-	0.90	0.88	0.72	0.75	1.00	[c]1.06	0.83	0.84	0.76	0.80	0.95	[e]0.95±0.1

*The repulsive parameters in the various potentials are taken from the following sources: TF and WTF potentials, from M. P. Tosi and F. G. Fumi, ref. [16], table 1, first column; SE potential, from M. P. Tosi, ref. [19], table VIII, second column; BM potential, from M. Born and J. E. Mayer, ref. [21], with the preexponential parameter fitted to the equation of state; FT potential, from F. G. Fumi and M. P. Tosi, ref. [15], table 2, first row. The Mayer values of the van der Waals coefficients (ref. [17]) are used in the TF and FT potentials, whereas the BM potential involves the use of the values reported by J. E. Mayer and L. Helmholz (Z. Phys. **75**, 19 (1932)).

[a] From the cohesive energy at room temperature reported by M. P. Tosi, ref. [19], after correction for the vibrational energy.

[b] From R. W. Dreyfus and A. S. Nowick, J. Appl. Phys. **33**, 473 (1962).

[c] From the activation energy for Cl^- diffusion in pure NaCl reported by N. Laurance (Phys. Rev. **120**, 57 (1960)), after subtraction of $\frac{1}{2}E_s = 1.06$ ev.

[d] From R. W. Dreyfus and A. S. Nowick, loc. cit.; A. R. Allnatt and P. W. M. Jacobs, Trans. Faraday Soc. **58**, 116 (1962); P. W. M. Jacobs and J. N. Maycock, Jr., J. Phys. Chem. Solids **24**, 1693 (1963); R. G. Fuller, Phys. Rev. **142**, 524 (1966).

[e] From R. G. Fuller, loc. cit.

errors between underestimates of the saddle point energy and of E_f [23]. In the FT potential [15], on the other hand, no assumption is made on the ionic radii, but the compressibility is still fitted on the average—using, of course, recent data. This procedure underestimates somewhat the hardness of the potential in sodium chloride, and this is reflected by the defect energies. The Huggins-Mayer potential [24] represents an intermediate stage of refinement between the BM and the FT potentials, and yields values for the defect energies which lie approximately midway between the BM and the FT results.

As an additional illustration of the sensitivity of defect energies to approximations in the potential, the columns labeled WTF report the results obtained by the TF potential with the van der Waals energy omitted. The crystal is moderately stiffened by this inconsistency and the binding of an ion in the crystal is sizably weakened.

In conclusion, two more questions may be touched upon. The first concerns possible improvements in the existing potentials based on the cohesive properties [19]. While the electron maps provide supporting experimental evidence for the ionic radii, it would be desirable to carry out other tests on the second neighbor interactions. An effort at refining the Mayer values for the van der Waals coefficients would also be desirable. Critical tests on the functional form of the potential would require accurate pressure-volume data over a large range of relative compression. Recent studies of the equation of state of NaCl [25] indicate, however, that the perfect crystal potential is quite accurate over a sizable range.

The second question is whether some defect configurations are indeed so far removed from the perfect crystal that the perfect crystal potential and the dipolar approximation become suspect. An example may be provided by the saddle-point configuration for vacancy migration; [23] and it was suggested, on the basis of the migration barriers obtained by us with the BM potential and by Mott and Littleton with the SE potential, that the perfect crystal potential is indeed inadequate in a treatment of this problem based on the dipole approximation. However, as is apparent from the first two columns of table 2, the ionic model yields reasonable values for these barriers. This remains nevertheless an outstanding theoretical question in the treatment of defect configurations where ions approach very closely. While a "molecule-in-crystal-field" method would clearly be the correct theoretical approach in principle, the Verwey potential [26,23] is a crude attempt at interpolating between the solid and the molecule. In the light of the sensitivity of defect energies to the potential parameters displayed above in the TF and BM columns, a careful reexamination of the interpolation scheme is needed.

Appendix

The Mott-Littleton model makes recourse to the macroscopic polarization to fix the long range displacements and dipoles around a charged defect. The macroscopic polarization enters also the model given previously by Jost [27]. The relationship between the two models has been the subject of some discussion at the Conference, and it has been suggested that the Mott-Littleton model is theoretically even less satisfactory than the Jost model. The writer deems it useful to give a detailed discussion of this point.

In a continuous dielectric medium, as considered in the Jost method, one has no difficulty in defining the macroscopic polarization around an extra point charge as a mathematical function of position over space. Integration of the field energy density of the charge in vacuo and in the dielectric yields the polarization energy as

$$E_{\text{pol}}=-\frac{1}{2}\frac{Q^2}{R}\left(1-\frac{1}{K}\right) \tag{1}$$

where R is the radius of a cavity in the dielectric. The method contains no prescription for determining this physically arbitrary limit of integration; Jost chose R equal to one-half the distance to neighboring ions to show that the polarization energy could be of the same order of magnitude as the rigid lattice energy, thereby reducing the defect formation energy from 8 to 10 eV to 1 to 2 eV as experimentally observed.

In a crystal of discrete ions, as considered in the Mott-Littleton method, the calculation of the macroscopic polarization around an extra point charge clearly requires an average of the ionic dipoles over macroscopic regions of space over which the field be essentially uniform. The equation

$$P(r)=\frac{1}{v_0}\left[\mu_+(r)+\mu_-(r)\right] \tag{2}$$

is the result of such an average over a region of space centered at r in the limit $r\to\infty$. Both sides of this equation have no meaning close to the point charge, and the method does not use the equation in these conditions. Equation (2) fixes in the method the sum of the dipoles in a lattice cell at large distance from the charge, whereas the ratio of these dipoles is fixed by the equation

$$\mu_+(r)/\mu_-(r)=\frac{\alpha_++\alpha}{\alpha_-+\alpha} \tag{3}$$

where the displacement polarizability α is also evaluated by taking the field as essentially uniform. The Mott-Littleton dipoles are therefore correct

only at large distance from the charge, a well known fact. The dipoles themselves are extrapolated into region II.

Let us examine the physical assumptions of the method on the dipoles in region II. Equation (2) fixes the inverse square distance dependence of the dipoles, that we may write in the form

$$\mu_{\pm}(r_i) = \frac{1}{2} v_0 M'_{\pm} \frac{Q}{r_i^2} \tag{4}$$

where r_i is the distance of the lattice site, occupied by either a positive or a negative ion, from the charge. The use of eqs (2) and (3) to determine M'_+ and M'_- implies then that the Mott-Littleton expression,

$$M'_{\pm} = \frac{1}{4\pi} \left(1 - \frac{1}{K}\right) \frac{\alpha_{\pm} + \alpha}{\frac{1}{2}(\alpha_+ + \alpha_-) + \alpha} \tag{5}$$

is taken directly from the atomic theory of dielectrics in a uniform field. Namely, the method is describing the response of the ions in region II to the field Q/r_i^2 of the charge by analogy with their response to a uniform field. The factor $\alpha_{\pm} + \alpha$ in eq (5) gives the response to a uniform effective field, and the other factors represent the effective field correction.

We may rederive these results in detail without using the macroscopic polarization. We consider an extra charge in a NaCl-type crystal, with coulomb interactions and short range interactions between first neighbors described by a potential $\varphi(r)$. The effective field $E_{\text{eff}}(r_i)$ at the lattice site r_i induces an electronic dipole $\alpha_{\pm} E_{\text{eff}}(r_i)$ and provides a driving force $\pm e E_{\text{eff}}(r_i)$. The restoring force is provided by the short range interactions and is derived by Mott and Littleton from the harmonic Hamiltonian written as $\frac{1}{2} k \sum_i u_i^2 + \frac{1}{2} k \sum_i u_i^2$; the first term follows from the diagonal elements of the force constants matrix and is exact, whereas the second follows from the nondiagonal elements [28] under the assumption that neighboring ions have equal and opposite displacements, as would be exact in a uniform field. The force constant k is given by Mott and Littleton as $2\nabla^2\varphi(r)|_{r=r_0}$; it is in fact the restoring force constant for long-wavelength optical vibrations and is related in the present model to the compressibility by $k = 6r_0/\beta$ [29]. Force balance yields the displacement dipole $\pm e u_i$ as equal to $\frac{e^2}{2k} E_{\text{eff}}(r_i)$, and the total dipole is

$$\mu_{\pm}(r_i) = (\alpha_{\pm} + \alpha) \frac{L}{K} \frac{Q}{r_i^2} \tag{6}$$

where [30] $\alpha = \frac{e^2}{2k}$ and we have written the effective field as $\frac{L}{K} Q/r_i^2$, with L an effective field correction factor. The assumption that L be independent of r_i is, again, correct only if the field is essentially uniform. If one uses eq (6) for all the dipoles around a vacancy, one finds for the Schottky defect

$$E_{\text{pol}} = -\frac{1}{2} \frac{e^2}{r_0^4} (\alpha_+ + \alpha_- + 2\alpha) \frac{L}{K} \sum_i \left(\frac{r_0}{r_i}\right)^4 \tag{7}$$

The quantity $\alpha_+ + \alpha_- + 2\alpha$ gives in fact the response of a lattice cell to a uniform field, and satisfies the relationship

$$\frac{1}{v_0} (\alpha_+ + \alpha_- + 2\alpha) \frac{L'}{K} = \frac{1}{4\pi} \left(1 - \frac{1}{K}\right) \tag{8}$$

where L' is the effective field correction factor for a uniform field. If one takes $L = L'$ in eq (6), as it should be by the manner in which this equation has been derived, one finds the Mott-Littleton formula for the dipoles in region II.

We note the following:

(1) equations (8) and (2) are in fact equivalent;

(2) the Mott-Littleton formula for the dipoles is independent of the value that dielectrics theory assigns to the effective field correction factor L' — although modern theory accepts the full Lorentz value $L' = (K+2)/3$ for ionic crystals when ionic overlap effects are accounted for by the Szigeti effective charge [31];

(3) the zeroth-order Mott-Littleton approximation for the Schottky defect energy, obtained by using eq (8) in eq (7), has the same formal structure as the Jost formula, but with the arbitrary limits of integration fixed by a lattice summation, because the Mott-Littleton method relates the defect problem to the atomic theory of dielectrics and one is summing over the two vacancies. The use of the macroscopic polarization in both methods does not imply that they are based on the same physical assumptions, and in fact the two methods give structurally different formulas for, say, the Frenkel defect energy. It implies, however, that the two methods will converge to the same limit as region I is enlarged.

We also note that, even under the assumptions specified above, the harmonic Hamiltonian that we have used is incorrect for the case of a vacancy, since the breaking of the bonds to the first neighbors of the vacancy implies a constant term and a modification to the linear term in the restoring force on these ions. This fact, as well as the fact that the above assumptions are most inappropriate for these ions, are accounted for in the first-order approximation of the method.

The relevant question on the usual scheme which decomposes the crystal around the vacancy into a region I and a region II to be described by approximate displacements and dipoles correct at large distance is, of course, the convergence of the energy results as region I is enlarged. Experience shows that the polarization energy is not as sensitive as the

dipoles to the assumptions of the method. Investigations of the convergence of the scheme for a crystal of polarizable but undisplaceable ions were carried out first by Mott and Littleton, who extended region I to include four shells of ions, and later by Rittner et al. [32], who included up to ten shells of ions. Several cases corresponding to different values of the dielectric constant and of the polarizability ratio were considered, and the results depend to some extent on these parameters. In all cases the dipoles keep fluctuating around the Mott-Littleton values but the polarization energy converges so rapidly that practically perfect convergence is attained after the third-order approximation. The first-order approximation is fairly accurate, the largest error being 4 percent of the polarization energy; the zeroth-order approximation itself is not poor, although the polarization energy is underestimated by as much as 10 percent in the same case. In most cases the first-order approximation overestimates the polarization energy. The convergence of the Jost method was also investigated and found to require up to eight successive approximations.

The Mott-Littleton model is therefore a quasi-continuum model whose accuracy has been tested in the dipole approximation. Since the displacements of the ions beyond first neighbors are sufficiently small to be equivalent to dipoles in their electrostatic effects, one expects that the foregoing results apply also in the real case. One also expects, however, that the method will become less reliable as the dielectric constant increases [1]. The treatment of the real case, on the other hand, involves a new set of difficulties already in the first-order approximation. These are the use of a reliable ion-ion potential and the inclusion of the long-range elastic distortion and of the coupling between ionic displacements and electronic deformations. A proper treatment of these effects has had to wait for developments of other aspects of the theory of ionic crystals. An examination of the first three columns of table 2 will show that the difficulties associated with the potential are at least as important as the convergence question, and, moreover, have a direct bearing on it.

The recent work of Scholz and of Simpson shows that an enlargement of region I is well within present capabilities, and the results of the first-order approximation are consistent with the results of these authors. It is nevertheless clear that even improved calculations of the Schottky defect energy will generally be affected by uncertainties of a few tenths of an eV. It is also clear that the uniform field response assumption of the zeroth-order Mott-Littleton approximation is a simple physical assumption which allows back-of-the-envelope calculations without requiring a fitting of parameters to the desired result. It should therefore be noted that it yields already very reasonable values of the Schottky defect energy. This fact is of little help to the study of other defect configurations.

I am indebted to Professor F. G. Fumi for helpful suggestions and to Dr. A. B. Lidiard for informative correspondence.

References and Notes

[1] N. F. Mott and M. J. Littleton, Trans. Faraday Soc. **34,** 485 (1938).
[2] B. Szigeti, Proc. Roy. Soc. (London) **A204,** 51 (1950).
[3] J. D. Eshelby, Solid State Physics **3,** 79 (1956).
[4] H. Kanzaki, J. Phys. Chem. Solids **2,** 24 (1957).
[5] T. Kurosawa, J. Phys. Soc. Japan **13,** 153 (1958).
[6] P. Brauer, Z. Naturforsch. **7a,** 372 (1952).
[7] F. G. Fumi and M. P. Tosi, Disc. Faraday Soc. **34,** 485 (1957).
[8] I. M. Boswarva and A. B. Lidiard, this conference.
[9] A. Scholz, Phys. Stat. Sol. **7,** 973 (1964).
[10] A. D. Franklin, this conference.
[11] J. D. Axe, Phys. Rev. **139,** A1215 (1965).
[12] P. O. Löwdin, Phil. Mag. Suppl. **5,** 1 (1956).
[13] M. I. Petrashen, L. V. Abarenkov, and N. N. Kristofel, Optics and Spectroscopy (USSR) **9,** 276 (1960); Vestnik Leningrad Univ. **16,** 7 (1960).
[14] H. Witte and E. Wölfel, Revs. Modern Phys. **30,** 51 (1958). (NaCl, LiF, CaF_2); G. Schoknecht, Z. Naturforsch. **12a,** 983 (1957). (NaCl); R. Brill, C. Hermann, and C. Peters, Z. anorg. u. allgem. Chem. **257,** 151 (1948) (MgO); U. Korhonen and M. Linkoaho, Ann Acad. Sci. Fenn., Series A VI, No. 195 (1966) (AgCl).
[15] F. G. Fumi and M. P. Tosi, J. Phys. Chem. Solids **25,** 31 (1964).
[16] M. P. Tosi and F. G. Fumi, J. Phys. Chem. Solids **25,** 45 (1964).
[17] J. E. Mayer, J. Chem. Phys. **1,** 270 (1933).
[18] D. W. Lynch, J. Phys. Chem. Solids, to appear. I am indebted to Professor Lynch for a preprint of his work.
[19] M. P. Tosi, Solid State Physics **16,** 1 (1964). The van der Waals interactions and partially covalent bonds will, of course, play an essential role for the stability of the silver interstitial [5].
[20] Details of the calculation and the comparison with experiment are discussed by M. P. Tosi and M. Doyama, Phys. Rev. **151,** 642 (1966).
[21] M. Born and J. E. Mayer, Z. Phys. **75,** 1 (1932). The BM potential has so far been approximated in defect calculations by omitting the van der Waals interactions, the pre-exponential parameter being refitted to the thermodynamic equations and the hardness parameter being left unchanged. These corrections are less rigorous than those adopted by Boswarva and Lidiard [8] but do not affect significantly the results. Thus these approximations lower the vacancy formation energies given in table 2 by about 0.1 eV, in agreement with previous results [23], but affect the values of the Schottky defect energy and of the motion energies by a few hundredths of an eV. The values of the motion energies given here are higher than those reported previously [23], by 0.2 eV in NaCl and 0.1 eV in KCl, because of the more accurate treatment of the dipole-dipole interaction in the treatment of the local relaxation energy.
[22] F. Bassani and F. G. Fumi, Suppl. Nuovo Cim. **1,** 114 (1955).
[23] R. Guccione, M. P. Tosi and M. Asdente, J. Phys. Chem. Solids **10,** 162 (1959).
[24] M. L. Huggins and J. E. Mayer, J. Chem. Phys. **1,** 643 (1933).
[25] D. L. Decker, J. Appl. Phys. **36,** 157 (1965).
[26] E. J. W. Verwey, Rec. Trav. Chim. **65,** 521 (1946).
[27] W. Jost, J. Chem. Phys. **1,** 466 (1933).
[28] One may use, e.g., eqs (35.1), (38.1), and (38.2) in G. Leib-

fried, Hand. d. Phys. VII/1 (Springer, Berlin 1955) to find the nondiagonal term as

$$-\frac{1}{2}\frac{\varphi'(r_0)}{r_0}\sum_{ij}\mathbf{u}_i\cdot\mathbf{u}_j-\frac{1}{2}\left[\varphi''(r_0)-\frac{\varphi'(r_0)}{r_0}\right]\sum_{ij}(\mathbf{n}_{ij}\cdot\mathbf{u}_i)(\mathbf{n}_{ij}\cdot\mathbf{u}_j)$$

Here, the index i runs over all the ions, the index j over the first neighbors of i, and $\mathbf{n}_{ij}$ is the unit vector joining the two ions. This may be used to find that the correction in the displacements falls as r^{-4}.

[29] This last result does not hold if second neighbor interactions are included. However, all the other relevant details remain correct, if one still interprets $\varphi(r)$ as the first-neighbor potential.

[30] The inclusion of the Szigeti effective charge in the manner discussed by Born and Huang [31] yields the result of Boswarva and Lidiard [8], $\alpha=e^{*2}/2k$.

[31] M. Born and K. Huang, Dynamical Theory of Crystal Lattices, section 9 (Oxford, 1954).

[32] E. S. Rittner, R. A. Hutner and F. K. du Pré, J. Chem. Phys. **17**, 198 (1949).

The Energy of Formation of Schottky Defects in Ionic Crystals

I. M. Boswarva

Metallurgy Department, Imperial College, London S.W.7

and

A. B. Lidiard

Theoretical Physics Division, U.K.A.E.R.E., Harwell, Didcot, Berks, England

The success of the Born ionic model in describing the cohesive properties of alkali halides has encouraged its use in calculations of characteristic energies of point defects. Several workers* have obtained good agreement with experiment for the formation energy of Schottky pairs, W_s, but the use of differing repulsive potentials and modifications to Mott and Littleton's basic description of the displacement field has, nevertheless, left a rather confusing picture. We present here, some of the main results of a systematic study made to clarify the effects of such differing descriptions. Our aim is thus not simply a comparison with experiment, but is also to assess the range of variation caused by reasonable alterations of the basic model. Further, we study 16 alkali halides with the NaCl structure so that a broader view is possible than when only NaCl and KCl are considered.

The basis of our calculations is a model in which each ion of the solid is described by its displacement from the perfect lattice and its electronic dipole moment. The energy function of the solid contains electrostatic terms coming from interactions among the ionic charges and dipoles, along with short-range closed-shell repulsions coming from ionic overlap. To calculate the energy needed to extract an ion from the perfect solid the crystal is divided into two regions, I and II. The six nearest neighbor ions of the vacancy, which constitute region I, are considered explicitly whilst we use a harmonic approximation for the rest of the lattice (region II). The general equations of this method were published in the abstracts of the International Conference on the Nature of Defects in Crystals, Melbourne, August 1965, Paper P3.

Previous calculations of vacancy formation energies have all used the traditional Born-Mayer exponential form for the overlap repulsion potential and we have also made computations for this model (BM). However, Guccione et al. [4], found it necessary to modify this to obtain sensible results for vacancy migration energies. They needed a harder potential for ions coming close together and used the so-called Born-Mayer-Verwey potential (a r^{-12} dependence for $r <$ anion-cation nearest neighbor separation). This potential was also used by Tharmalingam [10] for interstitial ion migration energies. We find that the general pattern of our results is the same with the B.M.V. potential as with the B.M. potential but each formation energy is higher. In general the B.M. formation energies are too low compared to experiment and the agreement with B.M.V. is better. The variations in W_s resulting from different choices of constants in these potentials (ionic radii etc.) are smaller than the difference between the W_s values for corresponding B.M. and B.M.V. potentials. We now consider various modifications to the description of region II in these calculations.

The description of the displacement field in region II in this model is essentially intuitive. The original method, due to Mott and Littleton [7], uses the electric polarization caused by the effective charge of the vacancy to determine the displacement field and our basic calculation (set A in the table) employs this approach. In an attempt to improve this description we consider the vacancy as an elastic singularity as well as an electrical one. The ion at r is then displaced radially outwards an amount $\xi = kr_0^3/r^2$ where r_0 is the perfect anion-cation separation and k is the elastic strength of the vacancy. If we take the displacement of region I ions as λr_0 then for continuity $\lambda = k + M'$ where $M'r_0$ is the electrical displacement of the neighbors to the vacancy as given by the Mott-Littleton theory. We include this elastic strength of the vacancy in the set of calculations labeled B in the table. Brauer [2] who first included this elastic displacement term in such calculations simply equated k to λ. It seems to us that in principle this would overemphasize the elastic component but we have also made computations using his assumption and these are given in Columns C.

*Brauer [2],† Tosi and Fumi [11], Kurosawa [6], Scholz [8], and Simpson [9].

†Figures in brackets indicate the literature references at the end of this paper.

TABLE I. *Experimental and theoretical values of the energy of formation of Schottky defects,* W_s *in eV, in alkali halides with the* NaCl *structure*

The corresponding theoretical values for the outward relaxation of the nearest neighbors to the vacancy are also given (in units of r_0 the anion-cation spacing). For description of the basis of the four different calculations A, B, C and D see text.

		W_s(exp)	A		B		C		D	
			λ	W_s	λ	W_s	λ	W_s	λ	W_s
LiF	+ion	2.20–2.68	0.0546	2.310	0.0445	2.339	0.0549	2.734	0.0410	2.218
	−ion		.0713		.0639		.0750		.0631	
LiCl	+ion	2.12	.0419	1.212	.0317	1.263	.0408	1.485	.0261	1.070
	−ion		.0785		.0738		.0845		.0731	
LiBr	+ion	1.80	.0388	0.970	.0288	1.024	.0378	1.214	.0225	0.798
	−ion		.0813		.0775		.0883		.0768	
LiI	+ion	1.34	.0358	0.607	.0265	0.665	.0352	0.818	.....	.....
	−ion		.0865		.0841		.0954			
NaF	+ion		.0596	2.818	.0518	2.892	.0612	3.181	.0510	2.865
	−ion		.0650		.0579		.0671		.0577	
NaCl	+ion	2.02–2.20	.0461	1.912	.0373	1.988	.0452	2.170	.0347	1.881
	−ion		.0693		.0644		.0727		.0642	
NaBr	+ion	1.68	.0424	1.653	.0333	1.727	.0410	1.887	.0306	1.600
	−ion		.0712		.0669		.0751		.0670	
NaI	+ion		.0384	1.300	.0295	1.372	.0367	1.506	.0268	1.248
	−ion		.0752		.0723		.0804		.0724	
KF	+ion		.0649	2.360	.0586	2.428	.0676	2.654	.0572	2.393
	−ion		.0571		.0492		.0577		.0491	
KCl	+ion	2.22–2.30	.0515	2.053	.0436	2.120	.0512	2.279	.0420	2.066
	−ion		.0609		.0546		.0621		.0547	
KBr	+ion	2.35–2.53	.0479	1.889	.0397	1.956	.0469	2.099	.0381	1.890
	−ion		.0622		.0565		.0638		.0567	
KI	+ion		.0433	1.657	.0346	1.722	.0416	1.845	.0330	1.636
	−ion		.0645		.0595		.0666		.0600	
RbF	+ion		.0672	2.074	.0612	2.135	.0703	2.345	.0606	2.121
	−ion		.0540		.0456		.0540		.0455	
RbCl	+ion		.0534	2.007	.0459	2.071	.0533	2.222	.0448	2.033
	−ion		.0582		.0514		.0588		.0516	
RbBr	+ion		.0502	1.868	.0423	1.931	.0496	2.068	.0411	1.888
	−ion		.0596		.0533		.0606		.0535	
RbI	+ion		.0526	1.879	.0448	1.937	.0524	2.081	.0434	1.894
	−ion		.0616		.0533		.0629		.0554	

The second major modifications which we introduce (columns D) allows for the deformation of the electron distribution of the ions resulting from their relative motion. The basic idea is that relative motion of the positive and negative ions leads to a distortion of the otherwise spherical charge distributions and this distortion can be represented as an additional dipole, the 'deformation dipole.' In region II the total polarizability per cell now is $\alpha_+ + \alpha_- + 2(e^*)^2/p$ where α_+, α_- are the electronic polarizabilities of the cations and anions respectively, e^* is the Szigeti effective charge and p is the force constant from Mott-Littleton theory. The last term of this total polarizability is the sum of the displacement dipole contribution of $2\,ee^*/p$ and the deformation dipole contribution $-2\ e^*(e-e^*)/p$. The deformation dipoles on the region I ions are readily found using the analysis of Hardy [5]. These deformation dipoles have been included as well as elastic terms with strength $k=\lambda-M'$ (set D).

General conclusions and features of the results obtained using the B.M.V. potential are as follows:

1. The outward relaxations of the cations neighboring an anion vacancy are more than those of the anion neighbors of a positive ion vacancy, except for KF and RbF. This is because they suffer less restraint from second neighbor repulsive interactions.

2. The work to remove a cation is less than that to remove an anion. The polarizability of the surrounding ions, which is much greater, appears to govern this feature although its effect is somewhat reduced by the larger second neighbor repulsions.

3. Reasonable agreement with experiment is obtained for LiF, NaCl, NaBr, and KCl with all modifications. The differences do not seem large enough to permit an empirical choice between the different assumptions for region II. However, none of the calculations give $W_s(\mathrm{KBr}) > W_s(\mathrm{KCl})$ as required by experiment, and the predicted values for the other Li halides are all too low.

4. If we use the B.M. potential the corresponding W_s values are reduced in most cases by 0.2–0.4 eV, although in LiF the reduction is as large as 1 eV. The first neighbor relaxations are increased up to 50 percent over the B.M.V. values.

5. An important energy term introduced by elastic distortion terms is an addition to the polarization

energy of region II of

$$(1.068-4.731\lambda)e^2(\lambda-M')/r_0.$$

The term in M' is missing in Brauer's method. The absence of the term in M' causes both the larger relaxations and the larger W_s values in this case.

6. Only the elastic term in the displacement field contributes to the change of volume of the crystal due to relaxation around the vacancy. The volume of formation per Schottky pair has been determined experimentally for NaCl and KCl by Biermann [1] and the results give, in both cases, the sum of the vacancy elastic strengths, $k_+ + k_- \sim 0.05$. This is considerably less than $\lambda_+ + \lambda_-$ (Brauer's assumption) but greater than $\lambda_+ + \lambda_- - 2M'$ (our assumption) which is 0.022 for both NaCl and KCl.

7. All the results for the alkali halides presented here have used the first set of values of interionic distance and compressibility compiled by Fumi and Tosi [3] along with the ionic radii evaluated by them. We have also considered (i) the second set of data from Fumi and Tosi and (ii) Goldschmidt radii, both of which give relatively small variations to W_s. Much early work used averaged values of strength and hardness parameters in the repulsive potential, although there is no theoretical reason for these parameters to be identical for a whole family of salts. We find that the traditional values ($\rho=0.345$ Å, $b=0.143$ eV) give lower values of W_s by 0.1–0.2 eV whilst Fumi and Tosi's new values averaged over all the alkali halides ($\rho=0.339$ Å, $b=0.159$ eV) give results close to those obtained using the particular values appropriate to each individual salt.

References

[1] Biermann, W., Z. f. Phys. Chem. **25**, 90 and 253 (1960).
[2] Brauer, P., Z. Naturf. **7A**, 372 (1952).
[3] Fumi, F. G. and Tosi, M. P., J. Phys. Chem. Solids **25**, 31 (1964).
[4] Guccione, R., Tosi, M. P. and Asdente, M., J. Phys. Chem. Solids **10**, 162 (1959).
[5] Hardy, J. R., Phil Mag. **7**, 315 (1962).
[6] Kurosawa, T., J. Phys. Soc. Japan **13**, 153 (1958).
[7] Mott, N. F. and Littleton, M. J., Trans. Farad. Soc. **34**, 485 (1938).
[8] Scholz, A., Phys. Stat. Solidi **7**, 973 (1964).
[9] Simpson, J. H., Paper No. 176 Conference on Color Centers in Alkali Halides, Urbana, Ill. (1965).
[10] Tharmalingam, K., J. Phys. Chem. Solids **25**, 255 (1964).
[11] Tosi, M. P. and Fumi, F. G., Disc. Farad. Soc. **23**, 92 (1957).

256-724 O-67—2

Recent Calculations Concerning Point Defects in Alkali Halides*

G. J. Dienes

Brookhaven National Laboratory, Upton, N.Y. 11973

R. D. Hatcher

Queens College, The City University of New York, Flushing, N.Y. 11367

R. Smolchowski

Princeton University, Princeton, N.J. 08540

and

W. D. Wilson

Queens College, The City University of New York, Flushing, N.Y. 11367

The presence of a defect in an alkali halide lattice causes the neighboring ions to be displaced from their normal positions, and consequently alters the interaction energies in the crystal. Evaluation of the energies involved coupled with the condition that the additional energy be a minimum with respect to certain variable parameters enables a solution to be found for the displaced position of the ions in the vicinity of the defect. The difference in the energy between the new configuration and the perfect lattice gives the formation energy and in addition, the activation energy for motion of the defect can be obtained by considering the defect in various positions.

The method used assigns variable parameters, P_i, to certain ions neighboring the defect and in some problems to the defect itself. These parameters indicate arbitrary displacements from normal lattice sites. The number of parameters vary with the problems handled, up to eight have been used, which when symmetry is taken into account allow for up to 30 neighboring ions to be varied. The energy is composed of several parts. The electrostatic terms are $\sum_{ij} e_i e_j / r_{ij}$ where r_{ij} is the distance between ions i and j in their relaxed positions and e_i the charge on the ions. From this term must be subtracted the electrostatic energy of the ions in the normal lattice. The Ewald summation method and a procedure of separating the ions into two groups, those that are allowed to relax, and those that are kept fixed enable several of the terms to be evaluated from well-known expressions leaving finite sums over the movable ions. The polarization energy is obtained from the expression $-\frac{1}{2}\sum_i \alpha_i \mathbf{E}_i^2$ where $\mathbf{E}_i$ is the electric field at ion i in its relaxed position and α_i is the polarizability of the ion. The summations here are handled hy the same procedures as in the case of the electrostatic terms. Since in the normal lattice the electric field at an ion is zero, there is no initial polarization energy. An additional term in the polarization series, the interaction between induced dipoles is sometimes included. Summations are taken over sufficient terms in the lattice that the model of a polarizable medium is not needed. The repulsive energy between ions is obtained from the Born-Mayer form $Ae^{-Br_{ij}}$ with A and B constants that depend on the particular ions involved. The summations required here are not extensive because of the rapid falling off of the interaction. In certain problems it is necessary to consider special types of interactions, usually of the nature of binding or covalent terms. These are calculated either quantum-mechanically or from experimental data. When all energy terms are computed the total energy as the sum of them is a function of the parameters $E=E(P_i)$. Initially the parameters are set at certain values and the energy obtained by a computer, then each parameter in turn is varied until a minimum is obtained relative to that parameter. After this has been done for all parameters it is run through several more times for smaller variations.

The polarizabilities of the ions were taken from the work of Tessman, Kahn, and Shockley [1].[1] The constants entering into the repulsive terms were taken from the papers by Tosi and Fumi [2].

*Work performed at Brookhaven National Laboratory and Supported by the Atomic Energy Commission.

[1] Figures in brackets indicate the literature references at the end of this paper.

This includes also such quantities as the radii of the ions. For the radius of neutral ions an average value of the radius was computed from wave functions and was suitably adjusted to compare with the radii of the charged ions. Radii for ions considered as sharing a charge was computed by interpolation.

Three applications will be considered here.

(a) *Interstitial* Cl° *in* NaCl. The method was initially applied to the case of an interstitial chlorine atom in NaCl to determine the amount of the relaxation involved and to find which position of the defect would give the least energy. Several positions for the Cl° were investigated: the cube-center, the face-center and various positions along the cube and face diagonals. The lowest energy configuration was found to be the body-center position. In this case four variable parameters were employed involving 20 movable ions. The nearest Cl^- ions relaxed outward 14 percent while the nearest Na^+ ions relaxed 16 percent. The energy relative to the perfect lattice was found to be 2.65 eV. For the face-center position six parameters were used involving 18 movable ions. Here the nearest Cl^- ions relaxed outward 23 percent while the nearest Na^+ relaxed 21 percent, the energy relative to the perfect lattice being 3.09 eV. The activation energy for motion between these two positions is then 0.4 eV. In the placement of the Cl° along the cube-diagonal in an asymmetrical position, the nearest Cl^- ion is considerably displaced; however a local minimum can be obtained using 9 parameters and 19 movable ions with an energy relative to the perfect lattice of approximately the same as for a cube-center position. The minimum position of the Cl° was found to be about 20 percent along the diagonal from the regular Cl^- site. A similar situation was found in the case of an asymmetrical face-diagonal position. Here the Cl° is found at about 32 percent along the diagonal with again only a small difference in energy from the face-center position. The activation energy along the ⟨111⟩ direction is about 0.2 eV and along the ⟨110⟩ is about 0.05 eV. It would appear then that motion of the Cl° along the diagonal is relatively easy. In these calculations crystal forces alone were used. However, it would appear that these forces alone might be able to push the Cl° into the diagonal or H-center type configuration.

(b) *The* H-*center in* KCl. The *H*-center in KCl is a Cl_2^- molecular ion oriented symmetrically along a ⟨110⟩ direction. This has been verified by experiments involving the absorption of polarized light and by electron spin resonance techniques. Using the defect calculation methods we investigated the problem of showing why the *H*-center preferred the ⟨110⟩ direction rather than the ⟨111⟩ which on the basis of the above work on the Cl° might seem to give rise to the most stable position. The interaction potential between the two halves of the Cl_2^- was first chosen as an average of the Cl^--Cl^- Born-Mayer interaction and the Cl°-Cl° Morse potential. The binding energy here was 0.2 eV with an interionic separation of 2.95 Å. This interaction was used for both the ⟨110⟩ and ⟨111⟩ orientations of the *H*-center with 8 parameters involving 23 movable ions. The resulting configuration showed a compression to 2.6 Å with the ⟨111⟩ direction having the lower energy by 0.2 eV. A better interaction potential was obtained from the wave function calculations of Wahl and Gilbert [3] for the ground state of the *H*-center, leading to an equilibrium separation of 2.70 Å with a binding energy of 0.93 eV. The interaction potential was put in the form of a polynomial for use in the defect work. Employing this new potential in the same two directions as before led to similar results—again a 0.2 eV. difference favoring the ⟨111⟩ direction. Corrections to the point ion model were considered first with respect to the polarization energy. Although for a point ion at its regular lattice position the electric field is zero, if the charge is considered as spread out there is an average electric field present, leading to a polarization energy. Similarly if the Cl_2^- is considered as spread out along the lines of their wave function, a polarization energy is also involved. Taking these aspects into account led to a correction of closely the same amount in each of the two orientations. The next modification of the point ion model was made by taking into account the fact that in the cyrstal the *H*-center involves attractive interactions with the two nearest Cl^- ions in the ⟨110⟩ direction. This has the effect of lowering the energy in this configuration. Considering that the wave function spreads to these ions as well, and that the hole spends 8 to 10 percent of the time on the end ions leads to a reduction of the energy for the ⟨110⟩ direction sufficient to make it the most favorable orientation by about 0.2 eV.

(c) *Off-center ions.* Recent experimental results [4] have indicated that a Li^+ substituted for K^+ in KCl does not end up on the lattice site but slightly away from it. We have investigated this in two ways. First the stability of the Li^+ at a lattice site was investigated, allowing the neighboring ions to relax and calculating the terms entering into a certain determinant [5] whose value indicates whether the location considered is stable or not. In this case, the Li^+ turned out to be unstable at a lattice site. Second the Li^+ was assigned a variable parameter so that it could move along the ⟨100⟩ direction and four other parameters were employed for the surrounding ions. The interaction of Li^+ with Cl^- was calculated from the Born-Mayer expression with the addition of a barrier to guard against too close contact. The minimum position turned out to be for the Li^+ about 12 percent of the distance along the cube edge; energywise this was stable with respect to the lattice site position by about 0.05 eV. At present positions other than the ⟨100⟩ are being investigated for the Li^+; it would appear that the ⟨111⟩ direction [6] would be most favorable. In addition the situation with respect to Li^+ in other crystals such as KBr is being fol-

lowed up (where initial results show the lattice site as a stable location), and as well an investigation of the conditions necessary for additional ions to go into off-center positions and especially the relation of off-center ions to the interaction potentials.

The method used above makes considerable use of the interaction potential between ions at close distances. An improvement in the calculation of these energies is needed for better accuracy in our work. Our method has so far been applied to the case of neutral defects in the sense that there is no net change in the total charge in the neighborhood of the defect. The case of charged defects, as for example, a positive ion vacancy gives rise to long range polarization effects. A method has been devised to take care of these effects by splitting the electric field into two parts, that due to a neutral lattice with displaced ions and that of a single charge at the defect. This enables the polarization energy to be calculated without using the concept of a polarizable medium.

References

[1] J. Tessman, A. Kahn, and W. Shockley, Phys. Rev. **92**, 890 (1953).

[2] F. G. Fumi and M. P. Tosi, J. Phys. Chem. Solids **25**, 31 (1964); M. P. Tosi and F. G. Fumi, J. Phys. Chem. Solids **25**, 45 (1964).

[3] Private communication.

[4] H. S. Sack and M. C. Moriarty, Solid State Comm. **3**, 93 (1965); G. Lombardo and A. O. Pohl, Phys. Rev. Letters **15**, 291 (1965).

[5] R. D. Hatcher and G. J. Dienes, Phys. Rev. **134**, A214 (1964).

[6] N. E. Byer, F. S. Welsh, and H. S. Sack, Bull. Am. Phys. Soc. **11**, 229 (1966).

Energy of Formation of Vacancy Pairs in KCl

K. Tharmalingam

Westfield College, London

It is a common practice in the calculation of the energies of (complex) defect crystals to assume for simplicity a restricted type of relaxation; for example the ten nearest neighbor ions of a vacancy pair in alkali halides are given a single relaxation parameter in the ⟨100⟩ directions. Such an approximation may be partially justified if the long-range forces are negligible. However, the electrical forces which are long-range in character and the next-nearest-neighbor anion-anion repulsive forces contribute significantly to determine the minimum energy configuration and the corresponding energy. Thus a more general relaxation is expected to lower the energy of the defect crystal and we have in this report examined this particular aspect.

The ten nearest neighbor ions (to be referred to as region I, and the rest of the lattice as region II) are given six relaxation parameters ξ_1, ξ_2, ξ_3, η_1, η_2, η_3, as shown in figure 1. The energy of the KCl defect crystal (with region II held rigid—nonpolarized, nondisplaced) was minimized with respect to the above six variables and the results are given in table 1. Also in this table are given the corresponding results with the restricted type of relaxation. We note that the energy of the defect crystal, at this stage, included coulombic, repulsive, and monopole polarization energies; the first two arising from changes in self-energy of region I and interaction of I with II and the latter essentially an estimate of the self-energy term (since region II is rigid). The effect of dipole-dipole interaction and the contributions from region II are estimated in the Mott and Littleton approximation.

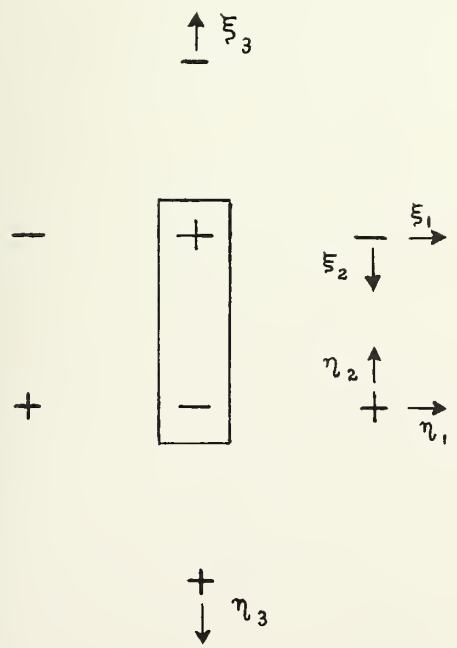

FIGURE 1

TABLE 1.

	B.M. potential		B.M.V. potential	
	Restricted relaxation	General relaxation	Restricted relaxation	General relaxation
ξ_1	0.065	0.034	0.045	0.026
ξ_2	.000	.055	.000	.038
ξ_3	.065	.031	.045	.027
η_1	.065	.072	.045	.052
η_2	.000	.053	.000	.029
η_3	.065	.061	.045	.048
ΔE	−1.23	−1.64	−1.11	−1.40
ΔE (Coul)	−1.80	−2.12	−1.28	−1.52
ΔE (Rep)	1.13	1.22	0.80	0.84
E (Pol-Mono)	−0.56	−0.74	−.63	−.72

We note from table 1 that:

(I) The energy of the defect crystal with general relaxation is, as expected, lower than that with restricted relaxation. The difference in the above energies is smaller for the B.M.V. potential than for the B.M. potential and is consistent with the fact that the B.M.V. potential is harder than the B.M. potential.

(II) The predominant contribution to the difference in energies of the restricted case and general case comes from the "electrical terms."

(III) The polarization energy combined with the next-nearest-neighbor repulsive forces ensure that the anions (in region I) are closer to the defects than the corresponding cations.

(IV) The fact that we have η_1, $\eta_3 > \eta_2$, for all cases, is consistent with the assumptions of restricted relaxation. This, however, is in contrast with the anions where $\xi_2 > \xi_1$, ξ_3.

Using the present results an estimate of the energy of formation of vacancy pairs in KCl can be obtained as follows, with the assumption that the B.M.V. potential is the better of the two.

(a) In the zeroth-order approximation (where both regions I and II are rigid, nonpolarized, and nondisplaced) the energy of formation in the rigid

lattice (for all four cases) is $E_f = 2.64$ eV.

(b) In the first order approximation where region II is rigid and region I is allowed to relax $E_f = 2.64 - 1.40 = 1.24$ eV.

(c) We note that so far the results are unambiguous with region II rigid. We must, however, include the electronic dipole-dipole interaction of region I before we can set a lowest value for the upper limit of E_f. Here again one can in principle evaluate this exactly but an estimate of this is ~ 0.1 eV. Hence the true $E_f < 1.3$ (4), since the effect of relaxing region II must be a negative contribution.

(d) An estimate of the contribution due to polarization (and coulombic relaxation) of region II may be obtained from the interaction of the Mott and Littleton dipoles of region II with the vacancy pair and is found to be -0.38 eV (for all four cases). Hence an estimate of E in third order approximation which does not include any dipole-dipole interaction is $1.24 - 0.38 = 0.86$ eV.

(e) In the next order approximation, since the dipoles are large close to the defects, an estimate of this (from the interaction of electronic dipoles of I amongst themselves and with those of II) is ~ 0.1 (5). Hence the E_f in the fourth order approximation becomes ~ 1 eV.

(f) We note that so far we have assumed that the region I "relaxation energy" is independent of the region II relaxation. An estimate of this may be obtained by minimizing the energy of region I (with Mott and Littleton displacement dipoles in II). We find the value -1.40 eV is now altered to -1.32 eV giving us an estimate of the energy of formation of vacancy pairs in KCl as ~ 1.1 eV.

In conclusion we remark that:

I. The effect of generalized relaxation in region I is not negligible compared with the less certain dipole-dipole terms in crystals containing neutral defects.

II. Due to the relatively large polarizability, and the next nearest neighbor repulsive interactions, care should be taken in treating the anion sublattice close to the defects on the same basis as for the cation sublattice.

Vacancies and Monovalent Cation Impurities in the Alkali Halides*

M. Doyama and M. P. Tosi

Argonne National Laboratory, Argonne, Ill. 60440

An accurate description of the short-range ionic interactions is generally important in lattice calculations of defect parameters in ionic crystals, and essential in the evaluation of the energies of motion of point defects. We have re-examined these calculations for several basic defect configurations in a few alkali halides, using the short-range potential recently proposed by Tosi and Fumi, and adopting consistently the Mott-Littleton scheme for the treatment of the lattice polarization.

The defect configurations that we have investigated are (a) an isolated vacancy at either lattice site, (b) a substitutional alkali impurity, (c) the saddle-point configuration for motion of both a (positive or negative) host ion and a substitutional alkali impurity into a vacancy. The energy of the latter configuration has been evaluated relative to the state in which the impurity and the vacancy are dissociated, so that the result is directly related to the activation energy for diffusion of the impurity. The calculations have been carried out for NaCl, KCl, and RbCl crystals, the impurities being Na^+, K^+, and Rb^+. The experimental information available for these systems is fairly extensive.

Although there is clearly room for further improvements in the model, particularly in the treatment of the lattice polarization, the agreement of the theory with experiment is generally semiquantitative. The main shortcoming of the model is the inability to yield a difference in the energies of motion of a positive and a negative host ion.

*Based on work performed under the auspices of the U.S. Atomic Energy Commission.

Born-Model Defect Energies for CaF_2

A. D. Franklin

Institute for Materials Research, National Bureau of Standards, Washington, D.C. 20234

The Born Model of an ionic solid is being applied to the calculation of the energies of formation of interstitial ions and vacancies of both kinds in the fluorite-structure alkaline earth fluorides, and to obtain estimates of the energy of replacement of Ca^{2+} in CaF_2 by Na^+ and Y^{3+}. Two-body interionic forces are assumed, including monopole-monopole, monopole-dipole, dipole-dipole, and Born-Mayer overlap repulsive forces. Arbitrary radial displacements and dipole moments are assigned the ions nearest and next-nearest each defect (region I), and their interactions with each other and with the defect are treated explicitly. The crystal beyond (region II) is considered to be a dielectric and elastic continuum, and its relaxation energy is calculated with the approximate methods of Mott-Littleton [1][1] and Brauer [2], suitably modified to take into account the effect of the region I ions. The energy as a function of the displacements and moments of the region I ions is calculated and minimized by computer to determine the equilibrium energy and configuration.

A major uncertainty arises from the parameters used to describe the repulsive forces. The Born-Mayer form for the repulsive energy between two ions, $U_{ij}=A_{ij}\exp(-r_{ij}/\rho)$, was used with a single value for ρ. Interactions were included for all ions separated by $\sqrt{2}a$ or less, where a is the fluorine-fluorine distance, thus involving anion-anion, anion-cation, and cation-cation interactions and requiring four parameters, A_{+-}, A_{--}, A_{++}, and ρ. These were obtained by fitting the model to two elastic constants ($(C_{11}-C_{12})$ and the mean of C_{12} and C_{44} to simulate the Cauchy relation were used in the manner of Reitz, Seitz, and Genberg [3]), to the equilibrium relation, and to the dielectric constants using the equation of Szigeti [4] modified for the CaF_2 lattice. Other sets of parameters have been calculated recently by Reitz, Seitz, and Genberg; Benson and Dempsey [5]; and Axe [6]. Comparison among the results suggests that reasonable values for A_{+-} and A_{--} can be found, but for A_{++} the uncertainty is large. The influence of A_{++} on the calculated defect energies in CaF_2 is illustrated in the following table:

Defect	A_{++}, eV	Formation energy, eV	Displacement, fraction of distance to origin	
			δ_1	δ_2
Anion vacancy	0	4.38	0.034	−0.107
	10^4	4.39	.030	−.110
Anion interstitial	0	−1.81	.057	−.046
	10^4	−1.77	.059	−.039
Cation vacancy	0	22.54	.152	.003
	10^4	22.36	.152	.003
Cation interstitial	0	−17.10	−.081	.075
	2.5×10^3	−16.55	−.078	.084
	10^4	−14.70	−.072	.104

in which the last two columns show the displacements of the nearest neighbor (δ_1) and next-nearest neighbor (δ_2) ions to the defect as fractions of their distances from it. Only for the cation interstitial is there a cation-cation distance sufficiently small to make A_{++} important.

A second major source of uncertainty is the relaxation of region II. Sufficiently far from the defect, it seems reasonable to assume a combination of a polarization and an elastic displacement (defined as a fraction of the distance r to the origin) both decreasing as r^{-3}. The problem is to evaluate the intensities of these responses in terms of the variational parameters of displacement and dipole moment assigned to region I ions. In the present calculations, the polarization part of the displacement of the lth region II ion at r_l was obtained from the Mott-Littleton approximation, $\delta_l^P=(Z_0/Z_l)(b/r_l)^3M_l'$, where Z_0 and Z_l are the effective valence of the defect and the valence of the lth ion, respectively, b^3 is the volume containing one CaF_2 molecular unit, and M_l' a constant containing the ionic total polarizabilities and the dielectric constant. The elastic part was written simply $\delta_l^E=\lambda/r_l^3$. The parameter λ was evaluated by setting the sum $\delta_l^P+\delta_l^E$ equal to the total displacement of either of the two kinds of ions in region I. The table below illustrates the effect of this choice.

The choice appears to be rather unimportant for all three defects tested. In general, propagation of δ_2 has been chosen, but as examination of the structure shows, a considerably larger region I would

[1] Figures in brackets indicate the literature references at the end of this paper.

Defect	Displacement propagated	Formation energy, eV	δ_1	δ_2
Anion vacancy....	None	4.41	0.048	−0.100
	δ_1	4.41	.049	−.101
	δ_2	4.38	.034	−.107
Anion interstitial..	None	−1.87	.058	−.048
	δ_1	−1.92	.061	−.047
	δ_2	−1.81	.057	−.046
Cation vacancy..	None	23.24	.150	.001
	δ_1	22.34	.190	.001
	δ_2	22.54	.152	.003

have to be taken before one could à priori have confidence that the approximations used for region II could have any real validity for even the outermost region I ions.

The energy of formation of a given defect can be subdivided in a number of ways. These calculations corresponded to the following conceptual steps: (1) creation of the defect in an otherwise undeformable, unpolarizable crystal, (2) displacement of region I ions into relaxed positions, (3) polarization of relaxed region I ions, (4) relaxation and polarization of region II. The division of the defect formation energies according to this scheme is set forth in the following table, in which the elastic term in region II was derived from δ_2 and A_{++} was set equal to zero:

Energy term	Anion vacancy	Anion interstitial	Cation interstitial
Rigid lattice, Madelung energy..	10.79	1.53 eV	−3.05 eV
Do....., repulsion.....	−1.81	1.54	5.77
Region I displacements, monopoles.	−3.85	−3.75	−13.60
Region I displacements, repulsion.	1.11	.42	2.87
Region I polarization.....	−.22	−.14	−1.98
Region II relaxation, polarization.	−1.51	−1.56	−6.16
Region II relaxation, repulsion.	−.04	.15	.25

The "best" values for the formation energies of defects in CaF_2 from these calculations are listed in the table below:

Defect	Formation energy, eV	δ_1	δ_2
Anion vacancy.....	4.5 ±0.2	0.034	−0.106
Cation vacancy.....	23.5 ±0.3	.149	.003
Anion interstitial.....	−1.8 ±0.2	.057	−.045
Cation interstitial.....	−15.9 ±0.5	−.080	.080

where the uncertainties shown reflect the uncertainty in A_{++} and in the elastic part of the region II relaxation. From these and the lattice energy the formation energies of anion and cation Frenkel pairs and of Schottky trios can be calculated. These are

Defect pair	Formation energy
Anion Frenkel.....	2.7 ±0.4 eV/pair
Cation Frenkel	7.5 ±0.6 eV/pair
Schottky.....	5.1 ±0.9 eV/trio

These energies are estimates of the enthalpies of formation of the various possible intrinsic defect sets. On the basis of these enthalpies alone, it would be expected that anion Frenkel pairs would be the dominant intrinsic defects, although the rather large uncertainties do not allow this conclusion to be definite. Generally speaking, entropies of formation of interstitials are found to be larger than those of vacancies, a fact tending still further to favor the anion Frenkel pair. The formation energy for the anion Frenkel pair calculated here agrees well with Ure's [7] experimental value of 2.8 eV. This agreement lends further support to the use of the Born model for defect calculations in CaF_2.

References

[1] N. F. Mott and M. J. Littleton, Trans. Faraday Soc. **34**, 485 (1938).
[2] P. Brauer, Z. Naturforsch. **6A**, 255 (1951).
[3] J. R. Reitz, R. N. Seitz, and R. W. Genberg, J. Phys. Chem. Solids **19**, 73 (1961).
[4] B. Szigeti, Proc. Roy. Soc. **A204**, 52 (1950).
[5] G. B. Benson, E. Dempsey, Proc. Roy. Soc. **266A**, 344 (1962).
[6] J. D. Axe, Phys. Rev. **139**, A1215 (1965).
[7] R. Ure, J. Chem. Phys. **26**, 1363 (1957).

Lattice Distortion Around Defects

Tatumi Kurosawa

Chuo University, Tokyo, Japan

A general procedure of determining the lattice distortion (or the electronic polarization) around a defect is presented.

The lattice distortion may be calculated by solving the equation of equilibrium of elasticity theory (or of electrostatic theory) in the corresponding continuous medium [1],[1] beyond the vicinity of the defect. There are many solutions of the equilibrium equation which tend to zero at infinity, and the lattice distortion should be represented by a linear combination of them, in general. In the case of a point defect, the displacement $\mathbf{u}(\mathbf{r})$ is given by

$$\mathbf{u}(\mathbf{r})=\sum_{n=2}^{\infty}\mathbf{u}_n(\mathbf{r}), \tag{1}$$

where

$$\mathbf{u}_n(\mathbf{r})=r^{-n}\sum_m a_{nm}\,\mathbf{f}_{nm}(\theta,\phi), \tag{2}$$

in which the $\mathbf{f}_{nm}(\theta,\phi)$ are analogous to the spherical harmonics in the case of the electrostatic field, and some of them can be omitted by the symmetry. In the case of a dislocation, the displacement is given by

$$\mathbf{u}(\mathbf{r})=\sum_{n=0}^{\infty}\mathbf{u}_n(\mathbf{r}), \tag{3}$$

where

$$\mathbf{u}_n(\mathbf{r})=r^{-n}\sum_{m=1}^{4}a_{nm}\,\mathbf{f}_{nm}(\theta), \tag{4}$$

in which the factor r^{-n} becomes a constant or $\log r$ if $n=0$. In either case, we can write $\mathbf{u}(\mathbf{r})$ as

$$\mathbf{u}(\mathbf{r})=\sum_{\mu}A_\mu\mathbf{u}_\mu(\mathbf{r}). \tag{5}$$

The coefficients A_μ are determined through a microscopic calculation of the defect structure. However, there has been no systematic method to do this. The procedure described below may be a reasonable way for this purpose.

We divide the whole crystal into two regions: the region C which is the immediate vicinity of the defect and the region D which is distant from it. First, we calculate the position of atoms in the region D using eq (5) with a tentatively given set of the coefficients. Namely, the position $\mathbf{r}_i$ of the ith atom is given by

$$\mathbf{r}_i=\mathbf{r}_{i0}+\mathbf{u}(\mathbf{r}_{i0}), \tag{6}$$

in which $\mathbf{r}_{i0}$ is the position before the formation of the defect. Next, we calculate the equilibrium position of atoms in the region C under the given position of the atoms in D. If the values of the coefficients are correctly given, all atoms in D as well as those in C are in equilibrium, at least approximately. If not, however, the atoms in D, particularly those bordering the region C, are not in equilibrium and suffer forces. In this case, it is convenient to the calculation to consider the following quantities:

$$F_\mu=\sum_{i\in D}\mathbf{F}_i\cdot\mathbf{u}_\mu(\mathbf{r}_i), \tag{7}$$

where $\mathbf{F}_i$ is the force on the ith atom and the sum is taken over the region D. Generally speaking, the sum converges quite rapidly for large r_i and is easily evaluated. If F_μ is positive, the force on the region D works to increase the coefficient A_μ, and vice versa. Therefore, F_μ may be regarded as a generalized force on the μth distortion mode $\mathbf{u}_\mu$. We should choose the coefficients so as to remove these forces F_μ's.

In practice, we retain a finite number of terms of (5), calculate the following symmetric matrix:

$$\begin{bmatrix} \partial F_1/\partial A_1 \ldots\ \partial F_1/\partial A_\mu \ldots, \\ \vdots\qquad\qquad \vdots \\ \partial F_\mu/\partial A_1 \ldots\ \partial F_\mu/\partial A_\mu \ldots, \\ \vdots\qquad\qquad \vdots \end{bmatrix}, \tag{8}$$

and evaluate the coefficients in the linear approximation.

The present method is useful for many problems concerning defects. For instance:

(1) A substitutional impurity atom or interstitial atom produces a strain field around it. However, the strength of the strain field cannot be determined by a simple application of the Mott-Littleton method [2]. The strain field of the distant region

[1] Figures in brackets indicate the literature references at the end of this paper.

should be known when we calculate the displacement of neighboring atoms to the defect, whereas the former depends on the latter. A similar situation is found in the case of vacancy pair in ionic crystals, the dipole moment of which is not unambiguously determined by the usual method. The present method is applicable to such cases.

(2) The first term is dominant in the expression (1) or (3) when r is large. However, the effect of higher order terms is not small unless the size of the region C is very large. Generally, the error produced by the neglect of the higher order terms is much larger than that by the use of the approximate expression (6), which replaces the distortion of a discrete lattice by that of a continuum, for the position of the atoms in D. The addition of the higher order terms to the distortion in D improves considerably the approximation. An example is illustrated in figure 1, which shows the sum[2] $\sum_{i \in D} |F_i|^2$ in the case of an edge dislocation. This demonstrates how the force on the atoms in D is relaxed by the addition of the higher order distortion modes; the abscissa means that the sum in (3) is taken from zero to $n_{\max}$.

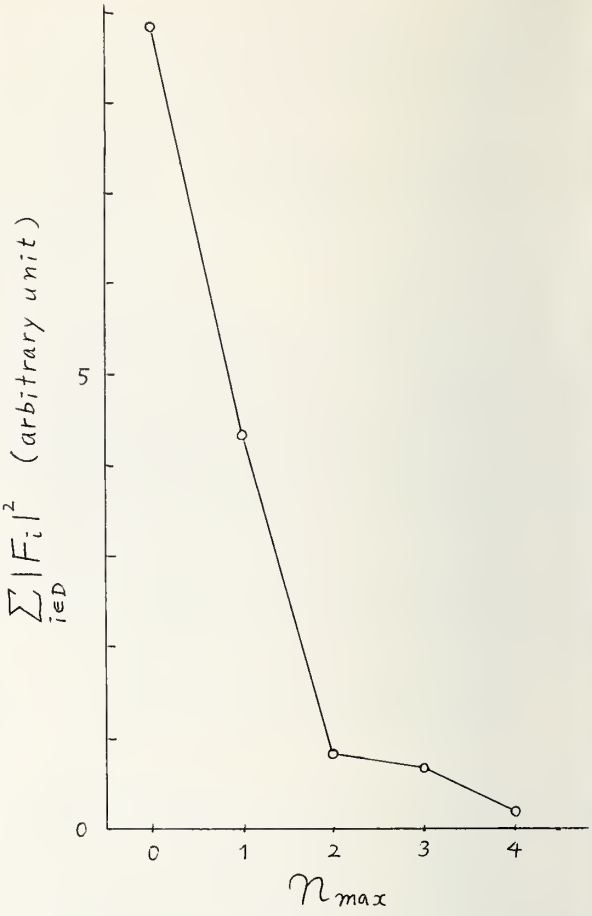

FIGURE 1

References

[1] J. D. Eshelby, Solid State Physics, Vol. **3** (Academic Press Inc., New York, 1957).

[2] Y. Fukai, J. Phys. Soc. Japan **18**, 1413 (1963).

[2] The sum $\sum_{i \in C} |F_i|^2$ is always zero except for calculational error.

Calculation of Lattice Distortion Around Point Defects By Lattice Statics

Hiroshi Kanzaki

Institute for Solid State Physics, University of Tokyo, Tokyo, Japan

In the ordinary procedure for calculating lattice distortions around point defects, the crystal containing the defect is divided into two regions: the region in the immediate vicinity of the defect will be called "region I"; "region II" is the region outside the region I. It is usually further assumed, at least in the case of a simple defect such as a vacancy, that displacements of atoms in the region II can be obtained by applying isotropic elasticity theory. Final expressions for lattice distortion in this procedure are obtained by "joining" the distortion in region II thus obtained to the distortion in region I where existence of the defect is taken into account in the discrete crystal lattice.

In the calculation of distortion around defects by lattice statics, discreteness of the crystal lattice is considered throughout the crystal. The method was first developed by Professor Pryce at Bristol, applied to vacancy in solid argon by the present writer [1],[1] and later very extensively applied to the K^+ impurity in NaCl by Hardy [2]. The procedure for obtaining displacements around defects is essentially to solve the problem of obtaining displacements of lattice points in the perfect lattice under a given external force representing the atomic nature of the defect. We start by expanding the displacements $\xi(\mathbf{r}^l)$ in a series of plane waves assuming the following expression in the harmonic approximation;

$$\xi(\mathbf{r}^l)=\sum_{\mathbf{q}} \mathbf{Q}(\mathbf{q})\cdot e^{i\mathbf{q}\cdot\mathbf{r}^l}, \qquad (1)$$

where $\mathbf{q}$ is the wave vector and the expansion coefficients $\mathbf{Q}(\mathbf{q})$ are the normal coordinates as in the theory of lattice dynamics. After having solved the equilibrium equations for $\mathbf{Q}(\mathbf{q})$ under the existence of generalized forces $\mathbf{G}(\mathbf{q})$ representing the defect, we can calculate the displacements $\xi(\mathbf{r}^l)$ at any lattice points $\mathbf{r}^l$ by using the eq (1).

Several features of the lattice statics method can be summarized as follows. (a) The whole crystal containing the defect is allowed to relax at the same time. It is not necessary to use the procedure of "dividing and joining" as in the ordinary method described above. The results thus obtained will be more reliable compared with these previous calculations not only for the distortion in the neighborhood of defects but for the distortion on the macroscopic scale. (b) Consideration of image forces due to the existence of the free surface can be introduced easily by relaxing the rigid cyclic lattice boundary and making the free surface the boundary. (c) It is generally possible without too much difficulty to take account of nonharmonic interactions in the immediate vicinity of the defect.

The lattice statics method can be applied to such types of crystals that can be represented by two-body interatomic potential functions. Ionic, van der Waals, and valency crystals are in this category [3]. Possible extension of the method to metals will be one of the future problems and will not be discussed at the present stage.

The following discussion based on the lattice statics method is concerned only with long-range distortion far from the point defects. The problem is essentially that of macroscopic distortion in the anisotropic elastic continuum as was already clarified by Hardy [2]. It will be shown that patterns of distortion are quite different from those expected from isotropic elasticity theory not only around noncubic axial defects but also around simple cubic defects in the case of the face-centered-cubic lattice.

1. The Model and Its Elastic Coefficients

In the following, we use the same model as in the calculation for solid argon [1]; each site in a face-centered-cubic lattice is connected by purely central interactions of Hookeian force Constant A with its twelve nearest neighbors.

Elastic coefficients of the crystal thus assumed are expressed as follows;

$$C_{11}=2A/a, \qquad C_{44}=C_{12}=A/a,$$

where $a/\sqrt{2}$ is the distance between nearest neighbor atoms (see figs. 1 and 2).

The elastic anisotropy factor in a cubic crystal is defined as the square of the ratio of velocities of shear waves propagating in the $\langle 100\rangle$ and $\langle 110\rangle$ directions, and in the case of our model, the anisotropy factor $=2C_{44}/(C_{11}-C_{12})=2$. The experimental value of anisotropy factor is not available for solid argon. The value is 0.76 for NaCl and 3.3 for Cu.

[1] Figures in brackets indicate the literature references at the end of this paper.

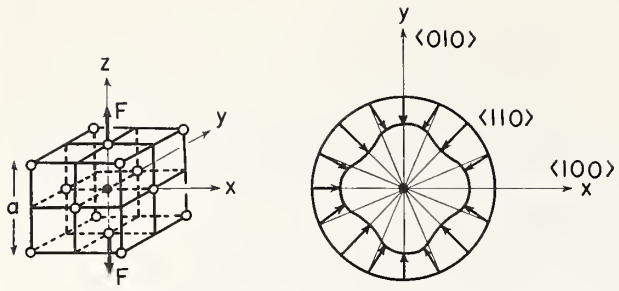

FIGURE 1. *Double forces along the* ⟨001⟩ *axis and anisotropic pattern of displacements in the* (001) *plane through the center.*

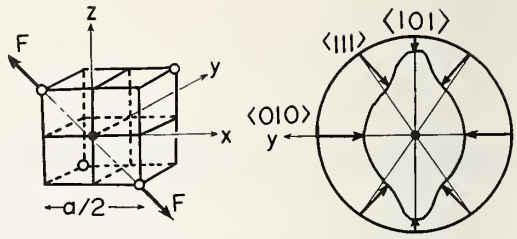

FIGURE 2. *Double forces along the* ⟨$\bar{1}$01⟩ *axis and anisotropic pattern of displacements in the* (101) *plane through the center.*

2. Anisotropic Long-Range Distortion in a Cubic Crystal Due to Defects of "Cubic" Character

The expression for this case has been already given [1]. Displacements at distance $r=\left(\frac{a}{2}\right)N$ from the defect are shown in table 1. In table 1, F is the magnitude of force acting radially (along ⟨110⟩) on each of the twelve first nearest neighbors of the substitutional defect. The results are exactly the same for applying force $\sqrt{2}F$ radially (along ⟨100⟩) on each of the six second nearest neighbors of the defect or applying $2\sqrt{2}F$ on each of the six nearest neighbors of interstitial atom in a body-centered-cubic position.

TABLE 1. *Displacements at distance* $\left(\frac{a}{2}\right)$N *around the "cubic" defect (a numerical error in ref. (1) has been corrected).*

Direction	Displacement in units of $\left(\frac{F}{A}\cdot\frac{1}{N^2}\right)$
⟨100⟩	0.079
⟨110⟩	.498
⟨111⟩	.670

In the case of K^+ in NaCl, Hardy evaluated long-range distortions in terms of the force F_R originating from repulsive interactions between ions. His results [2] are duplicated in table 2.

TABLE 2. *Displacements at distance* Xr_0 *around* K^+ *in* NaCl *(after Hardy)*

Direction	Displacement in units of $(F_R\cdot X^{-2})$
	cm dyne^{-1}
⟨100⟩	1.78×10^{-5}
⟨110⟩	1.24×10^{-5}
⟨111⟩	0.747×10^{-5}

The difference between the anisotropies of distortion shown in table 1 and table 2 can be understood in terms of the difference of elastic anisotropy factor between the two cases.

3. Long-Range Distortion in Cubic Crystal Due to "Noncubic" Axial Defects

There are several circumstances in which the treatment of distortion of this nature becomes necessary. (1) Substitutional impurity ions subjected to a Jahn-Teller distortion in a cubic lattice, such as Cu^{2+} or Ag^{2+} ions in alkali halides. Self-trapped holes in alkali halides are in a similar category. (2) Interstitial atoms in a cubic lattice, such as crowdions, split interstitials, pairs of vacancies, and saddle-point configurations of these and other "cubic" defects.

It can be understood that many defects of physically interesting nature are included in this group of defects. In the following, results of numerical calculations are presented for two kinds of lattice distortion in our model crystal. One is that due to two equal and opposite forces along the ⟨100⟩ axis and the other is due to those acting along the ⟨110⟩ axis.

3.1. Double Forces Along ⟨001⟩ Acting at Points Distance *h* Apart Along the Axis

Using the coordinate system shown in figure 1, displacements at distance r are evaluated for various directions as shown in table 3. It is interesting to notice that the value for ⟨001⟩ is comparable with that obtained from isotropic elastic theory, $\left(\frac{Fh}{4\pi G}\cdot\frac{1}{r^2}\right)$.

Also shown in figure 1 is the anisotropic pattern of displacements in the (001) plane through the

center. The pattern is always circular in an isotropic elastic body.

3.2. Double Forces Along $\langle \bar{1}01 \rangle$ Acting at the Points Distance h Apart Along the Axis

Figure 2 shows the coordinate system used and the anisotropic pattern in the (101) plane through the center. Displacements at distance r are shown in table 4. It is again interesting to notice that the axial displacement is $\sqrt{2}$ times that of the $\langle 001 \rangle$ double forces given in table 3.

3.3. Interaction Energy Between Two Anisotropic Defects

Especially interesting is the interaction energy between two defects as a function of relative orientations. Such evaluation has been made for K^+ in NaCl by Hardy [2]. In such anisotropic defects as discussed here, we can expect large attraction between two defects in perpendicular relative orientations and, furthermore, strong angular dependence in the perpendicular plane as seen in figures 1 and 2. This type of calculation of energy requires a knowledge of the distortion in the neighborhood of the defects where nonquadratic terms always become important, as shown already for the vacancy [1]. Here, we shall not enter into further details of this discussion, where the choice of interatomic potential becomes more critical, especially for the case of interstitial defects, such as the crowdion, as compared with vacancies.

TABLE 3. *Displacements at distance* r *due to double forces* F *along* $\langle 001 \rangle$ *acting at the points distance* h *apart*
Displacements expressed in unit of

$$\left(\frac{Fh}{4\pi C_{44}} \cdot \frac{1}{r^2}\right).$$

Direction	$\langle 001 \rangle$	$\langle 100 \rangle$	$\langle 110 \rangle$	$\langle 1, 0.414, 0 \rangle$ $\left(\langle \cos \frac{\pi}{8}, \sin \frac{\pi}{8}, 0 \rangle\right)$
ξ_x	0	−0.460	−0.527	−0.501
ξ_y	0	0	−0.527	−0.323
ξ_z	1.000	0	0	0
$\lvert\xi\rvert$	1.000	0.460	0.747	0.596

TABLE 4. *Displacements at distance* r *due to double forces* F *along* $\langle \bar{1}01 \rangle$ *acting at the points* h *apart*
Displacements in unit of

$$\left(\frac{Fh}{4\pi C_{44}} \cdot \frac{1}{r^2}\right).$$

Direction	$\langle \bar{1}01 \rangle$	$\langle 101 \rangle$	$\langle 010 \rangle$	$\langle 111 \rangle$
ξ_x	−1.000	−0.080	0	−0.204
ξ_y	0	0	−0.456	−0.303
ξ_z	1.000	−0.080	0	−0.204
$\lvert\xi\rvert$	1.413	0.113	0.456	0.418

The writer thanks Miss S. Ozawa for numerical calculations.

References

[1] H. Kanzaki, J. Phys. Chem. Solids **2**, 24 (1957).
[2] J. R. Hardy, J. Phys. Chem. Solids **15**, 39 (1960); **23**, 113 (1962).
[3] M. Born and K. Huang, Dynamical Theory of Crystal Lattices (Oxford University Press) 1964.

256-724 O-67—3

Calculation of Migration Energies of an Interstitial in Germanium and Silicon*

Ryukiti R. Hasiguti

Department of Metallurgy, University of Tokyo, Bunkyo-ku, Tokyo, Japan

1. Introduction

The formation and migration energies of an atomic vacancy and an interstitial atom of germanium and silicon have been offering many difficult and interesting problems to be solved. One of the important problems, which may be called the "triangular paradox," is as follows. Let us take as an example the migration energy of a vacancy. (1) The experimental results on germanium, (2) the experimental results on silicon, and (3) the theories of germanium and silicon, which give nearly the same but a little different calculated values for germanium and silicon, form the triangle of paradox. The migration energy, E_m, experimentally obtained for a vacancy in germanium is about 1 eV (refs. [1, 2, and 3],[1] and references therein). This value agrees well with theoretical estimations, which give the values of 0.95 eV [4] and 0.98 eV [5]. On the other hand, the experimental value of E_m for silicon, 0.33 eV [6], is considerably different from the theoretically estimated values, 1.06 eV [4] and 1.09 eV [5]. This situation may be taken as an indication that any one of the three components of the paradox triangle must equally be doubted and reinvestigated at this stage, and if any one of the components is found to be appropriately modifiable, then there would be a possibility of dissolution of the triangular paradox. Recently evidence was found that a vacancy of germanium may migrate at very low temperatures (at ~60 °K) [7]. This seems to make the paradox begin to dissolve.

The situation for the migration energies of an interstitial in germanium and silicon seems to be exactly the same as that of the above mentioned vacancy, although the situation for the interstitial is much less clear than that of the vacancy, because the experimental results for the interstitial are yet very insufficient [1], and only one theoretical result is available at this moment, worked out by Bennemann [5].

The objective of the present paper is to make a contribution to the theoretical evaluation of migration energies of an interstitial in germanium and silicon in the hope of diminishing the difficulties in the paradox. The method used here is an extension of Weiser's theory [8] which was successfully used in treating the migration energies of interstitial impurity atoms in germanium and silicon.

2. Theory and Results

We shall consider only a positive singly charged interstitial atom which is believed to exist in germanium [1, 2] and silicon [6]. Then the migration behavior of an interstitial can be treated as was that of a monovalent interstitial impurity atom such as lithium, copper and silver in germanium and silicon, although there may exist some differences between the above two cases as will be discussed later. The proposal of considering a positive singly charged interstitial is one of the unique features of the present theory.

The migration of a monovalent impurity atom in germanium and silicon was successfully treated by Weiser [8] considering an attractive potential due to the polarization of the host atoms and an exponential repulsive potential due to the overlapping of nonbonding electrons. This method will be, in the present paper, extended to the case of the interstitial migration.

As the two interstitial sites, the so-called [5, 8] tetrahedral sites (T site) and hexagonal site (H site) will be considered, of which one will be the stable site and the other the saddle point.

The attractive polarization energy, U_{pol}, due to the interaction of the positive singly charged interstitial ion with the dipoles it has induced in the host atoms was calculated by Weiser using the Mott-Littleton method [9] for the T and H interstitial sites. The details will be omitted here, because we use Weiser's result without any modification as far as U_{pol} is concerned. The result which we use is

$$\Delta U_{\text{pol}} = U^H_{\text{pol}} - U^T_{\text{pol}} = 0.75 \text{ eV}, \qquad (1)$$

*This research was partly performed at the Institute of Physical and Chemical Research, Bunkyo-ku, Tokyo.

[1] Figures in brackets indicate the literature references at the end of this paper.

where U_{pol}^{H} and U_{pol}^{T} are the polarization energies at H and T sites, respectively. The same result is applicable for both germanium and silicon.

2.1. Repulsive Energy

In order to obtain the repulsive energy, U_{rep}, we shall use the repulsive interaction of Born-Mayer type, as was done by Weiser in the case of impurity atoms. As this is a phenomenological method, the most important point is in the choice of Born-Mayer constants.

Now we shall express the Born-Mayer potential in the following form:

$$U_{rep} = A \exp[(r_0 - r)/\rho], \quad (2)$$

where A and ρ are the Born-Mayer constants, r_0 is the equilibrium distance between the nearest neighbor atoms, and r is the distance between respective pairs of atoms.

While Weiser uses the Born-Mayer constants which are appropriate for sodium chloride-type ionic crystals, the present author uses the Born-Mayer constants derived from the compressibilities of germanium and silicon using the method described by Leibfried [10] (potential 1 in table 1 and figs. 1 and 2).

In the derivation of the constants, the Madelung constant of 1.638 for zinc blend type crystals rather than that of 1.747 for sodium chloride type crystals was used.

Table 1 shows the Born-Mayer constants used in the present paper. Figures 1 and 2 shows the

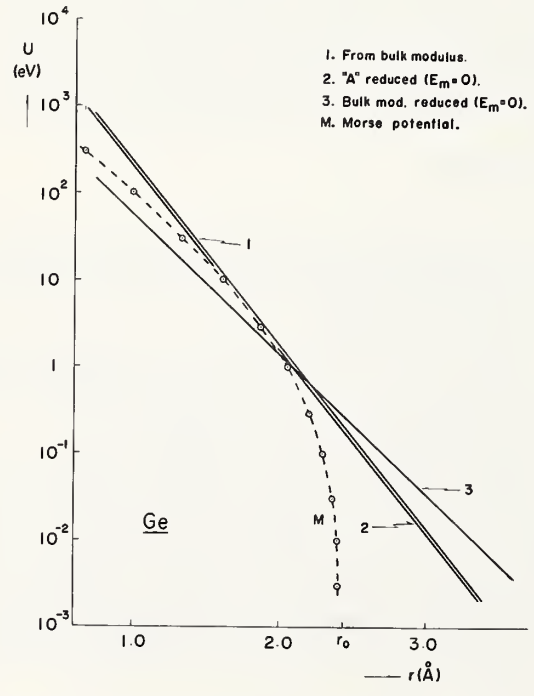

FIGURE 1. *Plots of Born-Mayer potential in germanium.*

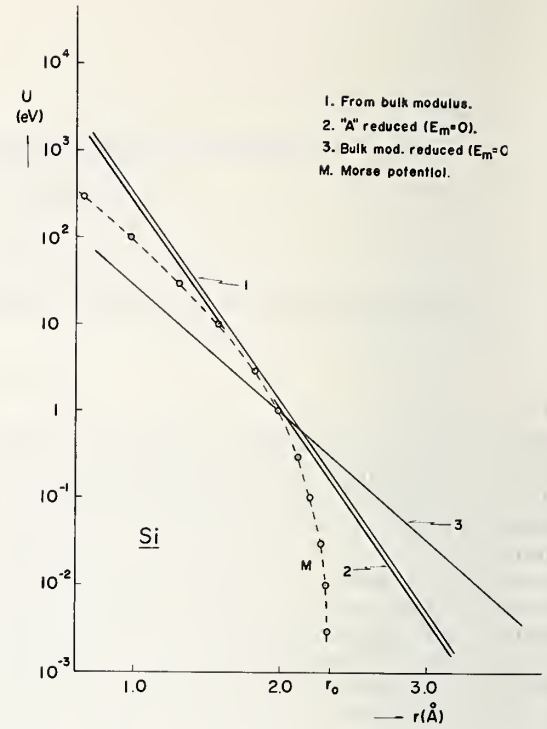

FIGURE 2. *Plots of Born-Mayer potential in silicon.*

TABLE 1. *Born-Mayer constants used in the present paper*

1	A(Ge) = 0.202 eV; A(Si) = 0.195 eV ρ(Ge) = 0.206 Å; ρ(Si) = 0.182 Å	From bulk modulus
2	A(Ge) = 0.177 eV; A(Si) = 0.150 eV ρ(Ge) = 0.206 Å; ρ(Si) = 0.182 Å	"A" reduced
3	A(Ge) = 0.267 eV; A(Si) = 0.305 eV ρ(Ge) = 0.272 Å; ρ(Si) = 0.296 Å	Bulk modulus reduced

plots of the Born-Mayer potentials for germanium and silicon.

The repulsive interaction energies are calculated for both H and T interstitial sites of germanium and silicon. The pair-wise interactions of an interstitial with the nearest and the next-nearest neighbors are included in the calculation for H and T sites, respectively, as follows:

$$U_{rep}^{H} = 6A \exp[(r_0 - r_H)/\rho] + 8A \exp[(r_0 - 1.56 r_H)/\rho], \quad (3)$$

$$U_{rep}^{T} = 4A \exp[(r_0 - r_T)/\rho] + 6A \exp[(r_0 - 1.15 r_T)/\rho], \quad (4)$$

where r_H is the distance between the H site and its nearest neighbor, and r_T is the distance between T site and its nearest neighbor, the latter being the same as r_0. Interactions with further neighbors

are negligible. Thus the difference between H and T sites are

$$\Delta U_{\text{rep}} = U^{H}_{\text{rep}} - U^{T}_{\text{rep}}. \tag{5}$$

Then the migration energy of an interstitial, E_{Im}, is obtained
to be

$$\begin{aligned} E_{Im} &= \Delta U_{\text{pol}} - \Delta U_{\text{rep}} \\ &= 0.75 \text{ eV} - \Delta U_{\text{rep}} \end{aligned} \tag{6}$$

for both germanium and silicon.

2.2. Results

The results obtained using the Born-Mayer potentials given in table 1 and figures 1 and 2 are shown in table 2.

3. Discussions

Now we shall make some discussion as to the choice of Born-Mayer constants. Before doing so, however, questions must be raised as to the applicability of Born-Mayer type repulsive potential in the case of germanium and silicon.

Objections against the use of Born-Mayer potential may arise concerning the following points: firstly, in the diamond lattice, the covalent bonding is important, so that the potential may be rather expressed by the Morse function [4], which is also an empirical form of expression in the case of diamond lattice. However, as the Morse potential consists of attractive and repulsive parts, it is possible to express the repulsive part of Morse potential by the Born-Mayer potential.

TABLE 2. *Migration energies of an interstitial* $E_m = U^{(H)} - U^{(T)}$ *in eV*

Born-Mayer potential	1	2	3
Ge	−0.25	0	0
Si	−0.22	0	0

Now the second objection may be expressed as follows. In such an open lattice as that of diamond structure, the overlapping of the wave function of closed-shell core-electrons may not be appreciable. If the Born-Mayer type potential is to express only the closed-shell repulsion, it may not be appropriate to use it in germanium and silicon. However, if all kinds of repulsive interactions including the one due to valence electrons are included in our expression of the Born-Mayer potential, this can be conveniently used as an empirical expression of the repulsive part of the potentials of germanium and silicon [11].

Thus if the Born-Mayer constants are determined from the elastic constants or the bulk modulus of the bulk crystal, then the above two objections are simultaneously solved.

The potentials 1 for germanium and silicon shown in table 1 and figures 1 and 2 are obtained from the bulk moduli of germanium and silicon, respectively. These potentials result in migration energies of 0.25 eV and 0.22 eV for germanium and silicon, respectively.

It is quite possible that the repulsive force exerted by a singly positively charged interstitial atom is rather smaller than that exerted by an atom at a regular site with covalent bonds, because three valence electrons of an interstitial atom do not make regular covalent bonds. The reduced repulsive force results in a reduced migration energy.

The extent of reduction of the repulsive force of an interstitial atom compared with that of a regular atom is not known at this moment. Therefore, the following approach was made; i.e., Born-Mayer potentials which give the zero migration energy were calculated, and were compared with the potentials 1.

Now in the potentials 2 shown in table 1 and figures 1 and 2 the constants A were reduced so that the migration energies for germanium and silicon will be zero.

In the potentials 3 the bulk moduli, from which Born-Mayer constants are obtained, were reduced so that the zero migration energy for both germanium and silicon was obtained. Thus-obtained Born-Mayer potentials 3 are shown in table 1 and figures 1 and 2. These potentials correspond to the bulk moduli reduced 29 percent and 45 percent for germanium and silicon, respectively.

Now the Born-Mayer potentials used here will be compared with the Morse potentials used by Swalin [4] when he calculated the energies of vacancies in germanium and silicon. In figures 1 and 2 the broken lines represent the Morse potentials. At larger distances the Morse potentials deviate from the Born-Mayer potentials because of the increase of attractive component. Actually the curves go to minus infinity at $r = r_0$. At smaller distances, neither Born-Mayer potentials nor Morse potentials are reliable, because they are determined at or near equilibrium separations. It is significant, therefore, that the potentials 1 and 2 agree fairly well with the Morse potentials at intermediate distances. Moreover, the potentials 2 agree the best with the Morse potentials.

Now if the above discussions are accepted, the migration energies obtained from the potentials 1 are rather the upper limits of migration energies. Although we do not know the extent of reduction of the repulsive force of a singly positively charged interstitial atom compared with that of a regular

atom in a regular site, it was shown above that a slight change of Born-Mayer potentials reduces the migration energy easily to zero. This is especially the case for the potentials 2. This suggests that the actual migration energies are somewhere between 0 and the above-shown upper limit values.

As shown in table 2, the migration energies have the minus sign, which means that the *T*-site is the saddle point and the *H*-site is the stable site. This is contrary to Bennemann's results.

Finally all the available theoretical results of formation and migration energies are collected in table 3.

TABLE 3. *Formation and migration energies of a vacancy and an interstitial in eV*

	E_{Vf}	E_{Vm}	E_{If}	E_{Im}	Authors
Ge	2.07	0.95			Swalin [4]
	1.62 ~ 2.54				Scholtz-Seeger [12, 13]
	1.91	0.98	0.93	0.44	Bennemann [5]
				0.25	Hasiguti (present result)
				0 ~ 0.25	
Si	2.32	1.06			Swalin [4]
	2.13	1.09	1.09	0.51	Bennemann [5]
				0.22	Hasiguti (present result)
				0 ~ 0.22	
Diamond	4.16	2.02			Swalin [4]
	3.68	1.85	1.76	0.85	Bennemann [5]

In conclusion the author thanks Miss S. Motomiya for her assistance in making calculations.

4. References

[1] R. R. Hasiguti and S. Ishino, Proc. Symp. on Radiation Damage in Semiconductors (7th Int. Conf. Phys. Semiconductors, Paris, 1964), Dunod, Paris (Academic Press, New York, 1965), p. 259.
[2] S. Ishino, F. Nakazawa and R. R. Hasiguti, J. Phys. Soc. Japan, **20,** 817 (1965).
[3] A. Hiraki and T. Suita, J. Phys. Soc. Japan **18,** Suppl. III, 254 (1963).
[4] R. A. Swalin, J. Phys. Chem. Solids **18,** 290 (1961).
[5] K. H. Bennemann, Phys. Rev. **137,** A1497 (1965).
[6] G. D. Watkins, Proc. Symp. on Radiation Damage in Semiconductors (7th Int. Conf. Phys. Semiconductors, Paris, 1964), Dunod, Paris (Academic Press, New York, 1965), p. 97.
[7] R. E. Whan, Appl. Phys. Letters **6,** 221 (1965).
[8] K. Weiser, Phys. Rev. **126,** 1427 (1962).
[9] N. F. Mott and M. J. Littleton, Trans. Faraday Soc. **34,** 485 (1938).
[10] G. Leibfried, Handbuch der Phys. edited by S. Flügge, VII-I, 1955, p. 104.
[11] The author appreciates Dr. K. H. Bennemann's private discussion on this point.
[12] A. Scholz, Phys. Stat. Solidi **3,** 42 (1963).
[13] A. Scholz and A. Seeger, Phys. Stat. Solidi **3,** 1480 (1963).

Calculation of the Physical Properties of Defects in Crystals by Approximate Self-Consistent-Field Methods

Emmett B. Moore, Jr.

Boeing Scientific Research Laboratories, Seattle, Wash. 98124

The rigorous Roothaan-Hartree-Fock linear-combination-of-atomic-orbitals self-consistent-field (RHF–LCAO–SCF) method [1, 2] [1] of calculating the physical properties of small molecules may be extended by the use of suitable approximations [3] and group theory to rather large molecules, or in our case to molecules which may be regarded as small regions of a crystal containing a defect. In this paper we outline the rigorous RHF–LCAO–SCF method, we show the relation between this method and the simpler extended-Hückel-theory (EHT) which has been used [4] to calculate some of the properties of defects in graphite, and we show how the RHF–LCAO–SCF method may be approximated to permit calculations of the physical properties of defects in crystals. This approximation of the SCF method has the advantage of being applicable to large molecules (or regions in a crystal) while being much more rigorous than the EHT method and nearly as rigorous as the parent SCF method.

In the Hartree-Fock self-consistent-field treatment the wave function Φ for the system is considered to be an antisymmetrized product of spin orbitals ψ^{ν},

$$\Phi = (N!)^{-1/2} A P |\psi_{\kappa}^{\nu}| \tag{1}$$

where each spin orbital contains one electron. There are N electrons in the system and they are referred to by the Greek letters μ and ν. There are also N spin orbitals which are referred to by the Greek letter κ. Each spin orbital is composed of two parts, an orbital part and a spin part:

$$\psi_{\kappa}^{\nu} = \phi_{i\kappa}^{\nu} \eta_{\kappa}^{\nu}. \tag{2}$$

There are thus $N/2$ orbitals $\phi_{i\kappa}^{\nu}$ which we shall designate as molecular orbitals (subscripts i and j) in anticipation of Roothaan's treatment.

When the wave function Φ is substituted into the Schrödinger equation the energy of the system is given by

$$E = \frac{\int \Phi \mathscr{H} \Phi d\tau}{\int \Phi \Phi d\tau} \tag{3}$$

where the integration is carried out over the space and spin coordinates of all the electrons. We omit the complex conjugate notation because, in the end, all our wave functions will be real. The Hamiltonian $\mathscr{H}$ of the system is given by

$$\mathscr{H} = \sum_{\nu=1}^{N} \left(-\frac{1}{2} \nabla_{\nu}^2 - \sum_{A=1}^{Q} \frac{Z_A}{r_{A\nu}} \right) + \frac{1}{2} \sum_{\mu \neq \nu=1}^{N} \frac{1}{r_{\mu\nu}} + \frac{1}{2} \sum_{A \neq B=1}^{Q} \frac{Z_A Z_B}{r_{AB}} \tag{4}$$

in atomic units where the terms in order are electron kinetic energy, electron-nuclear attraction energy, electron-electron repulsion energy, and nuclear-nuclear repulsion energy. The last term can be carried outside the Hamiltonian because the wave function Φ does not contain nuclear coordinates. There are Q nuclei in the system which are referred to by the letters A and B. Each nucleus carries a charge Z. When the energy expression is written out it becomes

$$E = 2 \sum_{i=1}^{N/2} H_i + \sum_{ij} (2J_{ij} - K_{ij}) + (NR) \tag{5}$$

where

$$H_i = \int \phi_i H \phi_i d\nu, \quad H = -\tfrac{1}{2} \nabla^2 - \sum_{A=1}^{Q} \frac{Z_A}{r_A}, \tag{6}$$

$$J_{ij} = \int \frac{\phi_i^{\mu} \phi_j^{\nu} \phi_i^{\mu} \phi_j^{\nu}}{r_{\mu\nu}} d\mu d\nu, \quad K_{ij} = \int \frac{\phi_i^{\mu} \phi_j^{\nu} \phi_j^{\mu} \phi_i^{\nu}}{r_{\mu\nu}} d\mu d\nu \tag{7}$$

and (NR) are the nuclear repulsion terms. Equations 5, 6, and 7 are included here only for completeness since we shall concern ourselves only with Roothaan's expression for the energy rather than the Hartree-Fock expression (eq (5)). For simplicity we drop the superscript ν in eq (6) and subsequent expressions when the integration is carried out over the coordinates of just one electron.

Roothaan's valuable contribution [1] was to extend Hartree-Fock theory (which mainly concerns atoms) to molecules explicitly by assuming the molecular orbitals to be linear combinations of atomic orbitals

[1] Figures in brackets indicate the literature references at the end of this paper.

χ centered on the atoms in the molecule.

$$\phi_i = \sum_{\alpha=1}^{n} c_{i\alpha}\chi_\alpha \tag{8}$$

The subscripts α and β refer to the atomic orbitals of which there are n in the system. It is customary to take $n > N/2$. When the energy (eq. (5)) is minimized with respect to the atomic orbital coefficients

$$\frac{\delta E}{\delta c_{i\alpha}} = 0 \tag{9}$$

there results the familiar set of equations

$$\sum_{\beta=1}^{n} (H_{\alpha\beta} - \epsilon_i S_{\alpha\beta})c_{i\beta} = 0, \ \alpha = 1 \ . \ . \ . \ n \tag{10}$$

where

$$H_{\alpha\beta} = [\alpha|\beta] + \sum_j \sum_{\gamma\delta} c_{j\gamma}c_{j\delta}(2[\alpha\beta|\gamma\delta] - [\alpha\delta|\gamma\beta]) \tag{11}$$

$$[\alpha|\beta] = \int \chi_\alpha \left(-\tfrac{1}{2} \nabla^2 - \sum_{A=1}^{Q} \frac{Z_A}{r_A} \right) \chi_\beta d\nu \tag{12}$$

$$[\alpha\beta|\gamma\delta] = \int \frac{\chi_\alpha^\mu \chi_\beta^\mu \chi_\gamma^\nu \chi_\delta^\nu}{r_{\mu\nu}} d\mu d\nu \tag{13}$$

and

$$S_{\alpha\beta} = \int \chi_\alpha \chi_\beta d\nu. \tag{14}$$

In the Roothaan treatment one evaluates all the intergrals explicitly, assumes a set of filled molecular orbitals, i.e., assumes the coefficients c_i, calculates $H_{\alpha\beta}$ and then solves eq (10) for the molecular orbital energies ϵ_i and a new set of molecular orbital coefficients c_i. This process is repeated iteratively until the set of coefficients from the solutions to eq (10) becomes the same as that used to calculate $H_{\alpha\beta}$. This process insures self-consistency within the framework of the method.

The energy of the system then becomes:

$$E = \sum_{i=1}^{N/2} H_i + \sum_{i=1}^{N/2} \epsilon_i + (NR) \tag{15}$$

$$= 2\sum_{i=1}^{N/2} \epsilon_i - \sum_{ij} (2J_{ij} - K_{ij}) + (NR) \tag{16}$$

where

$$H_i = \sum_{\alpha\beta} c_{i\alpha}c_{i\beta}[\alpha|\beta]. \tag{17}$$

In principle these equations can be solved for any size system but in practice the evaluation of the three and four center integrals is so difficult and time consuming that the method is limited at present to about eight atoms and thus is not really applicable at all to the problem of calculating the physical properties of defects in crystals. On the other hand, the extended-Hückel-theory method [5] has been used for 35 atoms [4] and simple application of group theory can make this number much larger. For instance in our graphite calculation [4] we considered a single layer containing 24 carbon atoms and 12 hydrogen atoms (to simulate boundary conditions), while use of the point group C_{2v} would have permitted us to consider a three layer structure containing 96 carbon atoms and 42 hydrogen atoms. In EHT one again assumes the molecular orbitals to be linear combinations of atomic orbitals (eq (8)) and carries out a variation procedure (eq (9)) which leads to a set of equations of exactly the same form as eq (10). Again the overlap integrals ($S_{\alpha\beta}$) are evaluated explicitly but here the similarity ends. The diagonal Hamiltonian matrix elements ($H_{\alpha\alpha}$) are approximated, usually by valence state ionization energies, and the off diagonal elements ($H_{\alpha\beta}$) are approximated, usually by the Wolfsberg-Helmholz approximation [6]. If the EHT Hamiltonian matrix elements turned out to be exactly the values obtained in the last cycle of the SCF method, then of course the EHT molecular orbital energies and coefficients would be exactly the same as those obtained by the RHF–LCAO–SCF method. This is one of the things we seek and a method for doing this will be outlined in the last part of this paper.

There is one further difficulty with the EHT method and this involves the way the total energy of the system is calculated. The EHT energy of the system is assumed to be just the first term of eq (16), i.e., twice the sum of the energies of the filled molecular orbitals. This includes electron kinetic energy and electron-nuclear attraction energy but ignores electron-electron repulsions (J_{ij} and K_{ij}) and the nuclear-nuclear repulsions. The success of our previous work [4] on the calculation of the energy of vacancy migration and Frenkel pair formation in graphite depends on the fact that these two terms partially cancel each other as well as on the fact that the sum of the energies of the filled molecular orbitals is sufficient in most cases to establish an energy minimum. The second thing we seek then is a better method of calculating the energy of the system so that we may have more confidence in the energies we calculate for defect formation and migration etc.

Newton, Boer, and Lipscomb [3] propose a refinement of the RHF–LCAO–SCF method (or improvement of the EHT method, depending on your point of view) which will allow calculation of values of the molecular orbital coefficients and energies more nearly equivalent to the exact RHF–LCAO–SCF values than the EHT method will allow. The major advantage is of course that the method can be extended to systems containing the same number of atoms as can be handled by EHT. They have

compared many small-molecule SCF calculations and have concluded that the Hamiltonian matrix elements from small-molecule calculations can be used to calculate the Hamiltonian matrix elements for similar but much larger molecules. They thus avoid the problem of calculating all the necessary integrals but at the same time simulate what eq (10) would be for an exact large molecule calculation. They write the diagonal Hamiltonian matrix elements as:

$$H_{\alpha\alpha}=\int \chi_\alpha(-\tfrac{1}{2}\nabla^2)\chi_\alpha d\nu+V_{\alpha\alpha} \tag{18}$$

and calculate the first term (kinetic energy) exactly. This term is subtracted from the $H_{\alpha\alpha}$ term, taken from small molecule calculations, to give $V_{\alpha\alpha}$. They have determined that the Wolfsberg-Helmholz approximation applies only to the potential energy part of the Hamiltonian matrix elements so for the off diagonal elements $H_{\alpha\beta}$ they use the expression

$$H_{\alpha\beta}=\int \chi_\alpha(-\tfrac{1}{2}\nabla^2)\chi_\beta d\nu+\text{"}KS_{\alpha\beta}(V_{\alpha\alpha}+V_{\beta\beta})/2\text{"} \tag{19}$$

where the kinetic energy term is again calculated exactly. We place the Wolfsberg-Helmholz approximation in quotation marks because the exact expression and value of K depend on which atomic orbitals are involved. Finally the energy of the system as calculated from eq (15) becomes

$$E=\sum_{i=1}^{N/2}\sum_{\alpha\beta}c_{i\alpha}c_{i\beta}\left[\int \chi_\alpha\left(-\tfrac{1}{2}\nabla^2-\sum_{A=1}^{Q}\frac{Z_A}{r_A}\right)\chi_\beta d\nu\right]+\sum_{i=1}^{N/2}\epsilon_i+(NR). \tag{20}$$

This expression necessitates the calculation of nuclear-electron attraction integrals and nuclear-nuclear repulsion terms as well as the kinetic energy integrals which were necessary to set up the Hamiltonian matrix elements in eq (10). The nuclear-nuclear repulsion terms are evaluated classically and the kinetic energy and nuclear-electron attraction integrals may be evaluated with the use of computer programs available from the Quantum Chemistry Program Exchange [7]. Programs are also available from the same source for solving eq (10).

Lipscomb and his co-workers are using this approximate SCF method with success to calculate the physical properties of a wide variety of large molecules for which prototype small molecule SCF calculations are available. These calculations, our success with EHT, the close relation between EHT and SCF theory, the impossibility of solving the Schrödinger equation directly, and the difficulty of carrying out complete SCF calculations on large systems, lead us to believe that this approximate self-consistent-field method will be very useful in calculating the physical properties of defects in crystals.

References

[1] C. C. J. Roothaan, Rev. Mod. Phys. **23**, 69 (1951).

[2] S. M. Blinder, Am. J. Phys. **33**, 431 (1965). This is a very readable account of the Hartree, Hartree-Fock, and Roothaan-Hartree-Fock self-consistent-field methods, although the author carries out the treatment for spin-orbitals rather than molecular orbitals and thus omits a factor of 2 in some of the expressions.

[3] M. D. Newton, F. P. Boer, and W. N. Lipscomb, J. Am. Chem. Soc. **88**, 2353 (1966).

[4] E. B. Moore, Jr. and C. M. Carlson, Solid State Comm. **4**, 47 (1966).

[5] R. Hoffmann, J. Chem. Phys. **39**, 1397 (1963).

[6] M. Wolfsberg and L. Helmholz, J. Chem. Phys. **20**, 837 (1952).

[7] Quantum Chemistry Program Exchange, Indiana University, Bloomington, Indiana.

Interatomic Potentials for Defect Calculations in Metals

H. B. Huntington

Rensselaer Polytechnic Institute, Troy, New York 12180

Ideally a paper with this title should answer two questions: "How are the calculation results influenced by the characteristics of the potentials?" and "What is the 'best' potential for defect calculations?" Neither answer is ready to hand at this time and this paper is for the most part only a chronological review of the topic with a few critical comments at the end. But first some general remarks on potentials in metals.

1. The problem is intrinsically more complex and intractable for metals than other solids because of the nature of the so-called metallic bond, which is really not a bond at all in the sense of an interatomic force but rather a cooperative interaction between the electrons and ions. The cohesion resides in such nonlocalized concepts as the Fermi surface and the electron-electron correlation. Of course, in principle any situation can be described by a complete set of interatomic force constants. Only in the case of metals such a description may converge slowly and has an artificial character in that it is difficult to assign physical meaning to the various coupling parameters. Actually, a potential dependent on volume only appears often to represent metallic cohesion better.

2. The metals share with all other types of solids a repulsion between atoms at close distances of approach as a consequence fundamentally of the Pauli Exclusion Principle. Unfortunately, it has not been possible to develop the magnitude of this repulsion directly from first principles, but the general form is certainly one where the repulsion increases rapidly at close distances of approach. The classical Born-Mayer form for this is a simple exponential and there is some theoretical justification for this at the separations of the usual lattice spacings in that the wave function tails fall off exponentially at large distance for most atoms. Positive potential terms varying as a large inverse power of r are another form for this closed shell repulsion as in the Lennard-Jones approach.

3. Although there has been considerable effort to treat the cohesive forces in metals from first principles, the repulsive forces have almost invariably been established by semiempirical methods. Naturally semiempirical considerations have played an important role in establishing the potentials used for all the large machine calculations. One is not likely to embark on an extensive program without first ensuring that the model will reproduce the most obvious parameters of the metal concerned. The parameters most usually chosen are the lattice constant and the compressibility, which respectively serve to establish the distance scale and the curvature of the potential. A third parameter to set the scale for the magnitude of the potential is most naturally the cohesive energy. On the other hand the potential has been required sometimes to give agreement for the calculation of vacancy formation or the radiation damage threshold for Frenkel pairs, as alternate procedures for setting the scale of the potential. For additional parameters there are the second order elastic constants. Since for most metals the Cauchy relations are not obeyed, exact fitting involves something other than two-body potentials. The addition of a volume dependent term as emphasized by De Launay [1][1] appears to be the simplest way to meet such a requirement. Currently third-order elastic data are becoming available [2] and it may be possible to fit such data later into more elaborate semiempirical potentials. The first results appear to indicate that the potentials as currently used give quite reasonable agreement in the main with the anharmonic results so that we may anticipate that such changes as might result will be in the nature of refinements only. Of course there is also a wealth of data on interatomic forces available from the dispersion curves obtained by the diffraction of neutrons and x rays, and attempts [3] have already been made to incorporate these results in defect calculations via Born Lattice coupling coefficients.

4. While the earliest calculations neglected atom motion at large distance from the defect, it was soon apparent that one should introduce an elastic solution in this region to be realistic and to find the volume change associated with the defect. The latter could be determined from the leading term in the expansion of the displacement in spherical harmonics about the defect:

$$u(r) = C\underline{r}/r^3.$$

From which it follows that the volume change was $\Delta V = 4\pi C$. Eshelby [4] showed that the requirement of the surface boundary condition increased ΔV by a factor

$$1 + \frac{2(1-2\nu)}{1+\nu}$$

[1] Figures in brackets indicate the literature references at the end of this paper.

or effectively about 50 percent. In general the elastic energy associated with the elastic field outside the first 100 atoms is small. For a defect with the symmetry of the lattice the higher order terms in the expansion of the strain are quite negligible. Defects with lower symmetry such as split-interstitials and divacancies will act as elastic dipoles and may be detected by mechanical or magnetic relaxation. Here the enhancement from the image force considerations may be even more substantial [5].

5. Consider the aspect of electron redistribution around point defects. For interstitials this problem has been largely honored in the breach. The single vacancy has been reasonably well treated by several different workers but the problem certainly does not lend itself to the treatment of defects of lower symmetry. As part of this general picture the Friedel oscillations may well play some role in this difficult problem.

6. As a summary item to this general introduction it should perhaps be remarked that to some extent different phases of the model potential are important for different applications. The part of the potential at short range is critical in determining energy thresholds for radiation production of defects. The fast changing repulsive potential plays a dominant role in the motion of crowded interstitial defects, whereas the energies for vacancy configurations appear to depend sensitively on the electron redistribution. We turn now to a chronological review of developments.

Probably the first effort to treat the defect potential in a metal was an attempt [6] that Seitz and the author made several years ago to establish the prevailing diffusion mechanism in a metal such as copper. We used a Born-Mayer repulsion and made an earnest effort to take into account the electron redistribution about the vacancy in a self-consistent way. This part of the work involved some serious errors which fortunately (?) to some extent canceled, but the main result, that the vacancy mechanism was preferred, seemed reasonably established. Later Zener's [7] stimulating suggestion as to a possible ring mechanism forced a reevaluation [8] of the original Born-Mayer potential and the introduction of a less rapidly varying alternative. The semiempirical considerations in back of this potential were again restudied at a still later time when the mechanism of interstitialcy motion was reexamined [9] as a possible explanation of low temperature anneal of radiation damage; it appeared to be a defect with a low energy of motion but a high energy of formation. We were inclined to play down certain oscillations in the self-consistent charge density at intermediate distance from the vacancy but Friedel pointed out [10] that such variation in charge and hence in potential were the natural consequences of the sharp Fermi Surface in a metal. These Friedel oscillations have subsequently turned out to be most important in the development of solid state physics.

Friedel's influence in this field has made itself felt in another important way. He showed [11] how one can calculate directly from a knowledge of the phase shifts η_l from a partial wave scattering problem for the wavelengths corresponding to the Fermi Surface the charge Z displaced by the scattering center. The formulation of this Friedel condition,

$$Z=\frac{2}{\pi}\sum_l (2_l+1)\,\eta_l,$$

is a most useful tool in developing a self-consistent solution in the neighborhood of a defect since it gives one an instant check as to when the defect is electrically neutral. While the satisfaction of this condition does not insure complete self-consistency, it is a most important first step—and to some extent sufficient in some applications. Fumi [12] employed the Friedel condition to develop a general treatment of the vacancy problem, applicable for any density of free electrons. This increase in flexibility was needed since any complete self-consistent treatment would be valid for only one particular electron density. The resulting predictions [12] for the energies of vacancy formation appear to be on the high side but to vary qualitatively in the right way with electron density. Comparison with experiment for the alkali metals has been limited for the most part to the activation energies for diffusion. However, this may have been more relevant than one would at first suppose since Fumi believed that the energy for motion would be small for these metals.

An even simpler approach to the electron redistribution problem was that of Brooks [13] who suggested that one could treat vacancy configurations as small internal voids whose intrinsic energy consisted primarily of the energy of the extra surface formed. Relaxation of the lattice inward about the vacancy then operated to minimize the total energy. The results of this method tended to give numbers that were somewhat too large for the formation energies of vacancy defects.

The general technique of the partial wave analysis hinged on the Friedel condition was the basis for many subsequent papers dealing with energy of point defects and their specific resistivity. While for the most part the work dealt with defects of high symmetry, Seeger and Bross [14] studied the divacancy with ellipsoidal coordinates and found for the noble metals a binding energy of about 0.06 of the Fermi Energy. Seeger [15] also made application to the vacancy in nickel and cobalt.

Around 1957 there began the somewhat simpler game of defect treatment by use of the two-body interaction only. The Lennard-Jones potential was used by two investigators that year, Kanzaki [16] and Hall [17]. The former was concerned primarily with the application to solid argon. The

latter introduced external pressure as a variable and explored the displacement pattern around both the vacancy and the cube-centered interstitial. The anisotropic nature of the displacement function pointed up the difficulty with the previous efforts to fit on an isotropic, elastic displacement, particularly in the case of the interstitial. In the next year Tewordt [18] showed a reasonable way to establish the elastic field at large distances by allowing the amplitudes of the respective harmonic components of the displacement to be treated as parameters for the energy minimization on a par with the displacements of the individual atoms near the defect. Tewordt used two alternate Born-Mayer potentials to treat the interstitial, the crowdion, and the vacancy. His work was also, I think, the first to make use of a large scale computer for defect calculations, the Illiac in Urbana.

In 1960 a much more ambitious machine program was first reported [19] in the literature, using the GRAPE program developed by the group at Brookhaven working with Vineyard. Here again a Born-Mayer potential was used but instead of fitting to an elastic solution at infinity the machine dealt with a finite number (1,000) of atoms, arranged in a rectangular chunk of lattice and constrained at an equilibrizing pressure by an elastic membrane at the boundary. The membrane also had some dissipative character so the specimen metal could lose energy to its environment at a reasonable rate. Vineyard and his colleagues gave considerable attention to the choice of Born-Mayer potential. Because their primary interest was to follow defect formation during fast particle irradiation, the behavior of the potential at close distances of approach was important. They considered the shielded coulomb potential of Bohr, presumably valid for $r \leq 0.1$ Å, and also the Fermi-Thomas modifications for somewhat greater distances. At normal interatomic distances possible Born-Mayer functions were considered. Lattice constant and compressibility as usual were input data but also the check with the threshold for radiation damage displacements was considered. The one finally chosen for the bulk of the work did not, as luck would have it, differ much from the form originally used by others in prior papers.

This potential was used again more recently in a revived treatment of the static defects of the fcc lattice by Johnson and Brown [20]. In addition to the calculations of energies and defect volumes the stabilities of the various configurations were investigated in a completely systematic way so that the energy profiles of the interconfigurational paths could be plotted.

Not all the two-body machine calculations, however, have used the Born-Mayer potential. In recent years there has been an increasing interest in the Morse potential for such purposes. Originally the group at Lewis Research Center in Cleveland developed [21] the parameters appropriate for a large number of fcc metals to put in the formula

$$V(r) = D\,[\exp\,(-2(r-r_0)/\alpha - 2\exp -(r-r_0)/\alpha].$$

Heat of sublimation, lattice constant and compressibility were used to determine D, α, and r_0, and the resulting $V(r)$ was applied to various vacancy and interstitial configurations. Benneman [22] applied both Born-Mayer and Morse potentials to two interstitial configurations apparently without essential difference in his findings. For reliable results with the Morse potential one considers quite distant neighbors and some artificial truncation schemes have been shown to give falacious results. Proponents for this potential usually feel that it offers an advantage in that attractive as well as repulsive forces are involved in minimizing the energy and in determining the atom positions. On the other hand this model uses only central forces and therefore can not be expected to adjust to departures from the Cauchy relations for the elastic constants. Recently Cotterill and Doyama have made extensive use of this potential in several kinds of defect problems. A thoroughgoing treatment [23], which involves elastic fields determined to minimize the energy, makes possible estimates of defect volumes—but this work will be reported directly later in this conference.

For some metals such as copper and silver, the Born-Mayer potential plus retaining pressure has been able to reproduce quite satisfactorily the observed elastic constants. Iron is an example where this is not possible and the Brookhaven group first applied a modified Morse potential for use in a dynamic treatment [24] of radiation damage events. Later Johnson [25] replaced the Morse curve with a cubic expression over a region including the range of nearest and next nearest neighbors. The cubic was chosen to give exactly the elastic constants minus the electronic contributions computed electrostatically. At large distances the fitted cubic was contrived to go to zero with zero slope at a distance halfway between second and third neighbors. This model has met with good success in several applications.

Lastly, for a long time we have been conscious of the influence of the Friedel oscillations for the potential of an impurity in a metallic lattice but the effect of these oscillations on defects calculations has not been explicitly explored. A step in this direction appears in a recent paper by Cotterill and Doyama [26] on line and plane defects wherein they investigate the stacking fault in aluminum by several potentials. Among these are two oscillating potentials, one determined experimentally by Johnson et al. [27], from neutron scattering data, the other evolved theoretically by Harrison [28] from a pseudopotential approach. Certainly these potentials will be used also in point defect problems [29].

After this chronological review a word is maybe in order by way of critical summary and perhaps suggested lines for progress.

First the electronic redistribution is especially important for the vacancy configurations. Its complete omission in the two-body-only force model leads to too small energies for formation and motion. On the other hand results of the partial wave analysis give somewhat too large values for sodium and values somewhat on the small side for the noble metals. One wonders if satisfying the Friedel condition alone is enough to establish satisfactory self-consistency. Also the neighbors' inward motion on the vacancy reduces its volume appreciably and thereby the charge to be removed. Clearly a thoroughgoing treatment of all these considerations would involve a very extensive program even for any real metal.

The application of large machines to explore interstitial configurations governed by two-body forces appears on the whole to give reasonably consistent and hence on the whole believable results. The addition of a volume-dependent force appears to be an improvement in that departure from the Cauchy relation can be incorporated. From the standpoint of macroscopic elasticity the use of two-body central forces plus a volume-dependent potential may suffice for a reasonably complete description in second order and maybe even in third order, although at this point there are only a few reliable third order measurements. The long range oscillations of the potential are also being quantitatively explored. Whether more refinement in this direction would significantly alter the results of defect calculations is still unknown.

There has up to now been relatively little effort to trying to understand the differences in the results of defect calculations in terms of differences in the underlying potentials. A simple example of such a consideration is the comparison of the volumes for defect formation against the anharmonic character of respective potentials. Detailed machine calculations have been carried out for the fcc lattice (Cu) using the Morse potential [23] and the Born-Mayer potential [20]. Let the anharmonic character of each be represented by a dimensionless parameter $\gamma_p = -\left[r \frac{d^3V}{dr^3} \Big/ \frac{d^2V}{dr^2} \right]_{r_1}$ where r_1 is set at some convenient interatomic distance such as the nearest neighbor distance. From the table below one sees that the higher γ_p goes with the larger volume expansion with the interstitial, the larger inward relaxation around a vacancy, and the larger volume increase for the moving atom at the saddle point, as might be expected. Further study of this sort should give worthwhile insight into the influence of potential parameters on calculated results.

	Morse potential	Born-Mayer potential
ΔV_I for split interstitial	1.34	2.20
ΔV_V for vacancy	0.83	0.43−0.62
ΔV_{MV} for vacancy motion	.03	.19− .38
γ_p	8.1	13.9
	(All ΔV in terms of atomic volume)	

References

[1] J. De Launay, Solid State Physics, Vol. **2**, p 283 (Academic Press, New York, 1956).
[2] Yosio Hiki and A. V. Granato, Phys. Rev. **144**, 411 (1966).
[3] A. Seeger, E. Mann, and R. N. Jan, J. Phys. Chem. Solids **23**, 639 (1962).
[4] J. D. Eshelby, Solid State Physics, Vol. **3**, p 79 (Academic Press, New York, 1956).
[5] H. B. Huntington and R. A. Johnson, Acta Met. **10**, 282 (1962).
[6] H. B. Huntington and F. Seitz, Phys. Rev. **61**, 315 (1942).
[7] C. Zener, Acta Cryst. **3**, 346 (1950).
[8] H. B. Huntington, Phys. Rev. **76**, 1728 (1949).
[9] H. B. Huntington, Phys. Rev. **91**, 1092 (1953).
[10] J. Friedel, Phil. Mag. **43**, 153 (1952); A. Blandin and J. L. Deplante, Metallic Solid Solution p IV-1 (W. A. Benjamin, Inc., New York, 1963).
[11] J. Friedel, Phil. Mag. **43**, 153 (1952).
[12] F. G. Fumi, Phil. Mag. **46**, 1007 (1955).
[13] H. Brooks, Impurities and Imperfections, pp 1–27 (ASM Cleveland, 1955).
[14] A. Seeger and H. Bross, Z. Physik **145**, 161 (1956).
[15] A. Seeger, Z. Physik **144**, 637 (1956).
[16] H. Kanzaki, J. Phys. Chem. Solids **2**, 24 (1957).
[17] C. L. Hall, J. Phys. Chem. Solids **3**, 210 (1957).
[18] L. Tewordt, Phys. Rev. **109**, 61 (1958).
[19] J. Gibson, A. N. Goland, M. Milgram, and G. H. Vineyard, Phys. Rev. **120**, 1229 (1960).
[20] R. A. Johnson and E. Brown, Phys. Rev. **127**, 446 (1962).
[21] L. A. Girifalco and V. G. Weizer, Phys. Rev. **114**, 687 (1959); P. Hockstra and D. R. Behrendt, Phys. Rev. **128**, 560 (1962).
[22] K. H. Bennemann, Phys. Rev. **124**, 669 (1961).
[23] M. Doyama and R. M. Cotterill, Phys. Rev. **137A**, 994 (1965).
[24] C. Erginsoy, G. H. Vineyard and A. Englert, Phys. Rev. **133A**, 595 (1964).
[25] R. A. Johnson, Phys. Rev. **134A**, 1329 (1964).
[26] R. M. J. Cotterill and M. Doyama, Phys. Rev. **145**, 465 (1966).
[27] M. D. Johnson, P. Hutchinson, and N. H. March, Proc. Roy. Soc. **A282**, 283 (1964).
[28] W. H. Harrison, Pseudopotentials in the Theory of Metals, p 45 (W. A. Benjamin, Inc., New York, 1966.)
[29] H. B. Huntington and Michael D. Feit, Structure Factor Approach to Energies of Migration, this symposium.

Calculations for Defects in an F.C.C. Lattice*

R. A. Johnson

Brookhaven National Laboratory, Upton, N.Y. 11973

1. Introduction

The properties of point defects in metals can be studied by lattice calculations in which the atoms near a defect are treated individually. In such calculations a model is devised which matches various known physical properties of a metal and which, one hopes, can be extrapolated to yield results about unknown properties of the metal, e.g., configurations and energies associated with lattice defects. These models normally represent the solid by a crystallite in which the atoms interact by two-body central forces surrounded by a boundary region which is meant to simulate the remainder of the lattice. An energy equation is written which includes the interatomic forces and the boundary forces, and parameters in this equation are adjusted to yield a reasonable approximation of the perfect lattice. Then the energy equation is investigated in a region of configuration space where it represents the defect lattice, i.e., the whole process may be thought of as very complicated and sophisticated curve fitting to one section of configuration space and extrapolation to another section. There is of course no unique way of fitting the perfect lattice: any number of quite different models can do a reasonably good job. Also, there is the question of whether or not the forces which describe the perfect lattice are adequate to describe the defect state, i.e., whether extrapolation is permissible.

Most of the work in this field has been carried out for copper, an f.c.c. metal, and the most extensive of these calculations have been reported by Johnson [1,2][1] and Brown [1], Seeger and coworkers [3-5] and more recently by Doyama and Cotterill [6]. All these authors used well-known potential interactions between the atoms: Johnson and Brown used a Born-Mayer interaction, Seeger et al., used a Born-Mayer for some calculations and modified it with Born lattice theory interactions in others, and Doyama and Cotterill are using a Morse function. All these calculations give unsatisfactory results pertaining to vacancies [2] and the reliability pertaining to interstitials is uncertain [7].

Johnson [8] has recently carried out corresponding calculations for α-iron with a different form of potential. In a b.c.c. lattice the first- and second-nearest neighbor separation distances are similar, while the third neighbor is at a much greater distance. Therefore a short-range interatomic interaction can reasonably be cutoff between the second- and third-neighbor separation distance. When this is done, the elastic moduli of α-iron are such that the first-neighbor interaction must be repulsive and the second-neighbor interaction must be attractive. A potential curve, shown in figure 1,

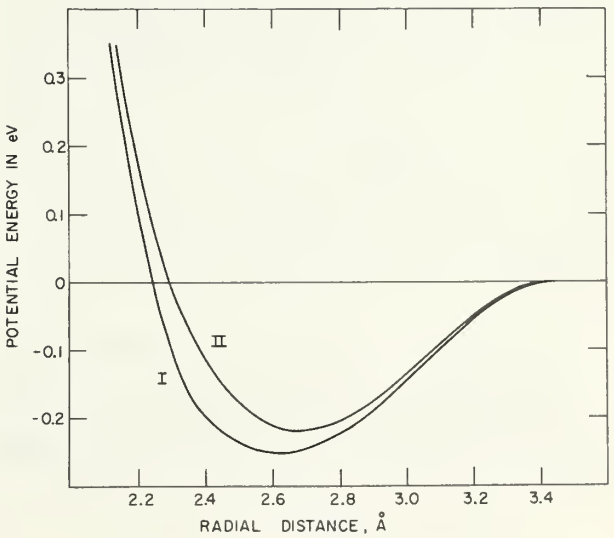

FIGURE 1. *The potential energy for the two-body central interaction of iron atoms in either the body-centered cubic or face-centered cubic phase.*

Interaction I together with an electronic contribution reproduce the elastic moduli of α-iron whereas interaction II by itself yields these data.

was devised which fit these criteria. In α-iron, the nearest neighbor distance is 2.48 Å and the second neighbor distance is 2.86 Å. Curve I is fitted to the elastic moduli with an electronic contribution corresponding primarily to the bulk modulus of a free electron gas, and curve II is fitted to the full experimental elastic moduli. The differences in the results given by these two curves were not significant.

Although there is not very much experimental data with which the calculated results can be

*Work performed under the auspices of the U. S. Atomic Energy Commission.

[1]Figures in brackets indicate the literature references at the end of this paper.

compared, what comparisons are available are quite encouraging. These calculations were extended to include the case of carbon interstitials in α-iron [9] and in iron martensite [10], a body-centered tetragonal phase of iron, and the structure and energy of Fe_3C (cementite) [9] were also investigated. Here too the results were encouraging.

When applied to an f.c.c. lattice structure with a nearest neighbor distance corresponding to γ-iron, 2.57 Å, the elastic moduli predicted by this interaction are very similar to those of nickel, (the elastic moduli of γ-iron are not known). If γ-iron or nickel are to be approximated by a short-range central interaction which fits the elastic moduli, this form of interaction is just as satisfactory as a purely repulsive interaction such as the Born-Mayer, and there is no a priori reason to choose one or the other. Since this form of interaction was required for the b.c.c. case, and since it yields reasonable elastic moduli for an f.c.c. structure, calculations were carried out to investigate the properties of vacancies and interstitials which it gives for an f.c.c. lattice.

The mathematical model used in the present f.c.c. calculations is as close as possible to being the same as that used in the earlier b.c.c. calculations [9]. A spherical set of 531 atoms was treated as a crystallite of independent particles and the atoms outside this set were treated as though they were imbedded in an elastic continuum. The changes in energy in this model were carefully monitored as defects were introduced and the set was allowed to relax to the minimum energy configuration. By applying constraints on the positions of some atoms, saddle point and intermediate configurations could be investigated.

2. Results

The stable vacancy configuration was that in which an atom is missing from a normal lattice site and the saddle point configuration for migration was found by moving one of the twelve nearest-neighboring atoms to the vacancy directly towards the vacancy until it is midway between its site and the vacancy site. The vacancy formation energy was found to be $E_{1V}^F = 1.49$ eV, the formation volume was $V_{1V}^F = 0.85\ \Omega$, where Ω is the atomic volume, the activation energy for migration was $E_{1V}^M = 1.32$ eV, and the activation volume was $V_{1V}^M = -0.05\ \Omega$. By adding the formation and migration energies a self-diffusion energy is found; $E_{1V}^{SD} = 2.81$ eV. The results are summarized in table 1.

TABLE 1. *Summary of results for vacancies and interstitials in an f.c.c. lattice model with an interatomic interaction appropriate for nickel*

The listing of experimental results is based on an interpretation of the data in which single interstitials migrate in the so-called stage I region, divacancies migrate in stage III and vacancies migrate in stage IV. Energies are given in eV, and E^F means formation energy, E^M means motion energy, E^{SD} means energy for self diffusion, E^B means binding energy, and E^S means energy by which a configuration is metastable.

Calculation		Experimental	Calculation	
E_{1V}^F	1.49	[a] 1.4	E_{1I}^S (⟨111⟩ split)	0.16
E_{1V}^M	1.32	[a] 1.5	E_{1I}^M (⟨111⟩ split)	.13
E^{SD}	2.81	[a] 2.9	E_{1I}^S (⟨110⟩ split)	.02
E_{2V}^M	0.90	[a] 0.8	E_{1I}^M (⟨110⟩ split)	.04
E_{1I}^F	4.08		E_{2I}^B	1.16
E_{1I}^M	0.15	[b] 0.15	E_{2I}^M	0.29

[a] For a summary of vacancy results see ref. [11].
[b] See ref. [12].

The stable divacancy configuration was that in which two atoms are missing from nearest-neighboring normal lattice sites. The saddle-point configuration has very little symmetry and involves the jump of an atom which is in a nearest-neighboring lattice site to both halves of the stable divacancy from its site to one of the vacant sites. The path goes out of the plane defined by the three sites and the jumping atom does not closely approach the center of the triangle of the three sites. The divacancy binding energy was found to be $E_{2V}^B = 0.25$ eV and the activation energy for migration was $E_{2V}^M = 0.90$ eV.

The most stable interstitial configuration was the ⟨100⟩ split configuration in which two atoms are symmetrically displaced in the ⟨100⟩ direction from a vacant lattice site. The migration mechanism consisted of one end of the split jumping to form a split at a nearest-neighboring lattice site. This involves rotation of the axis of the split as well as migration. The interstitial formation energy was found to be $E_{1I}^F = 4.08$ eV, the formation volume was $V_{1I}^F = 0.7\ \Omega$, the activation energy for migration was $E_{1I}^M = 0.15$ eV, and the activation volume was $V_{1I}^M = 0.1\ \Omega$.

Another metastable interstitial was found which gives rise to another migration mechanism—the ⟨111⟩ split, in which two atoms are symmetrically displaced in the ⟨111⟩ direction from a vacant lattice site. The migration mechanism consisted of one end of the split jumping to form a split at a nearest-neighboring lattice site. This configuration was metastable by E_{1I}^S(⟨111⟩ split) = 0.16 eV and the activation energy for migration was E_{1I}^M(⟨111⟩ split) = 0.13 eV.

The ⟨110⟩ split configuration, the so-called crowdion, was just barely metastable and migrated very easily: E_{1I}^S(⟨110⟩ split) = 0.02 eV and E_{1I}^M(⟨110⟩ split) = 0.04 eV.

The di-interstitial was found to be very tightly bound. The configuration consists of two parallel ⟨100⟩ single interstitial at nearest-neighboring lattice sites with the line joining their centers perpendicular to their axes. The binding energy was $E_{2I}^B = 1.16$ eV and the activation energy for migration was $E_{2I}^M = 0.29$ eV.

Close Frenkel pairs were investigated and it was found that the region of spontaneous interstitial

vacancy recombination was quite small—32 Ω—and that there was negligible interstitial-vacancy interaction at separation distances greater than several lattice constants.

3. Discussion

The object of this calculation was to investigate the consequences of using an interatomic interaction for an f.c.c. lattice with a form similar to that previously used for b.c.c. calculations. This type of interaction is somewhat intermediate between the purely repulsive short-range Born-Mayer and the long-range attractive-tail Morse interactions used in earlier calculations. The constants used should make the interaction reasonably appropriate for γ-iron or nickel, and the results are compared to the experimental values for nickel in table 1. The interpretation of the experimental data is not universally agreed upon, but these calculations certainly favor the interpretation in which interstitials freely migrate in the so-called stage I region, divacancies in stage III, and vacancies in stage IV. In contrast to earlier point defect calculations, the present calculations do not yield any results which are clearly inconsistent with experimental data, and although this certainly is not proof of its validity, the consistency is sufficiently good that this type of calculation warrants further study.

4. References

[1] R. A. Johnson and E. Brown, Phys. Rev. **127,** 446 (1962).
[2] R. A. Johnson, J. Phys. Chem. Solids **26,** 75 (1965).
[3] A. Seeger, E. Mann, and R. v. Jan, J. Phys. Chem. Solids **23,** 639 (1962).
[4] G. Schottky, A. Seeger, and G. Schmid, Phys. Stat. Solidi **4,** 419 (1964).
[5] G. Schottky, A. Seeger, and G. Schmid, Phys. Stat. Solidi **7,** K25 (1964).
[6] M. Doyama and R. M. J. Cotterill, Phys. Rev. **137,** A994 (1965).
[7] R. A. Johnson, Phys. Letters **19,** 191 (1965).
[8] R. A. Johnson, Phys. Rev. **134,** A1329 (1964).
[9] R. A. Johnson, G. J. Dienes, and A. C. Damask, Acta Met. **12,** 1215 (1964).
[10] R. A. Johnson, Acta Met. **13,** 1259 (1965).
[11] A. Seeger and D. Schumacher, in Lattice Defects in Quenched Metals, p. 15, edited by R. M. J. Cotterill, M. Doyama, J. J. Jackson, and M. Meshii (Academic Press, New York, 1965).
[12] J. Verdone, P. Peretto, P. Moser, D. Dautreppe, and J. Verdier, Compt. Rend. **260,** 5209 (1965).

256-724 O-67—4

Atomistic Calculations of Interstitials in F.C.C. Metals*

M. Doyama and R. M. J. Cotterill

Argonne National Laboratory, Argonne, Ill. 60440

1. Introduction

Interstitials and interstitial-type defects are particularly important in the study of radiation damage and plastic deformation. It has been apparent for many years that the process of irradiation damage is one of considerable complexity. When a property such as electrical resistivity is monitored during the warm up of a metal specimen irradiated at a low temperature, numerous annealing stages are observed. These have been classified into stages I, II, III, IV, and V, according to the temperature range in which they are observed in a given metal; and some of these stages exhibit substages. The point defects generated by the irradiation can interact with each other in a variety of different ways. Interstitials can interact with other interstitials and also with vacancies. Moreover, each of these interactions might itself occur in several different ways. For instance, several different stable interstitial-vacancy pairs might exist, each with its own binding and migration energy, and each with its own energy barrier against transition into another form.

Stage I annealing is generally considered to be due either to the annealing of close pairs of vacancies and interstitials or to the migration of free interstitials. There is an opposing school of thought which believes that free interstitials migrate in stage III rather than in stage I.

Important properties of these interstitial-type defects are the formation energy, the migration energy (or energies, if several types of interstitials exist), and the interaction energies between interstitials and other defects. Energies and atomic configurations of these defects are here studied by using an atomistic model. Central forces were assumed, and the pair-wise interaction between atoms was represented by a Morse potential function.

Several possible configurations of the single interstitial will be discussed, and it will be shown that a Morse potential [1][1] calculation gives essentially the same results as previous calculations which used a Born-Mayer potential [2].

Huntington and Seitz [3] examined both the interstitial and vacancy. For the former defect they considered an extra atom located at the cube center of the f.c.c. lattice (i.e., the so-called "body-centered" type). Paneth [4] considered a configuration in which the extra atom was located in a closest-packed row of atoms, the "crowdion." Several atomistic calculations on simple lattice defects have been published in recent years. Among these are the calculations due to Huntington [5], Fues and Stumpf [6], Kanzaki [7], Tewordt [8], Benneman [9], Girifalco and Weizer [10], Johnson and Brown [11], Johnson [12], and Dominigos [13]. These calculations are static calculations, and dynamical calculations [14] are not discussed here.

2. Method of Computation

The atoms close to a defect suffer displacements which are too large to be adequately described in terms of linear elastic theory. Because of this, these atoms are treated as individual atoms, the displacements of which are independent. This region is called region I. Atoms lying well away from the defect are displaced by small amounts which are susceptible to treatment by the elastic theory. Region I is surrounded by an array of atoms which are also regarded as discrete particles but whose displacements are given by linear elastic theory. This array can be divided into two regions (II and III). In region III none of the atoms interact with atoms in region I.

The interaction energy of the atoms in the crystal was represented by a Morse function. The interaction energy, $E(r_{ij})$, of a pair of isolated atoms is given by

$$E(r_{ij}) = D\{\exp[-2\alpha(r_{ij}-r_0)] - 2\exp[-\alpha(r_{ij}-r_0)]\},$$

where r_{ij} is the distance between the atoms, D is the dissociation energy of the pair, and r_0 is the equilibrium separation distance of the two atoms. α is a constant which effectively determines the

*Based on work performed under the auspices of the U. S. Atomic Energy Commission.

[1]Figures in brackets indicate the literature references at the end of this paper.

"hardness" of the potential. In the work described here, the interactions within a radius of $\sqrt{9.4}$ times the nearest-neighbor distances were taken into account. In a perfect crystal the number of atoms in this sphere of influence is 176. The constants were determined by the method used by Girifalco and Weizer [10, 15], using the Born stability criteria [16] and known experimental values of the lattice parameter and bulk modulus. Elastic constants calculated with the potential are in good agreement with experimental values.

The procedure for determining the equilibrium configuration and energy of a defect was as follows. All atoms were initially located on lattice sites. Atoms were then removed from or added to the center of region I so as to produce the desired defect. Each atom in region I was then moved in turn until the force on it was again zero. The atoms were moved in this manner in a series of cycles in which the atoms closest to the defect were moved more frequently than atoms more distant from the defect. The volume change and the total crystal energy were calculated after each cycle.

3. Results and Discussion

The formation energies of five different possible configurations of single interstitials in copper were calculated. The configurations that were examined are shown in figure 1. The relative formation energies of the various configurations, when they are artificially prevented from degenerating during the calculations, are shown in figure 1. It will be noted that the split-100 form has the lowest energy. When the constraint against degeneration is relaxed, it is found that all configurations spontaneously degenerate to the split-100 configuration. The latter is therefore the only stable form. This is in agreement with the conclusions drawn by Johnson and Brown [11] on the basis of their calculations, which involved the use of a Born-Mayer potential function. The absolute values of the formation energies of the various configurations are given in table 1. The potential used in obtaining these values was derived by use of the sublimation energy. Table 2 lists the corresponding values obtained with a potential which was derived from the vacancy formation energy. The discussion which follows refers only to the results listed in table 1. The difference between tables 1 and 2 is deferred to a later publication.

TABLE 1. *Energies and volumes of formation associated with interstitials (calculated with potential based on sublimation energy)*

Type	Formation volume	Formation energy	Energy above 100-split
	Ω	eV	eV
100-split	0.34	3.81	0.00
110-split	.34	3.96	.15
111-split	.36	4.07	.26
Body-center	.32	4.02	.21
Tetrahedral	.38	4.12	.31
Act 110	.36	3.97	.16

TABLE 2. *Energies and volumes of formation associated with interstitials (calculated with potential based on vacancy formation energy)*

Type	Formation volume	Formation energy	Energy above 100-split
	Ω	eV	eV
100-split	0.60	3.39	0.00
110-split	.56	3.77	.38
111-split	.78	3.96	.57
Body-center	.77	3.65	.26
Tetrahedral	.91	4.02	.63
Act 110	.80	3.77	.38

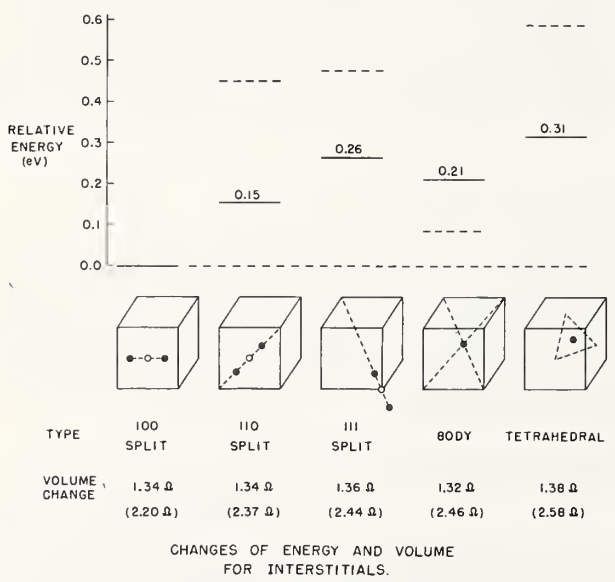

FIGURE 1. *Changes of energy and volume for interstitials.*
Dotted lines in the energy plot are the values by Johnson and Brown [11]. The values of volume changes in parenthesis are also by Johnson and Brown.

The volume change associated with the various types of interstitials are also given in figure 1. The actual increase in volume when an atom is removed from the surface and inserted into the interior of the crystal is about 0.4 atomic volumes.

Migration energies of the interstitials have also been calculated. The results are slightly different from the calculations using the Born-Mayer potential [11, 13]. The 100-split interstitial can migrate in a ⟨110⟩ direction with an activation energy of 0.15 eV. The 100-split interstitial can also rotate around the perfect lattice point on a {100} plane with an activation energy of 0.15 eV. The rotation is as easy as the migration.

Frenkel pairs were also studied. When the

vacancy and interstitial are nearest neighbors, there is no energy barrier against recombination. We may describe the various configurations of Frenkel pairs by quoting the distance between the vacancy and the interstitial and the angle between the axis of the dumbbell (split interstitial) and the line joining the vacancy to the center of the axis of the "dumbbell." Thus the nearest-neighbor pairs are described as the $d_0-90°$ type (of which there are four per interstitial) and the $d_0-45°$ type (of which there are eight). d_0 is the nearest-neighbor distance. Both of these types are unstable. There are four $d_0\sqrt{2}-90°$ and two $d_0\sqrt{2}-0°$ types, which are all unstable. All the types $d_0\sqrt{3}-\alpha$ are unstable, and so are all the types $2d_0-\alpha$ except the four pairs of type $2d_0-90°$. Thus the closest stable pair shows a separation distance of $2d_0$. Except for this last type of pair, the rule for spontaneous recombination seems to be that this occurs if the vacancy and interstitial have a common nearest-neighbor atom.

The greatest difficulty of these calculations is that the electron redistribution was not taken into account. Such effects could affect the results appreciably. The tetrahedral interstitial, for instance, has a high energy in the present calculations, but because of its high symmetry it may eventually be found stable when electron redistribution is taken into consideration.

4. Conclusions

Interstitials and Frenkel pairs in copper were studied. The formation energies and volume changes due to single interstitials are given in table 1. The 100-split interstitial was found to be the only stable interstitial. This interstitial can migrate into another 100-slit interstitial position with an activation energy of 0.15 eV, or it can rotate around the center of mass of the "dumbbell" with an activation energy of 0.15 eV.

The authors acknowledge the continuing interest and encouragement of T. H. Blewitt, H. H. Chiswik, F. G. Foote and O. C. Simpson. It is a pleasure also to acknowledge helpful discussions with K. H. Benneman, T. H. Blewitt, L. A. Girifalco, H. B. Huntington, R. A. Johnson, J. S. Koehler, F. Seitz, O. C. Simpson, L. Tewordt, and M. P. Tosi. The work described here was greatly facilitated by the help and cooperation of C. G. Le Vee and the scheduling, consulting, and operating personnel of the CDC 3600 computer at Argonne.

4. References

[1] P. M. Morse, Phys. Rev. **34**, 57 (1929).
[2] M. Born and E. Mayer, Z. Physik **75**, 1 (1932).
[3] H. B. Huntington and F. Seitz, Phys. Rev. **61**, 315 (1942).
[4] H. Paneth, Phys. Rev. **80**, 708 (1950).
[5] H. B. Huntington, Acta Met. **2**, 554 (1954).
[6] E. Fues and H. Stumpf, Z. Naturforsch. **109**, 136 (1955).
[7] H. Kanzaki, J. Phys. Chem. Solids **2**, 24 (1957).
[8] L. Tewordt, Phys. Rev. **109**, 61 (1958).
[9] K. H. Benneman, Z. Physik **165**, 445 (1951).
[10] L. A. Girifalco and V. G. Weizer, Phys. Rev. **114**, 687 (1959).
[11] R. A. Johnson and E. Brown, Phys. Rev. **127**, 446 (1962).
[12] R. A. Johnson, Phys. Rev. **134**, A1329 (1964).
[13] H. Dominigos, Bull. Am. Phys. Soc. II, **11**, 250 (1966).
[14] For example: J. B. Gibson, A. N. Goland, M. Milgram and G. H. Vineyard, Phys. Rev. **120**, 1229 (1960).
[15] L. A. Girifalco and V. G. Weizer, NASA, Report No. R-5 (1959).
[16] M. Born, Proc. Cambridge Phil. Soc. **36**, 360 (1940).

Morse Potential Calculations of Vacancy and Vacancy-Type Defect Properties in F.C.C. Metals*

R. M. J. Cotterill and M. Doyama

Argonne National Laboratory, Argonne, Ill. 60440

1. Introduction

Atomistic models and the central force approximation have been used in numerous studies of lattice defects in recent years. Among these are the calculations due to Huntington [1] [1], Fues and Stumpf [2], Kanzaki [3], Tewordt [4], Benneman [5], Girifalco and Weizer [6], and Johnson and Brown [7]. This paper describes calculations on vacancies and vacancy clusters, and the method of computation involves many of the features used by these authors. The interatomic potential was in all cases represented by a Morse [8] potential function.

Generally speaking, the atomic configurations of vacancy clusters are simpler than their interstitial counterparts. This is because the vacancy must of necessity be located at a lattice site, whereas the interstitial atom might be located at any other point in the Wigner-Seitz cell. The configuration of the divacancy is also obvious; two vacancies separated by a nearest-neighbor distance. The trivacancy is more complicated because it can exist in four different forms, each having a different binding energy. The tetravacancy is even more complicated. In this paper we examine all of these vacancy clusters in some detail. Also examined, but in less detail, are several larger clusters.

Large aggregates of vacancies usually find it energetically favorable to exist in the form of collapsed defects bounded by dislocations. This fact has been established by numerous experiments performed over the last eight years, the first direct evidence of this in metals being reported by Hirsch et al. [9], for quenched aluminum. More recently, however, open voids also have been seen [10]. If the aggregates are relatively large, their crystallographic nature can be determined quite precisely by transmission electron microscopy. The nature of the simplest clusters, such as the divacancy and trivacancy, is also well understood. It is the intermediate-sized clusters which now pose the main difficulty. Their energies and atomic configurations are not yet well known. A knowledge of their properties might permit a more complete interpretation of the quenching process and also perhaps the related processes of irradiation damage, diffusion, and mechanical deformation.

2. Method of Computation

The atoms immediately adjacent to a point defect, or a cluster of these defects, suffer displacements which are too large to be adequately described in terms of linear elastic theory. Because of this, these atoms must be treated as discrete particles. Atoms lying well away from the defect, on the other hand, are displaced by small amounts which are susceptible to treatment by the elastic theory. Because of this, the crystal containing the defect under examination was considered to consist of various regions. In the region immediately surrounding the defect, the atoms were discrete particles and their displacements were treated independently. The displacement of each atom in this region was determined by allowing it to interact with surrounding atoms according to a pair-wise central force law. This inner region was surrounded by an array of atoms which were also regarded as discrete particles but whose displacements were given by linear elastic theory.

The procedure for determining the equilibrium configuration and energy of a defect was as follows. All atoms were initially located on lattice sites. Atoms were then removed from or added to the center of region I so as to produce the desired defect. Each atom in region I was then moved in turn until the force on it was again zero. The atoms were moved in this manner in a series of cycles in which the atoms closest to the defect, which suffered the greatest disturbance, were moved more frequently than atoms more distant from the defect. After this variational process had been completed, the outer "elasto-atomic" region was displaced in such a way that equilibrium was restored. The

*Based on work performed under the auspices of the U. S. Atomic Energy Commission.

[1] Figures in brackets indicate the literature references at the end of this paper.

whole process was then repeated several times until the minimum energy condition was obtained. The number of iterations which were required to bring about complete stability was typically of the order of 25 to 50.

The formation energy of a cluster of λ point defects is

$$E^F_{\lambda V} = E'_{\lambda V} + \lambda E_S - E_p, \tag{1}$$

where $E'_{\lambda V}$ is the energy of the crystal containing the λ point defects (in the desired configuration), E_s is the energy of an atom on the surface of the crystal, and E_p is the energy of the perfect crystal with the λ atoms restored to their original positions. The binding energy against breakup into λ individual point defects is

$$E^B_{\lambda V} = \lambda E^F_V - E^F_{\lambda V}. \tag{2}$$

3. Calculation of the Constants of the Truncated Morse Potential

We follow the general method outlined by Girifalco and Weizer [11] by relating the potential to certain physical properties. The interaction energy, $E(r_{ij})$, of a pair of isolated atoms is then given by a Morse function,

$$E(r_{ij}) = D\{\exp[-2\alpha(r_{ij}-r_0)] - 2\exp[-\alpha(r_{ij}-r_0)]\}, \tag{3}$$

where r_{ij} is the distance between the two atoms, D is the dissociation energy of the pair, r_0 is the equilibrium separation distance of the two atoms, and α is a constant which effectively determines the "hardness" of the potential.

The energy of a crystal containing N atoms is

$$E = \frac{1}{2} ND \sum_{j=1}^{j=J} \{\exp(-2\alpha[r_j - r_0]) - 2\exp(-\alpha[r_j - r_0])\}, \tag{4}$$

where the factor $\frac{1}{2}$ is required to allow for the double counting of bonds. J is the total number of atoms which fall within the sphere of influence of a given atom. r_j is related to the lattice parameter by

$$r_j^2 = l_j^2 a^2 + m_j^2 a^2 + n_j^2 a^2 = M_j^2 a^2, \tag{5}$$

where a is the half-lattice parameter, l_j, m_j and n_j are integers, and their sum is always even for the f.c.c. lattice. The sublimation energy at zero temperature and pressure is given by

$$U_0(a_0) = E(a_0). \tag{6}$$

The Born stability criteria [12] require that

$$\left(\frac{dE}{da}\right)_{a=a_0} = 0, \tag{7}$$

and the compressibility at zero temperature and pressure, K_{00}, is given by

$$\frac{1}{K_{00}} = V_{00}\left(\frac{d^2E}{dV_0^2}\right)_{a=a_0}, \tag{8}$$

where V_{00} is the atomic volume at zero temperature and pressure and V_0 is the volume at zero temperature. Because the volume per atom in the f.c.c. structure is $2a^3$, eq (8) may be written

$$\frac{1}{K_{00}} = \frac{1}{18Na_0}\left(\frac{d^2E}{da^2}\right)_{a=a_0}. \tag{9}$$

Equations (6), (7), and (9), when used together, are sufficient to determine the three parameters D, α, and r_0 in the Morse potential. Equation (4) is used throughout in such a determination of constants, and the latter will clearly depend upon the value of J.

In the work described here, J was taken to be 176 and the constants were then $r_0 = 2.91295$ Å, $d_0 = 2.54756$ Å, $D = 0.32265$ eV and $\alpha = 1.28663$ Å^{-1}. Elastic constants calculated with the potential are in good agreement with experimental values.

4. Results

4.1. The Single Vacancy

The nearest-neighbor atoms of a single vacancy are found to relax inwards by a distance of 3.0 percent of the nearest-neighbor distance. The second neighbors relax outwards slightly by about 1.5 percent. The formation volume of the vacancy was found to be 0.83 Ω for copper, where Ω is the atomic volume. This compares with the experimental value for gold, which ranges from the value of De Sorbo [13] (0.57 Ω), to that of Simmons and Balluffi [14] (0.45 Ω). Theoretical values of ΔV^F_V have been reported for copper by Tewordt [4] (0.47–0.55 Ω), Seeger and Mann [15] (0.71–0.91 Ω), Benneman [5] (0.60 Ω), Johnson and Brown [7] (0.43–0.62 Ω), and Schottky, Seeger, and Schmid [16] (0.76–0.98 Ω). All these values were obtained by use of a Born-Mayer potential. The vacancy formation energy was found to be 3.2 eV. The activation energy of vacancy migration is found to be 0.69 eV. This compares with previous values of E^M_V calculated for copper by Huntington and Seitz [17] (1 eV), Fumi [18] (0.6 eV), Bartlett and Dienes [19] (0.97 eV), Damask, Dienes, and Weizer [20]

(1.3 eV), and Johnson and Brown [7] (0.43 eV). Direct experimental values of E_V^M have been reported by Schüle et al. [21], and by Hasiguti et al. [22]. They obtain 1.08 eV and 1.06 eV, respectively. The activation volume of self-diffusion was found to be 0.86 Ω in the present study, and activation volume for vacancy migration is therefore 0.03 Ω. Johnson and Brown [7] found a value $\Delta V_V^M = 0.19$–0.38 Ω. Schottky, Seeger, and Schmid [16] find 0.02–0.10 Ω. Emrick [23] has reported an experimental value of 0.15 Ω in gold.

4.2. Divacancies

The present calculation gives a divacancy binding energy in copper of 0.53 eV. Bartlett and Dienes [19] calculated 0.3 eV, and Weizer and Girifalco [24] give 0.64 eV. No experimental values of E_{VV}^B in copper have been reported. For gold it is greater than 0.3 eV [25]. For silver it is 0.38 eV [26]. The activation volume associated with the formation of a divacancy was found to be 1.53 Ω. The volume change associated with the formation of the divacancy from two isolated vacancies is 0.13 Ω. The binding energy for the loosely bound divacancy in which the two vacancies are separated by a second-nearest-neighbor distance was found to be 0.19 eV, and the volume change associated with this configuration is virtually the same as for two isolated vacancies.

When a divacancy migrates, the saddle point was found to be located at the center of the equilateral triangle defined by the original positions of the two vacancies and the position of the moving atom. The saddle point lies very close to the plane of that triangle. This saddle point is therefore equivalent to a triangular arrangement of three two-thirds vacancies surrounding the migrating atom. The energy barrier against motion was found to be 0.02 eV. This value is, of course, much lower than what would be expected. There are no experimental values of E_{2V}^M for copper, but this quantity has been measured in gold. Bauerle and Koehler [27] give 0.6 eV approximately.

4.3. Trivacancies

There are four possible types of trivacancies. They are the 60°, 90°, 120°, and 180° types, where the angles refer to the angles which the two outer vacancies subtend at the middle vacancy. The 60° type was investigated by Damask et al., [20]. They find that the atom located immediately above the three vacancies is able to relax downwards towards the center of the triangle and that its final equilibrium position is exactly at the center of the tetrahedron defined by the positions of the three vacancies and the moving atom. This configuration is equivalent to a symmetrical arrangement of four three-quarter vacancies surrounding an interstitial atom. Figure 1 shows the relative

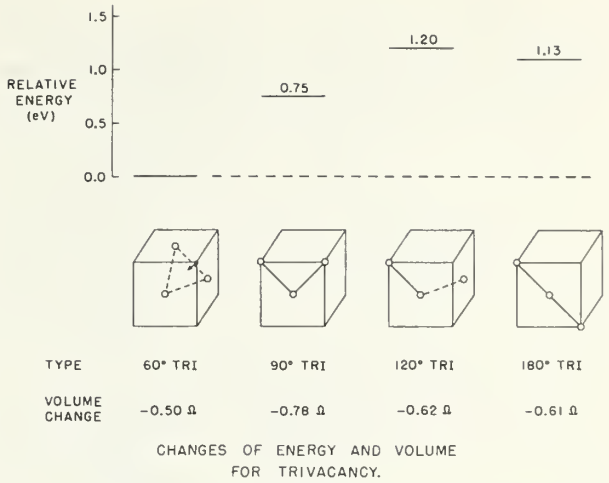

FIGURE 1. *Relative energies and activation volumes for trivacancies.*

binding energies of various trivacancies obtained in this study. It may be noted that the 60° is much more tightly bound than the other types. The actual formation volume of each defect is the number given in the figure plus 3 Ω, where Ω is the atomic volume. As might be expected, the 60° type shows the smallest contraction.

4.4. Tetravacancies

Calculations for some tetravacancy configurations have been reported by Vineyard and Gibson [28]. The configurations shown in figure 2 are of particular interest because they are quite compact. The relative binding energy of each of the

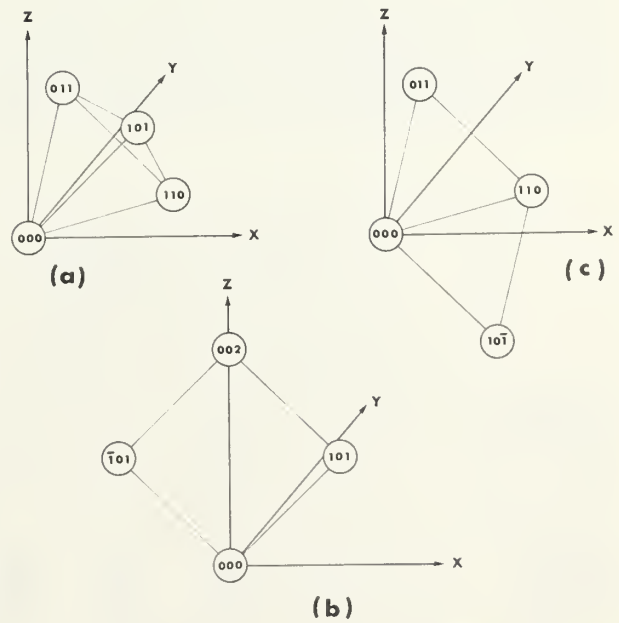

FIGURE 2. *Configurations of the three tetravacancies considered in the present study.*

only stable or metastable configurations is given in figure 3. The results do show that the rhombic form is the most stable. The rhombic form is related to the 60° trivacancy discussed earlier. It permits two of the relaxations which occur in that trivacancy, since it is effectively two adjacent 60° trivacancies joined along a common side. It has been shown that the low energy of the rhombic form may indicate collapse of vacancy clusters to dislocation loops at an early stage of growth.

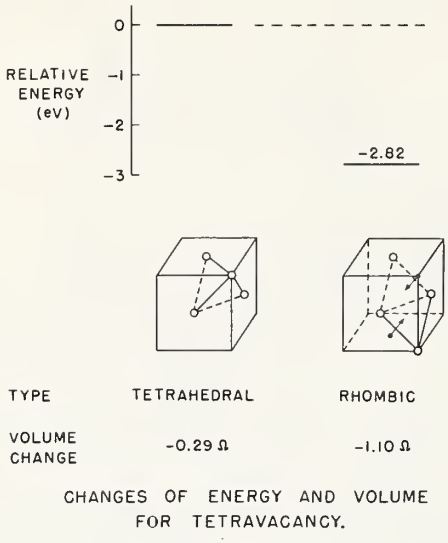

FIGURE 3. *Relative energies and activation volumes for tetravacancies.*

4.5. Larger Clusters of Vacancies

Calculations are now under way for larger clusters of vacancies. The smallest octahedral void, consisting of six vacancies, is stable. There is a vacant space of about two atomic volumes in the interior of the defect. This could be the nucleus of the large uncollapsed octahedral void observed by Yoshida et al., [10]. Larger clusters of vacancies on {111} planes are also being examined, and it is being found that the role of the 60° trivacancy as the "building block" of collapsed clusters, which was previously discussed in connection with the rhombic tetravacancy, is continued. The next larger octagonal void, which contains 19 vacancies, has also been examined recently. It too is found to be stable against spontaneous collapse. This result is intrinsically dependent upon the use of a potential which has an attractive term. A calculation which employed a Born-Mayer potential would not give stability.

5. Postscript

When a Morse potential is used to calculate the formation energy of point defects, the absolute values of the latter are always rather high. Electron redistribution around the defect must account for part of the discrepancy. Another source of error may arise from the fact that eq (6) implicitly assumes that the electron environment which applies when (4) is used is the same as the environment which prevails during the measurement of U_0. This is probably not true because the evaporation of a neutral atom from the surface requires first the localization of an electron at the atom which is to be removed. Because of these difficulties, an alternative approach could be used which links the Morse potential to the experimental value of E_V^F, the vacancy formation energy, rather than to E_S, the sublimation energy. The hope would then be that the absolute values of the binding, migration, and formation energies might also be more reliable. Table 1, which summarizes the energies obtained in the present calculations, includes entries for energies calculated by this alternative approach.

TABLE 1

Defect	Properties calculated by use of sublimation energy		Properties calculated by use of vacancy formation energy	
	Formation volume	Formation energy	Formation volume	Formation energy
	Ω	eV	Ω	eV
Single vacancy	0.83	3.19		1.17
Single vacancy motion	.86	3.88		
Divacancy	1.53	5.85	1.72	2.16
Divacancy motion	1.47	5.88		
Next-nearest neighbor divacancy	1.66	6.21		
60° trivacancy	2.50	7.33	2.49	3.05
90° trivacancy	2.26	8.09	2.59	3.10
120° trivacancy	2.38	8.54	2.67	3.14
180° trivacancy	2.39	8.46	2.65	3.14
Tetrahedral tetravacancy	3.71	11.73	3.85	3.70
Rhombic tetravacancy	2.90	8.96	3.42	3.82

The authors acknowledge the continuing interest and encouragement of T. H. Blewitt, H. H. Chiswik, F. G. Foote, and O. C. Simpson. It is a pleasure also to acknowledge helpful discussions with K. H. Benneman, T. H. Blewitt, L. A. Girifalco, H. B. Huntington, R. A. Johnson, J. S. Koehler, F. Seitz, O. C. Simpson, L. Tewordt, and M. P. Tosi. The work described here was greatly facilitated by the help and cooperation of C. G. Le Vee and the scheduling, consulting and operating personnel of the CDC 3600 computer at Argonne.

5. References

[1] H. B. Huntington, Acta Met. **2,** 554 (1954).
[2] E. Fues and H. Stumpf, Z. Naturforsch. **109,** 136 (1955).
[3] H. Kanzaki, J. Phys. Chem. Solids **2,** 24 (1957).
[4] L. Tewordt, Phys. Rev. **109,** 61 (1958).
[5] K. H. Benneman, Z. Physik **165,** 445 (1961).
[6] L. A. Girifalco and V. G. Weizer, Phys. Rev. **114,** 687 (1959).
[7] R. A. Johnson and E. Brown, Phys. Rev. **127,** 446 (1962).
[8] P. M. Morse, Phys. Rev. **34,** 57 (1929).
[9] P. B. Hirsch, J. Silcox, R. E. Smallman, and K. H. Westmacott, Phil. Mag. **3,** 897 (1958).
[10] M. Kiritani, J. Phys. Soc. Japan **19,** 618 (1964); M. Kiritani and S. Yoshida, Japan J. Appl. Phys. **4,** 148 (1965).
[11] L. A. Girifalco and V. G. Weizer, NASA Rept. No. R–5 (1959).
[12] M. Born, Proc. Cambridge Phil. Soc. **36,** 160 (1940).
[13] W. De Sorbo, Phys. Rev. **117,** 444 (1960).
[14] R. O. Simmons and R. W. Balluffi, Phys. Rev. **125,** 862 (1962).
[15] A. Seeger and E. Mann, J. Phys. Chem. Solids **12,** 326 (1960).
[16] G. Schottky, A. Seeger and G. Schmid, Phys. Stat. Solidi **4,** 419 (1964).
[17] H. B. Huntington and F. Seitz, Phys. Rev. **61,** 315 (1942).
[18] F. G. Fumi, Phil. Mag. **46,** 1007 (1955).
[19] S. H. Bartlett and G. J. Dienes, Phys. Rev. **89,** 848 (1953).
[20] A. C. Damask, G. J. Dienes and V. G. Weizer, Phys. Rev. **113,** 781 (1959).
[21] W. Schüle, A. Seeger, D. Schumacher and K. King, Phys. Stat. Solidi **2,** 1199 (1962).
[22] R. R. Hasiguti, Y. Nakao, and H. Kimura, J. Phys. Soc. Japan **20,** 553 (1965).
[23] R. M. Emrick, Phys. Rev. **122,** 1720 (1961).
[24] V. G. Weizer and L. A. Girifalco, Phys. Rev. **120,** 837 (1960).
[25] J. W. Kauffman and M. Meshii, Lattice Defects in Quenched Metals, p. 77, edited by R. M. J. Cotterill, M. Doyama, J. J. Jackson, and M. Meshii (Academic Press, New York, 1965).
[26] M. Doyama and J. S. Koehler, Phys. Rev. **127,** 21 (1962).
[27] J. E. Bauerle and J. S. Koehler, Phys. Rev. **107,** 1493 (1957).
[28] G. H. Vineyard and J. B. Gibson, Bull. Am. Phys. Soc. **6,** 158 (1961).

A Two-Body Central Force Interatomic Potential for Anharmonic Solids

Roger Chang and Lloyd J. Graham

North American Aviation Science Center, Thousand Oaks, California 91360

A prerequisite to the application of numerical methods with high speed computers to studying defects in solids is the availability of reliable interatomic potentials between the atoms. Previous investigations of the two-body central force interatomic potential in solids have not touched upon the effects of anharmonicity. Since nearly all solids have some degree of anharmonicity, it is the purpose of this paper to find an empirical approach to obtain an interatomic potential which takes into consideration the anharmonic effects.

The theory of anharmonic effects in crystalline solids has been discussed in considerable detail by Liebfried and Ludwig [1].[1] For a two-body central force model, explicit relationships exist between the second, third and higher order elastic constants of a solid and the interatomic potential, the details depending on the symmetry of the crystal and the number of shells used in computing the interactions. In this paper the body-centered cubic iron is used as an illustration where nearest and next-nearest neighbor interactions only are considered. If $\varphi(r)$ is the potential between a pair of atoms of separation r, r_1 the nearest neighbor separation and r_2 the next-nearest neighbor separation, the relationships between the second and third order elastic constants and the interatomic potential are, using the Voight notation [2],

$$C_{11}=\frac{2}{3r_2}\left[\frac{2\varphi'(r_1)}{r_1}+\varphi''(r_1)+3\varphi''(r_2)\right]+P$$

$$C_{12}=\frac{2}{3r_2}\left[\frac{-4\varphi'(r_1)}{r_1}+\varphi''(r_1)-\frac{3\varphi'(r_2)}{r_2}\right]-P$$

$$C_{44}=\frac{2}{3r_2}\left[\frac{2\varphi'(r_1)}{r_1}+\varphi''(r_1)+\frac{3\varphi'(r_2)}{r_2}\right]+P$$

$$C_{111}=\frac{\varphi'''(r_1)}{3\sqrt{3}}-\frac{\varphi''(r_1)}{\sqrt{3}\,r_1}-\frac{8\varphi'(r_1)}{r_1^2\sqrt{3}}+2\varphi'''(r_2)-\frac{6\varphi''(r_2)}{r_2}-3P$$

$$C_{112}=\frac{\varphi'''(r_1)}{3\sqrt{3}}-\frac{\varphi''(r_1)}{\sqrt{3}\,r_1}+\frac{4\varphi'(r_1)}{r_1^2\sqrt{3}}+\frac{2\varphi'(r_2)}{r_2^2}+P$$

$$C_{123}=\frac{\varphi'''(r_1)}{3\sqrt{3}}-\frac{\varphi''(r_1)}{\sqrt{3}\,r_1}-\frac{2\varphi'(r_1)}{r_1^2\sqrt{3}}-\frac{2\varphi'(r_2)}{r_2^2}-P \qquad (1)$$

where P is the external pressure and $\varphi'(r_i)$, $\varphi''(r_i)$ and $\varphi'''(r_i)$ are the first, second, and third derivatives of the potential $\varphi(r)$ with respect to r and evaluated at r_i, respectively.

We express the potential $\varphi(r)$ as a Taylor's expansion up the the fourth power in r (φ in eV, r in Angstroms),

$$\varphi(r)=A+Br+Cr^2+Dr^3+Er^4 \qquad (2)$$

Although higher orders in r may be included in eq (2), we feel that the expression to the fourth power in r is enough for the present purposes. The constant A in eq (2) goes out when it is fed into eq (1). Thus there are only four independent constants to be evaluated in eq (2). Since six experimental elastic constants are available for comparison, there is sufficient redundancy to check out the consistency of the computation.

Differentiating eq (2) with respect to r, one finds,

$$\begin{aligned}\varphi'(r)&=B+2Cr+3Dr^2+4Er^3\\ \varphi''(r)&=2C+6Dr+12Er^2\\ \varphi'''(r)&=6D+24Er.\end{aligned} \qquad (3)$$

We choose P in eq (1) to be equal to $(C_{12}-C_{44})/2$, where C_{12} and C_{44} are the experimental elastic constants. Substituting eq (3) into eq (1), one obtains a set of computed elastic constants which can be compared with the experimental values. The fitting is done numerically with the aid of computers. A reasonably good fit yields the following constants for eq (2),

$$B=-12.2404 \text{ eV } (\text{Å})^{-1}$$

$$C=1.24594 \text{ eV } (\text{Å})^{-2}$$

$$D=0.815729 \text{ eV } (\text{Å})^{-3}$$

$$E=-0.156140 \text{ eV } (\text{Å})^{-4}.$$

[1] Figures in brackets indicate the literature reference at the end of this paper.

The computed elastic constants using the above parameters are compared with the experimental values in table 1, showing reasonably good agreement. The force-distance plot is compared with those from three other potentials, the Morse [3], Lennard-Jones [4] and Johnson [5] potentials in figure 1. The comparison shows that our potential is very close to that of Johnson's. It is noted that the method yields the potential only within a region between and shortly beyond the nearest and next-nearest neighbor distances. Further information is needed to obtain a potential which will cover the full range. This is beyond the scope of the present paper.

TABLE 1. *Comparison of computed and experimental elastic constants (in units of 10^{12} dynes/cm^2)*

	Calculated (this paper)	Experimental	Reference
C_{11}	2.323	2.33	[6]
		2.28	[7]
C_{12}	1.327	1.35	[6]
		1.32	[7]
C_{44}	1.148	1.18	[6]
		1.165	[7]
C_{111}	−24.40	−33.5	[8]
C_{112}	−2.673	−3.3	[8]
C_{123}	−2.494	−3.1	[8]

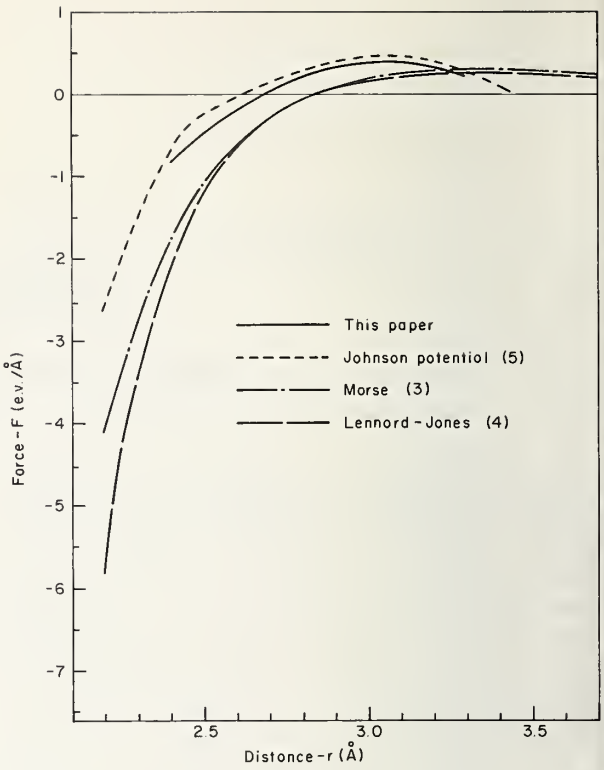

FIGURE 1. *Comparison of force-distance plots: body-centered cubic iron.*

References

[1] G. Leibfried and W. Ludwig, Solid State Physics **12**, 275 (1961).
[2] R. A. Coldwell-Horsfall, Phys. Rev. **129**, 22 (1963).
[3] L. A. Girifalco and V. G. Weizer, Phys. Rev. **114**, 687 (1959).
[4] R. Fürth, Proc. Roy. Soc. London **A183**, 87 (1944–45).
[5] R. A. Johnson, Phys. Rev. **134**, 1329 (1964).
[6] J. A. Rayne and B. S. Chandrasekhar, Phys. Rev. **122**, 1714 (1961).
[7] A. E. Lord and D. N. Beshers, J. Appl. Phys. **36**, 1620 (1965).
[8] A. Seeger and O. Buck, Z. Naturforsch. **15A**, 1056 (1960).

A Reexamination of the Born-Mayer Potential for Ion-Core Interactions in Copper*

S. S. Jaswal[1] and L. A. Girifalco

University of Pennsylvania, The School of Metallurgical Engineering and Laboratory for Research on the Structure of Matter, Philadelphia, Pa. 19104

Ion-core short-range interactions between nearest neighbors in copper have been approximated by the Born-Mayer potential by Huntington and Seitz [1],[2] Huntington [2], and others [3]. Huntington used the experimental values of the bulk and shear moduli, the free electron approximation with effective mass for valence electrons and Fuchs's calculations [4] reduced by one half for the electrostatic contribution to the shear moduli to compute the parameters in the Born-Mayer potential.

Fuchs computed the electrostatic contributions to the shear constants arising from distorting a lattice of positive point charges immersed in a uniform distribution of conduction electrons. As pointed out by Huntington it is hard to determine what these contributions really are in a case such as copper. The values, as computed by Fuchs, are listed in table 2. Since this contribution to C_{44} is significant, the uncertainty in C_{44} in large.

According to Fuchs [5] the contribution of the ground state energy to the bulk modulus is negligible and it is only through the Fermi energy that the conduction electrons contribute to the bulk modulus. Huntington's calculations are based on this idea.[3]

When a number of potentials of the Born-Mayer type were compared in radiation damage calculations [6], a potential which is close to that suggested by Huntington turned out to be quite good. However the contribution of this potential to $(C_{11}-C_{12})$, as listed in table 2, shows large disagreement with the experimental value [7] even when one takes into account the electrostatic contribution as computed by Fuchs. Since the electrostatic contribution to C_{44} is quite significant, due to the uncertainty in this contribution, it is difficult to make any meaningful comparison for this quantity.

In present calculations we use the experimental values of cohesive energy, lattice parameter and bulk modulus to determine the Born-Mayer parameters and hence avoid the uncertainties in theoretical estimates of the shear constants. Since we use the cohesive energy and its volume dependence, we must take into account all the volume dependent terms in the energy rather than just the Fermi energy.

The various terms considered in the interaction energy besides the Born-Mayer potential are the ground state energy of the conduction electrons based on a simplified theory due to Fröhlich [8], and the Fermi, Coulomb, exchange and correlation energies of conduction electrons based on the free electron model in the effective mass approximation. In Fröhlich's theory, the potential in the outer part of the unit cell is assumed to be hydrogenic and the conduction electrons are treated as free. An advantage of this theory is that one has an analytical expression for the ground state energy. Other terms in the energy mentioned above are computed on the assumption of a uniform conduction electron density. The correlation energy used is the interpolation result due to Nozieres and Pines [9].

The interaction energy per unit cell can be written as:

$$E_{\text{int}} = E_0 + E_{k.e} + E_{ex} + E_{c0} + E' + E_{c-c} \qquad (1)$$

where

$$E_0 = \text{ground state energy}$$

$$= -3/r_s + \rho_0^2/r_s^3$$

with ρ_0^2 being an unknown parameter:

$$E_{k.e} = \text{Fermi energy}$$

$$= 2.21/[(m^*/m)\, r_s^2]$$

*Supported by ARPA. A more detailed form of this paper has appeared in J. Phys. Chem. Solids **28**, 457 (1967).

[1] Present address: Physics Dept., Univ. of Nebraska, Lincoln, Neb. 68508.

[2] Figures in brackets indicate the literature references at the end of this paper.

[3] In reference 2 there is an error in equation (4). The number 5 in the denominator in first term on right-hand side should be replaced by 3.

with m^* being the effective mass and m, the free electron mass;

$$E_{ex} = \text{exchange energy}$$
$$= -0.916/r_s;$$
$$E_{c0} = \text{correlation energy}$$
$$= -.115 + 0.031 \ln r_s:$$
$$E' = \text{coulomb energy}$$
$$= 1.2/r_s;$$

and

$$E_{c-c} = \text{contribution of core-core interactions}$$
$$= 6\alpha \exp\left[(r_0 - r)\rho/r_0\right]$$

with r_0 being the equilibrium separation of ions and α and ρ are the parameters to be determined.

In this expression r_s, the radius of the equivalent sphere, is expressed in atomic units and energy in Rydbergs.

E_{int} can also be written as

$$E_{\text{int}} = E_I - E_{\text{sub}} \tag{2}$$

where E_I is the ionization potential of copper atom and E_{sub} is the sublimation energy of copper.

The equilibrium condition for the lattice gives

$$(dE_{\text{int}}/dr_s)|_0 = 0 \tag{3}$$

where $|_0$ stands for the value at equilibrium.

Also the second derivative of the interaction energy is related to the compressibility β by

$$(d^2E_{\text{int}}/dr_s^2)|_0 = 12\pi r_s/\beta. \tag{4}$$

Equations (2), (3), and (4) are used to determine the unknown parameters ρ_0^2, α and ρ.

Experimental values used in our calculations are as follows;

$E_I = -7.724$ eV; $\quad E_{\text{sub}} = 80.6$ kcal/mol

$r_s = 2.66$ a.u.; $\quad 1/\beta = 14.4 \times 10^{11}$ dynes/cm^2

and $m^* = 138$m as given by specific heat measurements [10].

TABLE 1. *Parameters of the present and some of the earlier Born-Mayer-potentials*

Potential	α (eV)	ρ
(1) Present	0.0958	13.34
(2) Huntington's	.053	13.9
(3) Gibson et al's	.051	13.0

Solving eqs (2), (3), and (4) for α and ρ we get $\alpha = 0.0958$ eV, $\rho = 13.34$ and $\rho_0 = 0.47$ a.u. We compare our results with some of the earlier potentials in table 1 and figures 1 and 2.

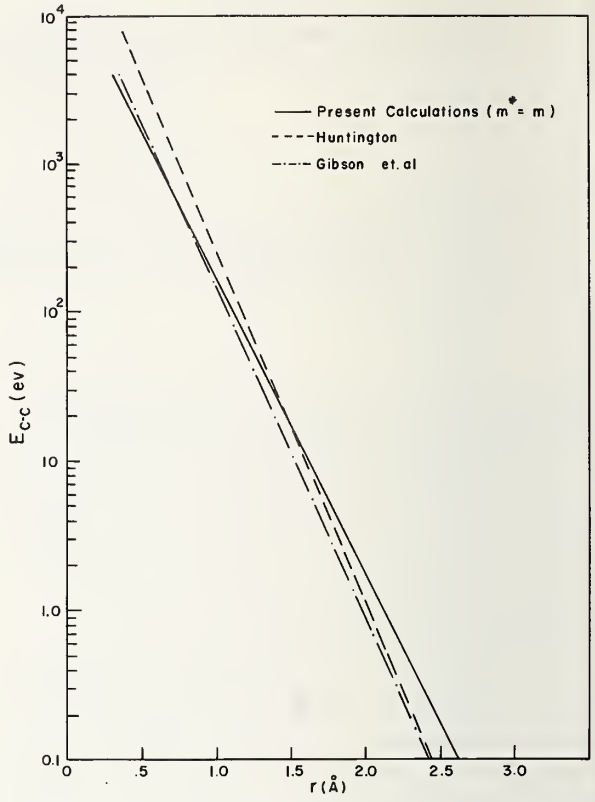

FIGURE 1. *Born-Mayer potential in eV as a function of core-core separation in Å when effective mass is equal to that of a free electron.*

The contributions due to the Born-Mayer potential to shear constants are given by [4]

$$(C_{11} - C_{12})_{c-c} = (1/2)N[r^2E''_{c-c} + 7\, rE'_{c-c}]r_0 \tag{5}$$

and

$$(C_{44})_{c-c} = (1/2)N[r^2E''_{c-c} + 3rE'_{c-c}]r_0 \tag{6}$$

where N is the number of ions per unit volume and primes indicate the derivatives with respect to r. Using eqs (5) and (6) we have computed Born-Mayer contributions to shear constants and results are given in table 2.

TABLE 2. *Shear constants* in units of 10^{11} dynes/cm^2*

	$(C_{11} - C_{12})$	C_{44}
Potential 1	5.55	9.06
Potential 2	3.49	5.51
Potential 3	2.8	4.5
Experiment, 0 °K	5.28	8.35
Electrostatic contribution	0.57	2.57

*First three lines list the contribution of Born-Mayer potential to shear constants. Last line list the electrostatic contribution as computed by Fuchs.

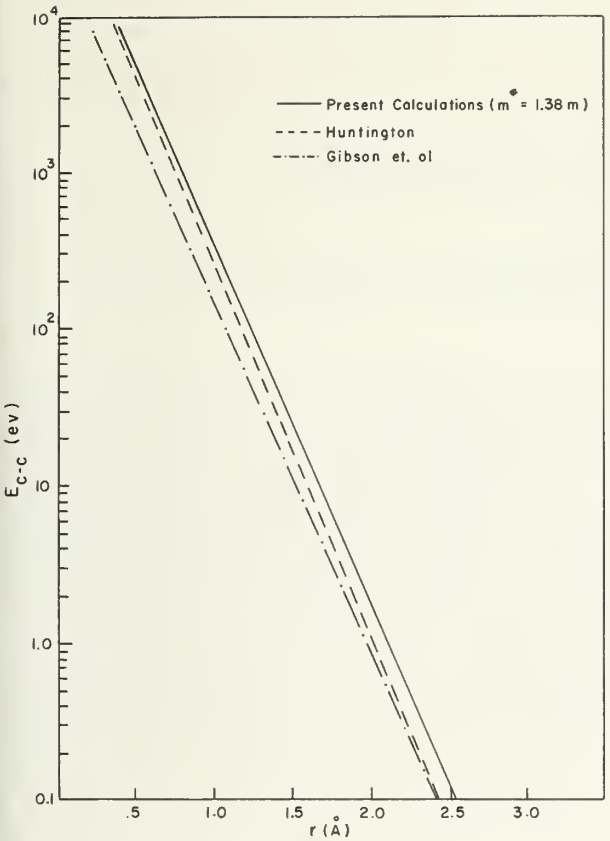

FIGURE 2. *Born-Mayer potential in eV as a function of core-core separation in Å when effective mass is 1.38 times that of a free-electron.*

Keeping in view the uncertainties in electrostatic contributions to the shear constants, agreement between our calculations and experimental results is quite good.

The potential based on the Thomas-Fermi-Dirac approximation (TFD) as computed by Abrahamson [6, 11] is considered reasonable around ion-core separation of about 0.5 Å. Our potential at such separations is in fair agreement with TFD.

Thus we have computed the Born-Mayer parameters which are of the same order of magnitude as have been used earlier by various people. However we have improved upon the earlier parameters by computing them in a self consistent manner within the approximations mentioned above and the agreement with shear constant $(C_{11}-C_{12})$ is much better in our case.

References

[1] H. B. Huntington and F. Seitz, Phys. Rev. **61**, 315 (1942).
[2] H. B. Huntington, Phys. Rev. **91**, 1092 (1953).
[3] C. Zener, Acta Cryst. **3**, 346 (1950); G. J. Diennes, Phys. Rev. **86**, 228 (1952).
[4] K. Fuchs, Proc. Roy. Soc. (London) **A153**, 622 (1936).
[5] K. Fuchs, Proc. Roy. Soc. (London) **A151**, 585 (1935).
[6] J. B. Gibson, A. N. Goland and G. H. Vineyard, Phys. Rev. **120**, 1229 (1960).
[7] H. B. Huntington, Solid State Physics **7** (1958).
[8] H. Fröhlich, Proc. Roy. Soc. **A158**, 97 (1937); H. Brooks, Supp. Nouvo Cimento **7**, 236 (1958).
[9] Nozieres and Pines, Phys. Rev. **111**, 442 (1958).
[10] W. S. Corak, M. P. Garfunkel, C. B. Satterthwaite, and A. Wexler, Phys. Rev. **98**, 1699 (1955); J. A. Rayne, Australian J. Physics, **9**, 189 (1956).
[11] A. A. Abrahamson, thesis, New York University, 1960 (unpublished); A. A. Abrahamson, R. D. Hatcher, and G. H. Vineyard, Bull. Am. Phys. Soc. **5**, 231 (1960).

256-724 O-67—5

The Interactions Between Point Defects*

J. S. Koehler

Department of Physics and Materials Research Laboratory, University of Illinois, Urbana, Ill. 61681

If it is assumed that the interaction between point defects in solids can be considered as a rapidly convergent series of two body interactions, three body interactions and higher order terms, then if one supposes that three body interactions and higher order interactions are negligible, information can be obtained concerning the strength of the two body forces provided their variation with distance and with the orientation of the defect separation relative to the crystal axes is known. The experimental information used is the formation energy of various point defects and the binding energy of various defect clusters. In addition the experimental stacking fault energy of both intrinsic and extrinsic stacking faults provide valuable data. From the fact that interstitials do precipitate in the form of low energy stacking faults it is shown that either interstitials attract one another or that three body and other multibody forces are of importance. A similar statement can be made for lattice vacancies. The equivalence of vacancies and interstitials for producing a given platelike precipitate is shown. The present formulation when it includes only two body interactions can be checked against experiment provided that enough experimental data is available. Although not enough data exists at present for any material, such a check would be valuable since it would determine the magnitude of the three body and higher multibody forces.

*Supported by the U.S. Atomic Energy Commission under Contract AT(11-1)-1198.

The Energies and Configurations of Point Defects in Solids

A. B. Lidiard

Theoretical Physics Division, U.K.A.E.R.E., Harwell, Didcot, Berks, England

(Panel Members: R. Bullough, H. Kanzaki, A. B. Lidiard, A. Seeger, M. P. Tosi and G. H. Vineyard)

1. Introduction

The topics included for discussion by Panel I were the energies and configurations of defects—especially those questions raised by the papers presented in the first two sessions. It was possible to group these questions as follows.

1.1. Ionic Crystals

(i) General relations of the new calculations presented at the conference (papers by Boswarva and Lidiard, Dienes et al., Franklin, Tosi and Doyama and Tharmalingam) among themselves and to previous calculations.

(ii) Specific questions of the method of treating the long-range displacement and polarization fields around charged defects. Here one had the papers by Kanzaki and Kurosawa and the discussion remarks by McCombie and Mullen among others.

(iii) Comparison of the interionic potentials used in these calculations, e.g., choice between Born-Mayer and Born-Mayer-Verwey forms, and the significance of van der Waals terms for these calculations. This aspect of the subject gave rise to a rather varied discussion.

1.2. Covalent Semiconductors

The discussions and contributions of the conference to this class of materials were disappointingly few. This remains an area where there appears no very consistent approach to defect problems. The most general approach is that of Bennemann but this has not yet been related to more conventional methods, e.g., those of Hasiguti and of Moore and Carlson.

1.3. Metals

(i) The whole question of the use of 2-body potential models for metals is important. While a general justification can be found in the method of pseudopotentials it is not evident that one can in this way find a justification for the particular forms of potential convenient for computer calculations e.g., Morse potentials, polynomials, etc. as used in the papers by Cotterill and Doyama and by Johnson. The panel also had before it two papers on the empirical determination of potentials by Chang and Graham (α-Fe) and by Jaswal and Girifalco (Cu).

(ii) The complexity of some of the larger computer calculations now being made means that, as with experimental work, the results cannot be verified by inspection in the way that theoretical arguments usually can be checked. The repetition of these computations by other workers is therefore equally as valuable as the verification of the experimental results of one laboratory by another. This sort of comparison was made at the conference for α-Fe (Beeler, Chang, and Johnson) and for Cu (Doyama, Johnson, and Seeger). Many of these calculations are made for model crystallites containing several hundred atoms and such comparisons are therefore valuable not simply to avoid program mistakes, truncation errors etc. but also to assess the sensitivity of the results to the size of the model.

We shall report on these topics in the way they were dealt with during the panel discussion but we also include a number of pertinent remarks made from the floor.[1]

[1] In presenting this report I have had the benefit of written contributions from Drs. Beeler, Hatcher, McCombie, Tosi, and Vineyard and I have not hesitated to use these as submitted where appropriate. The extensive remarks of Dr. Vineyard form the basis of section 3 on metals. However I have edited all this material substantially and accept responsibility for the correctness or otherwise of the views and comments presented.

2. Ionic Crystals

2.1. Interrelations Between Different Calculations

The defects one is concerned with in ionic crystals often have an effective electrical charge, e.g., ion vacancies and interstitial ions. As was shown long ago by Jost, the polarization of the lattice by these charges is important in lowering the energy of the defects, but the long range of electrical interactions makes it difficult to deal with them as one

deals with short-range forces. One cannot, for example, set up crystallite models on a computer in the same way as has been done for metals. Owing to the presence of these long-range electrical interactions it has been customary, following the original paper of Mott and Littleton, to divide the crystal into two regions, I and II; the first includes the defect and as much of its immediate surroundings as is judged desirable, while the second is the rest of the crystal. The idea is that in the outer region II the displacements and electronic dipole moments of the ions are small enough that a harmonic theory can be used; this is important as it allows the incorporation of information from other studies, e.g., dielectric constants and lattice dynamics. In region I on the other hand the harmonic approximation may not be adequate and the ionic interactions are represented explicitly by an assumed potential function (electrical plus overlap interactions). This division of the crystal into two regions is followed in the papers presented by Boswarva and Lidiard, Franklin and Tosi and Doyama, as well as in a number of previously published papers [1],[2] which also broadly follow the Mott and Littleton method.

Let us look more closely at the formal aspects of this division into regions I and II. It is basic to all models that we can specify the state of the system by the nuclear coordinates and the electronic moments of the ions. In regions I and II we specify the positions of the ions collectively by x, ξ and the moments by m, μ respectively. Then the potential energy function of the defect solid is written

$$V = V_1(x, m) + V_2(x, m; \xi, \mu) + V_3(\xi, \mu). \quad (1)$$

It is convenient to group terms so that $V_3(\xi, \mu)$ contains only quadratic terms in ξ and μ, i.e., so that it is the potential energy of a distorted and polarized region II filled with a perfect undistorted unpolarized lattice region I. The condition of equilibrium is that V should be a minimum with respect to variations in x, m, ξ, and μ, i.e.,

$$\frac{\partial V}{\partial x} = 0 \qquad \text{(I)}, \quad (2)$$

$$\frac{\partial V}{\partial m} = 0 \qquad \text{(I)}, \quad (3)$$

$$\frac{\partial V}{\partial \xi} = 0 = \frac{\partial V}{\partial \mu} \qquad \text{(II)}. \quad (4)$$

Equations (4) are not solved explicitly in methods derived from Mott and Littleton, but physically plausible approximations to the equilibrium values $\bar{\xi}$ and $\bar{\mu}$ are assumed instead. This applies to the greater part of the work in this field including the papers presented by Boswarva and Lidiard, Tosi and Doyama and Franklin. A convenient way to solve eq (4), which exploits the quadratic form of $V_3(\xi, \mu)$ was originally described by Kanzaki [2] and applied by him and by Hardy [3] to electrically neutral defects. It has now been applied to charged defects [4] and the long-range displacement and polarization fields so deduced provide an objective way of assessing the Mott-Littleton and related assumptions (see below).

The dependence of V upon m is also generally assumed to be quadratic so that eq (3) is equivalent to the elementary relation $m = (\text{polarizability} \times \text{electric field})$. Polarizabilities of many ions are believed to be well known, but it is not obvious that this linear relation between field and moment still holds at the large fields existing near a defect ($e/r_0^2 \sim 10^8$ V/cm). In addition as pointed out by Mullen these polarizabilities might also be changed in the vicinity of the defect due to the mechanical stresses there. Neither of these effects has yet been evaluated.

These assumptions of harmonic dependence upon m, μ, and ξ enable V to be put in a more convenient form, but here a difference arises between some of the calculations. Equilibrium values of m, μ, and ξ can be obtained for any configurations, x, of region I; call these $\bar{m}(x)$, $\bar{\mu}(x)$ and $\bar{\xi}(x)$. By eqs (3) and (4) we then have

$$\frac{d}{dx} V(x, \bar{m}; \bar{\xi}, \bar{\mu}) = \frac{\partial}{\partial x} V(x, m; \xi, \mu)\Big|_{\bar{m}, \bar{\xi}, \bar{\mu}} = 0 \quad (5)$$

as equivalent equations for the equilibrium x. In the papers of Boswarva and Lidiard and of Franklin the first member of (5) is used whereas in the paper of Tosi and Doyama the second is used, as in the earlier work of Kurosawa. If the assumptions made about $\bar{m}(x)$, $\bar{\mu}(x)$ and $\bar{\xi}(x)$ were exact then the calculated values of the equilibrium V would be identical, whichever path is followed. Any divergence may therefore be a measure of the inaccuracy of these assumptions. However, the divergence in the numerical results presented to the conference by Boswarva and Lidiard on one side and by Tosi and Doyama on the other is not due principally to such inaccuracies but comes from different choices of potential. When the Tosi-Doyama model is used in the Boswarva-Lidiard program the results are nearly coincident [5]. The inclusion of van der Waals terms in the potential function is important for this agreement, however.

It is worth noting that the form of the equilibrium polarization energy is $-\frac{1}{2}\bar{\mathbf{m}} \cdot \mathbf{F}^{(1)}$ summed over all the ions; in region II we can replace the moment

[2] Figures in brackets indicate the literature references at the end of this paper.

$\overline{m}$ by the sum of $\overline{\mu}$ with the moment resulting from the displacement of the ion charge. In both regions, however, $F^{(1)}$ is due only to the effective monopoles. in region I, e.g., the missing charge on the vacancy. The moments $\overline{m}$, of course, depend on all the dipole sources as well (field $\mathbf{F}^{(2)}$). It is not correct to represent the polarization energy as $-\frac{1}{2}\alpha|\mathbf{F}|^2$ with $\mathbf{F}=\mathbf{F}^{(1)}+\mathbf{F}^{(2)}$. This would count dipole-dipole interactions twice. Such a double counting may lead to large errors; the original results of Dienes [6] on the activation energy for vacancy pair migration are very low, apparently for this reason [7]. But Scholz presented to the conference results for the formation energy of Schottky defects in NaCl which showed that use of the incorrect form gave energies only about 0.1 eV too high -2.55 eV compared to 2.44 eV. These numbers were obtained using the small crystallite method with the Tosi and Fumi potential [8]. They stand rather high relative to the values coming from a Mott-Littleton approach, but this is almost certainly because the crystallite is too small—the additional polarization energy of an infinite crystal would be $\sim -\frac{e^2}{2R}\left(1-\frac{1}{\epsilon}\right)$ where R is the equivalent radius of Scholz' crystallite and ϵ is the dielectric constant. For NaCl this is about -0.4 eV per vacancy.

2.2. The Displacement and Polarization Fields

As noted above the use of the Kanzaki method to solve eq (4) enables an independent assessment of the assumptions of methods derived from Mott and Littleton. A recent study for the NaCl structure has determined the displacement and polarizations at large distances from the defect [4]. The displacements of the ions are made up of an elastic term ξ_{elas}, of the same sign for anions and cations, and an electrical polarization term ξ_{elec} which is opposite for anions and cations. This electrical term can be written

$$\xi_{\text{elec}}=\pm\frac{ee^*}{2\overline{M}\omega_\ell^2}\left(\frac{\epsilon_\infty+2}{3\epsilon_\infty}\right)\frac{\mathbf{r}}{r^3} \tag{6}$$

where e^* is the effective ionic charge of Szigeti, ω_ℓ is the frequency of the longitudinal optic mode at long-wavelengths, $\overline{M}$ is the harmonic mean of the masses of the anions and cations $(M_+M_-)/(M_++M_-)$ and ϵ_∞ is the high frequency dielectric constant, related to the electronic polarizabilities by the Clausius-Mosotti formula. If the Szigeti charge $e^*=e$ and if only nearest neighbor closed-shell repulsions are significant then one can show that (6) reduces exactly to the Mott-Littleton assumption, i.e.,

$$\xi_{\text{elec}}=\frac{\pm\alpha_c}{(\alpha_++\alpha_-+2\alpha_c)}\frac{v}{4\pi}\left(1-\frac{1}{\epsilon_0}\right)\frac{\mathbf{r}}{r^3} \tag{7}$$

where v is the molecular volume, ϵ_0 is the static dielectric constant and α_c is the displacement polarizability as defined by Mott and Littleton. On the other hand if $e^*\neq e$ then (6) reduces to the formulae used in the paper by Boswarva and Lidiard for the 'deformation dipole' model. In all cases the electrically induced electronic moments on the ions are as assumed in Mott-Littleton theory. However, with the deformation dipole model $e^*\neq e$ there are additional electronic dipoles (on the anions) caused by the relative displacement of the ions and the form assumed for these by Boswarva and Lidiard agrees with that obtained from the examination by the Kanzaki method.

Finally, this examination shows that for an elastically isotropic solid the elastic term is

$$\xi_{\text{elas}}=\frac{G}{4\pi C_{11}}\frac{\mathbf{r}}{r^3} \tag{8}$$

where C_{11} is the elastic constant and G is proportional to the force on the near neighbors of the vacancy (actually to that product which in a dynamical problem would be the virial of these forces). This differs from the proposal of Brauer [1] and the modification suggested by Boswarva and Lidiard in fixing the elastic strength of the vacancy by the force on the near neighbors rather than by their displacement. The magnitude of the strength, however, appears generally to be less than one obtains following Brauer's suggestion.

Mullen criticized the Mott-Littleton type of calculation for the way it assigns the moments and displacements to the ions of the crystal. While this assignment was originally intuitive the above results obtained by the Kanzaki method provide a rigorous basis for it and therefore answer this criticism. A more important aspect of the criticism is the use of the forms valid at large distances from the defect right up to the first shell of neighbors, i.e., that a region I containing only the vacancy and its six nearest neighbors is not large enough. The work of Scholz on a crystallite model shows how one can make computations with a much enlarged region I—although as previously noted it is not correct to neglect region II altogether. The importance of examining and establishing the validity of the Mott-Littleton approach is that if one is confident of its correctness for simple defects one can then proceed to more complex ones, e.g., vacancy clusters. At present the study of unsymmetrical and complex defects in ionic crystals is well behind that in metals.

It was recognized that the elastic strength of the defect may present problems especially in these more complex cases e.g., elastically anisotropic crystals (nearly all) or unsymmetrical defects such as dumbbell interstitials or vacancy pairs. Some results of Kanzaki's lattice statics method for these

cases were contained in the paper he put before the conference.

An alternative approach is contained in the paper of Kurosawa and was independently emphasized by McCombie. The idea here is that whenever one considers all degrees of freedom of a few shells of atoms round the defect but forces the behavior of all more remote atoms to conform to a continuum form specified by only a limited number of parameters (e.g., elastic strength) there is a problem of matching the solutions in the two regions. Because of the limitations imposed on the long range displacements and polarizations it will not be possible to choose the local displacements and polarizations and the long range parameters in such a way that every atom has zero force on it and also has exactly the dipole moment required by the electric field on it.

A reasonable procedure (which avoids attaching excessive weight to the exact equilibrium of the first shell of the continuum region) is to choose the local coordinates, local polarizations and long range parameters in such a way as to minimize the sum of the squares of the "error forces" and "error polarizations" for the local atoms and for a few shells of atoms in the region treated as a continuum. One can check that the results obtained are reasonably insensitive to the number of shells of the continuum region taken into account.

Slater and McCombie in Aberdeen some years ago applied essentially this method to investigating low frequency spherically symmetric vibrations round a vacancy in diamond. For a given low frequency they determined the amplitudes of vibration of the first few neighboring shells and of the parameters describing the long range displacement by minimizing the sum of the squares of the error forces in the equation of motion of the neighboring shells and of the first few shells of the continuum region. The linear equations embodying the least squares condition were easily set up and solved on a computer. The results were satisfactorily insensitive to both the number of neighboring shells treated as local, and the number of shells of the continuum region included with them in the least squares calculation. It would be very interesting to see this method applied to static defect calculations.

2.3. Potentials in Ionic Crystals

The most widely used closed-shell interaction potential is the Born-Mayer exponential form $\exp(-r/\rho)$. We would intuitively expect this form from the exponential decay of charge density on the periphery of an atom or ion, and Hartree-Fock calculations for the interactions of two Ne atoms support the expectation. Even the Thomas-Fermi model leads to an interatomic potential which is exponential over a fair range of separations (9). In ionic crystals the potential is generally written in an expanded form, e.g.,

$$V_{ij}(r) = b_{ij} \exp(r_i + r_j - r)/\rho,$$

for the interaction between ions i and j; r_i and r_j are ionic radii. The preexponential coefficient is generally fixed by a relation due to Pauling. The paper by Franklin on CaF_2 drew attention to this relation and indicated that it may be misleading. It is, *faute de mieux*, almost always used for the alkali halides.

If one tries to develop a detailed theory of defects in the framework of the ionic model, there are some conditions that the potential adopted ought to satisfy. One is on the radii, which ought to be consistent with the electron maps. The other is consistency with the cohesive properties, i.e., the first and second derivative of the potential must fit the interionic distance and the compressibility. Under these conditions, one might expect that calculations on vacancies would not be very sensitive to the fundamental form of the potential, on which, of course, the cohesive energy gives only broad indications. The results of Tosi and of Boswarva and Lidiard, however, show that the variations may be important if one desires accuracy of, say, 10 to 20 percent.

A number of defect calculations in the alkali halides which included second-neighbor interactions have been based on the Born-Mayer potential (BM), of an exponential form with parameters determined by Born and Mayer by fitting the interionic distance and (on the average) the compressibility of the alkali halides under the assumption that the Goldschmidt radii are representative of the ionic sizes in crystals. This potential in both NaCl and KCl gives only a small restoring force on the positive ions neighboring a negative ion vacancy. This leads to incorrectly low energies of formation for the negative-ion vacancy and for the Schottky pair.

The Born-Mayer-Verwey potential (BMV) which stiffens the interionic repulsions at distances smaller than the equilibrium nearest-neighbor distance, was used by Tosi et al. [10], to test empirically the sensitivity of migration barriers to the hardness of the potential. It has led to reasonable results in activation energy calculations; this success is however achieved at the expense of having an unphysical discontinuity in the second derivative of the short-range interaction energy at the equilibrium interionic distance.

Tosi has also emphasized that the r^{-12} form of the BMV potential varies much more rapidly than is allowed by the compressibilities of the alkali halide crystals. Thus fitting the exponent n in an assumed form r^{-n} leads to values between about 6 for LiF and 11 for CsI. Probably the BMV potential should now be discarded. There are, how-

ever, situations where the r^{-n} form is still useful, but for these the appropriate values of n should be obtained from crystal data.

The Tosi-Fumi potential [8] retains the BM form: it involves a careful determination of the parameters from recent data, and yields values of the ionic radii in crystals in agreement with the electron maps. When used in defect calculations the van der Waals energy should however also be included. This may be avoided, as Boswarva and Lidiard have done, by adopting the Tosi-Fumi values of the ionic radii and refitting the other parameters of the potential to the interionic distance and the compressibility. Nevertheless, as noted above, explicit inclusion of the van der Waals terms leads to small but significant increases in the calculated formation energies of Schottky defects. They appear to be more significant in defect calculations than previously supposed.

Further work is needed on the vacancy migration problem in the alkali halides. So far, it has not been clear that one could obtain a reasonable barrier for the direct path along the face diagonal with a potential appropriate to the perfect crystal. The results presented by Tosi and Doyama assuming a direct path show a near equality of anion and cation vacancy activation energies for NaCl, KCl, and RbCl. Haven pointed out that the experimental differences between anion and cation activation energies may be too large due to the predominance of multivalent *cation* impurities in even highly pure crystals. Nevertheless the best experimental values are considerably farther apart than the calculated ones. Haven also pointed out that one needs now to investigate indirect paths through the body of the cell. Tosi believes that indirect paths are favored in the case of large alkali impurities: in particular, for Rb^+ in NaCl, for which the impurity diffusion measurements of Arai and Mullen [11] indicate a moderate energy and a considerable entropy of diffusion.

Hatcher drew attention to the difficulty of dealing satisfactorily with the small impurity ion e.g., Li^+ in KCl and KBr. In KCl the equilibrium position of the Li^+ ion is known experimentally to be displaced from the exact cation site, whereas in KBr it is not. The small Li^+ ion can polarize the anion by moving towards it and the induced moment attracts the Li^+. According to Hatcher the Tosi-Fumi form of BM potential cannot account for the different behavior in KBr and KCl. Tosi regards this as a severe test of the potential function since the energy differences between the displaced and undisplaced positions are only ~ 0.01 eV.

However, from the paper of Dienes et al., it is clear that this system tests the model in a more drastic way. Thus the small Li^+ ion can move sufficiently close to the anion that the attraction resulting from the induced polarization, which in the point dipole model varies like r^{-4}, can outweigh the BM repulsion ($\sim \exp -r/\rho$) and the model breaks down completely. Scholz reported that in some crystals he found related divergences of the displacement of the ions around a vacancy. These occurred when a BM potential was used although not with the BMV form. The r^{-12} form of the BMV potential clearly prevented the r^{-4} attraction from taking over. Dienes et al., also modified the BM potential to guard against this effect in their calculations. These difficulties are of the same kind as originally led Verwey to propose his modification of the BM potential in order to account for the properties of both alkali halide molecules and crystals with the same ionic model. This problem, however, remains one worthy of further attention.

It will be clear that with the BM potential there may always be a risk of these divergences occurring. Even if actual divergences do not occur ions may approach too close together so that the energy is too low. As Tosi noted this is very likely to happen when the BM form is used in conjunction with Goldschmidt radii which are small for cations. Tharmalingam reported that the use of Goldschmidt radii in a BM potential gave a very low energy of formation for the vacancy pair in NaCl, only 0.07 eV, whereas the use of the Tosi-Fumi crystal radii gave a sensible value -0.91 eV including the van der Waals Term.

We may perhaps summarize this section by saying that fundamental knowledge of interaction potentials is rather meager. The choice of forms available to anyone setting out on defect calculations is still as it was 30 years ago, i.e., Born-Mayer and r^{-n}. However there is no doubt that the particular BM potential given by Tosi and Fumi, supplemented by a van der Waals term, is very superior to the original Born-Mayer form. This is apparent from the manner of its derivation and also from the results which it gives for defect formation and migration energies. However, it is evident that there are difficulties with the model, stemming from the point-dipole approximation, at small separations which are avoided by using r^{-n} potentials. Although the color center calculations were not the subject for the present panel it is nevertheless worth noting that BM and r^{-n} may lead to rather different predictions especially for the relaxation occurring in excited electronic states (papers by Bennett and by Öpik and Wood). We note that little attempt to derive interionic potentials from fused salts seems so far to have been made.

3. Metals

Several calculations of defects in metals were discussed at this conference, and Professor Huntington gave an expert history of the subject. These calculations all start from the common assumption

that the Born-Oppenheimer approximation is valid, which is to say that the complete dynamical problem of a crystal can be separated into a calculation of the eigenstate of the electrons for arbitrary, fixed positions of the nuclei, $R_1, R_2 \ldots R_n$, and a calculation of the effective potential for nuclear configurations associated with this eigenstate, $V(R_1, \ldots R_n)$. This potential for nuclear configurations determines the energies of formation and the energies of migration of the various lattice defects. Once V is known, the calculation of these energies reduces to a mathematical exercise in finding extremal values of a function of very many variables. Although this exercise is by no means trivial, numerical solutions to satisfactory accuracy can be found with modern computers, and this part of the problem is now relatively satisfactory.

The papers presented at this conference expounded two different approaches for estimating the function $V(R_1, \ldots R_n)$, either over all of configuration space, or at least at several points in this space. In what may be called the fundamental approach, one attempts to calculate the potential properly for selected nuclear configurations by solving the wave equation for all the electrons of the metal in the nuclear field. In the other method, which might be called the phenomenological method, one deduces a plausible function $V(R_1, \ldots R_n)$ by using many diverse bits of information, some theoretical and some empirical.

Historically, as pointed out by Huntington, the first serious attempts to calculate properties of defects in metals proceeded by the fundamental method, and for many years this was the only method of any importance [12]. The fundamental treatments that have been given have the obvious advantage that they start from a well-grounded position, and use respectable quantum mechanical procedures throughout. Because of the complexity of the quantum mechanical problem, however, they only yield definite answers after various approximations. There are so many ways in which these approximations may be arranged that it is impossible to describe the situation adequately briefly. Professor Seeger described some new methods of this sort which may well provide important improvements, and Dr. Moore opened some new avenues with his numerical calculations for a quasi-molecule representing a portion of a crystal containing a defect. However, detailed consequences of the approach of Seeger and Mann are still being worked out, and the greater quantum mechanical rigor of Moore's calculations has been purchased at the price of limiting the quasi-molecule to a very small number of atoms. In all of the fundamental calculations that have been made, one has been limited to defect configurations of high symmetry, with relaxations of neighboring atoms either assumed small, or neglected altogether. In principle, these relaxations could be perfected in a self-consistent way, but the process is most laborious. These remarks are meant not to disparage the various fundamental calculations which have been made, but to put them in some perspective.

The phenomenological procedures have come upon the scene relatively recently. They have been prompted, at least in some part, by the power of modern computers to give elaborate and detailed results about defects once a potential has been assumed. An older view would have been that such potentials can only be deduced sensibly for van der Waals crystals, and that the attempt to apply them to metals reveals less about defects in metals than of the judgement of he who applies them. This view is too harsh, even as the literal acceptance of all energies calculated with phenomenological potentials would be naïve. It should be mentioned that the pseudopotential approach (see e.g., the paper of Huntington and Feit) allows one to represent the energy of the solid as a sum of three terms (1) a free-electron volume-dependent term, (2) the coulomb interaction energy of the bare ions, and (3) a band structure term which is reducible to a sum of two body potentials which ought to tie up with the phenomenological potentials. The volume dependent term is left out in some treatments, e.g., the Morse potential treatment of Doyama and Cotterill; this is a step which has not been justified by those taking it. In other treatments simple volume-dependent forces are included—a situation colloquially described as putting the crystallite in an elastic bag. In general these treatments have not included the long-range oscillations known to occur in the band-structure term. Bullough, pointed out the need to include these oscillations in some calculations, e.g., stacking fault energies, where interactions at long range are important. This might also be true for interstitial vacancy close-pair interactions.

3.1. Phenomenological Calculations

Vineyard presented the general case for phenomenological methods as useful and fruitful complements of more fundamental methods as follows.

In setting up a phenomenological potential to describe any crystal, whether metal or insulator, the essential considerations are as follows. One knows that the crystal will be at equilibrium in the configuration of a perfect lattice of a certain form, with a certain lattice constant and a certain binding energy. Thinking in terms of the many dimensional configuration space of the system (with a finite number, n, of atoms), one thus knows that the potential function $V(R_1, \ldots R_n)$ possesses minima at the perfect lattice points of configuration space, and one knows the depths of these minima. Now a good deal is also known about V in the neighborhood of such a minima. First, the elastic constants determine a small number of second order coefficients in the Taylor expansion of V (considered in a suitable set of axes). Moreover, if one can find

all the Born-von Karman coupling constants of the lattice through techniques such as neutron inelastic scattering, one can determine all of the Taylor coefficients of the second order. Higher order elastic coefficients and anharmonic coupling constants determine higher order Taylor coefficients. Besides the minima, V possesses poles at all points where two or more nuclei coincide. Information on V in the neighborhood of these poles is obtainable in other ways. Two-body interactions clearly dominate here, and the strength of two-body interactions is found from gas scattering experiments and from direct calculations, either fully quantum mechanical, or on the basis of statistical models. Moreover, sputtering and radiation damage experiments shed light on the problem. Threshold studies of radiation damage are particularly sensitive indicators of the strength of two-body interactions. Finally all other available information on special configurations should be used. March pointed out the value of the pair correlation function for liquids in providing information about the hard-core part of the interatomic potential. Bullough mentioned the stacking fault energy of f.c.c. metals for its sensitivity to the long-range part of the potential and reported that in Al the oscillations in this potential were vital to the accurate calculation of stacking fault energies. There was some argument between Bullough and Cotterill about the speed of convergence of the lattice sums occuring in the stacking fault problem; the size of the computer model is an important feature in the accuracy of these calculations with oscillatory potentials. Owing to the different structure of b.c.c. metals their stacking fault energies depend also on near neighbor interactions; they thus provide a check on the potential at short range as well.

Out of all this one constructs a function $V(R_1 \ldots R_n)$ which goes as far as possible toward matching all of the data. Clearly such functions are not unique. Their construction is essentially an interpolation in configuration space. In this way various potentials have been deduced and have been employed for calculating the properties of defects.

An important advantage of the phenomenlolgical approach is that it allows far more complicated defects to be studied than will soon be handled on anything approaching a fundamental basis. At worst, one is studying defects on a model, which has some resemblance to a real crystal. Thus many clusters of point defects, and even realistic three-dimensional dislocations have recently been subjected to study. At this conference, papers were presented by Doyama and Cotterill and by Johnson that fall into this category. Such work in progress was also described in discussion by Beeler and by Bullough.

A rather large number of independent calculations with somewhat different forms of V have produced concordant results on several defects, and it seems these results must be right. The small relaxation of the neighbors of the vacancy, and the ⟨100⟩ split form of the interstitial, with larger lattice distortion, seem well established in f.c.c. lattices. Likewise the ⟨110⟩ split form of the interstitial in b.c.c. lattices is rather strongly supported. The low migration energy of the interstitial compared with the vacancy is a common feature of all calculations, even though actual values of these migration energies are not very certain. The conference was not, unfortunately, able to get to grips with the long standing problem of the divergence between the well-known calculation of Seeger, Mann, and von Jan [13] for the Cu interstitial ($E_m = 0.6$ ev) and other calculations which have, as in the paper of Doyama and Cotterill, generally led to much lower values (~ 0.1 eV). Johnson has been unable to reproduce the value of Seeger et al., but it appeared from the discussion that the original calculations have not been exactly repeated. This point is an important one for the subject and should be followed up further—quite independently of the question of experimental interpretations.

In the calculations reported at this meeting, certain interesting features deserve emphasis. These features are unquestionably valid for the model potentials employed, even though they may or may not prove to be true for the real crystals simulated. In general, the great complexity of possible point defects and their migration processes is, for the first time, becoming clear. Frenkel pairs appear to have very different properties in their different configurations, and a number of close pairs appear to be unstable. In addition, more distant pairs may exhibit reduced activation energies for recombination, or show binding, or even trapping. The interstitial in the f.c.c. lattice appears to migrate in a complex way in which it moves to a neighboring site in its plane and changes its axis in so doing. A consequence of this migration process is that, without reorientation, which may involve a higher activation energy, a given interstitial can only reach three out of the four types of interpenetrating simple cubic lattices into which the f.c.c. lattice may be resolved. Furthermore, Johnson's model shows four metastable configurations of the interstitial, in addition to the stable form, and the differences in energy between these are surprisingly small. Plots of lattice energy versus a reaction coordinate for the migration of the interstitial prove to be complicated by intermediate saddle points in addition to the principal saddle point. With combinations of point defects more and more kinds of stable or metastable clusters are being found as more calculations are being done. Although, as has been emphasized, these results are demonstrably valid only for model crystals, there seems no reason to believe that defects in real crystals are less complex. As more calculations are carried out, the apparent complexity will probably continue to increase.

One important practical point in these calculations is the size of the crystallite which is simulated on the computer. Beeler drew attention here to the differences between vacancy and interstitial calculations. The calculations on α-Fe show that the relaxations around interstitials are large enough that the continuum elastic region surrounding the discrete crystallite exerts a significant constraint and may not be ignored. It is less important for vacancies and vacancy clusters.

There is a proper balance between the degree of sophistication of a model and the extent of the numerical calculations that are worth carrying out. There is now a danger that the crudities of the phenomenological model will be forgotten in the enthusiasm to exploit the computer in more and more detailed investigations. The practitioner of these methods should feel the obligation to perfect his phenomenological potentials by making them harmonize with as many of the various separate bits of information, outlined above, as he can get his hands on and can trust. As more data becomes available, more considerations of this kind must be taken. Finally, these calculators should have a proper scepticism of their own results, and should feel a responsibility to prevent their results from being taken too literally by nonspecialists. In the present stages, calculated activation energies of motion surely do not have significance to two decimals—possibly not to one! Nevertheless, the range of defect phenomena which the calculations suggest, and their broader features, are sufficiently plausible that they warrant extensive experimental testing, and also cross-checking by fundamental calculations to the fullest extent that is feasible.

4. References

[1] See N. F. Mott and M. J. Littleton, Trans. Far. Soc. **34**, 485 (1938); P. Brauer, Z. Naturforsch **7a**, 372 (1952); F. G. Fumi and M. P. Tosi, Disc. Far. Soc. No. 23, 92 (1957); T. Kurosawa, J. Phys. Soc. Japan **13**, 153 (1958); K. Tharmalingam, J. Phys. Chem. Solids **25**, 255 (1964).

[2] H. Kanzaki, J. Phys. Chem. Solids **2**, 24 (1957).

[3] J. R. Hardy, J. Phys. Chem. Solids **15**, 39 (1960); ibid. **23**, 113 (1962).

[4] J. R. Hardy and A. B. Lidiard, Phil. Mag. **15**, 825 (1967).

[5] I. M. Boswarva and A. B. Lidiard, Phil. Mag. (in press).

[6] G. J. Dienes, J. Chem. Phys. **16**, 620 (1948).

[7] K. Tharmalingam and A. B. Lidiard, Phil. Mag. **6**, 1157 (1961).

[8] F. G. Fumi and M. P. Tosi, J. Phys. Chem. Solids **25**, 31 (1964); M. P. Tosi and F. G. Fumi Ibid **25**, 45 (1964).

[9] A. A. Abrahamson, Phys. Rev. **133**, A990 (1964).

[10] R. Guccione, M. P. Tosi and M. Asdente, J. Phys. Chem. Solids **10**, 162 (1959).

[11] G. Arai and J. G. Mullen, Phys. Rev. **143**, 663 (1966).

[12] H. B. Huntington, Acta Met. **2**, 554 (1954); E. Fues and H. Stumpf, Z. Naturforsch **109**, 136 (1955); L. Tewordt. Phys. Rev. **109**, 61 (1958).

[13] A. Seeger, E. Mann and R. v. Jan, J. Phys. Chem. Solids **12**, 314 (1960).

II. Electronic States

Vacancies, Phonons, and Dielectric Screening in Close-Packed Metals

N. H. March

Laboratory of Atomic and Solid State Physics, Cornell University, Ithaca, New York 14850

and

B. Oli

Department of Physics, The University, Sheffield, England

The role of dielectric screening in determining the electronic configuration round a vacancy in close-packed metals is emphasized. In particular (i) Mukherjee's relation between vacancies and phonons is interpreted in a first order theory, the essential link being the response of the Fermi gas, described by its wave number dependent dielectric constant, to the two different perturbations. (ii) The Fermi energy E_f times the valency Z is shown to be a natural unit in which to measure the vacancy formation energy E_v. For simple metals, the experimental results then vary systematically with Z, and yield Fumi's value (4/15) for the limit of small Z. (iii) Utilizing the semiempirical method of Kohn and Vosko, vacancies in Cu and Al are shown to lead to displaced charge densities which correlate fairly well with results for impurities in these same matrices. Again, the concept of a dielectric constant seems entirely meaningful, if not quantitative for the stronger scattering centers. The dielectric constant should also describe the interaction between a pair of ions. Some difficulties are encountered for Al.

1. Introduction

Since the classic studies of Huntington [1],[1] it has been clear that the electronic wave functions of the conduction electrons are markedly distorted around vacant lattice sites in metals. That the displaced charge around the vacancy also oscillated with distance from the vacancy was apparent in the work of Huntington, and was perhaps especially clear in the later work of March and Murray [2].

In spite of this, it is perhaps fair to say that no very direct experimental evidence has been forthcoming about the relevance of such oscillatory screening of the vacant lattice site. Nevertheless, without explicit appeal to dielectric screening (see 2, below), Fumi [3] recognized the importance of the Fermi energy E_f, and of complete shielding, inserted through the Friedel sum rule, in the problem of calculating vacancy formation energies in monovalent metals. Another step forward, which we believe will prove of considerable importance, came with the observation by Mukherjee [4], that there is an accurate empirical relation between the vacancy formation energy E_v and the Debye temperature θ for close-packed metals. A first-order theory based on linear screening has been given by one of us (March [5],) and a more general formulation has been considered recently (see especially Enderby and March [6],). The essential argument is briefly summarized in 3. In 4, some evidence is brought forward that a dielectric constant can be defined which is relevant for a variety of charged perturbations in Cu and Al. In particular, displaced charges and corresponding potentials for the vacancy correlate well with those for impurities in these matrices. Some difficulties, however, are apparent for Pb, which have not as yet been resolved.

2. Wave-Number-Dependent Dielectric Constant

Before proceeding to discuss the Mukherjee relation, it is worth stressing that, in the work of Huntington and the later studies of March and Murray [2] on the electronic redistribution round the vacancy, individual electronic wave functions were calculated explicitly. Such an approach makes the problem appear quite complex.

The first clear demonstration that a simpler point of view could be adopted was in fact given earlier by Mott [7], who stressed that an excellent physical description of a Zn impurity in Cu, say, was to view the Zn ion as 'dressed' with a very

[1] Figures in brackets indicate the literature references at the end of this paper.

localized screening cloud of electrons; the displaced charge. Mott's model was linear and the screened potential energy $V(r)$ around a point charge Z (Z being the excess valence, i.e., 1 for Zn in Cu)[2] was

$$V(r)=\frac{-Z}{r}\exp(-qr): \qquad q^2=\frac{4k_f}{\pi}, \tag{2.1}$$

where the inverse screening radius q was determined solely by the properties of the unperturbed Fermi gas, that is the Fermi wave number k_f. The corresponding displaced charge density $\rho(r)-\rho_0$, ρ_0 being the unperturbed constant density in a simple free electron description, was given by

$$\rho(r)-\rho_0=\frac{q^2}{4\pi}V(r). \tag{2.2}$$

The charge piles up around an attractive impurity, of course, but is repelled from a vacant site.

In addition to this important idea of an ion or defect, 'dressed' with a localized electron cloud which screens it perfectly, the Mott theory also implies that the screening of the defect center is simply to be described by a dielectric constant. Thus, introducing the Fourier transform of the screened potential

$$\tilde{V}(k)=\int V(r)e^{i\mathbf{k}\cdot\mathbf{r}}\,d\mathbf{r}, \tag{2.3}$$

we may write

$$\tilde{V}(k)=\frac{-4\pi Z}{k^2\epsilon(k)}, \tag{2.4}$$

where $\epsilon(k)$ is the wave number dependent dielectric constant. From (2.3) it follows that

$$\epsilon(k)=\frac{k^2+q^2}{k^2}. \tag{2.5}$$

A more correct result was given by Lindhard as

$$\epsilon(k)=\frac{k^2+\frac{k_f}{\pi}g\left(\frac{k}{2k_f}\right)}{k^2}, \tag{2.6}$$

where

$$g(x)=2+\frac{x^2-1}{x}\ln\left|\frac{1-x}{1+x}\right|. \tag{2.7}$$

This leads to Friedel 'wiggles' in $V(r)$.

But now the question arises: are the defects or impurity centers of interest in metal physics sufficiently weak probes so that we can describe their effect by such a dielectric constant? For point charges, Boardman and March [8] have calculated $\tilde{V}(k)$ beyond a linear theory and the failure of the dielectric constant picture is evident when Z is 3 or 4 in a Fermi gas of density ρ_0 appropriate to Cu metal (see especially the curves of figure 1 of their paper).

The pseudopotential theory, on the other hand, contends that with core electrons present, the effect of the ions on the conduction electrons is much weaker, and that the dielectric constant picture therefore is still valid even for large Z. We present some evidence below which suggests that pseudopotential theory should be a useful starting point in practice, particularly if the valence Z is not too large.

In the case of the vacancy, of course, the picture is that in a zeroth order approximation, we pluck a 'dressed' ion (Ziman [9] terms it a pseudoatom) out of the metal, and the electron redistribution is thereby almost accounted for. We obviously should include relaxation, and once again, in another paper of this Conference, Huntington has led the way by showing how ideally suited is Harrison's approach, using pseudopotentials, to this problem. The Dexter model, to which we now turn, is a very simple example of such an idea, and was indeed developed precisely for point-ions by Corless and March [10]. However, the approach of 3 will have, of course, to be generalized eventually to include core electrons (and therefore explicit pseudopotentials: see some further remarks at the end of sec. 3).

3. Phonons and Vacancies

It might seem, at first sight, surprising that there should be a simple relation between the Debye temperature θ and the vacancy formation energy E_v. But, as Mukherjee [4] emphasized, the experimental results are well represented by

$$\theta=\frac{CE_v^{1/2}}{M^{1/2}\Omega^{1/3}}, \tag{3.1}$$

where M is the atomic mass and Ω the atomic volume. The constant C is the same for eight close-packed metals, for which experimental results are available. These include however, Ni and Pt, which are not at all appropriately described by the considerations below. We have in mind then, specifically the noble metals, Mg, Al and Pb.

In the simplest model of a vacancy, due to Dexter, we represent the vacant site as a 'dressed' charge $-Ze$ in a Fermi gas, where Z is the valency of the metal, in complete accord with the ideas outlined in Z. The Fourier components $\tilde{V}(k)$ of the screened potential $V(r)$ are given by eq (2.4), with the dielectric constant of eq (2.6). Now following essentially the argument of Fumi [3], we calculate the

[2] We use atomic units in which $e=1$, $m=1$, $\hbar=1$.

shift in the individual electronic levels using perturbation theory. Obviously, in a metal of volume $\mathcal{V}$, the first-order perturbation energy is given by

$$\frac{1}{\mathcal{V}}\int d\mathbf{r} e^{-i\mathbf{k}\cdot\mathbf{r}} V(r) e^{i\mathbf{k}\cdot\mathbf{r}} . \tag{3.2}$$

Obviously, eq (3.2) is independent of $\mathbf{k}$ and from eq (2.3) is simply $\mathcal{V}^{-1}$ multiplied by the long-wavelength limit $\tilde{V}(0)$ of $\tilde{V}(k)$. This is immediately obtained from eqs (2.4) and (2.6), and if we add up the electronic energy change over N electrons and use the free electron relation between the electronic density and the Fermi energy, we find the result $\frac{2}{3} ZE_f$. But, if we neglect relaxation, the wave functions now extend into an extra atomic volume, when we remove an atom from the interior of the metal and place it on the surface. Hence the kinetic energy is lowered by a calculable amount (Fumi, [3]), which for free electrons is simply $\frac{2}{5} ZE_f$. We have then as our starting approximation

$$E_v = \left(\frac{2}{5} - \frac{2}{3}\right) ZE_f$$

$$= \frac{4}{15} ZE_f. \tag{3.3}$$

Lidiard and Tharmalingam (private communication) have looked at the numerous corrections to this result for the noble metals, and while the various energies arising from electron-electron interactions tend to cancel, the errors look somewhat serious. But taking the simplest picture, and recalling that (3.3) is obtained from first-order perturbation theory, it would seem that the natural unit in which to measure the vacancy formation energy is ZE_f. Following Enderby and March [6], we have collected in table 1 the experimental results for E_v in these units. It is readily shown from the last column that the result of extrapolating back to $Z=0$ is quite consistent with the value $\frac{4}{15}$ of (3.3). Following Fumi [3], if we correct for the fact that (with his model square-well potential now) the s waves are strongly perturbed and therefore their phase shift η_0 is not adequately given by the Born approximation employed in (3.2), then we find a reasonable estimate for the slope of E_v/ZE_f against Z at the origin. This is gratifying and therefore further calculations of the phase shifts of the p, d, etc. waves for larger valencies are now being carried out by S. Baranovsky and one of us (N.H.M.), to see whether Fumi's model can reproduce the experimental data in table 1, which flatten out in a very striking way around $Z=3$.

This all seems to indicate, therefore, that we can indeed obtain a sensible account of the vacancy

Table 1

Metal	Measured vacancy formation energy E_v in eV	Valency	Valency multiplied by free electron value of Fermi energy E_f in eV	E_v in units of ZE_f
Au.....	0.94	1	5.5	0.17
Ag.....	1.09	1	5.5	.19
Cu.....	1.17	1	7.0	.17
Mg.....	0.89	2	10.4	.09
Al.....	.75	3	33	.02
Pb.....	.53	4	36	.01(4)

formation energy in the simpler metals by summing the one-electron eigenvalues, though the self-energy of the displaced charge and the other interaction energies considered above may perhaps play a more important role in the polyvalent metals. But the situation is even more interesting in the light of the Mukherjee relation. For, in the Dexter model, the screened potential scattering the electrons is simply the negative of the electron-positive ion scattering potential in the linear theory. And this latter potential gives us, after multiplication by Ze, the pair potential $\phi(r)$ according to the theory of Corless and March [10]. Thus, since the ion-ion interaction determines the phonon spectrum, and hence the Debye temperature, it is entirely reasonable in a linear theory that it is connected with the vacancy formation energy. Thus, from elementary Debye theory (cf. Mott and Jones [7]), we have for the Debye temperature,

$$\theta = \frac{v_s}{\Omega^{1/3}} \left(\frac{3}{4\pi}\right)^{1/3} \frac{h}{k} . \tag{3.4}$$

The velocity of sound v_s is given, in the most elementary theory, by the Bohm-Staver result (cf. Bardeen and Pines [11]),

$$v_s = \sqrt{\frac{Zm}{3M}}\, v_f, \tag{3.5}$$

where v_f is the Fermi velocity. Eliminating ZE_f between (3.3), (3.4) and (3.5), Mukherjee's relation (3.1) follows immediately. The constant C is given to much better than order of magnitude and no more could be expected since the Debye temperature is calculated from (3.4) assuming a common velocity for transverse and longitudinal waves.

But while this proof of (3.1) is strictly valid only for small Z, the Mukherjee result has wider generality. The reason for its validity appears from the studies of Dr. S. H. Vosko and one of us (N.H.M.) to be clearly related to pseudopotential concepts, the essential quantity in the theory being a generalization of (2.4) in which $V(r)$ of the point ion model is replaced by a pseudopotential (see Vosko, Taylor, and Keech [12], for a detailed discussion of the phonon problem). We believe that Mukherjee's relation is direct experimental evidence of the picture of a metal built up as a superposition of 'dressed' ions. Such a superposition result leads directly to a description of ion-ion interactions in

terms of pair potentials (Corless and March [10], Johnson and March [13]), a result widely employed in defect calculations reported in this Conference (see, for example, the contribution by R. Johnson). Finally, we might stress here that in some cases a calculation of the properties of the 'dressed' ion, that is the single-center problem, may necessitate transcending the Born approximation. Even then, it may be possible still to build up the metal, to a good approximation, by superposing such 'dressed' ions. The work of section 4 below bears on this argument.

4. Dielectric Constant and Vacancies in Cu and Al

Though we have indicated that the argument of section 2 may be generalizable to include pseudopotentials, as presented in this paper it treats the conduction electrons as though they were free, and furthermore neglects core electrons.

At this point, we shall therefore consider the scattering of the Bloch waves representing the conduction electrons by a vacancy, following the semiempirical method of Kohn and Vosko [14]. Since this theory has been widely applied, we shall give only a brief summary before presenting some new results for vacancies in Cu and Al.

The idea is that we can represent the scattering of Bloch waves by a spherical defect potential $V(r)$ in terms of only two phase shifts for the s and p waves. If $\psi_{\mathbf{k}}(\mathbf{r})$ is the perturbed wave function and $\phi_{k}(\mathbf{r})$ is the unperturbed Bloch function, then we may write

$$\psi_{\mathbf{k}}(\mathbf{r}) = \phi_{\mathbf{k}}(\mathbf{r}) + [f(\mathbf{k}, \mathbf{k}')/r]\phi_{\mathbf{k}'}(\mathbf{r}) \qquad (4.1)$$

for the asymptotic form of $\psi(\mathbf{r})$. Then we can expand f, assuming it depends only on $|\mathbf{k}|$ and the scattering angle θ between $\mathbf{k}$ and $\mathbf{k}'$ $\left(\mathbf{k}' = |\mathbf{k}'\frac{\mathbf{r}}{r}\right)$, the initial and final wave vectors, in the usual way as

$$f_k(\theta) = \frac{1}{2ik}\sum_{0}^{\infty}(2l+1)[e^{2i\eta_l(k)} - 1]P_l(\cos\theta). \qquad (4.2)$$

If we write

$$\psi_{\mathbf{k}}(\mathbf{r}) = U_{\mathbf{k}}(r)e^{i\mathbf{k}\cdot\mathbf{r}}, \qquad (4.3)$$

then the displaced charge $\Delta\rho$ may be written

$$\Delta\rho(r) = -\left(\frac{1}{4\pi^2 r^3}\right)\left\{\exp(2ik_f r)|U_{k_f}(r)|^2 k_f f_{k_f}(\pi) + \text{complex conjugate}\right\}. \qquad (4.4)$$

The method hinges now on the fact that if we use
(a) the Friedel sum rule, and
(b) the measured residual resistivity,
then we can evaluate the s and p phase shifts, assuming the other phase shifts are negligibly small. We discuss these phase shifts below, but to avoid the complication of graphically representing (4.4), thus requiring knowledge of $U_{k_f}(r)$, we have put $U_{k_f}(r)=1$. Roughly then, we can consider that we are getting an envelope, or a spherical average, of the displaced charge. To make closer contact with dielectric screening, we have then put the results in terms of a 'screened potential,' using Poisson's equation. We want to stress of course, that for some purposes (especially the interpretation of nuclear magnetic resonance intensity) the retention of $U_k(r)$ in (4.4) is crucial. But our main interest is to compare results for different defect centers in the same matrix, and for this the present representation proves convenient.

We now turn to the results for the vacancies in Cu. Table 2 shows the phase shifts obtained for

TABLE 2

Phase shifts for vacancies in Cu	$\Delta\rho_v$ (micro-ohm-cm per atomic %)	η_0	η_1	η_2
Semiempirical	1.0	−0.52	−0.35	0
	1.25	−.71	−.29	0
	1.5	−.80	−.26	0
Theoretical Lee and March [16]	0.94	−.61	−.10	−0.03
Theoretical Jongenburger [17]	1.25	−.73	−.23	−.01

various choices of the vacancy resistivity $\Delta\rho_v$ per atomic percent vacancies. The values of η_2 calculated on theoretical models are very small, indicating that the approximation of neglecting η_2 in the semiempirical method is probably a good one.

We show the form of the vacancy potential thereby obtained in figure 1. We have plotted results for both $\Delta\rho_v = 1.0$ and 1.5, and for comparison, we have plotted, with a sign change of course, the results of Kohn and Vosko for $Z=+1$. The pointion result is also shown for comparison. The overall agreement among the results is good, and indicates that, to a useful first approximation we can regard these results as reflecting the dielectric function of Cu metal, though some differences in phase are evident from figure 1.

We have also carried out calculations for Mg, Al, and Pb, but only for Al was a result known to us for the vacancy resistivity at the time the calculations were carried out. However, it seems clear that already the perturbation is such that the phase shift η_2 may be beginning to play a significant role. We plot the results for Al in figure 2, for a vacancy, and for Zn, Mg, and Ge impurities. The curves, scaled with Z of course to be directly comparable, show a scatter which is a good deal larger than for Cu. Presumably, the smallest perturbation (Mg)

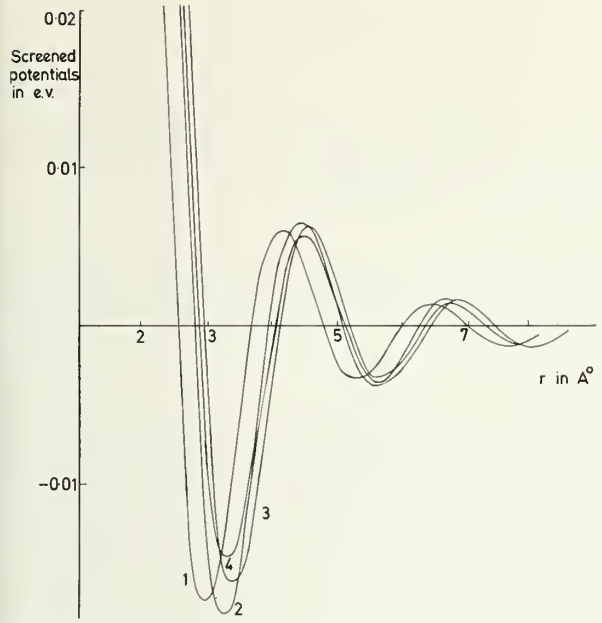

FIGURE 1. *Asymptotic form of 'screened potentials' round vacancy and positively charged impurity in* Cu.

Curve (1) Vacancy $\Delta\rho_i = 1.5$ μ ohm cm per atomic percent.
Curve (2) Kohn and Vosko result for $Z = 1$.
Curve (3) Vacancy $\Delta\rho_i = 1.0$ μ ohm cm.
Curve (4) Point-ion shielding (cf. eqs (2.4) and (2.6)).

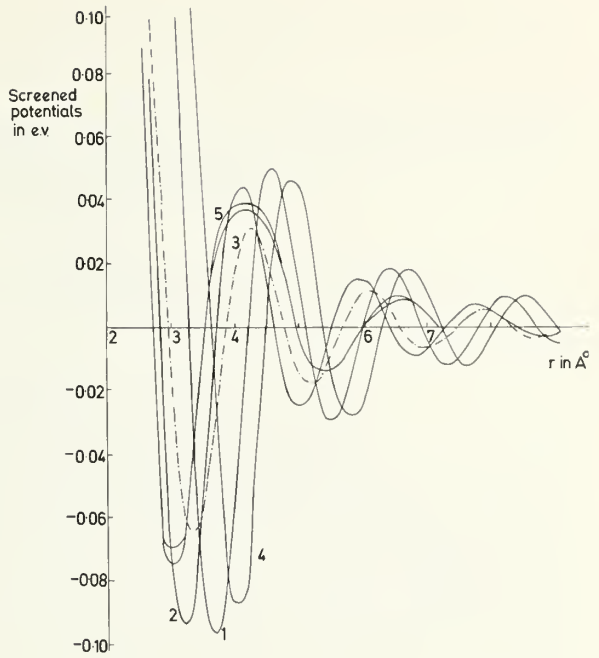

FIGURE 2. *Asymptotic form of 'screened potentials' round vacancy and various impurities in* Al.

Curve (1) Vacancy in Al.
Curve (2) Mg in Al ($Z = -1$).
Curve (3) Zn in Al ($Z = -1$).
Curve (4) Ge in Al ($Z = +1$).
Curve (5) Liquid metal ion-ion interaction.

should best reflect the dielectric function of the Al matrix. The situation for Pb is even worse and indicated that we may have to use a somewhat different approach in this case for a vacancy. The perturbation appears strong. Other evidence that this is indeed so seems to be contained in the marked curvature with Z of the vacancy formation energy, evident in table 1. It seemed of interest finally to plot in figure 2 the ion-ion interaction energy for liquid Al, derived by Johnson, Hutchinson, and March [15] from the liquid structure data. There is some agreement with the one-center potentials, but the use of a common dielectric function for one and two-center problems seems rather rough. This may be connected with the remarks at the end of section 3.

Nevertheless, we suggest that the considerations of the present paper lend weight to the view that the vacancy, as well as impurities which do not strain the lattice too greatly, can be usefully described in terms of a dielectric constant characteristic of the Fermi gas. Whether the description can be made entirely quantitative may seem in some doubt, particularly for the polyvalent metals. But Mukherjee's relation, on the other hand, suggests that with appropriate choice of pseudopotentials, a quantitative relation between forces characteristic of the perfect crystal and the vacancy should emerge.

Thanks are due to Drs. J. E. Enderby and S. H. Vosko, and to Messrs. S. Baranovsky and J. Worster for valuable discussion and correspondence. One of us (N.H.M.) wishes to acknowledge that his contribution to the present paper was partially supported by the U.S. Atomic Energy Commission.

5. References

[1] H. B. Huntington, Phys. Rev. **61**, 325 (1942).
[2] N. H. March and A. M. Murray, Proc. Roy. Soc. (London) **A256**, 400 (1960).
[3] F. G. Fumi, Phil. Mag. **46**, 1007 (1955).
[4] K. Mukherjee, Phil. Mag. **12**, 915 (1965).
[5] N. H. March, Phys. Letters **20**, 231 (1966).
[6] J. E. Enderby and N. H. March, "Phase Stability in Metals and Alloys," Editors, Rudman, P. S., Stringer, J., Jaffe, R. I., McGraw Hill (New York), 1967, p. 479
[7] N. F. Mott, Proc. Camb. Phil. Soc. **32**, 281 (1936); N. F. Mott and H. Jones, The Theory of the Properties of Metals and Alloys (Clarendon Press, Oxford, 1936).
[8] A. D. Boardman and N. H. March, Proc. Kyoto Conference on Crystal Lattice Defects, Vol. **II**, 80 (1962).
[9] J. M. Ziman, Adv. Phys. **13**, 89 (1964).
[10] G. K. Corless and N. H. March, Phil. Mag. **6**, 1285, 1961 and **7**, 1765 (1962).
[11] J. Bardeen and D. Pines, Phys. Rev. **99**, 1140 (1955).
[12] S. H. Vosko, R. Taylor, and G. H. Keech, Can. J. Phys. **43**, 1187 (1965).
[13] M. D. Johnson and N. H. March, Phys. Letters **3**, 313 (1963).
[14] W. Kohn and S. H. Vosko, Phys. Rev. **119**, 912 (1960).
[15] M. D. Johnson, P. Hutchinson, and N. H. March, Proc. Roy. Soc. (London) **A282**, 283 (1964).
[16] P. M. Lee and N. H. March, Phys. Rev. **118**, 138 (1960).
[17] P. Jongenburger, Appl. Sci. Research **3B**, 237 (1953).

256-724 O-67—6

Calculations on Point Defects in Metals Allowing for Realistic Fermi Surfaces and Scattering Mechanisms

A. Seeger and E. Mann

Institut für Physik am Max-Planck-Institut für Metallforschung, Stuttgart, Germany

1. Introduction

The majority of the calculations on point defects in metals have used either one of two approaches [1]:[1] (i) The model calculation or (ii) the free electron theory calculation.

(i) In the model type of calculation a model for the interactions between the atoms or ions of the metal is adopted, the characteristic parameters of which are usually fixed by using empirical data such as elastic constants, force constants, cohesive energies, etc., and/or calculations on individual ions, e.g., for determining the ion-ion interaction potentials. Typical properties of point defects for the calculation of which this kind of model is usually employed, include the configurations of the atoms surrounding a point defect, defect entropies, and the energies of migration of point defects.

(ii) The electron theory calculations are used to calculate the "electronic properties" of point defects [2], such as the electrical resistivity and the thermoelectric power. The majority of these calculations have been carried out for free electrons, which has the advantage of simplicity and generality. Calculations based on pseudopotentials, which have recently become fashionable, will be discussed separately (sec. 14).

Up to now these two approaches have remained rather unrelated to each other. It is true that in the more advanced theoretical treatments of some point defect properties, e.g., energies of formation and binding, both types of theories have been combined, but even here they have remained essentially unrelated, the results of the different calculations simply being superimposed on each other.

From the point of view of a theoretician who seeks a fundamental understanding of the properties of point defects in metals, it is clearly an unsatisfactory state of affairs that quite different approaches have to be used to treat different properties of point defects. The use of simple models and the restriction to easy-to-carry-out free electron theory calculations was a necessity when the computational work had to be done on small electronic computors or even on desk machines. With the present capacity of large electronic computors available, one should be able to do better and to make some progress towards a unified approach to the problem.

A number of years ago we have started a program of research, which, we hope, will finally unite the two theoretical methods mentioned above and permit reliable calculations of point defects properties in specific metals to be carried out. It appears still to be outside the realm of present possibilities to base such an approach entirely on first principles. What does seem possible, however, is to develop a quantum-mechanical framework which enables us to incorporate in an unambiguous manner the kind of empirical information which at present is used in the model calculations.

Such an approach will of necessity have to be developed along similar lines as the theory of perfect metal crystals. This means that at one stage we shall have to arrive at a one-electron Hamiltonian for the perturbed crystal, and that from this the one-electron wave functions and the one-electron energies (or rather their variations caused by the presence of the defects) will have

[1] Figures in brackets indicate the literature references at the end of this paper.

to be calculated. In order to be able to account for the individualities of the various metals, this stage must not be based on the free electron picture of a metal but on realistic electron energy surfaces and wave functions. The calculation of changes in wave functions, electron energies, and other electronic properties due to arbitrary localized perturbations for (within reasonable limits) general energy surfaces and wave functions of the perfect metal is central to the whole problem. Most of our efforts have gone into this question. The present account is mainly a summary on the results so far achieved in this field, an early progress report having been given a number of years ago [3].

The next stage will have to be the numerical evaluation of the general expressions for individual metals. This requires a detailed knowledge of the energy surfaces and the wave functions of the perfect crystals. Due to the experimental studies of the Fermi surfaces and the large theoretical efforts in band calculations, the present information on the electron energies is satisfactory for quite a few metals. Unfortunately, this cannot be said of our knowledge of the wave functions. It is hoped that the calculation of wave functions will see enough progress within the next few years to provide the background information necessary for the defect calculations.

The final step, leading to the merger of the approaches (i) and (ii), will be the numerical determination of the one-electron Hamiltonian of the perturbed crystal. The potential acting on the electrons will, among other things, depend on the configuration of the atoms surrounding the point defect. This configuration, however, depends on the electron redistribution caused by the point defect. Clearly, a problem of self-consistency arises here, and the many-body aspects of the problem must be included. At this stage it may well be found expedient to determine some of the parameters of the problem empirically or semiempirically. Some work on these questions has already been carried out, but in the interest of the coherency of the presentation we shall not report on it here. In sec. 14, we shall comment, however, on one proposal made in the literature in order to solve this self-consistency problem for metals, the method of "pseudoatoms" [4].

2. Basic Formulas

In a perfect crystal, the one-electron energies $E_n(\mathbf{k})$ are periodic functions of the wave vector $\mathbf{k}$. They may therefore be written as a Fourier series (n = band index) [5]

$$E_n(\mathbf{k}) = \sum_{\mathbf{R}_s} \epsilon_n(\mathbf{R}_s) e^{-i\mathbf{k}\cdot\mathbf{R}_s}, \tag{2.1}$$

where the summation extends over the Bravais lattice of the crystal. The Fourier coefficients may be expressed as matrix elements between the Wannier functions $a_n(\mathbf{r}-\mathbf{R}_i)$ (a^* = complex conjugate of a)

$$\epsilon_n(\mathbf{R}_s) = \int a_n^*(\mathbf{r}-\mathbf{R}_s) H_0(\mathbf{r}) a_n(\mathbf{r})\, d\mathbf{r}. \tag{2.2}$$

The Wannier functions $a_n(\mathbf{r}-\mathbf{R}_i)$ are localized around the lattice site $\mathbf{R}_i$ and are related to the Bloch functions $\varphi_{n,\mathbf{k}}(\mathbf{r})$ by the equations

$$a_n(\mathbf{r}-\mathbf{R}_i) = \frac{1}{\sqrt{N}} \sum_{\mathbf{k}} e^{-i\mathbf{k}\cdot\mathbf{R}_i} \varphi_{n,\mathbf{k}}(\mathbf{r}); \qquad \varphi_{n,\mathbf{k}}(\mathbf{r}) = \frac{1}{\sqrt{N}} \sum_{\mathbf{R}_i} e^{i\mathbf{k}\cdot\mathbf{R}_i} a_n(\mathbf{r}-\mathbf{R}_i). \tag{2.3}$$

The Bloch functions satisfy the one-electron Schroedinger equation

$$H_0(\mathbf{r})\varphi_{n,\mathbf{k}}(\mathbf{r}) = E_n(\mathbf{k})\varphi_{n,\mathbf{k}}(\mathbf{r}), \tag{2.4}$$

where H_0 is the one-electron Hamiltonian operator of the ideal crystal.

The Schroedinger equation of the perturbed crystal is written in the form

$$(H_0+V(\mathbf{r}))\psi(\mathbf{r})=E\psi(\mathbf{r}), \tag{2.5}$$

where the "perturbation" $V(\mathbf{r})$ may be an "ordinary potential" or an operator. It enters into the following expressions usually through its matrix elements

$$V_{nm}(\mathbf{R}_i,\ \mathbf{R}_j)=\int a_n^*(\mathbf{r}-\mathbf{R}_i)V(\mathbf{r})a_m(\mathbf{r}-\mathbf{R}_j)d\mathbf{r}. \tag{2.6}$$

The solution $\psi(\mathbf{r})$ of the Schroedinger eq (2.5) of the perturbed crystal is expanded in terms of Wannier functions:

$$\psi(\mathbf{r})=\sum_{n,\ \mathbf{R}_i} U_n(\mathbf{R}_i)a_n(\mathbf{r}-\mathbf{R}_i). \tag{2.7}$$

The coefficients $U_n(\mathbf{R}_i)$ satisfy the equation [6]

$$U_n(\mathbf{R}_l)-\sum_{m,\ \mathbf{R}_i,\ \mathbf{R}_j}\hat{G}_{n,E}(\mathbf{R}_l-\mathbf{R}_i)V_{nm}(\mathbf{R}_i,\ \mathbf{R}_j)U_m(\mathbf{R}_j)=0, \tag{2.8}$$

where

$$\hat{G}_{n,E}(\mathbf{R}_l-\mathbf{R}_i)=\frac{1}{N}\sum_{\mathbf{k}}\frac{e^{i\mathbf{k}\cdot(\mathbf{R}_l-\mathbf{R}_i)}}{E-E_n(\mathbf{k})} \tag{2.9}$$

may be denoted as Green's function of a crystal with periodic boundary conditions.

The condition for the solubility of the system of homogeneous linear equations (2.8) is the vanishing of the determinant

$$\hat{D}(E)\equiv|\delta_{nm}\delta_{lj}-\sum_{\mathbf{R}_i}\hat{G}_{n,E}(\mathbf{R}_l-\mathbf{R}_i)V_{nm}(\mathbf{R}_i,\ \mathbf{R}_j)|=0. \tag{2.10}$$

Equation (2.10) is the equation from which the (discrete) energy values $E=E^k$ of the perturbed problem are to be determined.

3. Change in Energy

The energy change associated with an energy value $E_n(\mathbf{k})=E_k$ of the ideal crystal is given by (E^k-E_k), where E^k reduces to E_k when the perturbation V is "switched off." In a metal (with compensated spins) the total change in one-electron energies is given by (Im = imaginary part)

$$\Delta E=2\sum_k^{\zeta}(E^k-E_k)=\frac{2}{\pi}\int^{\zeta}\text{arc}\ D(E)dE=\frac{2}{\pi}\int^{\zeta}\text{Im log}\ D(E)dE, \tag{3.1}$$

where the summation extends over all eigenvalues up to the Fermi surface, which is characterized by the Fermi energy ζ. In eq (3.1) the transition to a continuous distribution of energies has been made. This has the consequence that the Green's function (2.9) has to be replaced by the Green's function for a continuous energy spectrum (V_B = volume of the Brillouin zone)

$$G_n(E,\ \mathbf{R})=\lim_{\epsilon\to 0}\frac{1}{V_B}\int\frac{e^{i\mathbf{k}\cdot\mathbf{R}}}{E-E_n(\mathbf{k})+i\epsilon}\,d\mathbf{k}. \tag{3.2}$$

$D(E)$ is defined by eq (2.10) with $\hat{G}_{n,E}(\mathbf{R})$ replaced by $G_n(E, \mathbf{R})$. Bound states (outside the bands of continuous energy values) are included in eq (2.10), but not in the last two expressions of eq (3.1). They have to be added separately in order to obtain ΔE.

Equation (3.1) may either be derived by a heuristic argument [7], or by a technique based on the theory of functions that was first employed by Wentzel [8] in his meson pair theory. The application of this technique to electrons in metals [7] differs from that in the theory of lattice vibrations [9] in that in the metal case the integration in eq (3.1) ends at the Fermi energy, whereas in the lattice vibration case one always deals with "full bands."

4. Symmetry Considerations

We call a lattice site $\mathbf{R}_i$ "affected by the perturbation $V(\mathbf{r})$," if $V_{nm}(\mathbf{R}_i, \mathbf{R}_j)$ is different from zero for any $\mathbf{R}_j$. The order of the determinant D in eq (3.1) is equal to the number of energy bands to be taken into account, times the number of sites affected by the perturbation. The latter number will be the smaller the more localized the perturbation is. The method is therefore suitable for localized perturbations, e.g., for the treatment of point defects. Nevertheless, the order of D may be relatively large even in simple problems. Consider as an example a vacant site in an f.c.c. crystal and assume that in addition to the vacant site ($\mathbf{R}_i = 0$) only the twelve nearest neighbor sites are affected. When only one band is taken into account, the order of D is 13.

Fortunately, the secular problem eq (2.7) and (2.10) may be considerably simplified and reduced to a set of smaller problems, if the point symmetry of the problem is taken into account. In particular, the determinant D may be represented as a product in the form

$$D = \prod_{\mu} (D_{\mu}^{m_\mu})^{n_\mu} . \tag{4.1}$$

Here D_μ is the secular determinant associated with the irreducible representation μ. The superscript m_μ denotes the multiplicity with which the irreducible representation μ occurs in the problem and is equal to the order of D_μ. The multiple occurrence of the irreducible representation μ may either be associated with shells containing a relatively large number of sites, or with different shells. The quantity m_μ depends therefore on the number of shells affected by the perturbation. The exponent n_μ is equal to the dimension of the irreducible representation μ. For a problem involving a fixed number of sites, the order of the determinant D of the total problem is given by $\sum_{\mu} m_\mu n_\mu$.

In the example considered at the beginning of the section, eq (4.1) takes the form (employing the usual notation of the cubic point group O_h [10]) [7]

$$D = D^2_{\Gamma_1} (D^1_{\Gamma_{12}})^2 (D^1_{\Gamma_{25'}})^3 (D^1_{\Gamma_{15}})^3 (D^1_{\Gamma_{25}})^3. \tag{4.2}$$

The symmetry eigenvectors of the problem are easily obtained from the basis functions of the irreducible representations.

5. Phase Constants

Defining generalized phase constants $\alpha_\mu(E)$ associated with the irreducible representations μ by

$$\alpha_\mu(E) = \frac{1}{\pi} \operatorname{arc} D_\mu(E), \tag{5.1}$$

we may write the total energy change eq (3.1) as

$$\Delta E = 2\int^{\zeta} \alpha(E)\, dE. \tag{5.2}$$

where

$$\alpha(E) = \sum_{\mu} n_{\mu}\alpha_{\mu}(E) = \frac{1}{\pi}\,\mathrm{arc}\;\; D(E)\,. \tag{5.3}$$

Equations (5.2) and (5.3) are analogous to the expression of the energy change of a gas of free electrons perturbed by a potential of spherical symmetry [11, 12]

$$\Delta E^{\mathrm{free}} = -\frac{2}{\pi}\sum_{l=0}^{\infty}(2l+1)\int_0^{\zeta}\eta_l(E)\,dE \tag{5.4}$$

in terms of the phase shifts η_l of the partial waves. This demonstrates that the generalized phase constants are indeed generalizations of the quantities $-\frac{1}{\pi}\,\eta_l(E)$.

Since in problems of point symmetry in crystals the number of irreducible representations is limited, the present formulation of the phase-shift problem comprises only a finite number of terms [12a, 12b], in contrast to the free electron case, where on account of the higher symmetry the number of phase shifts is infinite.

6. Scattering Problems

In section 5 we have introduced the generalized phase constants α_{μ} by considering the effect of the perturbation on the spectrum of discrete energy eigenvalues. They may also be introduced through the scattering problem, i.e., in a formulation based on a continuous spectrum of energy eigenvalues.

In such a formulation one considers a fixed energy value $E_n(\mathbf{k})$ and writes the total wave function

$$\psi_{n,\mathbf{k}}(\mathbf{r}) = \sum_{m}\sum_{\mathbf{R}_j} U_m^{n,\mathbf{k}}(\mathbf{R}_j)\,a_m(\mathbf{r}-\mathbf{R}_j) \tag{6.1}$$

as a sum of the unperturbed function $\varphi_{n,\mathbf{k}}(\mathbf{r})$ (see eq 2.4) and the so-called scattered wave. Subdividing the expansion coefficients $U_m^{n,\mathbf{k}}(\mathbf{R}_j)$ in the same way gives us

$$U_m^{n,\mathbf{k}}(\mathbf{R}_j) = \frac{1}{\sqrt{V_B}}\,e^{i\mathbf{k}\cdot\mathbf{R}_j}\delta_{nm} + \bar{U}_m^{n,\mathbf{k}}(\mathbf{R}_j). \tag{6.2}$$

By a procedure analogous to that of section 2, the following equation for $U_m^{n,\mathbf{k}}(\mathbf{R}_j)$ is obtained [13, 14]:

$$U_m^{n,\mathbf{k}}(\mathbf{R}_l) = V_B^{-1/2}e^{i\mathbf{k}\cdot\mathbf{R}_l}\delta_{nm} + \sum_{m'}\sum_{\mathbf{R}_i,\mathbf{R}_j} G_m^{E_n(\mathbf{k})}(\mathbf{R}_l-\mathbf{R}_i)\,V_{mm'}(\mathbf{R}_i,\mathbf{R}_j)\,U_{m'}^{n,\mathbf{k}}(\mathbf{R}_j). \tag{6.3}$$

Here

$$G_m^{E_n(\mathbf{k})}(\mathbf{R}_l-\mathbf{R}_j) = \lim_{\epsilon\to 0}\frac{1}{V_B}\int\frac{e^{i\mathbf{k}'\cdot(\mathbf{R}_l-\mathbf{R}_j)}}{E_n(\mathbf{k})-E_m(\mathbf{k}')+i\epsilon}\,d\mathbf{k}' \tag{6.4}$$

is the Green's function of the scattering problem.

In matrix notation eq (6.3) may be written as

$$\mathbf{u}_{\mathbf{k}} = \mathbf{e}_{\mathbf{k}} + G^E V \mathbf{u}_{\mathbf{k}} \ . \tag{6.5}$$

The solution of eq (6.5) is

$$\mathbf{u}_{\mathbf{k}} = (M^E)^{-1} \mathbf{e}_{\mathbf{k}}, \tag{6.6a}$$

where

$$M^E = 1 - G^E V. \tag{6.6b}$$

The determinant of M^E is equal to the determinant D introduced in section 3, i.e.,

$$\det M^E = D(E). \tag{6.7}$$

Inserting eq (6.6) into the right-hand side of eq (6.5) gives us

$$\mathbf{u}_{\mathbf{k}} = \mathbf{e}_{\mathbf{k}} + G^E T^E \mathbf{e}_{\mathbf{k}}, \tag{6.8a}$$

where

$$T^E = V(M^E)^{-1} \tag{6.8b}$$

is the so-called transition matrix.

The preceding treatment is exact. From now on we consider the asymptotic behavior of the scattered wave function. Provided $\mathbf{R}_l$ lies sufficiently far outside the region affected by the perturbing potential, we may write the expansion coefficients

$$U_m^{n,\mathbf{k}}(\mathbf{R}_l) \simeq V_B^{-1/2} \left(e^{i\mathbf{k}\cdot\mathbf{R}_l} \delta_{nm} + \sum_{\nu} S_{m,\mathbf{k}'_\nu}^{n,\mathbf{k}} \frac{e^{i\mathbf{k}_\nu \cdot \mathbf{R}_l}}{R_l} \right), \tag{6.9}$$

where

$$S_{m,\mathbf{k}'_\nu}^{n,\mathbf{k}} = g_{m,\mathbf{k}'_\nu} A_{m,\mathbf{k}'_\nu}^{n,\mathbf{k}} \tag{6.10}$$

is the scattering amplitude.

The coefficients [15]

$$g_{m,\mathbf{k}'_\nu} = \frac{4\pi^2}{i} \frac{e^{-i\frac{\pi}{2}\lambda_m(\mathbf{k}'_\nu)}}{|\nabla E_m(\mathbf{k}'_\nu)| \ |K_m(\mathbf{k}'_\nu)|^{1/2}} \tag{6.11}$$

are entirely determined by the energy functions $E_m(\mathbf{k})$ of those energy bands that contain the energy E under consideration; the contributions of the other bands are negligible in the asymptotic region.

In eq (6.9) to (6.11) the wave vectors $\mathbf{k}'_\nu$ are defined by (see figure 1, with $\mathbf{r}$ replaced by $\mathbf{R}_l$)

$$E_m(\mathbf{k}'_\nu) = E \ \text{ and } \ \nabla E_m(\mathbf{k}'_\nu) \text{ parallel to } \mathbf{R}_l. \tag{6.12}$$

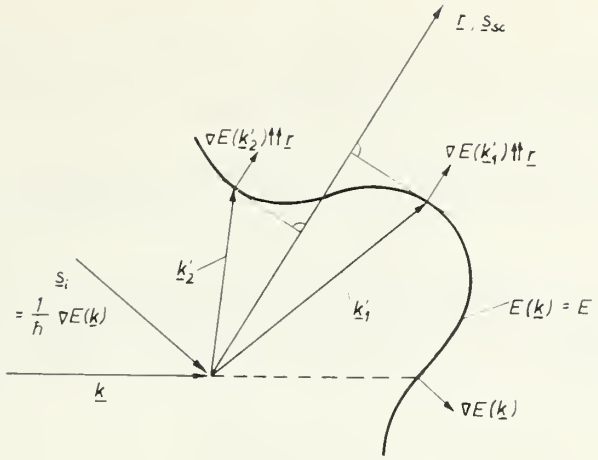

FIGURE 1. *Relation between an incident Bloch wave (wave vector* $\mathbf{k}$*) and the waves (wave vectors* $\mathbf{k}'_\nu$*) scattered into the direction* $\mathbf{r}$*:* $\mathbf{s}_i$ *and* $\mathbf{s}_{sc}$ *denote the directions of the incident and the scattered particle fluxes.*

The subscript ν enumerates the wave vectors that fulfill eq (6.12). $K_m(\mathbf{k}'_\nu)$ is the Gaussian curvature of the energy surface $E_m(\mathbf{k})$ at the point $\mathbf{k}'_\nu$. $\lambda_m(\mathbf{k}'_\nu)$ is 1 if the curvature at $\mathbf{k}'_\nu$ is elliptic concave when looking in the direction of $\mathbf{R}_l$, -1 if the curvature is elliptic convex, and 0 if the curvature is hyperbolic.

As we shall see below,

$$A^{n,\mathbf{k}}_{m,\mathbf{k}'_\nu} = V_B^{-1} \sum_{\mathbf{R}_i,\mathbf{R}_j} e^{-i\mathbf{k}'_\nu\cdot\mathbf{R}_i}\, T^E_{mn}(\mathbf{R}_i,\mathbf{R}_j) e^{i\mathbf{k}\cdot\mathbf{R}_j} \tag{6.13}$$

has the physical meaning of the transition amplitude from a state with wave vector $\mathbf{k}$ in the nth band to a state with wave vector $\mathbf{k}'_\nu$ in the mth band. In eq (6.13) $T^E_{mn}(\mathbf{R}_i, \mathbf{R}_j)$ denotes an element of the matrix T^E introduced in eq (6.8b).

As shown in detail elsewhere [16], the transition amplitude may be written as (for a similar expression, however without introducing phase shifts, see [16a])

$$A^{n,\mathbf{k}}_{m,\mathbf{k}'_\nu} = \sum_\mu Q^{n,\mathbf{k}}_{m,\mathbf{k}'_\nu,\mu} \sin\,\pi\alpha_\mu e^{-i\pi\alpha_\mu}. \tag{6.14}$$

$Q^{n,\mathbf{k}}_{m,\mathbf{k}'_\nu,\mu}$ is a quantity which, in addition to the functional dependencies indicated, depends also on the matrix V of the perturbing potential. For free electrons and spherically symmetric potentials the transition amplitude for the transition from $\mathbf{k}$ to $\mathbf{k}'$ reads

$$A^{\text{free}}_{\mathbf{k},\mathbf{k}'} = \frac{-1}{\pi(2\pi)^3 n(E)} \sum_{l=0}^{\infty} (2l+1) P_l(\cos\theta) \sin\eta_l e^{i\eta_l}, \tag{6.15}$$

where $n(E)$ denotes the density of states, θ the angle between $\mathbf{k}$ and $\mathbf{k}'$, and P_l, as usual, the Legendre's polynomial of degree l. The η_l are the phase shifts already introduced in section 5. As in section 5, we recognize again the close analogy between the $\alpha_\mu(E)$ and the quantities $-\frac{1}{\pi}\eta_l(E)$.

By inserting eqs (6.10) and (6.14) into the expression (6.9), we see that the contribution of the scattered wave to the coefficients $U^{n,\mathbf{k}}_m(\mathbf{R}_l)$ is made up of a linear combination of terms of the form $\exp[i(\mathbf{k}'_\nu\cdot\mathbf{R}_l - \pi\alpha_\mu)]/R_l$. This shows that the α_μ have indeed the physical meaning of phase shifts of partial waves.

7. Neutrality Condition

From the exact solution of the scattering problem given at the beginning of section 6 we may calculate the change of the electron density per unit energy

$$\Delta\rho(\mathbf{r};\, E)=2\sum_n \int_{E=\text{const}} (|\psi_{n,\mathbf{k}}(\mathbf{r})|^2-|\varphi_{n,\mathbf{k}}(\mathbf{r})|^2)d^2\mathbf{k}. \tag{7.1}$$

where the integration extends over an energy shell in $\mathbf{k}$-space and the summation includes all bands containing E. By integrating eq (7.1) over all space, one obtains the change in the number of electrons per unit energy, i.e., twice the change, $\sigma(E)$, of the density of states. Carrying out these integrations [14] gives

$$\sigma(E)=-\frac{1}{\pi}\,\text{Im trace}\,(G^E T^E G^E), \tag{7.2}$$

which can be transformed into

$$\sigma(E)=-\frac{d}{dE}\left(\frac{1}{\pi}\,\text{Im log det}\,M^E\right). \tag{7.3}$$

By virtue of eq (6.7) and the relations given in section 3, eq (7.3) is equivalent to

$$\sigma(E)=-\frac{d}{dE}\alpha(E). \tag{7.4}$$

Equation (7.4) establishes the relation between the change in the density of states $\sigma(E)$, defined for a continuous energy spectrum, and the relative energy change $\alpha(E)$ in the picture of discrete energies.

Going back to the original meaning of $2\sigma(E)$ as a change in the electron density per unit energy,

$$s_{\text{bands}}=2\int^{\zeta}\sigma(E)\,dE \tag{7.5}$$

gives the total change in the number of electrons within the bands caused by the perturbation. The change in the electron density decreases sufficiently rapidly to zero at large distances (sec. 8) for s_{bands} to be equal to the number of electrons introduced within the bands in the immediate environment of the perturbation. An additional number s_{bound} of electrons may be localized in bound states at the perturbation. The sum $s=s_{\text{bands}}+s_{\text{bound}}$ has therefore the meaning of the screening charge Z (in elementary charge units) of the perturbation.

It can be shown that fully occupied bands give a zero contribution to s. It suffices therefore to extend the integration in eq (7.5) upwards from the minimum energy E_{min} of the bands containing the Fermi energy, provided bound states split off at the bottom of these bands are properly allowed for. Integrating the right-hand side of eq (7.4) gives us

$$s_{\text{bands}}=-2[\alpha(\zeta)-\alpha(E_{\text{min}})]. \tag{7.6}$$

In the one-electron picture, in which all bound states below E_{min} are occupied by two electrons, the relation

$$s_{\text{bound}}=-2\alpha(E_{\text{min}}) \tag{7.7}$$

holds [14]. We have finally

$$Z=-2\alpha(\zeta), \tag{7.8}$$

which is one of the formulations of Friedel's condition for the neutrality of a perturbation in a metal. The present derivation of eq (7.8) has the advantage over the usual derivations that the supposition of the conservation of the Fermi energy is not required.

8. Asymptotic Charge Density

By inserting the asymptotic expressions for $\psi_{n,\mathbf{k}}(\mathbf{r})$ into eq (7.1) and integrating over E, one obtains for the change in the electron density at large distances r from the perturbation (Re = real part)

$$\Delta\rho(\mathbf{r}) \simeq \frac{2}{\pi}\,\mathrm{Re}\left[\sum_{\substack{m,\nu\\ m',\nu'}} \frac{g_{m,\mathbf{k}'_\nu} g_{m',\mathbf{k}'_{\nu'}} A^{m',-\mathbf{k}'_{\nu'}}_{m,\mathbf{k}'_\nu}}{\dfrac{1}{|\nabla E_m(\mathbf{k}'_\nu)|}+\dfrac{1}{|\nabla E_{m'}(\mathbf{k}'_{\nu'})|}} \frac{\varphi_{m,\mathbf{k}'_\nu}(\mathbf{r})\,\varphi_{m',\mathbf{k}'_{\nu'}}(\mathbf{r})}{r^3}\right]_{E=\zeta}, \tag{8.1}$$

where the $\mathbf{k}'_\nu$ are to be taken at the Fermi surface. Equation (8.1) was first derived by Blandin [17], although in a way different from that outlined here. Equation (8.1) exhibits a characteristic variation of $\Delta\rho$ as a function of $\mathbf{r}$, containing the product of r^{-3} times sinusoidal terms. This variation is brought out more clearly by averaging the additional charge density over the extension of the Wannier functions. The result is [14]

$$\overline{\Delta\rho}(\mathbf{R}_l) \simeq \frac{2}{\pi(2\pi)^3}\,\mathrm{Re}\left[\sum_m \sum_{\nu,\nu'} \frac{g'_{m,\mathbf{k}_\nu} g_{m,\mathbf{k}'_{\nu'}} A^{m,-\mathbf{k}'_{\nu'}}_{m,\mathbf{k}'_\nu}}{\dfrac{1}{|\nabla E_m(\mathbf{k}'_\nu)|}+\dfrac{1}{|\nabla E_m(\mathbf{k}'_{\nu'})|}} \frac{e^{i(\mathbf{k}'_\nu+\mathbf{k}'_{\nu'})\cdot\mathbf{R}_l}}{R_l^3}\right]_{E=\zeta}. \tag{8.2}$$

As the simplest special case of eq (8.2) we consider one band only and confine the perturbation to $\mathbf{R}_i=\mathbf{R}_j=0$. This means that we have only one nonvanishing matrix element $V_{00}=V_{nn}(0,0)$. Making use of the relation (6.14) between the transition amplitudes and the generalized phase constants $\alpha_\mu(E)$, we obtain

$$\overline{\Delta\rho}(\mathbf{R}_l) \simeq 2\,\frac{\sin\pi\alpha_{\Gamma_1}(\zeta)}{\pi^2(2\pi)^6 n(\zeta)}\,\mathrm{Re}\left[\sum_{\nu,\nu'} \frac{g_{\mathbf{k}'_\nu} g_{\mathbf{k}'_{\nu'}}}{\dfrac{1}{|\nabla E(\mathbf{k}'_\nu)|}+\dfrac{1}{|\nabla E(\mathbf{k}'_{\nu'})|}} \frac{e^{i\{(\mathbf{k}'_\nu+\mathbf{k}'_{\nu'})\cdot\mathbf{R}_l-\pi\alpha_{\Gamma_1}(E)\}}}{R_l^3}\right]_{E=\zeta}. \tag{8.3}$$

In the special case considered here we have

$$\alpha(E)=\alpha_{\Gamma_1}(E), \tag{8.4}$$

so that for a substitutional atom of valency two in a monovalent metal the neutrality condition takes the form

$$\alpha_{\Gamma_1}(\zeta)=-\frac{1}{2}. \tag{8.5}$$

giving a phase shift in eq (8.3) of $\frac{\pi}{2}$.

Figures 2 to 4 show the results of a numerical evaluation of the asymptotic average charge density according to eq (8.3). The parameters describing the shape of the energy surfaces have

been calculated by fitting the Fermi surface of Cu as determined by Roaf [18] to eq (2.1), taking into account one band only. Figures 2 and 3 give the lines of constant $\overline{\Delta\rho}$ in the {100}- and {110} planes. One can see a very pronounced anisotropy of $\overline{\Delta\rho}$. Figure 4 gives polar plots of $\overline{\Delta\rho}$ in the {100}- and {110}-planes for two different radii $|\mathbf{R}_l/a|=$ const.

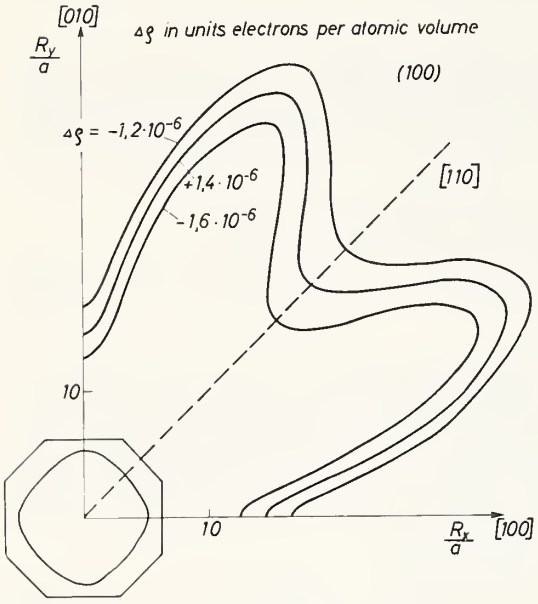

FIGURE 2. *Lines of constant electron density* $\Delta\rho$ *in a* {100}*-plane, calculated according to eq (8.3) for a substitutional atom of valency two in copper.*

R denotes the lattice vector, a is the lattice parameter. The figure near the origin shows a {100}-section through the first Brillouin zone and the Fermi surface.

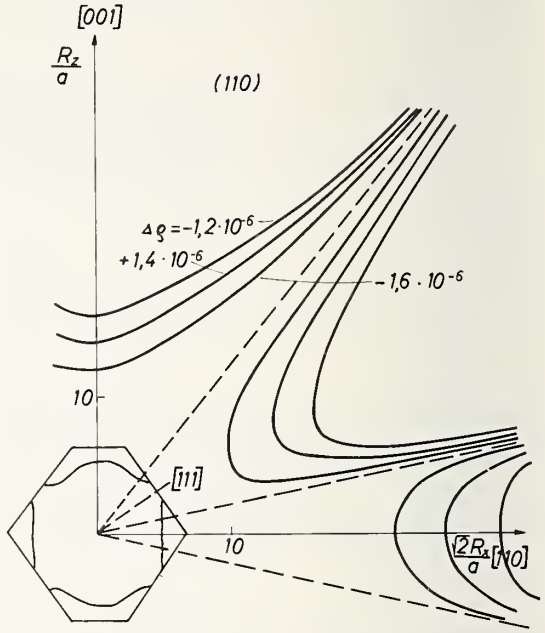

FIGURE 3. *Lines of constant electron density* $\Delta\rho$ *in a* {110}*-plane (for details cf. fig. 2).*

The figure near the origin gives the {110}-section through the Brillouin zone and the Fermi surface.

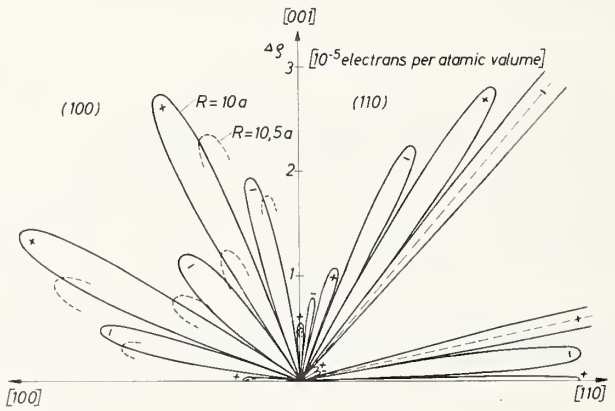

FIGURE 4. *Polar plots of the change in electron density* $\Delta\rho$ *in the* {100}*-and* {110}*-planes for two different radii* $R=$ *const.*

The radii of the plots give the additional electron density $\Delta\rho$ in units 10^{-5} electrons per atomic volume.

For directions $\mathbf{R}_l$ that according to figure 1 are associated with points $\mathbf{k}'_\nu$ on the Fermi surface with $K(\mathbf{k}'_\nu)=0$ eqs (8.1) to (8.3) lead to an infinity in $\overline{\Delta\rho}\,(\mathbf{R}_l)$ (comp. eq 6.11). In such situations these equations are no longer applicable. A more detailed investigation shows that such points of parabolic curvature give rise to an asymptotic contribution to the scattered wave function (6.9)

whose amplitude decreases with distance more slowly than $\frac{1}{R_l}$. If in a point $K(\mathbf{k}'_\nu)=0$ only one of the radii of curvature is infinite, and if the next higher derivative of the surface associated with that curvature is finite, the amplitude varies as $R^{-5/6}$. Even slower variations are possible, if the preceding conditions are violated. This means that in the special directions indicated above the amplitude of $\overline{\Delta\rho}\ (\mathbf{R}_l)$ decreases more slowly than R_l^{-3}. At sufficiently large distances from the defects the average charge density $\overline{\Delta\rho}\ (\mathbf{R}_l)$ will be larger for directions associated with $K(\mathbf{k}'_\nu)=0$ than for others.

If we had not carried out the E-integration mentioned at the beginning of the section, we would have obtained for the change of the average electron density per unit energy, instead of eq (8.3),

$$\overline{\Delta\rho}\ (\mathbf{R}_l;\ E) \simeq -2\,\frac{\sin\ \pi\alpha_{\Gamma_1}(E)}{\pi^2(2\pi)^6 n(E)}\ \mathrm{Im}\left[\sum_{\nu,\nu'} g_{\mathbf{k}_\nu}\, g_{\mathbf{k}'_{\nu'}}\,\frac{e^{i\{(\mathbf{k}'_{\nu'}+\mathbf{k}'_\nu)\cdot\mathbf{R}_l-\pi\alpha_{\Gamma_1}(E)\}}}{R_l^2}\right]. \tag{8.6}$$

Characteristic of (8.6) and all the other asymptotic expressions associated with $\Delta\rho\ (\mathbf{r};\ E)$ is that it varies with r as r^{-2} times oscillating terms, i.e., that it descreases more slowly than the total electron density.

9. Interactions Between Defects

The expressions of sections 3 and 7 remain valid if the potential matrix elements $V_{nm}(\mathbf{R}_i,\ \mathbf{R}_j)$ describe several defects separated in space. It is possible to obtain from them the electronic interaction energy ΔE_i between the defects as a function of their relative positions. We give the results for two equal defects characterized by the matrix elements

$$V_{nn}(0,\ 0)=V_{nn}(\mathbf{R}_l,\ \mathbf{R}_l)=V_{00}, \tag{9.1}$$

assuming the separation $\mathbf{R}_l$ between the defects to be large enough to allow the application of the asymptotic formulas.

The one-electron interaction energy is defined as

$$\Delta E_i=\frac{2}{\pi}\int^{\zeta}\mathrm{arc}\ D_2(E)dE-2\,\frac{2}{\pi}\int^{\zeta}\mathrm{arc}\ D_1(E)dE, \tag{9.2}$$

where

$$D_1(E)=1-G(E,\ 0)V'_{00} \tag{9.3a}$$

describes an isolated defect, whereas

$$D_2(E)=\begin{bmatrix} 1-G(E,0)\ V''_{00} & -G(E,\ \mathbf{R}_l)V''_{00} \\ -G(E,\ \mathbf{R}_l)V''_{00} & 1-G(E,\ 0)V''_{00} \end{bmatrix} \tag{9.3b}$$

is the determinant in the presence of both defects. The values V'_{00} and V''_{00} of the matrix elements V_{00} are to be determined from the neutrality conditions, eqs (5.3) and (7.8),

$$\frac{2}{\pi}\ \mathrm{arc}\ \mathrm{D}_1(\zeta)\equiv 2\alpha_{\Gamma_1}(\zeta)=-Z, \tag{9.4a}$$

$$\frac{2}{\pi}\ \mathrm{arc}\ D_2(\zeta)=-2Z. \tag{9.4b}$$

For large distances $\mathbf{R}_l$ one obtains

$$V''_{00} \simeq V'_{00} + \frac{V_B V'^2_{00}}{(2\pi)^4 n(\zeta)} \operatorname{Im}\left[G^2(\zeta, \mathbf{R}_l) e^{-2i\pi\alpha_{\Gamma_1}(\zeta)}\right] \tag{9.5}$$

with

$$G(E, \mathbf{R}_l) \simeq \frac{1}{V_B} \sum_{\nu} g_{\mathbf{k}'_\nu} \frac{e^{i\mathbf{k}'_\nu \cdot \mathbf{R}_l}}{R_l}. \tag{9.6}$$

The one-electron interaction energy becomes

$$\Delta E_i = \frac{2}{\pi^3 (2\pi)^6 n(\zeta)} \int^{\zeta} \frac{\sin^2 \pi\alpha_{\Gamma_1}(E)}{n(E)} dE \operatorname{Im}\left[\sum_{\nu,\nu'} g_{\mathbf{k}'_\nu} g_{\mathbf{k}'_{\nu'}} \frac{e^{i\{(\mathbf{k}'_\nu + \mathbf{k}'_{\nu'}) \cdot \mathbf{R}_l - 2\pi\alpha_{\Gamma_1}(E)\}}}{R_l^2}\right]_{E=\zeta} \tag{9.7}$$

and shows that the dependence on the separation is (apart from a different phase shift) that of $\overline{\Delta\rho}(\mathbf{R}_l; E)$ and not that of the total charge density $\overline{\Delta\rho}(\mathbf{R}_l)$. This at first sight surprising result is directly related to the fact that the charge neutrality condition has been applied to both defects taken together and not to each defect individually. It means that the electronic interaction between two point defects in metals is rather far-reaching and should definitely be taken into account in considerations of long-range interactions between defects.

With regard to the dependence of the interaction energy on the direction of the line joining the defects, we have to expect a similarly strong anisotropy as has been discussed in section 8 for the asymptotic change in the charge density.

10. Extended Defects

We have seen that the change in electron density associated with a localized perturbation extends rather far out. The effect of a point defect on the self-consistent potential of a metal will therefore also extend rather far out from the site of the defect. Elastic strains associated with the defects have a similar effect, too. However, the perturbing potential at the more distant sites will in general be small enough to be treated as a small perturbation. This suggests the following approach:

The large matrix elements $V_{nm}(\mathbf{R}_i, \mathbf{R}_j)$ for a limited number of sites in the immediate environment of the defect are taken into account exactly by the methods outlined in the preceding sections. The remaining small matrix elements are allowed for by a small perturbation of that exact solution, using the standard techniques of perturbation theory.

We shall not discuss this approach in detail here. As an example, its application to the calculation of the energy may be found in reference [7].

11. Transition Probability

In order to treat the effect of a perturbing potential on transport properties, the transition probability $W(\mathbf{k}, \mathbf{k}')$ for the transition from state $\mathbf{k}$ to state $\mathbf{k}'$ is required (see sec. 12). (From now on we shall confine ourselves to one band—the conduction band—and drop all band indices.) $W(\mathbf{k}, \mathbf{k}')$ is related to the ratio of the scattered particle flux (built up from Bloch waves with wave vector $\mathbf{k}'$) to the particle flux of the incident Bloch waves of wave vector $\mathbf{k}$ [19] (compare fig. 1). When calculating the particle fluxes from the wave function $\psi_{\mathbf{k}}(\mathbf{r})$, it suffices to consider the asymptotic solution. This brings the scattering amplitudes $S^{\mathbf{k}}_{\mathbf{k}'}$ into the expression for $W(\mathbf{k}, \mathbf{k}')$. When the geometry of the Fermi surface is taken into account properly, it is seen that the final expression does not contain the scattering amplitudes $S^{\mathbf{k}}_{\mathbf{k}'}$ but the quantities $A^{\mathbf{k}}_{\mathbf{k}'}$ (defined by eq (6.13)), which

for non-spherical energy surfaces have a $\mathbf{k}'$-dependence different from that of $S_{\mathbf{k}'}^{\mathbf{k}}$. The formula for the transition probability is [16] (V_c = volume of the crystal)

$$W(\mathbf{k}, \mathbf{k}') = \frac{(2\pi)^7}{\hbar V_c^2} |A_{\mathbf{k}'}^{\mathbf{k}}|^2 \delta(E(\mathbf{k}) - E(\mathbf{k}')), \tag{11.1}$$

justifying the name "transition amplitude" for $A_{\mathbf{k}'}^{\mathbf{k}}$.

The δ-function results from the fact that during the scattering the energy is preserved. It is convenient to introduce the function

$$w(\mathbf{k}, \mathbf{k}') = \frac{(2\pi)^7}{\hbar V_c^2} |A_{\mathbf{k}'}^{\mathbf{k}}|^2, \tag{11.2}$$

which is related to the transition probability by

$$W(\mathbf{k}, \mathbf{k}') = w(\mathbf{k}, \mathbf{k}') \delta(E(\mathbf{k}) - E(\mathbf{k}')). \tag{11.3}$$

From the definition of $A_{\mathbf{k}'}^{\mathbf{k}}$ (eq (6.13)) we see that $w(\mathbf{k}, \mathbf{k}')$ may be written in the form

$$w(\mathbf{k}, \mathbf{k}') = \sum_{\alpha}^{m} \bar{u}_\alpha(\mathbf{k}) \bar{v}_\alpha(\mathbf{k}'), \tag{11.4}$$

i.e., as a linear combination of products of functions $\bar{u}_\alpha(\mathbf{k})$, depending on $\mathbf{k}$, and $\bar{v}_\alpha(\mathbf{k}')$, depending on $\mathbf{k}'$. The number m of terms in this decomposition is equal to the square of the number of sites affected by the perturbation.

12. Electrical Resistivity and Thermoelectric Power [16]

We shall base the treatment of the effects of localized perturbations on the electrical resistivity and the thermoelectric power on the Boltzmann equation

$$\left(\frac{df}{dt}\right)_{\text{fields}} + \left(\frac{df}{dt}\right)_{\text{scattering}} = 0. \tag{12.1}$$

The rate of change of the distribution function of the electrons (occupation probability of the $\mathbf{k}$-states) $f(\mathbf{k}, \mathbf{r})$ due to fields is given by

$$\left(\frac{df}{dt}\right)_{\text{fields}} = -\frac{1}{\hbar} \nabla_{\mathbf{k}} E(\mathbf{k}) \cdot \nabla_{\mathbf{r}} f(\mathbf{k}, \mathbf{r}) - \frac{1}{\hbar} \mathbf{F} \cdot \nabla_{\mathbf{k}} f(\mathbf{k}, \mathbf{r}), \tag{12.2}$$

where $\hbar$ is Planck's constant and $\mathbf{F} = -e\mathbf{E}$ is the force exerted on an electron by the electrical field $\mathbf{E}$. The rate of change of the distribution function due to the scattering of the electrons may be written as

$$\left(\frac{df}{dt}\right)_{\text{scattering}} = \frac{V_c}{(2\pi)^3} \int \{W(\mathbf{k}', \mathbf{k}) f(\mathbf{k}') [1 - f(\mathbf{k})] - W(\mathbf{k}, \mathbf{k}') f(\mathbf{k}) [1 - f(\mathbf{k}')]\} d\mathbf{k}'. \tag{12.3}$$

where $W(\mathbf{k}, \mathbf{k}')$ is the transition probability introduced in section 11. If only the scattering by static imperfections is taken into account (very low temperatures), or if the temperature is higher than the Debye temperature, the scattering is to a very good approximation elastic. In this case,

to which we shall confine ourselves in the present paper, the transition probability may be written in the form of eq (11.3). It is then convenient to write the distribution function as

$$f(\mathbf{k}, \mathbf{r}) = f_0(\mathbf{k}) - \frac{\partial f_0}{\partial E}\, \mathbf{F}^* \cdot \mathbf{X}(\mathbf{k}), \tag{12.4}$$

where

$$f_0(\mathbf{k}) = f_0(E(\mathbf{k})) = \frac{1}{e^{(E(\mathbf{k})-\zeta)/kT}+1} \tag{12.5}$$

is the Fermi distribution function in the absence of external fields and

$$\mathbf{F}^* = \mathbf{F} - \frac{E-\zeta}{T}\, \nabla_{\mathbf{r}} T(\mathbf{r}). \tag{12.6}$$

$\nabla_{\mathbf{r}} T(\mathbf{r})$ is the temperature gradient. Linearizing the Boltzmann equation in $\mathbf{F}^*$ leads to the following integral equation (inhomogeneous Fredholm equation of the 2d kind) for the unknown vector function $\mathbf{X}(\mathbf{k})$:

$$\mathbf{X}(\mathbf{k}) \int W(\mathbf{k}, \mathbf{k}')\, d\mathbf{k}' - \int W(\mathbf{k}, \mathbf{k}')\, \mathbf{X}(\mathbf{k}')\, d\mathbf{k}' = \frac{(2\pi)^3}{\hbar V_c}\, \nabla E(\mathbf{k}) \tag{12.7a}$$

or, employing eq (11.3),

$$\mathbf{X}(\mathbf{k}) - \int_{E'=E(\mathbf{k})} K(\mathbf{k}, \mathbf{k}')\, \mathbf{X}(\mathbf{k}')\, d^2\mathbf{k}' = \mathbf{g}(\mathbf{k}) \tag{12.7b}$$

with $d^2\mathbf{k}' = dS_{\mathbf{k}'}/|\nabla E(\mathbf{k}')|$ ($dS_{\mathbf{k}'}$ = surface element).
Here

$$\mathbf{g}(\mathbf{k}) = \frac{(2\pi)^3}{\hbar V_c}\, \frac{\nabla E(\mathbf{k})}{\int_E w(\mathbf{k}, \mathbf{k}')\, d^2\mathbf{k}'}, \tag{12.8a}$$

$$K(\mathbf{k}, \mathbf{k}') = \frac{w(\mathbf{k}, \mathbf{k}')}{\int_E w(\mathbf{k}, \mathbf{k}')\, d^2\mathbf{k}'}. \tag{12.8b}$$

The electrical conductivity tensor $\underline{\underline{\sigma}}$ and the tensor of the absolute thermoelectric power $\underline{\underline{S}}$ are given in terms of the solution $\mathbf{X}(\mathbf{k})$ of eq (12.7) as

$$\underline{\underline{\sigma}} = e^2 \underline{\underline{\Lambda}}(\zeta), \tag{12.9}$$

$$\underline{\underline{S}} = -\frac{\pi^2 k^2 T}{3e} \left[\underline{\underline{\Lambda}}^{-1}(E)\, \frac{d}{dE}\, \underline{\underline{\Lambda}}(E) \right]_{E=\zeta} = -\frac{\pi^2 k^2 T}{3e} \left[\underline{\underline{\sigma}}^{-1}(E)\, \frac{d}{dE}\, \underline{\underline{\sigma}}(E) \right]_{E=\zeta}, \tag{12.10}$$

where

$$\underline{\underline{\Lambda}}(E) = \frac{2}{(2\pi)^3 \hbar} \int_{E=\text{const.}} \nabla E(\mathbf{k})\, \mathbf{X}(\mathbf{k})\, d^2\mathbf{k} \tag{12.11}$$

is a second rank tensor.

The integral equation (12.7b) may be solved simply in the two limiting cases already mentioned, namely either at very low temperatures, where the scattering is caused by the crystal defects only, or at temperatures above the Debye temperature, where the scattering by the static imperfections is small compared with that due to thermal vibrations and where the latter may to a sufficient approximation be described by a relaxation time, τ_{th}.

In the low-temperature case $W(\mathbf{k}, \mathbf{k}')$ and $w(\mathbf{k}, \mathbf{k}')$ are given by the equations of sec. 11. The kernel of the integral equation (12.7b) may therefore be written in the form

$$K(\mathbf{k}, \mathbf{k}') = \sum_{\nu=1}^{m} u_\nu(\mathbf{k}) v_\nu(\mathbf{k}'), \tag{12.12}$$

i.e., it is degenerate. In such a case, it is well known [20, 21] that the solution of eq (12.7b) may be expressed as

$$\mathbf{X}(\mathbf{k}) = \mathbf{g}(\mathbf{k}) + \sum_{\nu} u_\nu(\mathbf{k}) \mathbf{Y}_\nu, \tag{12.13}$$

where

$$\mathbf{Y}_\nu = \int_E v_\nu(\mathbf{k}') \mathbf{X}(\mathbf{k}') d^2\mathbf{k}' \tag{12.14}$$

has to satisfy the set of linear inhomogeneous equations

$$\mathbf{Y}_\nu - \sum_{\mu} \int_E v_\nu(\mathbf{k}') u_\mu(\mathbf{k}') d^2\mathbf{k}' \; \mathbf{Y}_\mu = \int_E v_\nu(\mathbf{k}') \mathbf{g}(\mathbf{k}') d^2\mathbf{k}'; \; \nu = 1 \; . \; . \; . \; m. \tag{12.15}$$

In the preceding equations, the integrations have to be carried out over surfaces of constant energy in $\mathbf{k}$-space, as indicated by the suffix E.

The order of the system (12.15) is equal to the square of the number of sites affected by the perturbation $V(\mathbf{r})$. In many cases of practical interest the problem of solving this equation can be reduced to smaller problems by use of symmetry considerations. The fact that the linearized Boltzmann equation may be solved exactly is a substantial advantage of the present formulation of the scattering problem. In marked contrast to this, the usual formulation of the scattering of free electrons by anisotropic defects does in general not permit the exact solution of the transport problem and necessitates the use of approximations or of the variational principle [22].

In the other limiting case, that of high temperatures, the scattering term (12.3) of the Boltzmann equation is rewritten in the form

$$\left(\frac{df}{dt}\right)_{\text{scattering}} = \left(\frac{df}{dt}\right)_{\text{defects}} - \frac{f - f_0}{\tau_{\text{th}}}, \tag{12.16}$$

where $(df/dt)_{\text{defects}}$ is given by $(df/dt)_{\text{scattering}}$ of the low-temperature case just discussed. Introducing again the vector function $\mathbf{X}(\mathbf{k})$ by eq (12.4), the integral equation

$$\frac{1}{\hbar} \nabla E(\mathbf{k}) - \frac{1}{\tau_{\text{th}}} \mathbf{X}(\mathbf{k}) + \frac{V_c}{(2\pi)^3} \int W(\mathbf{k}, \mathbf{k}') (\mathbf{X}(\mathbf{k}') - \mathbf{X}(\mathbf{k})) d\mathbf{k}' = 0 \tag{12.17}$$

is obtained. Since the second term of eq (12.17) is much larger than the third, the solution of eq (12.17) may be written as

$$\mathbf{X}(\mathbf{k}) = \frac{\tau_{\text{th}}}{\hbar} \nabla E(\mathbf{k}) + \mathbf{X}_1(\mathbf{k}), \tag{12.18}$$

256-724 O-67—7

where $\mathbf{X}_1(\mathbf{k})$ is small enough to be treated by perturbation theory. This leads to

$$\mathbf{X}_1(\mathbf{k}) = \frac{\tau_{th}^2}{\hbar} \frac{V_c}{(2\pi)^3} \int_E w(\mathbf{k}, \mathbf{k}') (\nabla E(\mathbf{k}') - \nabla E(\mathbf{k})) d^2\mathbf{k}'. \tag{12.19}$$

Inserting $\mathbf{X}(\mathbf{k})$ into eqs (12.9) to (12.11) gives us

$$\underline{\underline{\sigma}} = \underline{\underline{\sigma}}_{th} + \Delta\underline{\underline{\sigma}}, \tag{12.20}$$

$$\underline{\underline{\sigma}}_{th} = \frac{2e^2}{(2\pi)^3} \frac{\tau_{th}}{\hbar^2} \int_{E=\zeta} \nabla E(\mathbf{k}) \nabla E(\mathbf{k}) d^2\mathbf{k}, \tag{12.21}$$

$$\Delta\underline{\underline{\sigma}} = \frac{2e^2}{(2\pi)^3} \frac{\tau_{th}^2}{\hbar^2} \frac{V_c}{(2\pi)^3} \iint_{E=E'=\zeta} w(\mathbf{k}, \mathbf{k}') [\nabla E(\mathbf{k}) \nabla E(\mathbf{k}') - \nabla E(\mathbf{k}) \nabla E(\mathbf{k})] d^2\mathbf{k} d^2\mathbf{k}'. \tag{12.22}$$

It is convenient to express the effect of the lattice defects on the transport properties in terms of the change $\Delta\underline{\underline{\rho}}$ of the electrical resistivity $\underline{\underline{\rho}}$ and the change $\Delta\underline{\underline{S}}$ of the absolute thermoelectric power $\underline{\underline{S}}$. Making use of $\Delta\underline{\underline{\sigma}} \ll \underline{\underline{\sigma}}_{th}$, one obtains with $\underline{\underline{\rho}}_{th} = \underline{\underline{\sigma}}_{th}^{-1}$

$$\Delta\underline{\underline{\rho}} = \underline{\underline{\rho}} - \underline{\underline{\rho}}_{th} \approx -\underline{\underline{\sigma}}_{th}^{-1} \Delta\underline{\underline{\sigma}} \underline{\underline{\sigma}}_{th}^{-1}. \tag{12.23}$$

The general expression for the change in the thermoelectric power is

$$\Delta\underline{\underline{S}} = -\frac{\pi^2 k^2 T}{3e} \left[(\underline{\underline{\sigma}}_{th} + \Delta\sigma)^{-1} \frac{d}{dE} (\underline{\underline{\sigma}}_{th} + \Delta\underline{\underline{\sigma}}) - \sigma_{th}^{-1} \frac{d}{dE} \underline{\underline{\sigma}}_{th} \right]_{E=\zeta}, \tag{12.24}$$

or, making use of the tensor generalization of an expression first given by Friedel [23],

$$\Delta\underline{\underline{S}} = \frac{\pi^2 k^2 T}{3e} \left[(1 + \Delta\underline{\underline{\sigma}}^{-1} \underline{\underline{\sigma}}_{th})^{-1} \left(\underline{\underline{\sigma}}_{th}^{-1} \frac{d}{dE} \underline{\underline{\sigma}}_{th} - \Delta\underline{\underline{\sigma}}^{-1} \frac{d}{dE} \Delta\underline{\underline{\sigma}} \right) \right]_{E=\zeta}. \tag{12.25}$$

In the high-temperature case, the preceding exact expressions may be replaced by

$$\Delta\underline{\underline{S}} \approx -\frac{\pi^2 k^2 T}{3e} \underline{\underline{\sigma}}_{th}^{-1} \Delta\underline{\underline{\sigma}} \left[\Delta\underline{\underline{\sigma}}^{-1} \frac{d}{dE} \Delta\underline{\underline{\sigma}} - \underline{\underline{\sigma}}_{th}^{-1} \frac{d}{dE} \underline{\underline{\sigma}}_{th} \right] \Bigg|_{E=\zeta} \tag{12.26}$$

$$\approx \frac{\pi^2 k^2 T}{3e} \left[\left(\frac{d}{dE} \Delta\underline{\underline{\rho}} \right) \Delta\underline{\underline{\rho}}^{-1} - \left(\frac{d}{dE} \underline{\underline{\rho}}_{th} \right) \underline{\underline{\rho}}_{th}^{-1} \right] \Delta\underline{\underline{\rho}} \underline{\underline{\rho}}_{th}^{-1} \Bigg|_{E=\zeta}. \tag{12.27}$$

The last expression for $\Delta\underline{\underline{S}}$ shows that at high temperatures the thermoelectric power is (as is the electrical resistivity) proportional to the concentration of defects. (This does not hold for low temperatures.) As long as the high-temperature resistivity is proportional to the absolute temperature T, the high-temperature value of $\Delta\underline{\underline{S}}$ due to the defects is independent of temperature. At low temperatures the electronic contribution to $\Delta\underline{\underline{S}}$ is proportional to T.

Table 1 gives numerical examples for the electrical resistivity and the change in thermoelectric power for vacancies and divacancies in the noble metals as computed by Thierer [24] from the preceding formulas. They are based on the energy surfaces of Roaf [18] and on the assumptions that only the following matrix elements are different from zero:

(a) Single vacancy: $$V_{00}, V_{11} = V(\mathbf{R}_n, \mathbf{R}_n) = \frac{1}{10} V_{00}$$

($\mathbf{R}_n$ = nearest neighbors of the vacant site)

(b) Divacancy: $V_{00} = V(\mathbf{R}_s, \mathbf{R}_s)$, $V_{11} = V(\mathbf{R}_n, \mathbf{R}_n) = \frac{1}{10} V_{00}$

($\mathbf{R}_s$ = vacant sites,

$\mathbf{R}_n$ = nearest neighbors of both vacant sites).

The absolute magnitude of the matrix elements was determined by using the neutrality condition (sec. 7). In the results on the electrical resistivity the energy function $E(\mathbf{k})$ enters only through the shape of the Fermi surface, which is well known from experiments. For the thermoelectric power, however, the magnitude of $\nabla E(\mathbf{k})$ at the Fermi surface must be known. It has been fixed by using a one-band expression, eq (2.1), and giving to the Fermi energy ζ its free electron value. For comparison with experiments, the results of Huebener on the effect of vacancies on the thermoelectric power of gold [25] are given in parentheses.

TABLE 1. *Electrical resistivity* $\Delta\rho$ *and change in thermoelectric power* ΔS *at low* (l) *and high* (h) *temperatures for monovacancies* (1v) *and divacancies* (2v) *in noble metals (preliminary resalts)*

The values for divacancies are averaged over all directions. The differences between $\Delta\rho^l$ and $\Delta\rho^h$ are negligibly small. T = absolute temperature, exp = experimental values.

	Cu	Ag	Au
$\Delta\rho_{1v}^{l,h}$ [$\mu\Omega$ cm/at.%]	1,47	1,73	1,80
$\Delta\rho_{2v}^{l,h}/\Delta\rho_{1v}^{l,h}$	1,78	1,75	1,82
ΔS_{1v}^{l} [$10^{-2}\mu V/(°K)^2$]	−0,28 T	−0,36 T	−0,53 T (exp −0,5 T)
ΔS_{2v}^{l} [$10^{-2}\mu V/(°K)^2$]	−0,30 T	−0,38 T	−0,56 T
ΔS_{1v}^{h} [$\mu V/^2$K at.%]	−0,98	−1,31	−1,47 (exp −1,67)
$\Delta S_{2v}^{h}/\Delta S_{1v}^{h}$	1,86	1,89	1,85

13. Magnetoresistivity

As a tool for studying the anisotropy of Fermi surfaces, the magnetoresistivity at low temperatures has proven very important [26-29]. The scattering theory outlined in the present paper allows us to treat not only the anisotropy of the energy surfaces, but also the anisotropy of the scattering mechanism in an exact way [30].

As usual, we base our treatment on the Lorentz-force formula and the Boltzmann equation. The wave-number space is described by the coordinates ϵ, k_z and ϕ, where $\epsilon(\mathbf{k})$ is the energy, k_z the component of the wave vector parallel to the magnetic field $\mathbf{H}$, and

$$\phi = \omega_H \frac{c\hbar}{eH} \int \frac{dk}{v_\perp} \tag{13.1}$$

a phase variable measuring the position of a point in $\mathbf{k}$-space in its orbit in a plane k_z = const. [31, 32]. The quantity $v_\perp$ is the component of the electron velocity $\mathbf{v} = \frac{1}{\hbar} \nabla\epsilon(\mathbf{k})$ perpendicular to $\mathbf{H}$, and dk is a path element in $\mathbf{k}$-space. The cyclotron frequency ω_H is given by the integral over a closed orbit

$$\frac{2\pi}{\omega_H} = \frac{c\hbar}{eH} \oint \frac{dk}{v_\perp} = \frac{c}{eH} \hbar^2 \frac{\partial A(\epsilon, k_z)}{\partial \epsilon}, \tag{13.2}$$

where $A(\epsilon, k_z)$ is the area in $\mathbf{k}$-space enclosed by the orbit.

Writing the distribution function as in eq (12.4), the Boltzmann equation for elastic scattering reads to first order in $\mathbf{X}(\mathbf{k})$ [31]

$$\omega_H \frac{\partial \mathbf{X}}{\partial \phi} - \mathbf{v} = \frac{V_c}{(2\pi)^3} \int W(\mathbf{k}, \mathbf{k}') \mathbf{X}(\mathbf{k}') d\mathbf{k}' - \frac{V_c}{(2\pi)^3} \mathbf{X}(\mathbf{k}) \int W(\mathbf{k}, \mathbf{k}') d\mathbf{k}'. \tag{13.3}$$

Inserting the expressions of section 11 for the transition probability and evaluating the integrals over $\mathbf{k}'$ gives us for $\epsilon = \zeta$

$$\omega_H \frac{\partial \mathbf{X}(\phi; k_z)}{\partial \phi} - \mathbf{v} = \sum_{\nu}^{m} \bar{u}_\nu(\phi; k_z) \bar{\mathbf{Y}}_\nu - \mathbf{X}(\phi; k_z) \sum_{\nu}^{m} \bar{u}_\nu(\phi; k_z) A_\nu. \tag{13.4}$$

Here

$$A_\nu = \frac{V_c}{(2\pi)^3} \int_{\epsilon=\zeta} \bar{v}_\nu(\mathbf{k}') d^2\mathbf{k}'; \quad \bar{\mathbf{Y}}_\nu = \frac{V_c}{(2\pi)^3} \int_{\epsilon=\zeta} \mathbf{X}(\mathbf{k}') \bar{v}_\nu(\mathbf{k}') d^2\mathbf{k}', \tag{13.5}$$

where the integrals extend over the Fermi surface $\epsilon = \zeta$. If we introduce the function

$$F(\phi; k_z) = \frac{1}{\omega_H} \sum_{\nu}^{m} A_\nu \int_{\phi' = \phi_0}^{\phi' = \phi} \bar{u}_\nu(\phi'; k_z) d\phi', \tag{13.6}$$

we may write the solution of eqs (13.3) and (13.4) as

$$\mathbf{X}(\phi; k_z) = \frac{\exp[-F(\phi; k_z)]}{\omega_H} \int_{\phi'' = \infty}^{\phi'' = \phi} \left[\sum_{\nu}^{m} \bar{u}_\nu(\phi''; k_z) \bar{\mathbf{Y}}_\nu + \mathbf{v} \right] \exp[F(\phi''; k_z)] d\phi''. \tag{13.7}$$

The constants $\bar{\mathbf{Y}}_\nu$ are obtained by solving the following system of linear equations:

$$\bar{\mathbf{Y}}_\mu = \int_{\epsilon=\zeta} \frac{1}{\omega_H} \bar{v}_\mu(\phi, k_z) \exp[-F(\phi, k_z)] \left\{ \int_{-\infty}^{\phi} \left[\sum_{\nu}^{m} \bar{u}_\nu(\phi''; k_z) \bar{\mathbf{Y}}_\nu + \mathbf{v} \right] \exp[F(\phi''; k_z)] d\phi'' \right\} d^2\mathbf{k}; \quad \mu = 1 \ldots m. \tag{13.8}$$

Inserting the solutions of eq (13.8) into eq (13.7) completes the solution of the Boltzmann equation. The tensors of the electrical conductivity and the thermoelectric power are obtained by inserting this solution into the expressions (12.9) to (12.11).

These solutions are valid for all magnetic fields below the quantum oscillation region. Following the procedure of Mertsching [32], the quantum oscillations may also be included in the treatment by allowing for the density of states of the energy levels quantized in the magnetic field. From eqs (13.7) and (12.9) to (12.11) the magnetoresistivity, the Hall effect, and the analogous thermoelectric effects at high and intermediate fields can be obtained in a convenient form by expanding the exponential functions in powers of ω_H^{-1}.

14. Pseudopotentials and Pseudoatoms

In recent years the theory of pseudopotentials has been repeatedly applied to the calculation of defect properties in metals [4, 33]. The basic idea of the pseudopotential approach, viz., supplanting the condition of orthogonality of a state of high principal quantum number to the states of lower quantum numbers by a short-range repulsive "pseudopotential," is a fairly old one [34, 35]. Its first application to the theory of crystals appears to have been made by Fues and Statz [36]. Recently, the idea has been extended to the concept of "pseudoatoms" [37]. A pseudoatom is an ion in a metal plus its screening charge; on account of the large spatial extension of the screening

charge in a metal (see sec. 8) it is considerably more extended than a free atom.

In applying the pseudoatom idea to defect calculations, the assumption is made that not only the perfect metal but also a perturbed metal may be built up from pseudoatoms carrying their screening charges with them while they are displaced to off—lattice-sites positions. This implies that the pseudopotentials associated with each ion superimpose without perturbing each other, which in turn means that they must be well localized within each atomic cell. In actually solving the Schrödinger equation of the perturbed crystal, the further assumption is made that the pseudopotentials are so weak that they may be treated by second-order perturbation theory, starting from plane waves. Although this additional assumption is not inherent in the physical concept of pseudoatoms, it has so far been a practical necessity in the applications of the pseudopotential method to defects in metals, since the pseudopotential is usually formulated in terms of matrix elements between plane waves.

Let us first examine whether the pseudopotential approach as outlined above, based on the superposition principle, the quasi-free electron picture, and the use of second-order perturbation theory can be expected to give reasonable results for point defect calculations. Unfortunately it will turn out that the basic assumptions made in this treatment, which is the one almost exclusively adopted in the recent book by Harrison [33], are incompatible with each other. This can be seen as follows: In order to permit the linear superposition of the pseudopotentials of neighboring pseudoatoms, each of these pseudopotentials must be well concentrated within the atomic cell. In order to hold the screening charge of one electron per atom in monovalent metals (or even of two or more electrons in polyvalent metals) this potential must at the same time have sufficient strength. The more concentrated the potential is, the deeper has the potential well to be in order to attract a given screening charge. From the calculations on vacancies and interstitials based on the free electron approach (see, e.g., [3, 2]) it is well known that even in monovalent metals a potential repelling or attracting one electron is much too strong to be treated by perturbation theory, if localized within the unit cell. A physical measure of the failure of the second-order perturbation theory is the phase constant φ_F in the asymptotic charge density

$$\Delta\rho(\mathbf{r}) \simeq -\frac{\alpha_F}{2\pi^2 r^3}\cos(2k_F r+\varphi_F) \tag{14.1}$$

around a defect localized at $r=0$. The parameters α_F and φ_F are given in terms of the free electron phase shifts η_l by [17]

$$\alpha_F \sin\varphi_F = \sum_l (-1)^l(2l+1)\sin^2\eta_l(E_F) \tag{14.2}$$

$$\alpha_F \cos\varphi_F = \frac{1}{2}\sum_l (-1)^l(2l+1)\sin 2\eta_l(E_F). \tag{14.3}$$

In the perturbation theory treatment we have $\varphi_F=0$ [38]; the expression for α_F is invalid if $\alpha_F \ll 1$ is not fulfilled. As numerical examples for the exact evaluation of eqs (14.2) and (14.3), we consider a potential based on the Hartree-Fock solution for a Cu-ion determined by Stehle [39] for vacancy calculations, and an attractive square-well potential used by Seeger and Mann [40] for interstitial atoms in monovalent metals. In order to make the situation least unfavorable for the pseudopotential theory, we choose the radius for the square-well potential as large as possible within the framework of the pseudoatom approach, namely equal to the radius r_s of the Wigner-Seitz sphere. The numerical results are in the first case

$$\alpha_F=-0.478, \qquad \varphi_F=-\frac{\pi}{2}+0.198=-1.313$$

and in the second case

$$\alpha_F=0.159, \qquad \varphi_F=-0.733.$$

We see that in none of these examples φ_F is negligible. In typical situations in monovalent metals $|\varphi_F|$ will lie between $\pi/4$ and $\pi/2$. For polyvalent metals the asymptotic phase φ_F will be even larger. Phase shifts $|\varphi_F|$ comparable with or larger than $\pi/4$ will completely invalidate the theory of interactions between ions based on pair potentials derived from the pseudopotential theory. This can be seen by comparing the pair interactions for Al determined experimentally from liquid metal scattering data with the theoretical curve [41]. While these data confirm the existence of the long-range charge oscillations (compare sec. 8), they demonstrate at the same time that the phase of these oscillations differs from the one calculated by the pseudopotential theory by approximately π, in agreement with our predictions. This difference in phase is extremely serious whenever the charge oscillations enter into the final result of pseudopotential theory. In the case of Al it leads to a reversal of sign in the interaction potential. Any agreement of pseudopotential calculations of such properties as interaction energies between point defects, stacking-fault energies etc., must therefore be considered as fortuitous.

We cannot therefore support Ziman's claim [4] that in calculations on defects in metals the usual pseudopotential approach is superior to the free electron calculations. The latter have at least the advantage that, once a potential describing the defect has been adopted, the results follow in a mathematically reliable way from the model, whereas the pseudopotential approach makes assumptions which are certainly not justified and which become more and more serious, the higher the valency of the metal. On the other hand, the polyvalent metals are just those for which the pseudopotential theory is claimed to be best applicable. It appears to us that the only way in which the success of the quasi-free electron picture in describing the Fermi surface of aluminum can be utilized for defect calculations is to start from an exact free electron solution of the defect problem (if obtainable) and to allow subsequently for the small deviations of the Fermi surface from sphericity by perturbation theory.

15. References

[1] A. C. Damask and G. J. Dienes, Point Defects in Metals (Gordon and Breach, New York, 1963).
[2] H. Bross, in: A. Seeger, Moderne Probleme der Metallphysik, Vol. I (Springer, Berlin-Heidelberg-New York, 1965).
[3] A. Seeger, J. Phys. Radium **23**, 616 (1962).
[4] J. M. Ziman, Adv. in Phys. **13**, 49 (1964).
[5] J. C. Slater, Handbuch der Physik, Vol. **XIX** (Springer, Berlin-Göttingen-Heidelberg, 1956); Quantum Theory of Molecules and Solids, Vol. **2** (McGraw-Hill Book Co., New York, 1965).
[6] G. F. Koster and J. C. Slater, Phys. Rev. **95**, 1167 (1954).
[7] E. Mann, Phys. Stat. Sol. **11**, 753 and 767 (1965).
[8] G. Wentzel, Helv. Phys. Acta **15**, 111 (1942).
[9] A. A. Maradudin, E. W. Montroll, and G. H. Weiss, Solid State Physics, Suppl. **3** (Academic Press, New York and London, 1963).
[10] H. Jones, The Theory of Brillouin Zones and Electronic States in Crystals (North-Holland, Amsterdam, 1960).
[11] J. Friedel, Adv. in Phys. **3**, 446 (1954).
[12] F. G. Fumi, Phil. Mag. **46**, 1007 (1955).
[12a] F. Gautier and P. Lenglart, Phys. Rev. **139**, A705 (1965).
[12b] E. Mann, Phys. Letters **18**, 110 (1965).
[13] G. F. Koster, Phys. Rev. **95**, 1436 (1954).
[14] E. Mann, Phys. Stat. Sol. **13**, 293 (1966).
[15] I. M. Lifshitz, Suppl. Nuovo Cimento [X] **3**, 716 (1956).
[16] E. Mann, A. Seeger, and G. Thierer, Z. Physik **193**, 295 (1966).
[16a] J. Callaway, J. Math. Phys. **5**, 783 (1964).
[17] A. Blandin, J. Phys. Radium **22**, 507 (1961).
[18] D. J. Roaf, Phil. Trans. Roy. Soc. (London) **A255**, 135 (1962).
[19] L. M. Roth, Thesis, Harvard University, Cambridge, Mass., 1957.
[20] W. Schmeidler, Integralgleichungen I (Akademische Verlagsgesellschaft, Leipzig, 1950).
[21] S. G. Mikhlin, Integral Equations (Pergamon Press, London-New York-Paris-Los Angeles, 1957).
[22] H. Bross and A. Seeger, J. Phys. Chem. Solids **4**, 161 (1958).
[23] J. Friedel, J. Phys. Radium **14**, 561 (1953).
[24] G. Thierer, Diplomarbeit, Technische Hochschule Stuttgart, (1966).
[25] R. P. Huebener, Phys. Rev. **135**, A1281 (1964).

[26] I. M. Lifshitz, M. Ya. Azbel', and M. I. Kaganov, Zh. eksper. teor. fiz. **30**, 220 (1955); **31**, 63 (1956).
[27] I. M. Lifshitz and V. G. Peschanskii, Zh. eksper. teor. fiz. **35**, 1251 (1959); **38**, 188 (1960).
[28] I. M. Lifshitz and M. I. Kaganov, Uspekhi fiz. nauk **69**, 419 (1960).
[29] R. G. Chambers, The Fermi Surface, p. 100 (W. A. Harrison, M. B. Webb, eds.), (John Wiley & Sons, New York-London 1960).
[30] A. Seeger, Phys. Letters **20**, 608 (1966).
[31] J. M. Ziman, Electrons and Phonons (Clarendon Press, Oxford 1960).
[32] J. Mertsching, Phys. Stat. Sol. **14**, 3 (1966).
[33] W. A. Harrison, Pseudopotentials in the Theory of Metals (Benjamin, New York and Amsterdam, 1966).
[34] H. Hellmann, Einführung in die Quantenchemie, sec. 8 (Deuticke, Leipzig und Wien, 1937).
[35] P. Gombas, Die statistische Theorie des Atoms und ihre Anwendungen, sec. 19 (Springer, Wien, 1949).
[36] E. Fues und H. Statz, Z. Naturforschung **7a**, 2 (1952).
[37] J. M. Ziman, in: Physikertagung 1965 Frankfurt (M)-Hoechst, Plenarvorträge, Deutsche Physikalische Gesellschaft (Teubner, Stuttgart, 1965).
[38] A. Blandin, in: Alloying Behavior and Effects in Concentrated Solid Solutions, Metallurgical Society Conferences, Vol. **29** (Gordon and Breach, New York, 1965).
[39] H. Stehle, Dissertation, Technische Hochschule Stuttgart, 1957; cf. also A. Seeger [3].
[40] A. Seeger and E. Mann, J. Phys. Chem. Solids **12**, 326 (1960).
[41] cf. W. A. Harrison [33], fig. 8–10, p. 319.

Electrical Resistivity of Impurities and Vacancies in Aluminum

Yuh Fukai

Department of Physics, Chuo University, Bunkyo-ku, Tokyo, Japan

Electrical resistivities due to impurities and vacancies in Al have been calculated in a pseudopotential formalism. Comparison with experimental values suggests that the atomic displacement is outward around a vacancy in Al in contrast to noble metals.

1. Introduction

Although most of the existing calculations of defect scattering have been based on an approximate phase shift analysis, recent progress in the pseudopotential approach now allows us to attack this problem in a more reliable way, provided a screened lattice potential is weak enough to be treated by perturbation theory. Now we have a potential of Al, well examined both theoretically and experimentally: also we have good reason to expect that calculations could be more reliable in Al than in noble metals.

2. Pseudopotentials Adopted

Considering only elastic scattering of electrons on the Fermi surface, $\mathbf{k}\rightarrow\mathbf{k}+\mathbf{q}$, where $|\mathbf{k}|=|\mathbf{k}+\mathbf{q}|=k_F$, we need a Fourier component of the potential $w(q)$ in the range $0\leq q\leq 2k_F$ for the calculation of electrical resistivity. For this we use "experimental" values corresponding to a few lattice wave numbers deduced from de Haas-van Alphen experiments on Zn [1],[1] al [2], and from optical experiments on Si and Ge [3]. Potential curves calculated by Animalu and Heine [4] were used for the interpolation of experimental points.

Potential curves of atoms as solutes in the Al lattice, $w_i(q)$, are constructed from the ones in their own lattice $v_i(q)$ in the manner,

$$w_i(q)=\frac{\Omega_i\epsilon_i(q)}{\Omega_0\epsilon_0(q)}v_i(q).$$

The ratio of atomic volumes Ω_i/Ω_0 comes from the different normalization volume of wave functions, and the ratio of the SCF dielectric function $\epsilon_i(q)/\epsilon_0(q)$ from different screening by conduction electrons of impurities embedded in the Al lattice from that in their own lattice. The validity of this simple transformation was examined by Harrison theoretically [5], and also by our NMR experiments on Al-alloys [6].

3. Electrical Resistivity Due to Impurity Atoms

The electrical resistivity is calculated, treating the lattice pseudopotential as a first order perturbation. The formula is given by

$$\Delta\rho=\frac{1}{4.58}\frac{3\pi\Omega_0}{16E_F}\int_0^2[w_i(x)-w_0(x)+N\Delta S(x)w_0(x)]^2x^3dx\ \mu\Omega\cdot\text{cm./at.\%},$$

where $x=q/k_F$, $w_i(x)$ and $w_0(x)$ are pseudopotentials of the impurity and the host atoms, respectively, $\Delta S(x)$ is the change in the geometrical structure factor due to lattice distortion. The Fermi energy E_F and potential w's are written in Rydbergs.

In the absence of any exact knowledge of lattice distortion, we shall here calculate $\Delta\rho$ originating from the difference in pseudopotentials only. It turned out that approximate inclusion of distortion as described in the next section does not affect our results by more than 10 percent in the case of impurity scattering, if we use lattice distortion as estimated from lattice-parameter changes. Results of calculations are listed in table 1, together with experimental ones.

TABLE 1. *Electrical resistivity due to impurities in Al*
($\mu\Omega$cm/at.% solute)

Solute	$\Delta\rho_{calc.}$	$\Delta\rho_{exp.}$	$\Delta\rho_{exp.}/\Delta\rho_{calc.}$
Zn	0.16	0.24	1.5_0
Si	.41	.60	1.4_6
Ge	.59	.79	1.3_4

[1] Figures in brackets indicate the literature references at the end of this paper.

The agreement seems gratifying in view of approximations involved. Theoretical values will become even closer to experimental ones when we proceed to second order perturbation.

4. Electrical Resistivity Due to Vacancies

The same formula is applied to vacancies, putting $w_i(x)=0$. Neglecting, as before, the effect of lattice distortion, we obtain $\Delta\rho=0.66\ \mu\Omega\cdot\text{cm/at.\%}$, which is much smaller than the experimental value $\Delta\rho=2.2\pm0.6\ \mu\Omega\cdot\text{cm/at.\%}$ [7].

Let us tentatively assume that our calculation on vacancies is reliable to the same extent as on impurities, and take $(1.3\sim1.5)\times0.66\ \mu\Omega\cdot\text{cm}$ as a theoretical value, then we may estimate the amount of lattice distortion by comparison with experimental values ascribing the remaining discrepancy to distortion effects. For this purpose, we calculate a geometrical structure factor as a function of fractional displacement of nearest-neighbors, assuming the isotropic elastic solution for the atomic displacement:

$$\xi=\eta\left(\frac{a}{\sqrt{2}r}\right)^3\mathbf{r}.$$

Comparison with experimental value yields

$$\eta=+0.09\ {}^{-0.06}_{+0.11}.$$

The positive sign indicates that displacement is outward.

The outward displacement thus deduced, though apparently incompatible with our knowledge on noble metals, should not be taken as improbable. The same conclusion was reached by Harrison [8] on vacancies in Zn. We may rather regard it as fairly common to metals with small ion cores where repulsive forces are of long range character as distinct from noble metals where short range core repulsion is dominant.

The present work is of course roundabout as an approach to lattice distortion, and more direct calculation is necessary in drawing any definite conclusions. This is possible, in theory, within the same pseudopotential formalism, but we cannot be too optimistic about it. Very strong cancellation of electrostatic and band-structure energies in Al [9], as well as the long range, oscillating character of interatomic interactions via conduction electrons [10, 11] will make such calculations quite unreliable. This is the very reason why we have made a detour and have left a more orthodox way of approach for future studies.

5. References

[1] W. A. Harrison, Phys. Rev. **126**, 497 (1962).
[2] N. W. Ashcroft, Phil. Mag. **8**, 2055 (1963).
[3] D. Brust: Phys, Rev. **134**, A1337 (1964).
[4] A. O. E. Animalu and V. Heine, Phil. Mag. **12**, 1249 (1965).
[5] W. A. Harrison, Phys. Rev. **131**, 2433 (1963).
[6] Y. Fukai and K. Watanabe, To be published in J. Phys. Soc. Japan.
[7] J. Takamura, Lattice Defects in Quenched Metals, p. 521, (Academic Press, Inc., New York, 1965). The value is corrected for deviations from Matthiessen's rule.
[8] W. A. Harrison, Phys. Rev. **129**, 2512 (1963).
[9] W. A. Harrison, Phys. Rev. **136**, A1107, (1964).
[10] W. A. Harrison, Phys. Rev. **129**, 2503 (1963).
[11] M. H. Cohen, in Metallic Solid Solutions, (J. Friedel and A. Guinier, ed.) (W. A. Benjamin, Inc., New York, 1962).

Structure Factor Approach to Energies of Migration

H. B. Huntington and Michael D. Feit

Rensselaer Polytechnic Institute, Troy, New York 12180

Several crystal lattice defects move with hardly any activation volume. Examples of such are the interstitialcy, the crowdion, the dislocation, and possibly some interstitial impurities. Presumably their energy of motion is largely the difference in the ordering of the atoms between two rather similar configurations. The individual environment of each atom changes relatively little in going from one configuration to the next as far as its ambient electron density or cell volume. One would like a method of attack where energy could be tied very directly to structure. For this purpose Harrison's recent technique [1][1] growing out of his pseudopotential approach [2] seems made to order.

According to the Harrison approach the energy of any configuration can be represented by the sum of three terms: one of which is volume dependent and will be avoided in these applications, another of which is just the coulomb energy of the undressed ionic charges (as might be found by a modified Ewald method), and the third is the so-called band structure term, which has the following form,

$$E_{bs}=Nz\sum_{q}|S(q)|^2\,F(q).$$

Here N is the number of ions in the lattice and z is their valence. The summation is over all the points of wave number space. The $S(q)$ is just the structure factor as usually defined as in diffraction and $F(q)$ is called "the energy wave-number characteristic" with units of energy per electron. It is this function which embodies the particularities of the band structure of each metal and must be separately evaluated in each case via application of the pseudopotential technique. Harrison has carried out this evaluation [1] for sodium, magnesium, and aluminum. These functions are large and negative for small wave number, exhibit minima in magnitude where the form factor changes sign, and go rapidly to zero at large wave number. Defect calculations based on this formulation of the total energy would involve the electrons and their redistribution to a greater extent than prior approaches.

The formulation is, however, reducible to the use of a two-body potential. For multibody forces the perturbation development would need to be carried to higher order. The connection between $F(q)$ and the equivalent two-body potential $V(r)$ is easily demonstrated [3]. The latter exhibits the familiar Friedel oscillations at large distance since in developing $F(q)$ account is taken of the sharp Fermi cutoff in the dielectric response of the metal.

In our application we want to compare the energies of two related defect configurations involving several atoms on a nearly equal basis. Although the more recent defect calculations have used an elastic displacement function at large distances, the explicit evaluation of the structure factor in our method made it necessary to treat only a finite number of displaced atoms. With $\mathbf{r}_i'$ for the displaced positions of these atoms and $\mathbf{r}_i$ for their original locations the structure can be written as a small number of terms

$$NS(q)=\sum_{i}^{N}e^{-i\mathbf{q}\cdot\mathbf{r}_i'}=\sum_{i}^{n}(e^{-i\mathbf{q}\cdot\mathbf{r}_i'}-e^{i\mathbf{q}\cdot\mathbf{r}_i})\pm e^{i\mathbf{q}\cdot\mathbf{r}}+N\delta_{qK}$$

Here n stands for the number of atoms in the specimen that are displaced. The second term represents the lattice defect, + for interstitial and − for vacancy. The final term is now expressed as an integral plus a sum

$$E_{bs}=\frac{z\Omega_0}{(2\pi)^3}\int F(q)\left[\sum_{i,j}^{n}(e^{-iq\cdot r_i'}-e^{-iq\cdot r_i})(e^{iq\cdot r_j'}-e^{iq\cdot r_d})\right.$$

$$\left.\pm 2\sum_{i}\{\cos q(r_i'-r_d)-\cos q(r_i-r_d)\}+1\right]d^3q$$

$$+2z\sum_{K}F(K)\left[\sum_{i}(\cos K\cdot r_i'-\cos K\cdot r_i)\pm\cos K\cdot r\right].$$

As a test case, to give experience with this approach we calculated the restoring force for the motion of a single atom in an otherwise perfect aluminum lattice. In energy units of milli-rydbergs and with d the lattice constant we found for the energy of the atom displaced by δ,

Electrostatic energy	$46.3\,(\delta/d)^2$
Integral term in band structure energy	$-108.3\,(\delta/d)^2$
Discrete Sum term in band structure energy	$70.6\,(\delta/d)^2$
	$8.6\,(\delta/d)^2$

[1] Figures in brackets indicate the literature references at the end of this paper.

which is equivalent to an Einstein temperature of about 580 °K. Note the high degree of cancellation making it important to work to several significant figures.

We have applied this procedure so far only to a comparison of the "split interstitial" and cube center interstitial in the face-centered cubic lattice. In each case the same number of displaced atoms was used ($n \sim 87$) and since the outer atoms were held fixed, the volume was the same for both defects. For our configuration we have chosen the displacements found by Johnson and Brown [4] using a Born-Mayer type potential. The sensitivity of defect energy to atom positions near equilibrium is usually small but we intend to explore this point more later. Preliminary results from this calculation favors the split configuration. The energy difference between the two configurations has been calculated for aluminum and hypothetical fcc metals of magnesium and sodium at their normal density. The results are given below for $E_{cc} - E_{sc}$ in eV.

Note that the electrostatic contribution dominates and serves as an upper limit in these cases. This energy difference is associated with, but exceeds, the motion energy for the free interstitialcy.

	Aluminum	Magnesium	Sodium
Electrostatic energy	0.3488	0.1403	0.0288
Integral term	.0328	.0099	.0038
Discrete sum term	−.1278	−.0441	−.0129
Total	0.254	0.106	0.020

The method is of interest for several reasons. It may supply insight into how the energy difference between two configurations depends on the transform of the interaction potential. It attempts to take into account the energy of the electrons and of their redistribution in the presence of a defect. Once developed for the comparisons of a particular pair of defects the result can be quickly extended to any other material of the same crystal structure for which $F(q)$ is known.

References

[1] W. A. Harrison, Phys. Rev. **136A,** 1107 (1964).

[2] W. A. Harrison, Pseudopotentials in the Theory of Metals (W. A. Benjamin, Inc., New York, N.Y. 1966).

[3] Ref. [2] p. 43; M. H. Cohen, in Metallic Solid Solutions, J. Friedel and A. Guinier, editors (W. A. Benjamin, Inc., New York, N.Y. 1962).

[4] R. A. Johnson and E. Brown, Phys. Rev. **127,** 446 (1962).

Perturbed Bloch Functions Obtained from the Koster-Slater Perturbation Theory*

Bernard Mozer

Brookhaven National Laboratory, Upton, New York 11973

Approximations for Bloch functions for a crystal containing an impurity can be obtained from approximate solutions of the Koster-Slater equations. A well-known solution of the Koster-Slater equations for a single matrix element of the perturbation potential at the impurity site will yield perturbed Bloch functions whose scattered wave part corresponds to summing in a simple way an infinite number of terms in the perturbation series and hence a simple result for the scattering matrix or T matrix. Immediate comparison with the results of the Friedel method can be made as well as with results obtained for a δ function potential using a formal scattering theory solution. The question of the role of phase transformations on the unperturbed Bloch functions is answered and shown not to fix the perturbation potential but to help choose the most localized Wannier functions which allows reasonable truncation of the Koster-Slater equations.

1. The Koster-Slater Equations

We shall derive the Koster-Slater Equations [1][1] for a crystal containing a single impurity. We make use of the formal theory of scattering [2] to obtain an expression for the perturbed Bloch waves and then transform the formal solution of the scattering problem to a Wannier representation. Our approach is the same as that first put forth by Koster and Slater and others [1] except for the introduction of the Green's function to discuss the electron spin or charge density. Consider that we have a one-electron Hamiltonian H_0 which is a good first approximation for describing the band electrons in the perfect crystal. H_0 can be determined from a self-consistent potential. The Bloch eigenfunctions $\phi_{n,\mathbf{k}}$ have eigenvalues $E_{n,\mathbf{k}}$ of H_0 satisfying the unperturbed Schrödinger equation

$$H_0\varphi_{n,\mathbf{k}} = E_{n,\mathbf{k}}\varphi_{n,\mathbf{k}}. \tag{1}$$

We shall denote by V the perturbation potential which is the difference between the imperfect crystal potential and the perfect crystal potential. V can be determined in a self-consistent manner when we are interested in spin and correlation effects as well as charge difference as shown by Wolff [3] and Clogston [4]. The new eigenfunctions Ψ_E have eigenvalues E determined from the solution of the perturbed Schrödinger equation

$$H\Psi_E = E\Psi_E. \tag{2}$$

Formal solutions of Ψ are

$$\Psi_E = \{\varphi_{n,\mathbf{k}}\} + (E - H_0)^{-1} V \Psi_E \tag{3a}$$

or

$$\Psi_E = \{\varphi_{n,\mathbf{k}}\} + (E - H)^{-1} V \{\varphi_{n,\mathbf{k}}\}, \tag{3b}$$

where E is an energy in the allowed bands of the perfect crystal and $\{\varphi_{n,\mathbf{k}}\}$ are the set of solutions of the homogeneous equation or unperturbed Schrödinger equation. We have specified a set of unperturbed $\{\varphi_{n,\mathbf{k}}\}$ all having energy $E_{n,\mathbf{k}}=E$, but one could have chosen a single member of the set which we shall do in the future and leave the possibility of choosing a linear combination of Ψ's or φ's satisfying some symmetry property of the crystal Hamiltonian. When the energy E does not lie in any of the allowed bands of the perfect crystal, then the formal solution for Ψ is

$$\Psi_E = (E - H_0)^{-1} V \Psi_E. \tag{4}$$

The Green's functions that are used to describe the response of the system are in operator form

$$G^0(E) = (E - H_0)^{-1} \qquad \text{(for the unperturbed system)} \tag{5}$$

and

$$G(E) = (E - H)^{-1}, \qquad \text{(for the perturbed system).} \tag{6}$$

*Work performed under the auspices of the U.S. Atomic Energy Commission.

[1] Figures in brackets indicate the literature references at the end of this paper.

The perturbed Green's function can be obtained in terms of the unperturbed Green's function or as a Dyson equation by matrix manipulation to yield

$$G(E)=[1-G^0(E)V]^{-1}G^0(E)=G^0(E)[1-VG^0(E)]^{-1} \tag{7}$$

or

$$G(E)=G^0(E)-G^0(E)VG, \text{ etc.} \tag{8}$$

It is preferable to continue on in the Bloch representation and rewrite (3a) and (4) as follows:

$$\Psi_E=\varphi_{n,\mathbf{k}}+\sum_{\mathbf{n'k'}}\frac{\varphi_{n'\mathbf{k'}}}{E-E_{n'\mathbf{k'}}}\langle\varphi_{n,\mathbf{k'}}|V|\Psi_E\rangle \tag{9}$$

and

$$\Psi_E=\sum_{n,\mathbf{k}}\frac{\varphi_{n,\mathbf{k}}}{E-E_{n\mathbf{k}}}\langle\varphi_{n\mathbf{k}}|V|\Psi_E\rangle. \tag{10}$$

$\langle\varphi_{n\mathbf{k}}|V|\Psi_E\rangle$ is a matrix element of the T matrix and as we shall see that working in the Wannier representation or in the Koster-Slater equations gives us various approximations to the T matrix for the impurity problem. We can now transform our eqs (9) and (10) to a Wannier representation where we define the Wannier functions as follows:

$$a_n(\mathbf{x}-\mathbf{X}_i)=\sum_k\frac{e^{-i\mathbf{k}\cdot\mathbf{X}_i}}{N^{1/2}}\varphi_{n,\mathbf{k}}(\mathbf{x}) \tag{11}$$

and

$$\varphi_{n,\mathbf{k}}=\sum_{X_i}\frac{e^{i\mathbf{k}\cdot\mathbf{X}_i}}{N^{1/2}}a_n(\mathbf{x}-X_i). \tag{12}$$

There are other possible choices for the Wannier function for complicated bands as discussed by Blount [5] but we shall work with the simple transformation here. The perturbed wave function Ψ can be expanded in the Wannier representation as follows:

$$\Psi_E=\sum_{n,X_i}U_{ni}(E)a_n(\mathbf{x}-\mathbf{X}_i) \tag{13}$$

$$a_n(\mathbf{x}-\mathbf{X}_i)=\sum_E U_{ni}(E)\Psi(E). \tag{14}$$

The transformation coefficient U are elements of a unitary matrix as are the transformation coefficients

$$\frac{e^{i\mathbf{k}\cdot\mathbf{X}_i}}{N^{1/2}}$$

in (11) and (12).

If we make use of the orthogonality relations for the Wannier functions,

$$\langle a_n(\mathbf{x}-\mathbf{X}_i)|a_m(\mathbf{x}-\mathbf{X}_j)\rangle=\delta_{nm}\delta_{ij}, \tag{15}$$

we find the following expression for (9) and (10) in the space spanned by the transformation coefficients:

E in the band

$$U_{ni}(E)=\frac{e^{i\mathbf{k}\cdot\mathbf{X}_i}}{N^{1/2}}+\frac{1}{N}\sum_{\mathbf{k'}}\frac{e^{i\mathbf{k'}\cdot\mathbf{X}_i}}{E-E_{n,k'}}\sum_{m,s,t}e^{-i\mathbf{k'}\cdot\mathbf{X}_s}V^{(st)}_{nm}U^{(E)}_{mi}; \tag{16}$$

E not in the band

$$U_{ni}(E)=\frac{1}{N}\sum_{\mathbf{k}}\frac{e^{i\mathbf{k'}\cdot\mathbf{X}_i}}{E-E_{\mathbf{k}}}\sum_{m,s,t,}e^{-i\mathbf{k'}\cdot\mathbf{X}_s}V_{nm}(st)\,U_{mt}(E). \tag{17}$$

The above are the Koster-Slater equations. The matrix elements of the potential are

$$V_{nm}(st)=\langle a_n(\mathbf{x}-\mathbf{X}_s)|V|a_m(\mathbf{x}-\mathbf{X}_t)\rangle. \tag{18}$$

One should note that there are no restrictions on the number of Wannier functions required to specify the Bloch functions and no restrictions on the perturbation potential. In a straight-forward manner one can write similar Green's functions for the U's as was introduced in (5) and (6) for the φ's and Ψ's:

$$G^0_{nj;\,mi}(E)=N^{-1}\sum_{\mathbf{k}}\frac{e^{i\mathbf{k}\cdot(\mathbf{X}_i-\mathbf{X}_j)}}{E-E_{n\mathbf{k}}}\delta_{nm}, \tag{19}$$

$$G_{nj;\,mi}(E)=\sum_p\frac{U_{mi}(E_p)U_{nj}(E_p)}{E-E_p}, \tag{20}$$

and the solutions for U are

$$U=U^0+G^0VU \tag{21}$$

or

$$U=U^0+GVU^0 \tag{22}$$

where U^0 refers to the coefficients

$$\frac{e^{i\mathbf{k}\cdot\mathbf{X}_i}}{N^{1/2}}.$$

Algebraic manipulation of (21) and (22) will allow one to write the Green's function equations analogous to (7) and (8),

$$G(E)=[1-G^0(E)V]^{-1}G^0(E) \tag{23}$$

or

$$G(E)=G^0(E)-G^0(E)VG(E), \tag{24}$$

discussed by Goodings and Mozer [6].

2. Lowest Order Solutions to the Koster-Slater Equation

One can now see how the perturbation series in the Koster-Slater equations can yield perturbed Bloch functions. For the first example we consider the very simplest problem of using a single matrix element for V in a single band. All other matrix elements of V in this band and other bands are considered small and to be treated in higher order. This is a problem which has been studied in great detail, yet it will provide insight into more complicated problems. We shall drop all band indices and call the matrix element of the perturbation potential at the impurity site V_0.[3] The Koster-Slater equations become

$$U_i(E) = \frac{e^{i\mathbf{k}\cdot\mathbf{X}_i}}{N^{1/2}} + \frac{V_0}{N}\sum_{\mathbf{k}} \frac{e^{i\mathbf{k}\cdot\mathbf{X}_i}}{E-E_{\mathbf{k}}} U_0(E) \tag{25}$$

for energies in the band and

$$U_i(E) = \frac{V_0}{N}\sum_{\mathbf{k}} \frac{e^{i\mathbf{k}\cdot\mathbf{X}_i}}{E-E_{\mathbf{k}}} U_0(E) \tag{26}$$

for energies outside the band. U_0 is given by

$$U_0 = [1 - V_0\bar{G}(E)]^{-1} \tag{27}$$

for energies in the band. $\bar{G}$ has real and imaginary parts

$$\mathrm{Re}\,\bar{G}(E) = \int P\,\frac{g(E')\,dE'}{E-E'} \equiv f(E) \tag{28}$$

(P means principal value) and

$$\mathrm{Im}\,\bar{G}(E) = -i\pi g(E), \tag{29}$$

where $g(E)$ is the density of states in the band and we have added a small imaginary part to E which vanishes in the usual limiting procedure. The condition for the existence of a state outside the band is the vanishing of $1 - V\bar{G}(E)$ corresponding to a pole in the Green's function G of (23). U_0 can be obtained for the state outside the band by imposing the normality condition on the U's,

$$\sum_{\mathbf{X}_i} |U_{\mathbf{X}_i}(E)|^2 = 1, \tag{30}$$

and we find

$$|U_0(E)|^2 = \left[-V_0^2\frac{\partial}{\partial E}\bar{G}(E)\right]^{-1}. \tag{31}$$

The U's at other lattice sites are not so easy to obtain unless one knows the energy versus $\mathbf{k}$ in the Brillouin zone for the unperturbed crystal. Numerical techniques have been developed for obtaining the U's at other sites if the energy versus $\mathbf{k}$ is known.

[3] We take the impurity site at the origin of the coordinate system.

It is worthwhile at this stage to transform back to the Bloch representation. The resulting approximation for Ψ we call $\Psi^{(1)}$,

$$\Psi^{(1)} = \varphi_{\mathbf{k}} + N^{-1}\sum_{\mathbf{k}'} \frac{\varphi_{\mathbf{k}'}}{E-E_{\mathbf{k}'}} T(E) \tag{32}$$

where

$$T(E) = V_0[1 - V_0\bar{G}(E)]^{-1} \tag{33}$$

and

$$V_0 = \langle a_0(x)|V|a_0(x)\rangle = N^{-1}\sum_{\mathbf{k},\,\mathbf{k}'} \langle\varphi_{\mathbf{k}'}|V|\varphi_{\mathbf{k}}\rangle. \tag{34}$$

The state outside the band is

$$\Psi^{(1)} = N^{-1}\sum_{\mathbf{k}} \frac{\varphi_{\mathbf{k}'}}{E-E_{\mathbf{k}'}} T(E). \tag{35}$$

We see that the Koster-Slater equations have given us an approximation for the T matrix which is fairly simple in form as it depends only on the energy E but not on $\mathbf{k}'$ or $E_{\mathbf{k}'}$. $T(E)$ can be rewritten as follows:

$$T(E) = V_0|1 - V_0\bar{G}(E)|^{-1}e^{i\lambda}(E), \tag{36}$$

where

$$\lambda(E) = \tan^{-1}\frac{\pi V_0 g(E)}{[1 - V_0 f(E)]}, \tag{37}$$

and is in the familiar form of a phase shift that one expects from scattering theory except there is only one phase shift and not a sum whose terms contain the product of a spherical harmonic and the phase shift. An expression similar to (26) can be obtained from the formal solution (36) for Ψ, which we rewrite as follows

$$\psi_E = \sum_i (G^0V)^i\varphi_{\mathbf{k}}. \tag{38}$$

The approximation one uses in evaluating terms such as $(G^0V)^i$ in (38) to get a similar expression for $\psi^{(1)}$ given by (26) is to replace the operator G^0V by

$$G^0V|\varphi_{\mathbf{k}}\rangle = \sum_{\mathbf{k}'} \frac{|\varphi_{\mathbf{k}'}\rangle\langle\varphi_{\mathbf{k}'}|V|\varphi_{\mathbf{k}}\rangle}{E-E_{\mathbf{k}'}} = \{V\}\sum_{\mathbf{k}} \frac{\varphi_{\mathbf{k}'}}{E-E_{\mathbf{k}'}}, \tag{39}$$

where $\{V\}$ is some suitable average of $V_{\mathbf{k}\mathbf{k}'}$. In other words, the approximation consists in saying that $V_{k\mathbf{k}'}$ is a very slowly varying function of k and $\mathbf{k}'$ or $E_{\mathbf{k}}$ and $E_{\mathbf{k}'}$ compared to the energy denomina-

tor and the density of states $E_{k'}$ and we replace $V_{\mathbf{k}\mathbf{k}'}$ by a mean value and sum the series to yield (32). The mean value of $V_{\mathbf{k}\mathbf{k}'}$ is judiciously chosen by the approximation made in the Koster-Slater equations; it is an average over the various $\mathbf{k}$, $\mathbf{k}'$ states given by (34). Such approximations are common in perturbation theory but one usually makes the approximation only on the energy shell, $E_{\mathbf{k}'} \approx E$, and not for states both on and off the energy shell which is what we did here. One can argue that such approximations are very reasonable for problems in solids except for the *very unusual* accident of a real metal whose electrons are completely described by single plane waves. For any metal where the electrons are not described by plane waves, the one-electron wave function could be represented by a tight binding wave function

$$\varphi_{\mathbf{k}} = e^{i\mathbf{k}\cdot\mathbf{x}} \sum_j \chi_j$$

and the matrix elements of, say, a coulomb potential of the impurity will vary with $\mathbf{k}$ and $\mathbf{k}'$ as

$$V_{\mathbf{k}\mathbf{k}'} \propto \frac{1}{|\mathbf{k}-\mathbf{k}'|^2+\kappa^2} + 0\left(\frac{1}{\kappa^3}\right), \tag{40}$$

where κ is the minimum inverse decay length of the tight binding functions. The approximation considered above is reasonable only if $\kappa > \max |\mathbf{k} - \mathbf{k}'|$ and then perturbation theory could describe the fluctuations of the potential about the mean value. If one includes the correlation of the band electrons, the coulomb potential of the impurity is screened and (39) is then a better approximation as κ in (40) contains the screening parameter of the electron gas. One should be at least a little careful in using the argument given above if bands have configuration mixing as then the χ_j contain functions of $\mathbf{k}$, e.g., s–p mixing in the alkalis, *and* if the overlap of the tight binding functions is large then additional terms must be evaluated in (40). It seems what one would prefer to show is that the Wannier functions for most systems are quite localized and then taking only one or several matrix element of the potential in the Koster-Slater equations is sufficient to describe the impurity problem. For a discussion of the localization of Wannier functions we refer the reader to Blount's work [5], Kohn's work [7], or an extensive discussion by des Cloizeaux [8] which contains some remarks on tight binding functions that are of interest.

The perturbed Bloch functions have several interesting properties. One most important property is that the perturbed functions are orthonormal since the unitarity requirement was imposed upon the transformation coefficients U; it should be emphasized that if a bound state exists, the orthogonality conditions are still satisfied. Another interesting property is that the wave functions are approximate eigenstates of the Hamiltonian H in the sense that for states in the band

$$\langle \psi_{E_{\mathbf{k}}} | H | \psi_{E_{\mathbf{k}}} \rangle = E_{\mathbf{k}} + (V_d - V_0), \tag{41}$$

where V_d is the diagonal matrix element of the perturbation potential between two unperturbed Bloch states, $\langle \varphi_{\mathbf{k}} | V | \varphi_{\mathbf{k}} \rangle$. We have evaluated matrix elements of V occurring between

$$\sum_{\mathbf{k}'} \frac{\varphi_{\mathbf{k}'}}{E - E_{\mathbf{k}'}} T(E) \text{ and } \varphi^*_{\mathbf{k}}$$

or the quadratic term in $T(E)$ by using the average value for V. The term in parenthesis is the correaction to the energy $E_{\mathbf{k}}$ and is equal in magnitude to the average fluctuation of the potential about the mean value determined by (34). The shift given by this term is the same for all states $E_{\mathbf{k}}$ and hence the band is displaced by this amount. Since the perturbed states in the band are labeled by $E_{\mathbf{k}}$, a one-to-one correspondence can be made between the φ_k and $\psi_{\mathbf{k}}$ which is especially useful for counting states. If a bound state occurs because of the strength of the perturbing potential, the matrix elements of H are

$$\langle \psi_B | H | \psi_B \rangle = E_B, \tag{42}$$

where E_B is the energy of the bound state. The density of states of the system will not be perturbed until a finite concentration of impurities is considered; local densities of states or local charge density vary as pointed out previously [6].

Our results for the first approximation for the perturbed Bloch wave should be compared with results obtained for a δ function potential and a well or barrier. We immediately obtain the following result for a δ function potential using (3) and considering only one band,

$$\psi_E = \varphi_{\mathbf{k}} + V_\delta \sum_{\mathbf{k}'} \frac{\varphi_{\mathbf{k}'} \varphi^*_{\mathbf{k}'}(0)}{E - E_{\mathbf{k}'}} \psi^{(0)}_E; \tag{43}$$

and solving for $\psi_E(0)$ we find

$$\psi_E(0) = \frac{\varphi_k(0)}{1 - V_\delta G'(E)}, \tag{44}$$

where

$$G'(E) = \sum_{\mathbf{k}'} \frac{|\varphi_{\mathbf{k}'}(0)|^2}{E - E_{\mathbf{k}'}}. \tag{45}$$

The T matrix is simply

$$T_{\mathbf{k}\mathbf{k}'} = \frac{V_\delta \varphi^*_{\mathbf{k}}(0) \varphi_{\mathbf{k}'}(0)}{1 - V_\delta G'(E)}. \tag{46}$$

The poles in the T matrix, when $1 - VG'(E) \equiv 0$, define the bound states, which is very similar to the

condition for a bound state as determined from the Koster-Slater equations. We see one significant difference in the T matrix for the first approximation to the wave function $\psi^{(1)}$ given by the Koster-Slater equations and (46). This difference occurs in the definition of $G(E)$ in (28) and (29) and $G'(E)$ in (45). The latter is evaluated only for those states $\varphi_{\mathbf{k}}$ nonvanishing at the impurity. The T matrix has only matrix elements for nonvanishing states and hence the scattered wave must consist of only s-like waves. Only if the $\varphi_{\mathbf{k}}$ are plane waves, can the T matrix for the δ function potential have the same value as the T matrix for the first approximation in the Koster-Slater equations and generally the amplitude and phase shift of the scattered waves are vastly different for the two approximations. If one considers other bands, the δ function potential will force the T matrix to have elements between states nonvanishing at the impurity and again only s-wave scattering whereas the Koster-Slater equations allow one to take reasonable matrix elements for the potential for both interband and intraband transitions and the symmetry of the scattered waves depends on the symmetry of all the wave functions in the bands.

The scattering of electrons in a crystal when the impurity potential is represented by a well or barrier has been considered in detail by Friedel and coworkers [9]. The general solution for this well or barrier problem is given by the following:

$$\psi_E = \varphi_k + \sum_{\mathbf{k}'} \frac{\varphi_{\mathbf{k}'}}{E - E_{\mathbf{k}'}} V(\varphi_{\mathbf{k}'}|\psi_E), \tag{47}$$

where $(\varphi_{\mathbf{k}'}|\psi_E)$ represents the integral over the extent of the well or barrier. If we consider plane wave states of all possible energy $\mathbf{k}$, and a spherical well or barrier, and ask for the scattering solution corresponding to outgoing waves, (47) becomes

$$\psi_E = e^{i\mathbf{k}\cdot\mathbf{r}} - \frac{i}{2}\sum_n (2n+1)\frac{e^{ikr}}{kr}\sin\delta_n e^{i\delta_n} P_n(\cos\theta), \tag{48}$$

where δ_n is the phase shift of the nth partial wave with angular dependence given by the Legendre polynomials P_n. The T matrix, $\langle\varphi_{\mathbf{k}'}|V|\psi\rangle$, is required only on the energy shell (when $E = E_{\mathbf{k}'}$) for the solution to the scattering problem and can be written for each partial wave as $T_n = 2i \sin\delta_n e^{i\delta_n}$. The phase shifts are functions of the size of the well or barrier and its depth (height). To insure that the system is electrically neutral, the Friedel sum rule is invoked to fix the parameters of the well,

$$\Delta Z = \frac{2}{\pi}\sum_n (2n+1)\delta_n(E_f), \tag{49}$$

where ΔZ is the difference in charge between an impurity ion and lattice ion, and E_f is the Fermi energy of the system. There are large differences between (47) for Bloch waves and (48) for plane waves and greater differences between (47) or (48) and our first order expression obtained from the Koster-Slater equation which has only one phase shift. It is not at all apparent that if one needed only a single phase shift in (47) or (48) that this phase shift would disagree with the Koster-Slater result. Rather than go into detailed differences in the phase shifts, one can compare the two methods of approach. In the Friedel method, or a generalization of it where the potential is not restricted for example to a well or barrier (see W. Kohn and S. Vosko [10]), the formal solution or Green's function solution (3) is evaluated for a scattering problem using Bloch waves for the unperturbed crystal functions. As in most scattering problems, the Green's function is evaluated under boundary conditions for outgoing waves asymptotically far from the impurity and on the energy shell. One can then express the solution for ψ in terms of phase shifts where for most cases only a few phase shifts are needed to describe the problem. In order not to restrict oneself to a particular potential, a set of finite linear equations can be given to relate the phase shifts to known or experimentally determined quantities, i.e., the Friedel sum rule is invoked to conserve total charge, and the residual resistance expressed in terms of the phase shifts, etc. Thus with a few parameters one could account for a variety of phenomena in *dilute* alloys. Using the truncated Koster-Slater equations, one can obtain approximate perturbed Bloch waves with the following properties. The wave functions are orthonormal and thus one does not need the Friedel sum rule to conserve total charge. The first approximation to the T matrix yields a single phase shift [11] which supposedly is completely determined by the matrix element of the potential using the Wannier functions at the impurity site, or (34) if the Bloch waves are known, and the density of electron states for the perfect crystal. Since not too much is known about Wannier functions, potentials, Bloch waves, or density of states, one can do the same thing as for the Friedel method and determine the parameter V_o using the residual resistance and its relation to the phase shifts. One has then a perturbed wave function which can be used to describe transport phenomena and additional phenomena in dilute alloys associated with the impurity itself, for example the Knight shift, Mössbauer shifts or structure, and effects arising from local spin and charge density since in the Koster-Slater method one has a wave function defined over all the crystal and the T matrix both on and off the energy shell. Truncating the Koster-Slater equations so as to include additional terms involving matrix elements of the perturbation potential for Wannier functions off the impurity site will produce a T matrix with additional phase shifts and of course more parameters to describe the impurity. One needs the E versus $\mathbf{k}$ relations for the perfect crystal in addition to the density of states and Wannier func-

256-724 O-67—8

tions but one has considerable information on E versus $\mathbf{k}$ relations and hence the method is not so restrictive. If interband matrix elements are important, then both methods can be modified accordingly.

It appears from the preceeding paragraph that working with the truncated Koster-Slater equations would be more advantageous than the Friedel method or pure scattering solutions which require more parameters. There is a problem with using the truncated Koster-Slater equations that was first brought to the author's attention by V. Hiene in connection with the x-ray emission problem in lithium [12]. The problem is brought about when one considers general phase transformations of the Bloch waves. One wants to consider general phase transformations in order to achieve Wannier functions which are very localized. It is just such localized Wannier functions that make the Koster-Slater method acceptable since one would only need a few matrix elements of the perturbation potential to adequately describe a problem. The latter notion would be valid for even a moderately screened coulomb potential. Consider a phase transformation $e^{i\eta(\mathbf{k})}$ that produces the most localized Wannier functions $a'_n(\mathbf{x}-\mathbf{X}_i)$:

$$a'_n(\mathbf{x}-\mathbf{X}_i)=\sum_{\mathbf{k}}\frac{e^{i\mathbf{k}\cdot\mathbf{X}_i}}{N^{1/2}}\,e^{i\eta(\mathbf{k},\,n)}\varphi_{\mathbf{k},\,n}. \tag{50}$$

We know then that $\varphi_{\mathbf{k}}$ and ψ can be expanded in the quantities a',

$$\varphi_{\mathbf{k},\,n}=\sum_i\frac{e^{i\mathbf{k}\cdot\mathbf{X}_i}}{N^{1/2}}\,e^{-i\eta(\mathbf{k},\,n)}a'_n(\mathbf{x}-\mathbf{X}_i), \tag{51}$$

$$\psi_E=\sum_{n,\,E}U'_{ni}(E)e^{-i\eta(\mathbf{k},\,n)}a'_n(\mathbf{x}-\mathbf{X}_i). \tag{52}$$

One can obtain the Koster-Slater equations for the U' and the only modification coming in is a new definition of the matrix elements $V'_{nm}(st)$,

$$V'_{nm}\ (st)=\langle a'_n(\mathbf{x}-\mathbf{X}_s)|V|a'_m(\mathbf{x}-X_t)\rangle. \tag{53}$$

Truncating the Koster-Slater equations yields the following approximation to the perturbed Bloch wave

$$\psi_k^{(1)}=\varphi_{\mathbf{k}'}+\sum_{\mathbf{k}'}\frac{\varphi_{\mathbf{k}'}e^{i[\eta(\mathbf{k}')-\eta(\mathbf{k})]}}{E-E_{\mathbf{k}'}}\,T'(E), \tag{54}$$

where

$$T'(E)=V'_0[1-V'_0\bar{G}(E)]^{-1} \tag{55}$$

with

$$V'_0=\langle a'(X)|V|a'(X)\rangle=\frac{1}{N}\sum_{\mathbf{k},\,\mathbf{k}'}\langle\varphi'_{\mathbf{k}}|V|\varphi'_{\mathbf{k}'}\rangle, \tag{56}$$

where $\varphi'=e^{i\eta(\mathbf{k})}\varphi_{\mathbf{k}}$. It is possible to view the result obtained in (54) in several ways: (1) We have obtained a new T matrix, $T=e^{i\eta(\mathbf{k}')}T'(E)e^{-i\eta(\mathbf{k})}$, with matrix elements determined by the choice of phase for the Bloch waves in defining the a's; or (2) we have started out with a general phase transformation $e^{i\eta(\mathbf{k})}$ such that $\psi'_{\mathbf{k}}=e^{i\eta(\mathbf{k})}\psi_{\mathbf{k}}$ and $\varphi'_{\mathbf{k}}=e^{i\eta(\mathbf{k})}\varphi_{\mathbf{k}}$ and a solution

$$\psi'_{\mathbf{k}}=\varphi'_{\mathbf{k}}+\sum_{\mathbf{k}'}\frac{\varphi'_{\mathbf{k}'}}{E-E_{\mathbf{k}'}}T'(E). \tag{57}$$

New phase shifts of scattered waves appear because of the phase transformation used in defining the a's and, depending upon what use is made of the ψ', one could expect results different from those found for ψ. Another obvious difference seen to occur as a consequence of the phase transformation is the strength of the potential required to produce a bound state, when $1-V'_0\bar{G}(E)\equiv 0$. Thus in order to get any consistency in the method of using the Koster-Slater equations for continuum states or bound states one can require

$$|V_0-V'_0|=N^{-1}\Big|\sum_{\mathbf{k},\,\mathbf{k}'}(1-e^{-i[\eta(\mathbf{k})-\eta(\mathbf{k}')]})V_{\mathbf{k}\mathbf{k}'}\Big|<\epsilon \tag{58}$$

where ϵ is small compared to V_0 or V'_0. This means that some variation is allowed in the phase choice but according to (58) one would require that the Bloch functions that have been determined for the perfect crystal produce Wannier functions that are almost as localized as the phase transformed Bloch functions. It is the opinion of the author that one should use the most localized Wannier functions in the Koster-Slater method in order to have a tractable expression involving the truncated equations and thus, to first order, use (54), (55), and (56). If the Bloch functions are well represented by tight-binding functions such as to justify the approximation in (39), the inequality (58) will be satisfied and estimates of the matrix elements of the perturbation potential in (34) can be made using atomic functions.

In the previous paragraph we have shown the role of the phase transformations that should be used in conjunction with the Koster-Slater equations to obtain perturbed Bloch waves. Recently Turner and Goodings [13] have discussed the importance of phase transformations in what they call the localized approximation of the Koster-Slater theory. Their version of the localized approximation places such restrictions on the Koster-Slater theory as to bring into question the validity of its use. The reason this occurs is that they impose restrictions on the potential that can be used in the Koster-Slater theory. According to their expression (5) the localized approximation means in our notation

$$V_{nm}(st)=V_{nm}\delta_{s0}\delta_{t0}, \tag{T–G 5}$$

a potential having only matrix elements in the Wannier representation for Wannier functions at

the impurity. Consequently they conclude that the localized approximation in the Koster-Slater theory fixes the phase of the Bloch waves. They further remark that a potential yielding matrix elements such as (T–G 5) is hard to understand physically. We agree completely with this last statement and cannot imagine a physically realizable potential satisfying those requirements.

What is even more peculiar about the restriction of the potential according to (T–G 5) is that when one wants to extend the truncation of the Koster-Slater equations one has to introduce a *new* potential whose properties are completely different from the potential leading to (T–G 5). It is important then to restate what in the Koster-Slater theory is a local approximation [14]. For simple potential scattering, the local approximation means a potential which falls off fast enough with distance, e.g., a screened coulomb, and *localized* Wannier functions so that one can comfortably truncate the Koster-Slater equations using a few matrix elements of the potential and regard the remaining potential matrix elements as small and to be treated later by perturbation theory. This is the context in which Koster and Slater first proposed the method. As we have seen in this article phase-transformed Bloch waves are used to define localized Wannier functions in order to use the Koster-Slater theory to get an approximate expression for the T matrix which describes the effect of an impurity potential, and not to fix or define the potential being used.

Another comment on the paper of Turner and Goodings [13] can be made with respect to the approximate wave functions they suggest for the perturbed problem. If we consider as they do the first approximation for the wave function (32), then we may rewrite this as

$$\psi_{\mathbf{k}}=\varphi_{\mathbf{k}}P(E)+i\pi[g(E)\varphi_{\mathbf{k}}-\sum_{\mathbf{k}'}\varphi_{\mathbf{k}'}\delta(E-E_{\mathbf{k}'})]T(E)$$
$$-\left[f(E)\varphi_{\mathbf{k}}-P\int_{B.Z.}d\mathbf{k}'\,\frac{\varphi_{\mathbf{k}'}}{E-E_{\mathbf{k}'}}\right]T(E) \qquad (59)$$

where

$$P(E)=T(E)/V_0=[1-V_0\bar{G}(E)]^{-1}.$$

Turner and Goodings suggest using only the first term in (59), $\varphi_{\mathbf{k}}P(E)$, for the perturbed wave function, but this must be justified for each particular problem depending upon what use is made of $\psi_{\mathbf{k}}$. If one can show that the second term in (59) is small for a particular problem, the third term will also be small because of the Kramers-Kronig relation between the parts on and off the energy shell of the quantity $\sum_{\mathbf{k}}\frac{\varphi_{\mathbf{k}}}{E-E_{\mathbf{k}}}$. If $\varphi_{\mathbf{k}}$ is well approximated by a tight binding function, then the Knight shift for the impurity is given by the expression in Turner and Goodings,

$$K_{\text{imp}}=8\pi/3g\mu_B^2N\langle|\varphi_{\mathbf{k}}(0)|^2\rangle E_F\cdot|P(E)_F|^2g(E)_F. \qquad (T.\ G\text{–}21)$$

For other problems, say the x-ray emission problem, one might find it difficult to approximate $\psi_{\mathbf{k}}$ by $\varphi_{\mathbf{k}}P(E)$ even in the tight binding approximation, and the correction terms have to be estimated. One can also look at the correction terms in another way by expanding $\varphi_{\mathbf{k}}$ in Wannier functions; the first quantity in brackets is

$$\frac{i\pi}{N^{1/2}}\sum_{i\neq 0}a(\mathbf{x}-\mathbf{X}_i)\Big[e^{i\mathbf{k}\cdot\mathbf{x}_i}g(E)$$
$$-\sum_{\mathbf{k}'}\frac{e^{i\mathbf{k}'\cdot\mathbf{X}_i}}{N^{1/2}}\delta(E-E_{\mathbf{k}'})\Big]T(E), \qquad (60)$$

and here again if the a's are localized the correction terms can be small in a region confined to the impurity site. (60) is modified in a straightforward manner for phase-transformed φ's,

$$\frac{i\pi}{N^{1/2}}\sum_{i\,0\,0}a'(\mathbf{x}-\mathbf{X}_i)\Big[e^{i\mathbf{k}\cdot\mathbf{X}_i}e^{i\eta(\mathbf{k})}g(E)$$
$$-\sum_{\mathbf{k}'}e^{i\mathbf{k}'\cdot\mathbf{X}_i}e^{i[\eta(\mathbf{k}')-\eta(\mathbf{k})]}\delta(E-E_{\mathbf{k}'})\Big]T'(E). \qquad (61)$$

As a final remark one can point out that the approximation $\psi_{\mathbf{k}}\approx\varphi_{\mathbf{k}}P(E)$ must be used with care since to assume that it represents the perturbed wave function is incorrect because normalization of $\psi_{\mathbf{k}}$ would require replacing the factor $P(E)$ by unity and furthermore for scattering problems where ψ is needed far from the impurity the correction terms are most important.

In conclusion, we can say that the Koster-Slater-equations can yield useful estimates of perturbed Bloch functions for the impurity problem and that the role of phase transformations on the unperturbed Bloch waves should be to provide localized Wannier functions which allow a reasonable truncation of the Koster-Slater equations. This first approximation can be used in deriving a self-consistent potential where higher order effects of the scattering have been approximately taken into account. From our discussions of the simplest solution of the Koster-Slater equations one can easily see what the perturbed Bloch wave looks like when truncating the Koster-Slater equations so as to include matrix elements of the perturbation potential at sites in the neighborhood of the impurity. The T matrix is more complicated and has additional phase shifts; the perturbed Bloch waves show new effects in which scattered waves are introduced with an additional phase dependence corresponding to translations of the Bloch wave to sites in the neighborhood

of the impurity. Multiband effects can also be treated in the Koster-Slater theory, as is well known, and the result of their inclusion in the theory produces additional modifications of the approximate Bloch waves. A fuller discussion of the multiband effects and the effects of extending the truncated Koster-Slater equations to sites in the neighborhood of the impurity will be given elsewhere.

3. References and Notes

[1] G. F. Koster and J. C. Slater, Phys. Rev. **95**, 1167 (1954); G. F. Koster, Phys. Rev. **95**, 1436 (1954); and G. F. Koster and J. C. Slater, Phys. Rev. **96**, 1208 (1954). For generalized Green's function approach see ref. 6.

[2] We intend to use the Green's function approach that was introduced for scattering problems (L. F. Schiff, Quantum Mechanics, p. 110 (McGraw-Hill Book Co., New York, N.Y., 1949) and more general developments in M. L. Goldburger and K. M. Watson, Collision Theory (John Wiley & Sons, Inc., New York, N.Y., 1964) but can also be used for other problems by a proper choice of boundary conditions.

[3] P. A. Wolff, Phys. Rev. **124**, 1030 (1961).

[4] A. M. Clogston, Phys. Rev. **136**, A1417 (1964).

[5] E. I. Blount, Solid State Physics Vol. **13**, pp 306–370 (Academic Press, New York, 1962).

[6] D. A. Goodings and B. Mozer, Phys. Rev. **136**, A1093 (1964).

[7] W. Kohn, Phys. Rev. **115**, 809 (1959).

[8] J. des Cloizeaux, Phys. Rev. **135**, A698 (1964).

[9] Friedel's work and that of his school is described in Metallic Solid Solutions (W. A. Benjamin, Inc., New York, 1963).

[10] W. Kohn and S. H. Vosko, Phys. Rev. **119**, 912 (1960). See also A. Blandin and J. Friedel, J. Phys. Rad. **21**, 689 (1960).

[11] One should note that this does not imply only *s*-wave scattering unless one has completely spherical bands. If the bands are not spherical, then scattered waves of various symmetry appear, but a peculiar nature of the first Koster-Slater approximation is that all the scattered waves have an identical phase shift coming from the potential and perhaps different shifts coming from the nonspherical behavior of the energy. One should really talk about the scattered waves in cubic harmonics for the systems considered here but we will ignore this modification of the problem. Choosing the Wannier functions via phase transformed Bloch waves brings in additional phase shifts even if only one matrix element of the perturbation potential is used in the Koster-Slater equations.

[12] Interpretation of the soft x-ray emission spectrum of lithium metal, B. Mozer and D. A. Goodings, BNL # 7965 (unpublished); D. A. Goodings, Proc. Phys. Soc. **86**, 75 (1965). Heine's remarks concern the symmetry (parity) of the Wannier functions under phase transformations of the Bloch waves when the inversion operator and time reversal operator commute with the perfect crystal Hamiltonian. Arguments about the symmetry of the Wannier functions become rather subtle when one has overlapping bands or when free atom energy levels are close together.

[13] R. E. Turner and D. A. Goodings, Proc. Phys. Soc. **86**, 87 (1965).

[14] In ref. 6 we erroneously used $V_{nm}(st)=V_{nm}\delta_{so}\delta_{to}$ instead of considering the truncation of the matrix V as we have seen here is the correct view of the process. Unfortunately this has led to confusion regarding the generality of that paper. The method as introduced in that paper is quite general but the approximate solutions of the Green's functions should be considered only as a truncation of the perturbation potential. What is hidden in the Koster-Slater equations is that the theory provides a method for obtaining impurity energy levels, changes in density functions such as spin, charge, or energy states, but does not provide the behavior of the perturbed wave function which is also of great interest in the impurity problem. One uses the Green's functions to provide the coefficients in the Wannier expansion of the perturbed Bloch waves.

Residual Resistivities of Dilute Aluminum Alloys*

F. J. Blatt and H. R. Fankhauser

Physics Department, Michigan State University, East Lansing, Mich. 48823

We have performed calculations of the residual resistivities of several aluminum base alloys using the approach described by one of us some years ago [1].[1] Briefly, we represent the scattering potential by a square well (or barrier) whose range is given by

$$r' = r_s[1 + (\delta V/\Omega)]^{1/3}, \tag{1}$$

where r_s and Ω are the radius and volume of the Wigner-Seitz sphere of aluminum and δV is the increase in the volume of the cell containing the impurity atom. Values for δV were obtained from measured lattice parameter changes [2]. (See table 1.) The strength of the potential, V_0, was adjusted so as to satisfy the modified Friedel condition

$$\frac{2}{\pi}\sum_{l=0}^{\infty}(2l+1)\delta_l = N' = Z_1 - 3[1 + (\delta V/\Omega)], \tag{2}$$

where Z_1 is the valence of the impurity atom. The correction term, $3\delta V/\Omega$, is intended to account, at least roughly, for the partial screening (or antiscreening) due to local lattice distortion. The phase shifts were calculated numerically and residual resistivities determined from the relation

$$\Delta\rho(\mu\ \text{ohm-cm/atomic \%}) = \frac{5.1626}{n_{\text{eff}}k_F}\sum_{l=0}^{\infty}(l+1)\sin^2(\delta_l - \delta_{l+1}), \tag{3}$$

where n_{eff} is the effective number of free electrons per atom and k_F the wave vector at the Fermi surface of aluminum in reciprocal Angstroms.

The phase shifts and Friedel sums are listed in table 2. The calculated resistivities, experimental data, and calculated results obtained by Harrison [3], who used a pseudopotential method, are given in table 3. In Tables 2 and 3 we also present the calculated parameters for vacancies in aluminum, obtained under the assumption that this defect demands a screening charge $N' = -3$, i.e., we have neglected local distortion since it is not known.

The calculated residual resistivities are consistently too small if we take $n_{\text{eff}} = Z_{\text{Al}} = 3$. This choice of n_{eff} may well be inappropriate since in aluminum the first BZ is completely filled and the principal contribution to the current presumably derives from electrons in the partly filled second zone. Two independent observations support a choice of $n_{\text{eff}} \approx 1$. First, Sondheimer oscillations in thin aluminum films [4] are in excellent agreement with theory provided the Fermi momentum is that appropriate to $n_{\text{eff}} \approx 1$. Second, and more significant as regards resistivity calculations, is the

TABLE 1. *Lattice distortion due to impurities in aluminum*

Solute	Z_1	$\frac{\delta a}{a}$	$\frac{\delta V}{\Omega}$	N'	r' (Angstrom)
Li	1	−0.014	−0.0278	−1.9166	1.57
Cu	1	−.122	−.253	−1.241	1.43
Ag	1	.0	.0	−2.0	1.58
		+.101	+.201	−1.603	1.68
Mg	2	+.063	+.125	−1.375	1.64
Zn	2	−.0035	−.0069	−0.9793	1.58
Ge	4	+.035	+.0694	+.7918	1.62
		+.042	+.0833	+.7501	1.62
Si	4	−.045	−.0903	+1.2709	1.53

TABLE 2. *Range and strength of square well potentials*
Phase shifts and Friedel Sum.

Solute	r'	V_0(eV)	δ_0	δ_1	δ_2	δ_3	δ_4	$\frac{2}{\pi}\sum(2l+1)\delta_l$
Li	1.57	3.711	−0.9240	−0.4392	−0.1234	−0.0193	−0.0017	−1.9167
Cu	1.43	3.086	−.6782	−.2909	−.0669	−.0082	−.0006	−1.2411
Ag	1.58	3.822	−.9585	−.4566	−.1300	−.0207	−.0019	−2.0003
Mg	1.68	2.377	−.6271	−.3758	−.1190	−.0211	−.0022	−1.6031
Zn	1.64	2.172	−.5555	−.3269	−.0986	−.0164	−.0016	−1.3748
Ge	1.58	1.697	−.4106	−.2388	−.0665	−.0100	−.0009	−0.9792
Si	1.62	−1.152	+.2316	+.2082	+.0645	+.0093	+.0008	+0.7918
Vacancies	1.62	−1.093	+.2129	+.1971	+.0609	+.0088	+.0008	+0.7501
	1.53	−2.127	+.3790	+.3509	+.0969	+.0115	+.0009	+1.2706
	1.58	6.8	−1.4831	−.6587	−.1970	−.0336	−.0032	−2.9994

*Research supported in part by the National Science Foundation.

[1] Figures in brackets indicate the literature references at the end of this paper.

fact that the calculated ideal resistivity of aluminum, using a free-electron model, leads to a result about 3.6 times too small if $n_{\text{eff}}=3$, although the same calculation when performed for the alkali metals is in reasonably good agreement with experiment. If, then, we take $n_{\text{eff}}=1$ we obtain results in fairly good agreement with observation. The notable exception is Ge in Al. It would appear that in this instance the pseudopotential method, which should be superior to our crude model in any event, can come rather close to the measured result. It must be recognized, however, that in this instance the strength β of the repulsive delta function in the point-ion potential for germanium was adjusted to optimize agreement with experiment.

TABLE 3. *Residual resistivities of aluminum alloys—$\mu\Omega$-cm/atomic percent*

Solute	$\Delta\rho_{\text{exp}}$	$\Delta\rho_{\text{calc}}$	$\Delta\rho_{\text{calc}}$	$\Delta\rho_{\text{calc}}$
		$n_{\text{eff}}=3$	$n_{\text{eff}}=1$	Harrison [3]
Li	0.94 [a]	0.438	1.314	
Cu	0.75 [a], 0.8 [b]	.248	0.744	0.76
Ag	1.1 [a], 1.2 [b], 1.5 [c]	.468	1.404	.58
Mg	0.45 [a], 0.33 [b], 0.4 [c]	.218	0.654	.78
		.172	.516	
Zn	0.22 [a, b], 0.24 [d]	.097	.291	.1
		.050	.15	
Ge	0.79 [a, d], 0.98 [b]	.045	.135	1.0*
Si	0.7 [a], 0.56 [d]	.148	.444	
Vacancy	2.5±0.7 [e]	1.00	3.0	

*Parameters adjusted for optimum agreement with experiment.
[a] F. Pawlek and K. Reichel, Z. Metall **12**, (1), 1(1958).
[b] Quoted by W. A. Harrison, Pseudo-Potentials in the Theory of Metals, p. 150 (W. A. Benjamin, New York, 1966).
[c] Y. Fukai, private communication.
[d] Quoted by Y. Fukai (see preceding paper).
[e] J. Takamura: Lattice Defects in Quenched Metals, p. 521 (Academic Press, Inc., New York, 1965).

The value selected, $\beta_{\text{Ge}}=60$, corresponding to $(\beta_{\text{Ge}}-\beta_{\text{Al}})\equiv\delta\beta\approx 23$, is somewhat different from that deduced from preliminary results of Heine and Animalu (quoted by Harrison), for which $\delta\beta\approx 17$. Since in the pseudopotential formulation $\delta\beta$ and also $(\delta\beta)^2$ appear in the expression for $\Delta\rho$, varying this parameter may lead to significant changes in $\Delta\rho_{\text{calc}}$.

We are well aware of the gross inadequacy of our procedure, both as regards the choice of scattering potential as well as the selection of n_{eff}, and undertook these calculations primarily because we were curious to see if the rough manner by which we successfully incorporated the influence of lattice distortion in calculations of residual resistivities of noble metal base alloys, might perhaps reproduce the corresponding trends in aluminum, a metal which exhibits much larger local strains about imperfections than do the noble metals. In the case of monovalent and divalent impurities in aluminum, the indications are that lattice strains do provide some local screening; for example, the experimentally observed large difference between $\Delta\rho$ due to copper and silver in aluminum reappears in the calculated values, and

$$\left[\frac{\Delta\rho(\text{Mg})}{\Delta\rho(\text{Zn})}\right]_{\text{exp.}}\approx 2\approx\left[\frac{\Delta\rho(\text{Mg})}{\Delta\rho(\text{Zn})}\right]_{\text{calc.}}$$

We are, however, unable to account at this time for the wide disparity in the case of germanium impurities.

References

[1] F. J. Blatt, Phys. Rev. **108**, 285 (1957).
[2] W. B. Pearson, A Handbook of Lattice Spacings and Structures of Metals and Alloys (Pergamon Press, New York, 1958).
[3] W. A. Harrison, Pseudo-Potentials in the Theory of Metals, p. 150 (W. A. Benjamin, Inc., New York, 1966).
[4] K. Forsvoll and I. Holwech, Phil. Mag. **9**, 435 (1964).

Point Imperfections in Solid Rare Gases*

Albert Gold

Institute of Optics, University of Rochester, Rochester, N.Y. 14627

The low-lying electronic states of impurity atoms in rare gas crystals are well described by a tight-binding model in which the atomic wave functions of the impurity are Schmidt-orthogonalized to those centered on neighboring host atoms. It is necessary to account for the second order, van der Waals, energy differences between ground and excited states. A simple approximation is quite successful. Applications to the lowest transitions of hydrogen in argon and of argon in neon have been made. The extension of the model to include so-called charge-transfer states is discussed. The line shape for the Ar:H transition has been studied in detail, considering both the usual linear interactions with the lattice and the quadratic interaction with the local modes. The shape and associated isotope effects can be well understood provided that the quadratically coupled modes are treated fully quantum mechanically.

1. Introduction

Within the one-electron approximation the calculation of the electronic energy levels of impurities in rare gas crystals is, in principle, an entirely straightforward matter to be prosecuted in complete analogy with the computation of the eigenstates of any other molecular or solid state system. One may write the many-electron wave function for the αth level as

$$\Psi_\alpha = \sum_\mu c_{\alpha\mu}\Phi_\mu \tag{1}$$

where the Φ_μ are the members of any *arbitrary* complete orthonormal set and the $c_{\alpha\mu}$ are coefficients obtained variationally by solving the appropriate secular equation. The Hamiltonian to be diagonalized is, in the Born-Oppenheimer approximation,

$$H = \sum_i \left(\frac{\hbar^2}{2m}\nabla_i^2 - \sum_I \frac{Z_I e^2}{|\mathbf{R}_I - \mathbf{r}_i|} + \frac{1}{2}\sum_j{}' \frac{e^2}{r_{ij}} + \frac{1}{2}\sum_{I,J}{}' \frac{Z_I Z_J e^2}{R_{IJ}} + H_{i.\,s.o.} \right) \tag{2}$$

where i and j run over electron coordinate $\mathbf{r}_i$, I and J run over the coordinates $\mathbf{R}_I$ of the nuclei which carry charge Z_I and the final term schematically indicates the spin-orbit interaction of the ith electron.

Unfortunately, filling this prescription as given seems both computationally unfeasible and intellectually unrewarding. Hence, one usually begins by choosing the Φ_μ to be some particular set that experience, preference or prejudice indicates is convenient. Specifically, one hopes to make a choice such that only a few c's are substantially different from zero. However, even this limited task is often beyond practicality and instead one attempts to "model" a wave function; i.e., he chooses a *specific* $\Phi_\alpha \approx \Psi_\alpha$ and, assuming that it diagonalizes the Hamiltonian, proceeds to calculate levels, or at least excitation energies. The appropriateness of a model wave function to represent a given state of a system rests primarily on its empirical success; theosophical arguments over various descriptions can usually be expected to be devoid of physical content, even though they may be of some pictorial or heuristic value. Different states of the same system may, in fact, be best understood using vastly different models! The effective mass approximation seems to work well for donor states in valence semiconductors. The tight-binding approximation, with which we shall primarily concern ourselves, seems adequate for molecular crystals and the low lying states of rare gas systems. We shall also look briefly into the use of charge transfer states and pseudopotential techniques. We will find that sometimes apparently different models lead to equivalent or nearly equivalent descriptions.

*Research supported in part by the National Science Foundation.

2. The Tight Binding Model [1][1]

In the Heitler-London picture, the electronic wave functions for the ground and excited states are taken, respectively, to be of the forms

$$\Psi_g = \mathscr{A}\psi^g_{Aa}(\mathbf{r}_{Aa}) \prod_{I,i\neq a} \psi^g_{Ii}(\mathbf{r}_{I_i}). \tag{3a}$$

and

$$\Psi_e = \mathscr{A}\psi^e_{Aa}(\mathbf{r}_{Aa}) \prod_{I,i\neq a} \psi^g_{Ii}(\mathbf{r}_{I_i}). \tag{3b}$$

Here $\mathscr{A}$ is the antisymmetrization operator, the double subscript indicates the ith electron belonging to the Ith nucleus and the letters Aa are reserved for the optical electron bound to the impurity A. In the ground state all of the one-electron functions, ψ, are usually (but not necessarily) taken to be the corresponding ground state wave functions for the free atom. In the rare gases, overlap of atomic wave functions centered on different atoms, as measured by the overlap integrals

$$S_{IiJi} = \int \psi^{g*}_{Ii}\psi^g_{Jj}\, d\tau, (I \neq J) \tag{4}$$

are sufficiently small to be neglected without substantially affecting normalization of Ψ_g. The excited state is composed of the same ground state atomic functions for the host atoms and the corresponding excited state functions for the impurity. However, the overlaps of the excited optical electron are *not* generally negligible (they may be ~ 0.5) and hence, to obtain a normalized excited state, it is necessary to orthogonalize the excited one-electron function to those centered in the neighbors. A simple Schmidt procedure suffices, and so we take

$$\psi^e_{Aa} = \left(\varphi^e_{Aa} - \sum_{Ii} S_{AaIi}\psi^g_{Ii}\right)\left(1 - \sum_{Ii}(S_{AaIi})^2\right)^{-1/2} \tag{5}$$

where φ^e_{Aa} is the atomic excited state wave function for the optical electron. Insertion of (5) into (3b) gives an excited state wave function normalized to order S^2.

Excitation energies are now obtained by computing the difference of the expectation values $\langle \Psi_e|H|\Psi_e \rangle$ and $\langle \Psi_g|H|\Psi_g \rangle$. The resulting expression is complicated, involving coulomb, exchange and three-center interactions. Terms through second order in overlap are consistently retained. The form of the results will not be reproduced here. Suffice it to say that numerically they yield a small ($\lesssim 10\%$) correction to the corresponding atomic excitation energy but that this correction is composed of terms of both signs which are individually large in magnitude compared to that of their algebraic sum.

In undergoing excitation the impurity atom also suffers a considerable increase in polarizability. Recalling that the cohesion of rare gas systems is entirely due to van der Waals forces, it is not surprising that this in turn leads to an appreciable negative contribution to the excitation energy. No rigorous methods of including the van der Waals term in a tight-binding calculation has yet been given, but apparently satisfactory approximate estimates can be made [2]. We shall not go beyond mentioning their existence here.

3. Impurities in Rare Gas Crystals

Impurity states in solid rare gases have been the subject of recent study both experimentally [3–7] and theoretically [1, 2, 8–10]. Absorption spectra have been obtained for dilute alloys of rare gases [5], for hydrogen atoms in argon and for alkali atoms in various rare gas matrices [6, 7]. Calculations have been made for Ne : Ar [1, 2, 10] and Ar : H [8, 9]. The last is perhaps the simplest and most successful. The quantity of machine-performed numerical computation engenders unavoidable uncertainty in the calculation, but the predicted value of 10.6 ± 0.2 eV for the $1s$-$2p$ transition is in excellent agreement with Baldini's measurement of 10.56 eV. Further, the excitation energy has been calculated as a function of the breathing mode configuration coordinate and the use of these results together with a careful quantum treatment of interactions with the quadratically coupled local mode [9, 11] gives good fits to the line shape and the observed differences in width and peak position for Ar : H and Ar : D. Calculation for the lowest, ^1P and ^3P states of Ar in Ne also agree well with experiment [10].

4. Extensions of the Tight Binding Model

Recently Webber, Rice, and Jortner [10] have extended the Heitler-London model by including charge transfer states in the wave function for the excited electron. The wave function is taken to be of the form

$$\psi_{ct} = U_A\psi^e_{Aa} + \sum U_J\psi^i_{jj} \tag{6}$$

[1] Figures in brackets indicate the literature references at the end of this paper.

where ψ^e_{Aa} is defined by eq (5), ψ^j_{jj} are wave functions corresponding to the "extra" electron of the negative rare gas ion on the Jth neighboring nuclear sites orthogonalized in the same manner as ψ^e_{Aa} and the U's are variational parameters. They have applied this technique to Ne : Ar. The sum on J has been carried to third neighbors and the 4*s* excited state orbital of neutral Ne has been used for the "ionic" wave function. Analytic fits are used for all atomic functions. These authors find that a noticeable lowering of energy (~ 0.5 eV) takes place for ψ_{ct} compared to that which they obtain for ψ^e_{Aa} alone [12].

Though these results certainly reflect the superiority of a truly variational calculation, the very large increase computational labor and attendant necessary approximations somewhat obscure their quantitative significance. Some of the simplification made include neglect of the distinction between ^{1}P and ^{3}P states and the use of the Mulliken approximation in evaluating three center integrals. No estimated computational uncertainty is given; it seems likely that it is comparable in magnitude to the 0.5 eV difference found.

These same workers have also studied the $\mathbf{k}=0$ exciton state of pure solid Ne [13]. It is interesting to compare ψ^e_{Aa} and ψ_{ct} for the case, as shown in figure 1, taken from their paper. The resemblance of the orthogonalized tight-binding function to the charge-transfer function is striking. One is tempted to conjecture that the elaborate variational calculation has served to confirm the accuracy of the simpler model.

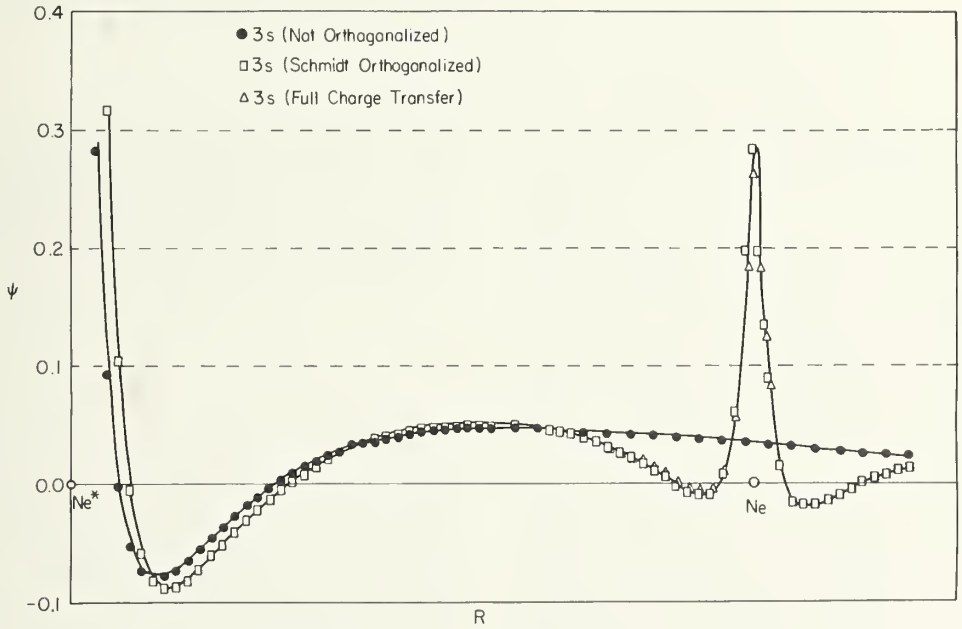

FIGURE 1. *Comparison of* ψ^e_{Aa} *and* ψ_{ct} *for the* $\mathbf{k}=0$ *exciton state of pure solid* Ne.

5. Summary

The lower lying excited states of impurities in rare gas crystals seem reasonably well accounted for by a simple Heitler-London model. Both excitation energies and line shapes are well predicted. Addition of charge-transfer states shows promise for somewhat improving results while generally confirming the original predictions. The higher excited states, however, seem to fall well outside the region of validity of these treatments. Hydrogenic series are observed at short wavelengths in both pure rare gases [14] and their alloys [3, 5]. They seem to correlate well with an effective mass model of the states [3, 5].

An attempt to unify the theory of the entire spectrum has been made through use of a pseudopotential model [10]. Application was made to Ne:Ar. Unfortunately no prediction of excitation energies were made. Only the absolute value of the excited state was calculated. Thus, though a single theory of the excited states of defects in rare gas crystals would be at least aesthetically pleasing, none is yet in sight. It is still necessary to apply models a posteriori to describe different portions of the spectra. On the other hand, this situation is not entirely unique. For example, one is still content to say that different excited states of the same atom may be best described in different coupling schemes ranging from *LS* to *jj*.

6. References

[1] A. Gold, Phys. Rev. **124,** 1740 (1961). References to earlier work on the tight binding model are contained in this paper.
[2] See, for example, A. Gold, J. Phys. Chem. Solids **18,** 218 (1961).
[3] G. Baldini and R. S. Knox, Phys. Rev. Letters **11,** 127 (1963).
[4] G. Baldini, Phys. Rev. **136,** A248 (1964).
[5] G. Baldini, Phys. Rev. **137,** A508 (1965).
[6] W. Weyhmann and F. M. Pipkin, Phys. Rev. **137,** A490 (1965).
[7] B. Meyer, J. Chem. Phys. **43,** 2986 (1965).
[8] T. H. Keil and A. Gold, Phys. Rev. **136,** A252 (1964).
[9] T. H. Keil and A. Gold, Phys. Rev. **140,** A906 (1965).
[10] S. Webber, S. A. Rice and J. Jortner, J. Chem. Phys. **42,** 1907 (1965).
[11] T. H. Keil, Phys. Rev. **140,** A601 (1965).
[12] The differences found between these results for ψ^c_{Aa} and those of reference 1, appear to be due to a numerical error in the latter.
[13] S. Webber, S. A. Rice and J. Jortner, J. Chem. Phys. **41,** 2911 (1964).
[14] G. Baldini, Phys. Rev. **128,** 1562 (1962).

The Use and Misuse of Models in the Calculation of Energy Levels in Insulators*

W. Beall Fowler

Lehigh University, Bethlehem, Pa. 18015

There exist a number of models which have been used to correlate and interpret data on energy levels in insulators. In this note we demonstrate by means of three examples that a model is not necessarily correct just because it appears to agree with experiment. The three phenomena considered have all been "explained" in terms of particular models; we show that for each of these a completely different model leads to an equally good "explanation."

1. The A and C Bands of Tl^+ in Alkali Halides

Ghosh [1] [1] compiled the available room-temperature data on peak positions of the so-called A and C absorption bands associated with Tl^+ in the alkali halides. He then found that the following expressions fit rather well the observed energies (with the exception of the simple cubic cesium halides):

$$E_A = 0.306r_+ - 1.789r_- + 7.845 \text{ eV},$$
$$E_C = 0.244r_+ - 2.722r_- + 10.925 \text{ eV}. \quad (1)$$

E_A and E_C are the peak positions of the A and C bands, respectively, while r_+ and r_- are the Goldschmidt radii of the alkali and halide ions in angstroms. Ghosh's fit is such that if δ is the difference between theoretical and experimental energies for a given alkali halide, then the sum of δ^2 for all 9 alkali halides considered is 0.0021 for E_A, 0.052 for E_C.

We have performed a least-squares fit in a similar attempt to optimize the values of E_A and E_C in terms of ionic polarizabilities. We obtain

$$E_A = 0.098\alpha_+ - 0.1991\alpha_- + 5.4452 \text{ eV},$$
$$E_C = 0.029\alpha_+ - 0.3036\alpha_- + 7.1307 \text{ eV}. \quad (2)$$

α_+ and α_-, in ($Å^3$), are the polarizabilities determined by Tessman, Kahn, and Shockley [2]. For E_A the sum of δ^2 is 0.0030, for E_C it is 0.056. Our fit is thus for all practical purposes as good as Ghosh's.

There may well be little theoretical content in either Ghosh's or our results. However, if one were to formulate a picture of what is going on in terms of the former result, he would probably guess that the presence of ionic radii implies that the energies of the Tl^+ depend mainly on the size of the "box" in which it finds itself. Things are actually a bit more complicated than this, because the interionic distance does not enter explicitly into eq (1).

In terms of our result a quite different picture might emerge. The presence of polarizabilities implies that perhaps in the excited state the electron and hole of Tl^+ are fairly well separated and are polarizing the neighboring ions. Thus Ghosh's result leads one to think in terms of a highly localized state, our result to a more diffuse state.

The fact that *both* pictures fit is simply a result of the fact that the larger an ion is, the more polarizable it is. The relationship is not generally linear, but it is sufficiently monotonic for data-fitting approaches to be unable to distinguish from among the two extreme possibilities or any intermediate ones.

2. Exciton Binding Energies

Several authors [3], including Fischer and Hilsch [4], have attempted to fit the observed binding energies of $n = 1$ excitons in alkali halides by means of an effective-mass model. In this model the binding energy G_n of the nth exciton state is

$$E_{opt} - E_{ex}^n \equiv G_n = \frac{13.6m^*}{K_0^2 n^2} \text{ eV}, \quad (3)$$

where n is the principal quantum number, K_0 the optical dielectric constant, and m^* the reduced electron-hole effective mass. E_{opt}, the optical band gap, is the least energy required to excite an electron from the valence band into the conduction band, E_{ex}^n the energy to create the nth exciton.

In an attempt to test the validity of eq (3), we have plotted in figure 1 K_0G_1 versus $1/K_0$ for a number of alkali halides. The values of G_1 have been obtained from various experimental sources

*Work supported in part by the Advanced Research Projects Agency under Contract SD-131 at the University of Illinois.

[1] Figures in brackets indicate the literature references at the end of this paper.

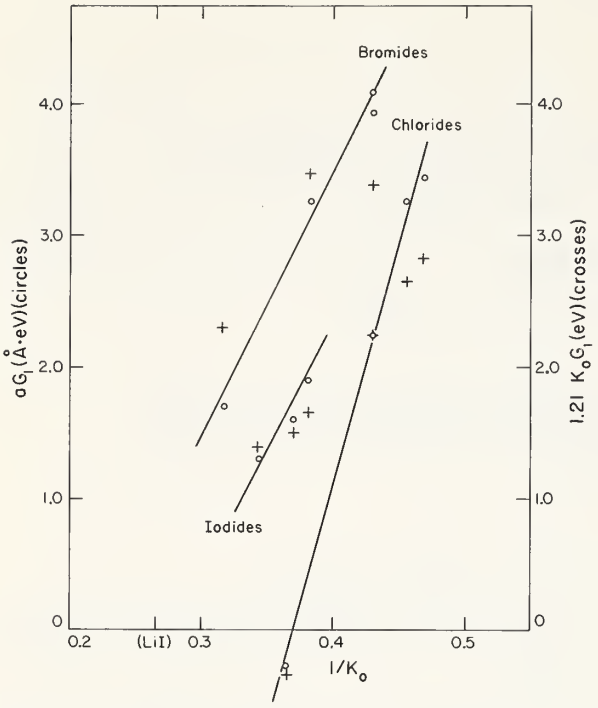

FIGURE 1. *Exciton binding energies for a number of alkali halides.*

The crosses and the circles represent data plotted according to the effective-mass model and the transfer model, respectively. The lines refer to the results of the latter model. Also shown is the value of $1/K_0$ for LiI, whose binding energy is not known. See the text and reference 5 for further discussion.

and are tabulated in reference 5. The data fall into such a pattern that one might try to fit them with three lines, one for each halogen. One might then try to argue that the existence of three lines instead of one implies that there is a core correction, different for different halogens, which has been ignored. The different slopes might come from different effective masses for different halogens.

The preceding arguments are rather weak, but they become extremely suspect if we recognize that in most of the alkali halides the $n=1$ excitons are so small that the effective-mass approximation should not work at all [5], and that there is really very little dielectric polarization between or around the electron and hole when in this state.

We then search for another description of the binding energies, particularly their dependence on dielectric effects. Such a description is obtained when we recognize, with Mott and Gurney [6], that when one excites an electron from the valence band into the conduction band, one is creating not "bare" particles but rather electronic polarons, with large self-energies associated with the *electronic* polarization surrounding the hole and the electron. Elsewhere [5] we have shown that the classical Mott-Littleton [7] approach is valid for calculating these self-energies in most of the alkali halides.

A simplified picture of the situation is then as follows: one creates an $n=1$ exciton by placing an electron and a hole into a state in which they are confined to the same unit cell; these are "bare" particles and little polarization is involved. But exciting the electron into the conduction band *does* involve large polarization effects; the binding energy, being the difference of these two energy states, thus depends on electronic polarization.

With very little quantitative justification, we describe this picture in terms of a transfer model. For discussions of the features and shortcomings of this model, see reference 8.

According to the semiclassical transfer model, the energy required to take an electron from a negative ion and place it into a state in which it spends its time on positive ions a distance R away is

$$E(R)=\frac{e^2}{2R}+H_{se}(R)+E' \tag{4}$$

The coulomb energy of the electron and hole is $(-e^2/R)$; the factor $\frac{1}{2}$ comes from the virial theorem and takes account of the kinetic energy. $H_{se}(R)$ is the polarization energy discussed above. E' contains a host of other important contributions, including ionization and Madelung energies, but it is assumed independent of R. We now assume that placing the electron into the conduction band requires $E(\infty)$, while creating an $n=1$ exciton requires $E(a)$, a being the nearest neighbor distance. We further assume that $H_{se}(a)$ is zero and write $H_{se}(\infty)$ as just H_{se}. Then G_1 is given by

$$G_1=\frac{e^2}{2a}+H_{se}. \tag{5}$$

Now, it turns out that the quantities H_{se} for all of the alkali halides are given very accurately by the expression [9]

$$H_{se}=\frac{14.6}{a}\left[\frac{1.5}{K_0}-1.43\right]\text{eV}. \tag{6}$$

Here a is in angstroms. Note that H_{se} may be as large as ≈ 5 eV.

Qualitatively, then, this model says that G_1 should vary as $[1/a]$ $[(1/K_0)+\text{const}]$, and it suggests that if we plot aG_1 versus $1/K_0$ we should obtain a straight line. Such a plot is given in figure 1 (circles), and we do indeed obtain 3 straight lines whose separation may again be due to core corrections. The slopes of the iodide and bromide lines even turn out to be very close to that predicted by eq (6).

Although these results may be quite fortuitous, we feel that the physical picture described is more accurate than that provided by the effective-mass model. Note that it is not surprising that both models work; empirically, a tends to be a monotonic, sometimes linear, function of K_0.

3. The Relaxed Excited *F* Center

Spinolo [10] has shown that the thermal ionization energies E_T of excited F centers in a number of alkali halides are fit quite well by an effective-mass model similar to that of eq (3): $E_T \approx 1/K^2$, where K is the static dielectric constant. In figure 2 we plot

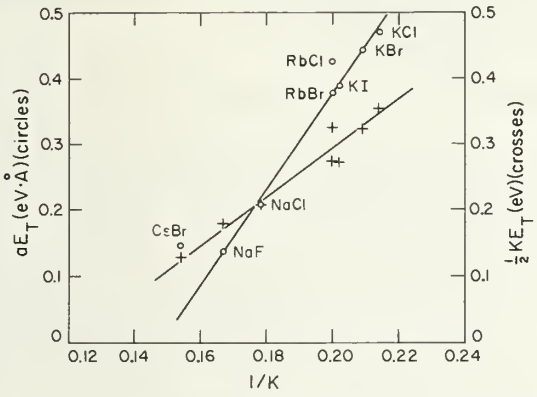

FIGURE 2. *Thermal ionization energies for the excited* F *center in a number of alkali halides.*

The crosses and the circles correspond to large-orbit and small-orbit models, respectively. The data for E_T were obtained from reference 10.

KE_T versus $1/K$, using Spinolo's data. A rather good straight line obtains. Such a fit is in the spirit of the "large-orbit" picture of the relaxed excited state developed by the author. In this picture there exists some lattice polarization between electron and vacancy which leads to an "effective" dielectric constant whose value is between K_0 and K.

Actually, it is possible to take account of the change in the lattice self-energy accompanying the thermal process and do a bit better than $1/K^2$. We neglect the effect of self-energy due to electronic polarization, assuming it to be the same in the excited state as in the ionized state.

Mott and Gurney [12] have shown how to compute this difference of lattice self-energies E_L in a continuum approximation. The result is

$$E_L = \frac{e^2}{2R}\left[\frac{1}{K_{\text{eff}}} - \frac{1}{K}\right]. \tag{7}$$

R is the "radius" of the electronic state, K the static dielectric constant, and K_{eff} the "effective" dielectric constant when the electron is in the excited state.

The optical ionization energy is

$$E_{\text{op}} = \frac{e^2}{2RK_{\text{eff}}}. \tag{8}$$

The thermal activation energy E_T equals $E_{\text{op}} - E_L$, or

$$E_T = \frac{e^2}{2KR}. \tag{9}$$

In the effective-mass theory [11] for the F-center $2p$ state, R approximately equals $4K_{\text{eff}}/m^*$, and so we have

$$E_T = \frac{13.6}{4}\frac{m^*}{KK_{\text{eff}}}\text{eV}; \qquad E_{\text{op}} = \frac{13.6}{4}\frac{m^*}{K_{\text{eff}}^2}\text{eV}. \tag{10}$$

Using the parameters $m^* = 0.6$, $K_{\text{eff}} = 4.2$ derived by the author [11] for NaCl, we find that E_T equals 0.09 eV and that E_{op} equals 0.12 eV. Since K_{eff} will tend to vary linearly with K, we see that the expression for E_T is consistent with Spinolo's law.

Now suppose that the state were not diffuse but were compact, and that $R \approx a$, the nearest neighbor distance. Then

$$E_T = \frac{e^2}{2Ka} \tag{11}$$

In fact, this fits Spinolo's data about as well as does $1/K^2$ (see fig. 2). The slope even turns out to be about correct, although the experimental line does not extrapolate to (0, 0). The reason that both models "work" is again that K tends to be a monotonic function of a.

In the small-orbit model, if we assume K_{eff} to be 2.3 for NaCl, we find that the difference between E_T and E_{op} is 0.7 eV. This is quite different from the 0.03 eV obtained for the large-orbit model; however, the thermal activation energies E_T turn out to be about the same for both models. Thus the thermal ionization energy is apparently not a very sensitive indicator of the nature of impurity states. If the state is compact and the optical binding energy large, there will be a large lattice energy E_L which tends to make E_T small. If the state is diffuse, E_{op} is already small, and E_T will also be small.

In the case of the relaxed excited F center, there are good reasons for thinking that the large-orbit model is valid [11]. The point stressed here is that the behavior of E_T does not by itself lead unambiguously to this conclusion.

As often happens, improvements in the amount and quality of experimental data seem to lead to poorer agreement with either model than indicated in figure 2. Lowndes [14] has recently measured static dielectric constants for a number of alkali halides, while Podini and Spinolo [15] have reported values of E_T for several more alkali halides. The situation in NaF is apparently more complex than earlier recognized [16].

The updated values of K, E_T, and a, plotted as in figure 2, indicate more scatter than the older values shown. In particular, RbI appears to have a value of E_T too small by nearly a factor of 2. The need for more data is clear; of the crystals for which both E_T and new values of K are known, only CsBr and NaCl have values of K which are outside the

range 4.6 to 4.8. For curve-fitting purposes this is not a desirable situation.

D. L. Dexter has told the author of another case in which two models have been used to fit the same data. The Mollwo-Ivey law [17], in which F-center absorption energies vary as a^{-n}, where n is about 2, has long been known to agree rather well with experiment. The physical interpretation of this model is that the F center in absorption behaves as a particle in a box. Wood has recently investigated the theoretical validity of this model [18]. In a note published ten years ago, Levy [19] exhibited another relationship, $E_{abs}=3e^2/8K_0R$, where R is the cation radius. This seems to agree with experiment to within 10 to 20 percent. The physical interpretation of the Levy model is not clear; it appears to contain some features of a continuum treatment, some features of a localized treatment. But it does work fairly well.

4. References

[1] A. K. Ghosh, J. Chem. Phys. **43,** 2978 (1965).
[2] J. R. Tessman, A. H. Kahn, and W. Shockley, Phys. Rev. **92,** 890 (1953).
[3] J. Hermanson, Phys. Rev. **150,** 660 (1966). Hermanson has made an extensive study of the corrections to eq (3) and has shown that in some cases these corrections cancel.
[4] F. Fischer and R. Hilsch, Nachr. Akad. Wiss. Göttingen, II Math.-Physik. Kl. **8,** 241 (1959); F. Fischer, Z. Physik **160,** 194 (1960).
[5] W. Beall Fowler, Phys. Rev. **151,** 657 (1966).
[6] N. F. Mott and R. W. Gurney, Electronic Processes in Ionic Crystals (The Clarendon Press, Oxford, 1948), 2d ed., reprinted by Dover Publications, Inc., New York, 1964.
[7] N. F. Mott and M. J. Littleton, Trans. Faraday Soc. **34,** 485 (1938).
[8] R. S. Knox, Theory of Excitons (Academic Press, Inc., New York, 1963).
[9] F. K. Du Pré, R. A. Hutner, and E. S. Rittner, J. Chem. Phys. **18,** 379 (1950).
[10] G. Spinolo, Phys. Rev. **137,** A1495 (1965).
[11] W. Beall Fowler, Phys. Rev. **135,** A1725 (1964).
[12] Ref. 6, p. 162.
[13] To be consistent with our earlier discussion of electronic polaron effects, and our omission of them here for the reason stated, we should assume that $R \gtrsim a$ in this case, and $R \lesssim a$ in the exciton problem. This distinction will not substantially affect the curve-fitting approach which we use.
[14] R. P. Lowndes, Physics Letters **21,** 26 (1966).
[15] P. Podini and G. Spinolo, to be published.
[16] P. Podini, Phys. Rev. **141,** 572 (1966).
[17] E. Mollwo, Nachr. Ges. Wiss. Göttingen Math.-Physik. Kl. p. 97 (1931); H. F. Ivey, Phys. Rev. **72,** 341 (1947).
[18] R. F. Wood, J. Phys. Chem. Solids **26,** 615 (1965).
[19] M. Levy, Nature **177,** 241 (1956).

Methods for Calculation of the Electronic Structure of Defects in Insulators*

U. Öpik and R. F. Wood**

Solid State Division, Oak Ridge National Laboratory, Oak Ridge, Tennessee, 38730

The comments which we shall make in this paper apply most directly to calculations of the electronic structure of the F center in alkali halides. We expect them, however, to be valid for a large number of defects in insulators, such as the U, M, and R centers in ionic crystals, the hydrogen interstitial in CaF_2, an yttrium ion in CaF_2, etc.

In calculating the electronic structure of the F center in the alkali halides two methods of representing the defect wave function, ψ_d, have generally been used. In the LCAO–DO method the defect orbital (DO) is expressed as a linear combination of atomic orbitals (LCAO) on the neighboring ions. Thus,

$$\psi_d = \sum_{\nu, j} c_{\nu, j}\, \phi_j(\mathbf{r} - \mathbf{R}_\nu), \tag{1}$$

where $\phi_j(\mathbf{r} - \mathbf{R}_\nu)$ is the jth unoccupied atomic orbital on the νth ion. This leads to a secular equation

$$|(\nu, j|h|\mu, k) - (\nu, j|\mu, k)\epsilon| = 0 \tag{2}$$

for the one-electron energies, ϵ. The difficulty with this method is that the functions $\phi_{\nu, j}$ are quite diffuse, whereas ψ_d will usually be rather well localized and hence the sum in eq (1) must contain several orbitals on each ion in order to give the proper degree of localization. In addition to the orthogonality problems encountered in evaluating $(\nu, j|\mu, k)$ one has a somewhat related problem in calculating the matrix elements of the Hamiltonian, $(\nu, j|h|\mu, k)$, in that they may have large contributions from regions of space in which ψ_d itself is practically vanishing. The point which we wish to make here is neither new nor surprising, but perhaps needs reemphasizing occasionally. Stated very simply, it is that it is not economical to express a localized function in terms of a basis set of diffuse functions, and conversely. Perhaps the most familiar case of this principle occurs in band theory where the OPW method circumvents the need to express the highly localized core states in terms of plane waves.

In calculating ψ_d for defects in alkali halide crystals, it seems more useful and natural to use what we shall call the defect centered (DC) method. In this method, ψ_d is written as

$$\psi_d(\mathbf{r}) = N[\phi_0(\mathbf{r}) - \sum_{\nu, j} (0|\nu, j)\phi_{\nu, j}(\mathbf{r})] \tag{3}$$

in which $\phi_0(\mathbf{r})$ is a fairly smooth function which may be chosen in various ways. The sum over ν, j ensures that ψ_d will be orthogonal to the occupied ion orbitals, $\phi_{\nu, j}(\mathbf{r}) \equiv \phi_j(\mathbf{r} - R_\nu)$. Equation (3) assumes, in effect, that the $\phi_{\nu, j}$ do not overlap with each other, and this simplification must be investigated in each case. If these overlaps are not negligible, it might prove convenient to first use the method of symmetrical orthogonalization to transform to a set of mutually orthogonal core functions.

Expressing ψ_d as in eq (3) and evaluating $(\psi_d|h|\psi_d)$, one obtains in addition to the familiar point ion approximation a contribution from exchange with the core orbitals, a coulomb term due to penetration of ϕ_0 into the core region, and a contribution, arising from the overlap terms in eq (3), which we shall refer to as the overlap energy. Table 1 shows the magnitude of these contributions in a number of cases [1].[1]

TABLE 1. *Defects in* KCl: *contributions to the total energy, in eV*

These are in addition to the point-ion energy.

Defect and state	Exchange	Penetration	Overlap	Total
F center ground.....	−3.016	−1.715	+6.993	−4.721
F center excited.....	−4.720	−3.178	+10.934	−1.978
U center ground.....	−1.422	−0.828	+4.391	−28.734

Since these terms are not negligible and do not even approximately cancel each other, we now wish to consider methods of calculating them. In fact, at the present level of approximation, only the exchange terms present a really difficult problem. A part of the one-electron Hamiltonian is the exchange operator, h_{ex}, defined by

$$h_{ex}u(\mathbf{r}) = \sum_\nu \sum_i \phi_{\nu i}(\mathbf{r}) \int \frac{\phi_{\nu i}(\mathbf{r}')u(\mathbf{r}')}{|\mathbf{r} - \mathbf{r}'|} d\mathbf{r}' \tag{4}$$

*Research sponsored by the U.S. Atomic Energy Commission under contract with Union Carbide Corporation.

**Visiting scientist from Queens University, Belfast, North Ireland.

[1] Figures in brackets indicate the literature references at the end of this paper.

where all wave functions are assumed real. To understand the difficulty, consider that each of the $\phi_{\nu,i}$ in eq (4) is supposed to be a Hartree-Fock free-ion orbital. The preferred method of calculating these orbitals now is to expand them in terms of Slater orbitals with nonlinear variation parameters [2]. This expansion may contain six or seven such orbitals in the case of positive alkali ions. In order to calculate the exchange integrals between ϕ_0 and $\phi_{\nu,j}$ accurately, it is customary to use elliptic coordinates. This method, though quite accurate, is very time consuming, involving as it does the calculation of the exchange between the defect electron and charge distributions given by products of the individual Slater orbitals. Furthermore, since ϕ_0 may also be expressed as a sum of orbitals

$$\phi_0=\sum_k a_k\phi_{0k}, \tag{5}$$

the number of two-center, two-electron integrals which must be calculated at each stage in the minimization procedure, can become very large. Even on a fast computer the computational time involved in this method becomes a very serious factor. Therefore, in the remainder of this paper we shall sketch a method which circumvents this difficulty and then end by giving a few comparisons of accuracy and time using the two methods.

Let

$$u_{nl}(r,\ \theta,\ \phi)=\frac{1}{r}\,P(nl|r)Y_{lm}(\theta,\ \phi) \tag{6}$$

be the orbital of an electron outside the spherically symmetrical closed shells of an ion, r, θ, ϕ being the spherical polar coordinates centered at the nucleus, l and m being the azimuthal and orbital magnetic quantum numbers, respectively, and Y_{lm} being a spherical harmonic. The Hartree-Fock equation for the radial function $P(nl|r)$, belonging to an energy value E [3], is

$$\left\{\frac{d^2}{dr^2}+\frac{2Z_p(r)}{r}-\frac{l(l+1)}{r^2}\right\}P(nl|r)$$

$$+\frac{2}{r}\sum_{l'}\frac{2l'+1}{2}\sum_{n'}\left[\sum_k C_{ll'k}Y_k(nl,\ n'l'|r)\right]$$

$$\times P(n'l'|r)-\sum_{n'}\epsilon_{nl,\ n'l}P(n'l|r)=-2EP(nl|r), \tag{7}$$

where

$$Y_k(nl,\ n'l'|r)=r^{-k}\int_0^r r'^kP(nl|r')P(n'l'|r')dr'$$

$$+r^{k+1}\int_r^\infty r'^{-k-1}P(nl|r')P(\mathrm{n}'l'|r')dr',$$

$Z_p(r)$ is Hartree's "effective nuclear charge for potential," primed quantities refer to the core orbitals, the constants $C_{ll'k}$ are defined by Condon and Shortley [4] (sec. 9[6]), and the so-called non-diagonal parameters, $\epsilon_{nl,\ n'l}$, are determined so as to make the function $P(nl|r)$ orthogonal to the core functions $P(n'l|r)$.

Defining δZ_p by

$$\delta Z_p(r)=\frac{1}{P(nl|r)}\sum_{n'l'}\left\{\frac{2l'+1}{2}\sum_k C_{ll'k}Y_k(nl,\ n'l'|r)\right.$$

$$\left.-\frac{1}{2}\delta_{ll'}r\epsilon_{nl,\ n'l}\right\}P(n'l'|r), \tag{8}$$

we may call $-\delta Z_p(r)/r$ and effective exchange potential energy, and rewrite the Hartree-Fock equation as

$$\left\{\frac{d^2}{dr^2}+2\frac{Z_p(r)+\delta Z_p(r)}{r}-\frac{l(l+1)}{r^2}+2E\right\}P(nl|r)=0. \tag{9}$$

In agreement with what has been previously found by other authors (see, e.g., Biermann and Lübeck [5], and Stone [6]), we find that the function $\delta Z_p(r)$ depends strongly on the azimuthal quantum number l but only slightly on the energy, E, provided that the energy E is well above the energies of the core orbitals.

We can thus replace the operator

$$-r^{-1}Z_p(r)+h_{\mathrm{ex}} \tag{10}$$

by an operator U, defined so that for an eigenfunction $v_l(\mathbf{r})$ of the square of the orbital angular momentum belonging to an eigenvalue $\hbar^2l(l+1)$,

$$Uv_l(\mathbf{r})=-r^{-1}[Z_p(r)+\delta Z_p^l(r)]v_l(r), \tag{11}$$

$\delta Z_p^{(l)}$ being the function defined by (8) for that value of l. Having tabulated the functions $\delta Z_p^{(l)}$ for each of the ions, we can use expansions of ϕ_{0k} and $\phi_{0k'}$ in spherical harmonics about the ionic nuclei to evaluate the matrix elements,

$$\langle\phi_{0k}|U|\phi_{0k'}\rangle, \tag{12}$$

thus avoiding the need for performing the time-consuming calculations of the matrix elements of h_{ex} coming from eq (4). In tabulating the functions $\delta Z_p(r)$, we have to smooth out the singularities that arise at the zeros of $P(nl|r)$. The functions $\delta Z_p(r)$ are so insensitive to the energy E that a rough knowledge of E is sufficient to enable us to calculate them with the required accuracy.

To summarize, the advantage of the present method is that, in determining the functions $\delta Z_p(r)$, we in effect calculate the exchange integrals once and for all, instead of having to recalculate them every time they are needed.

It should be realized that our procedure replaces the original one-electron Hamiltonian h by a new one, say h_{eff}, such that only those eigenvalues of h which are above the core eigenvalues, and the eigenfunctions belonging to these, are practically indentical to the corresponding eigenvalues and eigenfunctions of h_{eff}. This is not true of the core eigenstates of the two Hamiltonians, and it can be shown that in carrying out the orthogonalization procedures, we now have to use the core eigenvalues and eigenfunctions of h_{eff} and not those of h.

This method requires the expansion of each of the "smooth" trial functions ϕ_{0k} in spherical harmonics about the nucleus of each of those ions that are treated as extended ions, and this can in itself be very time consuming. It was therefore decided to gain speed by sacrificing a certain amount of mathematical accuracy. A computer program was written which expands an arbitrary function in spherical harmonics about an arbitrary center, on the assumption that terms of degree $l > L$, where $L \leqslant 12$, are negligible. Instead of numerical integration, the program uses summations over a set of judiciously chosen points within a sphere (whose radius is input data) outside which the expansion will be inaccurate. No spherical harmonics are evaluated during the expansion process; instead, the spherical harmonics at the required points, multiplied by suitable weight factors, were stored as constants of the program when the program was written. The method turned out to be more accurate than had been anticipated. Depending on circumstances, the expansion of a typical Slater-type function of not too high an azimuthal quantum number takes between 0.5 and 4.0 sec on the CDC 1604A computer.

These new methods have been tested on the F center in KCl, by comparing the results with those obtained by calculating the exchange and overlap integrals by more conventional methods (ref. 1). The energies agree to within 0.03 eV, but the energy *difference* between the ground and the first excited state was found to differ from that obtained by the conventional methods by only 0.005 eV. Most of the 0.03 eV inaccuracy in the energy probably arose from our failure to achieve complete self-consistency in solving the Hartree-Fock equation (7) for the free K^+ ion when we determined $\delta Z_p(r)$. According to some indications, the errors arising from our method of expansion in spherical harmonics are probably not greater than 0.003 eV. These are small sacrifices if one considers the gain in speed: a calculation which previously took over 2 hr can now be done in less than 5 min, provided that the functions δZ^l_p have been previously determined; but this probably overestimates the gain, because in the early calculations by the conventional methods we had used some quantum chemistry routines which had been written for problems in which much greater accuracy was required, and, moreover, we probably did not use these routines in the most efficient way. The determination of the functions δZ^l_p, which we do separately for six values of l, takes about 7 to 10 min for each ion; once determined, these functions can be used any number of times.

References

[1] Taken from unpublished calculations of R. F. Wood and H. W. Joy on the F center and R. L. Gilbert and R. F. Wood (to be published) on the U center. See also R. F. Wood and H. W. Joy, Phys. Rev. **136**, A451 (1964).

[2] The method used is that of C. C. J. Roothan, Rev. Mod. Phys. **23**, 69 (1951) and **32**, 179 (1960), with Slater orbitals as a basis set.

[3] D. R. Hartree, The calculation of Atomic Structures (John Wiley & Sons, Inc., New York, N.Y., and Chapman and Hall, London, 1957).

[4] E. U. Condon and G. H. Shortley, The Theory of Atomic Spectra (University Press, Cambridge, 1935).

[5] L. Biermann and K. Lübeck, Z. Astrophys. **25**, 325 (1948).

[6] P. M. Stone, Phys. Rev. **127**, 1151 (1962).

256-724 O-67—9

A Model to Treat Lattice Distortions and the F-Center Electron Consistently*

Herbert S. Bennett †

Department of Physics and Materials Research Laboratory, University of Illinois, Urbana, Ill. 61801

In this note we present a model of the lattice which is as simple as possible and yet which contains many of the features of an exact treatment. But most important we require that the same lattice model be able to accommodate either a spatially compact or diffuse vacancy-centered F-electron wave function. We feel that this last condition has not received sufficient consideration in the few previous consistent calculations of the F-electron wave function and the lattice distortions.

The F-center lattice defect in ionic crystals consists of an electron localized about a vacant negative ion site. Many calculations of the electronic structure of the F center appear in the literature [1,2]. [1] They all have one feature in common. Namely, the potential energy term in the electronic Hamiltonian is a constant for distances less than a distance of the order of the nearest neighbor distance. This constant potential (the potential well depth) contains at least one term which depends upon the electrostatic crystal potential at the vacant site (the Madelung potential).

Most of the calculations in references [1] and [2] consider the ground state and low lying excited states of the center in an undistorted lattice. Lattice distortions are present and may change the potential well depth. As far as we know, only a few authors have attempted to include the effect of the lattice distortions in a consistent manner [2]. The emission spectra of the F center in the alkali halides indicates the importance of lattice distortions. The emission band exhibits a large Stokes shift and the first excited state has a lifetime which is greater than the lifetime one expects from atomic spectra [3].

We shall take the view that the nature of the wave function of the F electron may change substantially between emission and absorption [3,4]. The F center originally in its ground state, $|a,0\rangle$, becomes excited into the state, $|a,n\rangle$, which is assumed to be a quasi-stationary state with an electronic wave function calculated from the same crystal potential as that for the state, $|a,0\rangle$. The lattice then relaxes and thereby the crystal potential which the F electron experiences changes. The excited electronic state, $|e,n\rangle$, calculated from the relaxed crystal potential may differ from the excited state, $|a,n\rangle$. The continuum model of W. B. Fowler [1] suggests that the relaxed excited state, $|e,n\rangle$, from which emission occurs, may be very diffuse; i.e., the wave function, $\langle r|e,n\rangle$, may have its maximum at four to five nearest-neighbor distances while the ground state, $|e,0\rangle$, into which emission occurs remains rather compact with a wave function, $\langle r|e,0\rangle$, confined mostly to the region within the nearest-neighbor distance.

The electronic part of the Hamiltonian contains the self-consistent potential which the electron experiences and which is a function of the lattice configuration. All calculations thus far represent this potential for distances less than the nearest-neighbor distance as a potential well whose depth is determined in part by the Madelung potential. We compute the Madelung potential by viewing the lattice as a collection of point ions and this suggests that we use the point ion approximation as a zeroth order approximation to the lattice. The electronic Hamiltonian yields an electronic wave function which may be either spatially diffuse or compact. This F-electron wave function gives rise to a charge density

$$\rho_F(\mathbf{r}) = -e\psi^*(\mathbf{r})\psi(\mathbf{r}).$$

The brevity of this note forces us to consider here only the two extreme cases; namely,

$$\text{diffuse:} \qquad \rho_F(\mathbf{r}) = 0,$$

$$\text{compact:} \qquad \rho_F(\mathbf{r}) = -e\delta^3(\mathbf{r}).$$

Even though we shall also neglect polarization and defect self-energies in our discussion below, such aspects are easily incorporated into the model.

We want to compute the change in the lattice energy due to replacing an anion with a F-center electron. We first create a vacancy at the anion site $\mathbf{r}_0 = 0$ of charge Z_0 and permit no lattice relaxation. This fictitious lattice state will serve as

*This work was supported in part by an United States Atomic Energy Commission Contract AT(11-1)-1198.

†Present address: National Bureau of Standards, Washington, D.C. 20234.

[1] Figures in brackets indicate the literature references at the end of this paper.

the reference energy for the lattice. Classical ionic lattice theory gives the lattice energy as a sum of the electrostatic (Coulombic) energy of the lattice, E_e, and the repulsive energy of interaction between the ionic cores of the lattice, E_r;

$$E_L = E_e + E_r, \tag{1}$$

where

$$E_e = \frac{1}{2}\sum_{\substack{i,\,j \\ i\neq j}} Z_i Z_j |\mathbf{r}_i - \mathbf{r}_j|^{-1} - Z_0 \sum_{j\neq 0} Z_j |\mathbf{r}_j|^{-1}, \tag{2}$$

and

$$E_r = \frac{1}{2}\sum_{\substack{i,\,j \\ i\neq j}} \varphi_r(\mathbf{r}_i - \mathbf{r}_j) - \sum_{j\neq 0} \varphi_r(\mathbf{r}_j). \tag{3}$$

We may interpret the second term of E_e by saying that we create a vacancy by adding an ion of charge $-Z_0$ at $\mathbf{r}_0 = 0$ or equivalently by saying that we remove the electrostatic "bonds" involving the point $i = 0$. The second term in E_r means that we remove the repulsive "bonds" involving the point $i = 0$. The repulsive energy $\varphi_r(\mathbf{r}_i - \mathbf{r}_j)$ between the ith and jth ions take the Pauli exclusion principle between the ith and jth cores into account and is a short-ranged function of $r_{ij} = |\mathbf{r}_i - \mathbf{r}_j|$. The function $\varphi_r(r_{ij})$ usually has the empirically determined Born inverse power law form,

$$\varphi_r(r_{ij}) = a r_{ij}^{-\lambda}, \qquad \lambda > 0, \tag{4}$$

the Born-Mayer exponential form,

$$\varphi_r(r_{ij}) = b b_i b_j \exp(-r_{ij}/\rho), \tag{5}$$

or some combination of the two forms (Verwey). The quantities a and λ, and b, b_i, b_j, and ρ are determined from experiment and are given in the literature [5]. Forms (4) and (5) assume no electronic polarization of the ionic cores and because the experiments used to determine their parameters involve only small ion displacements, we must at the least be cautious whenever the distance between ions becomes substantially less than the sum of their ionic radii.

We now allow the n nearest neighbors of the vacancy (defect ions) to move radially inward or outward to the sites $\mathbf{r}_i' = \mathbf{r}_i(1-\sigma)$ for $1 \leq i \leq n$. All other ions are to remain at their perfect lattice sites in this model. The change in lattice energy then assumes the form,

$$\Delta E_L \text{ (vacancy, distortion)} = E_L' - E_L = \Delta E_e + \Delta E_r, \tag{6}$$

where

$$\Delta E_e = E_1 + E_2 + E_3 + E_4, \tag{7}$$

$$E_1 = nZ_1 \sum_{j\neq 1} Z_j \{|\mathbf{r}_1' - \mathbf{r}_j|^{-1} - |\mathbf{r}_1 - \mathbf{r}_j|^{-1}\}, \tag{8}$$

$$E_2 = -nZ_1 \sum_{\substack{j\neq 1,\, j\neq 0 \\ j\leq n}} Z_j \{|\mathbf{r}_1' - \mathbf{r}_j|^{-1} - |\mathbf{r}_1 - \mathbf{r}_j|^{-1}\}, \tag{9}$$

$$E_3 = \tfrac{1}{2} \sum_{\substack{i\leq n \\ i\neq 0,\, i\neq j}} \sum_{\substack{j\leq n \\ j\neq 0,\, i\neq j}} Z_i Z_j \{|\mathbf{r}_i' - \mathbf{r}_j'|^{-1} - |\mathbf{r}_i - \mathbf{r}_j|^{-1}\}, \tag{10}$$

$$E_4 = -Z_0 \sum_{\substack{j\leq n \\ j\neq 0}} Z_j \{|\mathbf{r}_j'|^{-1} - |\mathbf{r}_j|^{-1}\}, \tag{11}$$

and

$$\Delta E_r = E_{r'} - E_r. \tag{12}$$

The lattice configuration obtains at that value of σ for which the change in the lattice energy is a minimum.

If we assume that the F electron has negligible repulsive interaction with the core electrons, then the limit of a very diffuse F-electron state corresponds to removing both the electrostatic and repulsive core "bonds" involving the point $i = 0$; i.e., we minimize $\Delta E_L(\sigma)$. On the other hand, the limit of a very compact F-electron state corresponds to removing only the repulsive core "bonds" involving the point $i = 0$; i.e., we minimize $\Delta E_L(\sigma) - E_4(\sigma)$.

Past authors [2] have assumed that the ions experience repulsive core interactions with only their nearest neighbors. Using a computer to minimize ΔE_L and $\Delta E_L - E_4$ for NaCl, we find that for the range $-.06 \geq \sigma_d \geq -.20$, $\Delta E_L(\sigma_d)$ is a minimum depending upon which form for ϕ_r we choose to describe the nearest-neighbor-only repulsive core interactions. The same examination of $\Delta E_L(\sigma) - E_4(\sigma)$ yields that $\Delta E_L(\sigma_c) - E_4(\sigma_c)$ will be a minimum only for values of σ_c greater than $+0.30$. This large inward motion of the ions to accommodate a very compact F-electron state results in the n defect ions, which are next nearest neighbors of each other, approaching within a distance roughly equal to the sum of their ionic radii. This means that we must include the next-nearest-neighbor core repulsions, particularly for the compact F-electron states.

A qualitative examination of the terms in ΔE_L and in $\Delta E_L - E_4$ as functions of σ also reveals the same results for the nearest-neighbor-only core interactions. To facilitate this qualitative examination, we summarize the contents of the terms E_1 to E_4. The term E_1 is the change in electrostatic energy which occurs when a neighboring cation moves in the background of a perfect point ion lattice potential. The quantity E_2 represents the change in the electrostatic energy which occurs when one of the n defect ions moves in the point ion potential of the remaining $(n-1)$ defect ions at undistorted lattice sites. The term E_3 is the change

in the electrostatic energy of the n defect ions when all n defect ions move radially inward or outward. And finally, E_4 represents the change in the electrostatic energy between the effective charge $(-Z_0)$ and the lattice due to the motion of the defect ions.

To be specific we use the form (4) for which $\lambda \approx 7.0$–9.0. The form (5) also leads to the same conclusions. Recall that a diffuse state corresponds to adding an effective charge $-Z_0$ at $i=0$ (remove electrostatic "bonds" to $i=0$). But $-Z_0$ has the same sign as the nearest-neighbors to $i=0$. Hence, the electrostatic part of ΔE_L, E_4, and also E_1 and E_3, decrease for $\sigma < 0$. Only the term E_2 increases for $\sigma < 0$. In addition we have $\lambda > 1$ and a sufficient number of repulsive nearest-neighbor "bonds" which decrease in length for $\sigma < 0$. These conditions combine to bring about an accompanying increase in ΔE_r which offsets the decrease in ΔE_e before $|\sigma|$ becomes too large. However, such a balance does not obtain for the case of a compact state, which is the limit of removing only the repulsive "bonds." In this case we consider $\Delta E_L - E_4$. The electrostatic terms E_1 and E_2 decrease for $\sigma > 0$. Only the term E_3 increases for $\sigma > 0$. Thus, the electrostatic forces tend to move the n defect ions inward, $\sigma > 0$. But most important, because there are no nearest-neighbor repulsive "bonds" which decrease for $\sigma > 0$ the defect ions move excessively inward until the electrostatic term E_3 increases sufficiently to offset the decrease in the remaining electrostatic part $\Delta E_e - E_3 - E_4$ and in the repulsive term ΔE_r.

Notice that when the next-nearest-neighbor repulsive "bonds" are included, those "bonds" among the n defect ions of $i=0$ decrease for $\sigma > 0$. In fact, upon minimizing $\Delta E_L - E_4$ with next-nearest-neighbor repulsive "bonds" we obtain a much smaller inward distortion for a compact F-electron state and about the same outward distortion for the diffuse F-electron state as before. The quantity σ_c is in the range $0.1 \gtrsim \sigma_c \gtrsim 0.01$ and the quantity σ_d is in the range $-0.2 \lesssim \sigma_d \lesssim -0.05$ depending upon the form and parameters of φ_r. Hence, we state that one must include next-nearest-neighbor core repulsions when considering a compact F-electron wave function in a model lattice in which only the nearest-neighbor ions to the defect move in the so-called breathing mode.

References

[1] S. I. Pekar, Uspekhi Fiz. Nauk. **50,** 197 (1953); T. Kojima, J. Phys. Soc. Japan **12,** 918 (1957); B. S. Gourary and F. J. Adrian, Phys. Rev. **105,** 1180 (1957); B. S. Gourary and A. E. Fein, J. Appl. Phys. **33,** Suppl., 331 (1962); W. B. Fowler, Phys. Rev. **135,** A1725 (1964); and J. K. Kübler and R. J. Friauf, Phys. Rev. **140,** A1742 (1965).

[2] R. F. Wood and J. Korringa, Phys. Rev. **123,** 1138 (1961); and R. F. Wood and H. W. Joy, Phys. Rev. **136,** A451 (1964).

[3] R. K. Swank and F. C. Brown, Phys. Rev. **130,** 34 (1963).

[4] W. B. Fowler and D. L. Dexter, Phys. Rev. **128,** 2154 (1962).

[5] G. C. Benson and E. Dempsey, Proc. Roy. Soc. **A266,** 344 (1962); and M. P. Tosi, Solid State Physics **16,** 38 (1964).

T-Matrix Theory of Localized Electronic States Due to a Vacancy With Application to Diamond

K. H. Bennemann

Institute for the Study of Metals, University of Chicago, Chicago, Ill. 60637

1. Introduction

The problem of determining the electronic state of a vacancy in semiconductors, particularly in diamond, has found some interest in the past and due to the remarkably sensitive derivative techniques used presently with great success in studying optical properties of solids, there is good reason to believe that this problem will soon become active again. First, I would like to describe briefly the work which has been done in the past on the vacancy problem. Then I would like to advertise a new method for determining the electronic structure of a vacancy and to apply the theory to diamond. Finally, I would like to introduce a new aspect on charged vacancies.

In the past Coulson and Kearsley [1][1], Yamaguchi [2], and more recently Stoneham [3] have made detailed studies of localized electronic states at neutral and (positively or negatively) charged vacancies in diamond. In all these studies the electronic structure of the vacancy has been determined by applying a molecular-orbital technique using one-electron wave functions centered at the vacancy or using linear combinations of atomic orbitals (LCAO). The molecular orbitals were constructed from the tetrahedrally hybridized $2s$ and $2p$ atomic orbitals. Then from such "vacancy"-electronic orbitals Slater determinantal wave functions were formed representing a special electronic vacancy configuration taking into account properly lattice symmetry of the vacancy and electron spins. Finally several Slater wave functions with the same spin multiplicity and space symmetry were linearly combined. The spectrum of energies for the localized electronic states were then determined from the appropriate secular determinant including configuration interaction and interaction among the localized electrons and among the localized electrons and lattice atoms. The results obtained differed mainly due to uncertainties in determining the interatomic electronic coulomb interaction matrix elements.

Instead of improving these previous methods which are all very much in the spirit of "dangling bonds," we would like to propose a very different method for treating vacancies in semiconductors. Recently the pseudopotential theory as developed by Kleinman, Phillips, Cohen, Heine, et al., which replaces the crystal potential by an effective potential, in many cases much weaker and smoother, has been successfully applied to semiconductors such as C, Si, Ge, etc. Using such an effective crystal potential permitted one to treat the valence electrons approximately as quasi free-electrons. This suggested that we determine the electronic structure of defects in semiconductors using scattering theory; this is in a way an extension of Friedel's theory of defects in metals.

Therefore using T-matrices a theory of the electronic structure of vacancies in semiconductors is developed and applied to diamond. This theory unifies the effective mass approximation, which is adequate to treat shallow localized states (Kohn, Luttinger, et al.), and the localized perturbation theory (Lifshitz, Clogston-Slater et al.), which is adequate to treat deeply bound states.

2. Theory

The most remarkable feature of the diamond-type lattice is that each atom sits at the center of a regular tetrahedron formed by its four nearest neighbors to which it is covalently bound. Therefore we have four broken covalent bonds around the vacancy. This gives rise to a strong change in the valence electron distribution in the vicinity of the vacancy and leads to a lattice distortion around the vacancy. Therefore, it is not reasonable to determine the redistribution of the valence electrons around the vacancy by perturbation theory using the perfect crystal as the unperturbed state. Instead, we determine self-consistently the electronic distribution and crystal potential in the vicinity of the vacancy by scattering theory. By including multiple electron scattering involving different lattice atoms we take explicitly into account the atomic configuration of the lattice. A

[1] Figures in brackets indicate the literature references at the end of this paper.

vacancy means that an atomic scatterer is missing in the lattice. In detail the crystal potential is obtained as follows: after replacing the crystal potential V by the appropriate pseudopotential V_S, resulting from using orthogonalized wave functions, we introduce the one-electron Green's function G and the T-matrix T by

$$G = G_0 + G_0 T G_0, \tag{1}$$

and

$$T = V + V G_0 T. \tag{2}$$

The scattering matrix T describes the electron scattering by the self-consistent crystal potential V. The atomic configuration of the crystal comes in through T as is seen by the following expansion:

$$T(k, q, E) = \sum_l T_l(k, q, E) e^{i(\mathbf{q}-\mathbf{k})\cdot\mathbf{r}_l}, \tag{3}$$

with

$$T_l(k, q, E) = t_l(k, q, E) + \sum_{l' \neq l} \int t_l(k, p, E) G_0(p, E) \cdot T_{l'}(p, q, E) e^{i(\mathbf{p}-\mathbf{k})\cdot\mathbf{r}_{l'}} dp^3 + \ldots . \tag{4}$$

The higher terms result from multiple scattering due to 3, 4, and more atoms. T_l gives the electron scattering associated with the atom l. If a vacancy is present, then $l \neq V$, where V denotes the vacant lattice site. t_l results from V_l neglecting the crystalline environment of the ion l, and T_l results if the multiple electron scattering involving the

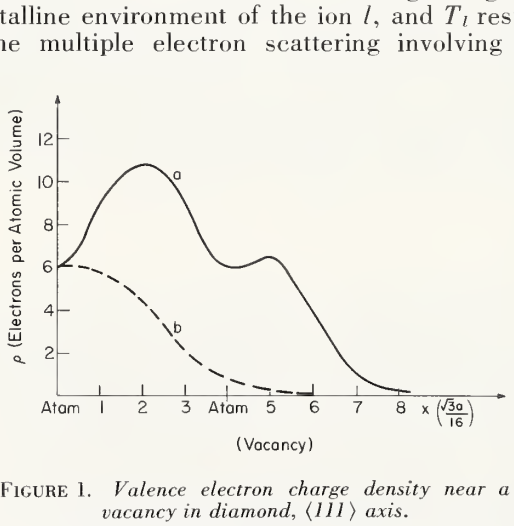

FIGURE 1. *Valence electron charge density near a vacancy in diamond, ⟨111⟩ axis.*
Curve "a" refers to the perfect crystal, and "b" to a crystal with a vacancy. Distance is measured in terms of the cubic lattice parameter, a.

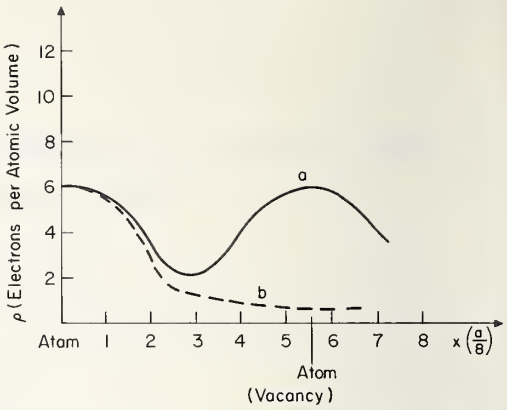

FIGURE 2. *Valence electron charge density near a vacancy in diamond, ⟨1–10⟩ axis.*
Curve "a" refers to the perfect crystal, and "b" to a crystal with a vacancy. Distance is measured in terms of the cubic lattice parameter, a.

surrounding lattice atoms of the atom l is taken into account.

From T the electron distribution in the vicinity of the vacancy is determined. Figure 1 shows the valence electron charge density along a ⟨111⟩-axis and figure 2 shows the charge density at the vacancy along a ⟨1, −1, 0⟩-axis. The lattice relaxation has been neglected (which probably leads at most to about 10% corrections). These calculations shed some light on the validity of the often used concepts of dangling covalent bonds, of stretching covalent bonds, and of reforming covalent bonds from the four electrons in the broken covalent bonds. The results indicate the strong deviation from spherical symmetry of the potentials at the nearest neighbor lattice sites of the vacancy and suggest that a point ion approximation and a dielectric screening treatment, neglecting *local field corrections*, are bound to be poor approximations for such strong lattice perturbations as given by a vacancy.

After having determined the crystal potential the localized states in the resulting crystal potential at the vacancy are given by the poles of the T-matrix. To obtain the localized states within the forbidden gap we look for the poles of

$$T(E) = V G_0(E) T(E). \tag{5}$$

In determining the poles of $T_{l_0}(E)$ it is necessary to take into account the poles associated with the other three $T_{l_0}(E)$ which appear for the same energies E for symmetry reasons. Such a self-consistent determination of the poles is probably equivalent to configuration interaction. However, contrary to configuration interaction such a self-consistent procedure does not lift the degeneracy of the localized states at the four nearest neighbors. This might happen via Jahn-Teller lattice distortion. If the wave functions associated with the before-mentioned localized states do not overlap, then it is also possible that this degeneracy just persists

(see degeneracy of 1s core electrons, ϵ_{1s} same for each atom). It follows that the spectrum of bound states is approximately given by

$$1-\frac{1}{\Omega}\sum_{p} V_{l_0}(k,\,p)\,G_0(p,E)$$

$$-\frac{1}{\Omega}\sum_{p,\,l'} e^{i(\mathbf{p}-\mathbf{k})\cdot R_{l'l}} V_{l'}(k,\,p)\,G_0(p,E)=0 \qquad (6)$$

if (a) the potential V is highly localized in real space and if (b) the Fourier transformed potential is sharply peaked, which case is adequate for shallow bound states described by the effective mass approximation. Using eq (6) the spectrum of bound states is determined. The results are given in figure 3. Notice please, that the top of the valence band refers to the crystal point symmetry Γ_{25} and the bottom of the conduction electron band to Γ_{15}. The symmetry of the bound states is $E_1(l=0)$: $E_2(l=1)$: $E_3(l=2)$: $E_4(l=3)$.

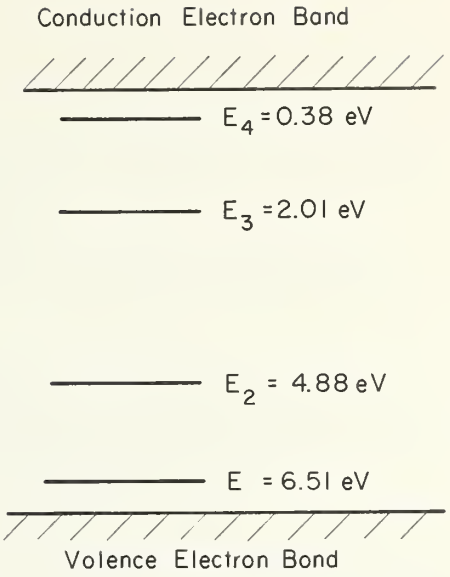

FIGURE 3. *Energy spectrum of bound states at a vacancy in diamond.*

3. Charged Vacancy

The vacancy might trap electrons in the localized states and also might release electrons from the broken covalent bonds to the conduction band and become charged in this way. It would be nice to get these charged vacancy states from the theory, without introducing explicitly wave functions for the electrons in the localized states. This can be done if one performs a self-consistent (bootstrap-like) calculation taking carefully into account the localized states in determining the crystal potential which gives rise to the bound states.

Charged vacancies and also neutral vacancies might be in paramagnetic states. They act then like paramagnetic impurities having an exchange interaction with the conduction electrons. Therefore paramagnetic vacancies should give rise to anomalous conduction electron scattering (Kondo Effect) possibly exhibited in resistivity, magnetoresistivity, magnetic nuclear relaxation rate, etc. Possibly the observed anomalies in the conductance of semiconductor-oxide-metal junctions are due to anomalous electron exchange scattering from vacancy-like paramagnetic defects in the interface of semiconductors and oxide. As will be shown in detail in another paper these paramagnetic defects in semiconductors and their interaction with conduction electrons can be treated very elegantly by using Anderson's Hamiltonian used in connection with localized magnetic moments in metals. With respect to the optical properties of the vacancy one should notice that the exchange scattering of the electrons involves spin flips and therefore the selection rule $\Delta S=0$ for optical transitions is no longer valid for paramagnetic vacancies.

It would be of considerable interest to include electron-phonon interaction in the theory. This will be of importance, for example, in determining the lifetime of the higher excited bound states at defects in semiconductors.

It is hoped that the large contrast between the previous theories and the one proposed here will help in the study of the shortcomings and limitations of the existing theories.

4. References

[1] C. A. Coulson and H. J. Kearsley, Proc. Roy. Soc., **A241**, 433 (1957).

[2] T. Yamaguchi, J. Phys. Soc. Japan **17**, 1359 (1962).

[3] Stoneham, preprint (Harwell, 1966).

Energy Levels Associated with Isolated Vacancies in Silicon*

Joseph Callaway

Department of Physics, University of California, Riverside, Calif. 92507

and

A. James Hughes

Applied Research Laboratory, Aeronutronic Division of Philco Corporation, Newport Beach, Calif. 92660

The energy levels of bound electronic states associated with defects in semiconductors can be studied through the use of methods based on scattering theory [1]. The approach is most useful for the consideration of levels lying deep within the band gap for which the usual effective mass theory is not valid. As an example of the use of this technique, we have investigated the bound states associated with vacancies in silicon.

The energy levels of interest are the roots of the equation $\det(I-GV)=0$ which lie in the band gap, in which I is a unit matrix, V is the matrix representing the perturbing potential, and G is the matrix $(E-H_0)^{-1}$ usually called the Green's function matrix. These matrices are referred to a basis of Wannier functions characterized by band and site indices. The Green's functions are obtained by numerical integration using energy bands calculated by Brust [2]. The lowest eight bands were considered. The perturbing potential is taken to be the negative of the contribution to the usual pseudopotential from a single atomic site. Formulas have been developed to enable the calculation of matrix elements of the perturbation directly from results of a pseudopotential band calculation. As a byproduct of this work some interesting results concerning the symmetries of Wannier functions have been obtained.

*Supported in part by the Air Force Cambridge Research Laboratories.

References

[1] J. Callaway, J. Math. Phys. **5**, 783 (1964).

[2] D. Brust, Phys. Rev. **134**, A1337 (1964). We are indebted to Dr. Brust for furnishing us numerical tables of energy bands.

Electron Trapping as a Function of Normal Modes

A. M. Lemos*

Adelphi University, Garden City, New York 11530

Within the framework of the "adiabatic-harmonic" approximation there exists a unique set of normal lattice coordinates corresponding to each bound F-center electron state. This is due to the one to one correspondence between electron state and lattice equilibrium configuration. The various sets of normal coordinates are related to one another by means of unitary transformations. The transformation matrices depend on the lattice equilibrium configurations which in turn are functions of the F-center electron state.

In the first portion of this paper, the matrices defining the transformation between two arbitrary, different sets of normal coordinates are developed. The unitary properties are then established. From these results it can be seen that given a set of normal coordinates corresponding to a particular F-center state, one may generate the spectrum of different sets by successive applications of unitary transformations. In this sense the ground state normal coordinates can be used as a basis set.

In the second part of this paper, the transformation matrices developed in part 1, are used to express the electron trapping energy [1][1] for any bound state F-center transition in terms of phonon eigenfrequencies and a basis set of normal coordinates. This formulation is quite general. It includes degenerate and nondegenerate modes and does not require the solution of Feynman-Hellman [2,3] integrals. This is in contrast to previous work [1].

As a result of bound state F-center electron transitions, phonons are stored in the various lattice modes. From the trapping energy the number of phonons stored in these modes is determined. Only Frank-Condon transitions are considered. General expressions are then developed for the Huang-Rhys [4] factors in terms of the number of stored phonons. It is shown that in general the Huang-Rhys factors are *not* equal to the number of stored phonons. The factors for absorption and emission of light by deep electron traps are compared with the corresponding expressions in a recent publication [5]. The factors developed here are quadratic polynomials in Δ, the distortion parameter. The zeroth order term is exactly the form previously published. Therefore the present formulation for the Huang-Rhys factors includes the previous ones as a special case. The last item developed in this section is a general expression for the Stokes Shift. The Shift is shown to be a function of stored phonons and phonon eigenfrequencies.

In the third part of the paper, the general expressions developed in the previous two sections are specialized to the tight binding model of the F-center in the alkali halides. We have assumed that both the adsorption and emission F-bands are essentially due to electronic transitions between two bound states. The states are "s-like" in the ground state and "p-like" in the excited state. The local lattice symmetry is O_h in the "s-like" state and D_{4h} in the "p-like" state. The unitary transformation matrices are displayed for this system. The recent experimental results of Gebhardt and Kuhnert [6] and the theoretical results of Wood and Joy [7] have been used in carrying out the numerical calculations. From their work and our analysis it was found that an effective mode approximation was in order. This was the A_{1g} mode of the O_h group (for the "s-like" state) and the A_{1g} mode of the D_{4h} group (for the "p-like" state). Since the F-center electronic charge distribution is a function of state, then clearly the electron-phonon interaction should also depend on the F-center electron state. In a conventional one dimensional configuration coordinate scheme, this fact is not considered. In an attempt to use the one dimensional (single mode approximation) scheme and yet to account for the difference in electron-phonon interactions we have introduced effective ion masses for each state. The formulation is completely consistent and in addition has precedence in the work of Williams [8], Klick [9], and Luty [10].

On this basis we have calculated numerical results for the number of phonons stored in the "p-like" and "s-like" states of the lattice, the Huang-Rhys factors for absorption and emission and the Stokes Shift. The specific alkali halides considered were NaCl, KCl, and KBr. These were the only crystals for which compatible absorption, emission and "distortion-parameter" data are available. The results of the computation are displayed in table 1. In this table the first column, $R_{\text{eff.}}$, is the ratio of the ground state to the excited state effective alkali ion mass: the second column is the sum of

*Work supported in part by the National Aeronautics and Space Administration.

[1] Figures in brackets indicate the literature references at the end of this paper.

Table 1

	$R_{eff.}$	$\Sigma(\Delta X_k)^2$	$N_{cal}(p)$	$N_{exp}(p)$	$S_{cal}(a)$	$N_{cal}(s)$	$N_{exp}(s)$	$S_{cal}(e)$	ΔE_{cal}	ΔE_{exp}
		Å							*eV*	*eV*
NaCl	1.97	0.659	20.7	28.8	27.8	30.6	42.5	25.4	1.085	1.695
KCl	2.81	.664	21.4	24.6	33.2	39.0	45.0	25.3	0.900	1.098
KBr	2.00	.710	25.3	28.0	34.2	37.8	41.6	28.2	0.846	1.148

the squares of the equilibrium displacements as measured in the "*p*-like" and "*s*-like" state; the third and fourth columns ($N_{cal}(p)$ and $N_{exp}(p)$) are the calculated and experimental values for the number of phonons stored in the "*p*-like" state of the lattice: the fifth and eighth columns ($S_{cal}(a)$ and $S_{cal}(e)$ are the calculated values for the emission and absorption Huang-Rhys factors: the sixth and seventh columns ($N_{cal}(s)$ and $N_{exp}(s)$) are the calculated and experimental values for the number of phonons stored in the "*s*-like" state of the lattice: the ninth and tenth columns ΔE_{cal} and ΔE_{exp} represent the calculated and experimental values for the Stokes Shift. The experimental results are obtained from the recent work of Gebhardt and Kuhnert. Since there appears to be an inconsistency in their interpretation of the Huang-Rhys factors, we did not include in the table any experimental results for *S*. However the values that appear in most publications is 30 ± 5. With the exception of the Stokes Shift the agreement with the experimental results is surprisingly good. The treatment while sophisticated in its general form, is quite crude in the actual numerical calculation. While a tight binding approximation might be reasonable for the "*s*-like" ground state, it is certainly suspect in the case of the relaxed "*p*-like" excited state. This is because in the "*p*-like" state the electronic charge distribution apparently spreads over several lattice parameters. Hence one would expect that the localized approximation of the *F*-center electron-phonon interaction would break down. In addition we have used a one-mode scheme which we do not believe is correct. Recent work supports this contention. It is our opinion that the basic reason for the discrepancy in the Stokes Shift is due to the fact that not all of the significant modes were accounted for. This means that "in effect" we were using a one-dimensional configuration coordinate approximation. In such a scheme there seems to be no consistent way of interpreting both absorption and emission data.

Wood and co-workers have been reformulating some of their previous work. A significant variation in this calculation of the distortion parameters would introduce other modes into our calculation.

Although we have restricted our numerical calculation to the *F*-center, the general equations we have developed hold for any deep electronic or hole trap in the alkali halides. One problem in which we are presently interested in the determination of the entries in table 1 for the system KCl:Tl. Although the Thallium ion is large, apparently its charge distribution is quite localized. This means that this system is probably amenable to our tight binding scheme of approximation.

References

[1] Markham J. J., Rev. Mod. Phys. **31**, 956 (1959).
[2] Feynman R. P., Phys. Rev. **56**, 340 (1939).
[3] Hellman H., Einfuhrung in die Quanten Chemie, p. 285. Teuber, Leipzig (1937).
[4] Huang K. and Rhys A., Proc. Roy. Soc. (London) **A204**, 406 (1950).
[5] Lemos A. M. and Markham J. J., J. Phys. Chem. Solids **26**, 1937 (1965).
[6] Gebhardt and Kuhnert H., Phys. Letters (Netherlands) **11**, 15 (1964).
[7] Wood R. F. and Joy H. W., Phys. Rev. **136**, A451 (1964).
[8] Williams F. E., Phys. Rev. **82**, 281 (1951).
[9] Klick C. C., Phys. Rev. **85**, 154 (1952).
[10] Luty F. and Gebhardt W., Z. Physik **169**, 475 (1962).

Electronic Properties of Point Defects in Solids.

Report of the Panel II Discussion

J. A. Krumhansl

Department of Physics, Clarendon Laboratory, Oxford University, Oxford, England

(Panel Members: F. Blatt, W. B. Fowler, N. H. March, and R. Wood)

1. Introduction

The topics discussed by this panel dealt primarily with the theory of and concepts regarding electrons, considerations which underlie much of our understanding of the properties of defects.

The panel I discussion presented in some detail how defect structures and their configurational dynamics may be determined from ionic and electronic properties, so reference to specific systems was not the primary concern of panel II. Rather, it seemed appropriate to develop some perspective regarding the limits or relevance of current descriptions of electronic properties.

In subject matter, the material falls naturally into divisions: materials (metals or insulators), individual defects, defect interactions. In examining the electronic properties (particularly in nonmetals) one frequently studies the excited (electronic) states with the atomic configuration fixed. This, it is to be recognized, is different than the primary concern in studying "energies and configurations"—for in this latter case it is almost invariably implicit that the electronic configuration assumes its lowest energy.

This differentiation is worth emphasizing as it is quite possible that an approximation method suitable for one purpose may not suffice for the other; we probably can always do much better in computing elementary excitations from some ground state than we can in determining the absolute energies or configurations starting from some remote standard state in many body configuration space. Again, one should recall the comments by Vineyard [sec. 3, Panel I] on this configuration space description; the point of the present remarks is that there obviously are not only the nuclear coordinates R_1, R_2, . . ., but also all of the electronic coordinates $\underline{r}_1, \underline{r}_2, \ldots$. It is remarkable that frequently [e.g., in the case of electronic polarization] one can rather successfully account for the electronic system by relatively few parameters such as the electronic moment μ or Fermi wave number K_F in the computation of configurations and energy. The principal reason for this must be that in many systems the electronic structure is strongly determined by factors other than the specific ion locations, e.g., core potentials in ionic insulators, or valence electron-densities in good metals. Based on this observation one may expect that by contrast the situation in covalent small band gap semiconductors or semimetals is rather more complex; this seems to be the case.

2. Particular Problems

The subject of electronic properties is vast; what is of concern in the present summary are particular topics which received discussion in relation to defects. For nonmetals these were: electronic contributions to ion pair interactions, the ground electronic and excited electronic states of point defects, and the coupling of lattice motion and electronic configurations. In the case of metals the principal topics were: ion-electron interactions, defect-electron gas interactions, charge distribution around a point defect, scattering by a point defect, energy of formation of defects, and defect-defect interaction. We proceed to note some of the main points.

3. Nonmetals

The electronic contributions to ionic interactions have been discussed at length over the years, and tests of the better known models appeared in many of the conference papers, particularly those of Boswarva and Lidiard, Franklin, Tosi, and Doyama. Since this topic has already been discussed extensively by Lidiard in reporting on Panel I, and has received particularly thorough examination in relat-

ing theory and experiment for phonon spectra we are now reasonably convinced that in the regime of small displacements from the normal equilibrium positions the electronic polarization contributions to potential, particularly at long range, are well described by a few "electronic" degrees of freedom, which might for example be the dominant terms in a perturbation expansion. However, it is unlikely that the short range potentials can be developed similarly from first principles beyond the Slater-Morse work. Nor is it likely that an extensive machine calculation of ion pair electronic configurations at short range could give much more than qualitation information for obviously the symmetry of the interactions must play an important role. Thus when defects are not at symmetry sites the use of simple phenomenological potentials is something of an act of blind faith; perhaps this effect already appears in Franklin's findings for CaF_2. However, no further light was shed on this question in conference discussion.

The electronic states of defects in nonmetals have received most attention in alkali halides and especially for color centers. The papers by Wood and by Fowler, together with their panel remarks, comprise complementary views. On the one hand it must be recognized, as demonstrated by the Wood and Gilbert calculation of the effective force constants for motion of the neighbors around a *U*-center, that it is in fact possible to compute successfully a substantial amount about the electronic excitation and lattice coupling for these centers. To this extent the last few years have led to physically meaningful improvements in previous computations—including some ideas on autoionization of excited states and related questions for tightly bound excitons. On the other hand it is not amiss to recognize that one must always examine and reexamine how much credit should go to the calculation and how much to the appropriateness of the physical assumptions underlying the computer approach. The nonuniqueness begins already with the models, as emphasized by Fowler in his paper on the "use and misuse" of them. In the panel discussion he summarized his views, and I will attempt to paraphrase them.

Fowler again draws attention to the fact that there are two types of approximations in theoretical physics, (1) physical, and (2) mathematical. By "physical" is meant approximations which a theorist feels will not do too very great injustice to nature. [The role of close contact between experiment and theory is all important in this respect.] Once the physical chaff is eliminated the solution of the resulting problem invariably calls for some mathematical approximations, and here is where large computational capacity has allowed new gains. But it is all too easy to abuse the physics then and carry 10 percent models to five decimal place accuracy. One could not help but have a feeling that this danger did exist in many of the present day calculations.

I do not interpret these views, which are mine also, to mean that no more calculations on *F*-center systems should be done, but rather careful attention should be given to whether it is more important to call in a computer for extensive Hartree-Fock computations or to focus attention on the simpler of the known many body contributions to correlation and polarization. Ideally an analysis which involves extensive computation should make direct contact both with *other* theory and with experiments. This is what appeals to me about the Wood and Gilbert work; in this case both the theory of localized lattice vibrations, and experimental studies of optical properties of *U*-centers have led to estimates of the force constants—the results have considerable value.

4. Metals

In passing on to metals, it is useful to compare the dominant electronic factors with those for nonmetals. The essential point is, of course, that in the electronic phenomena just treated a "localized" basis for electron states was implicit, and usually only a few electrons were involved at one time [e.g., in localizing electronic polarization, ion by ion]. By contrast, in metals the electronic behavior, frequently collective, of the conduction electrons dominate.

Again there is a long history. The summary by Huntington together with March's paper accompanying his Panel III remarks cover the traditional approaches quite completely, showing that a number of point defect properties are given quite well in leading approximation by one-electron theory in the Hartree-Fock sense, neglecting band structure effects. However, developments in three aspects have supplemented the traditional quantum mechanical methods and may be examined in the context of the point defect problem: (i) dielectric response properties of the interacting electron gas, (ii) psuedopotential methods, (iii) introduction of real band structure corrections to the isotropic electron gas. March discussed various aspects of (i); unfortunately there was too little discussion of (ii), but (iii) received considerable discussion by Seeger and Mann, and by Mozer. Again, we attempt here briefly to develop relations between these several aspects.

First of all, there are good physical reasons why a number of the properties in metals are interrelated. This has become apparent from dielectric response concepts and psuedopotentials. From these studies we recognize that two complex parts of the electron dynamics, namely, the collective properties of the electron gas and the strong interactions between the conduction electrons and the ion cores (both many electron effects), may for many purposes be replaced by effective one-elec-

tron potentials. If at the same time the ion core—ion core interactions are represented by a suitable phenomenological potential, the following may be seen:

(1) When a point test charge is introduced into the lattice, the conduction electron gas responds and a particular charge or potential distribution is set up around the defect [Friedel; Vosko et al., March]. A prominent feature is the oscillating character of the potential.

(2) Closely related is the effective potential which the conduction electrons see around a lattice ion for forming one electron Bloch states, in other words the pseudopotential. Regarding the ion core as a charge immersed in a responding electron gas, the long range (small q) part of the potential may be closely approximated from (i). The short range part reflects the physical difference between a test charge and the electrons of the core which may exchange with the conduction electrons; in the Hartree-Fock approximation this leads to the famous cancellation effects developed by Cohen and Heine. Thus the pseudopotential and the potential found in (i) may differ inside of an ion core radius (or at large q in momentum space), but obviously over much of the range the pseudopotential and test charge potential in the electron gas are similar.

(3) Taking this view one step further one may develop an effective interaction potential between a pair of ions by simply computing the energy of one charged ion in the polarized charge distribution due to the other. We may expect this to be most in error for close approach of the ions. In at least two applications this effective potential seems to be a sensible one: first, the structure factors in liquid metals as analyzed by March et al., are in fair agreement with this theory; second; phonon frequencies as estimated by this method [Cochran; Harrison; Shom and Ziman; Vosko, Taylor and Keech] show very good consistency. While not exactly given by the pseudopotential for electrons the relationship is sufficiently close that electron band structure information may thus be used to estimate this ion—ion interaction, except at short ranges.

(4) Still another obviously related quantity is that contribution to a point defect formation energy which derives from a rearrangement of the conduction electron gas. Neglecting band structure effects, and to first order in perturbation theory, this may be shown again to depend on the long wavelength limit of the polarization potential: March discusses this in some detail in his paper.

Of course, what the contributors to this viewpoint have emphasized is that the electron gas responds to probes in a characteristic manner whose features are very similar whether the probe be a test charge, an ion core, an ion pair, a point defect, or a phonon displacement of the ions. Any one of these probes may thus be used to characterize the electron gas to a very good first approximation. Moreover, there are some cross-relations to be expected; one example is that between Debye temperature and vacancy formation energy as proposed by Mukherjee and interpreted by March.

To a large extent these considerations, though relatively recent, were assumed by the conference as established and were not really discussed at great length. However, in several aspects we know that improvements are needed.

First of all there are the explicitly many-body corrections to the dielectric response function; these are very difficult to handle beyond the random phase approximation; fortunately, for small q they may perhaps be small enough to neglect. No discussion of this matter was attempted, since it seems apparent that other effects will produce the more important corrections to the linear screening—perturbation approximation. For instance, it is probable that the Born approximation fails seriously as the defect charge ΔZ increases, and band structure effects require consideration as well.

As long as the effective mass dynamics are ignored one may still go beyond the Born approximation by doing a phase shift analysis along the lines developed by Friedel, care being taken to conserve charge through an appropriate sum rule. Indeed, it is to be expected that as ΔZ increases neither the defect resistivity nor the formation energy will vary linearly with ΔZ.

Mathematically, the phase shift method is computable in principle for arbitrary ΔZ, for a spherical potential. However, as soon as effective mass dynamics are introduced the differential equation defining the electron wave function no longer has spherical symmetry and a partial wave analysis becomes intractable. It is here that the integral equation method, i.e., electron Green's functions developed by Mozer and by Seeger and Mann, can be applied. Not only can one easily go beyond the Born approximation, but also the explicit effects of anisotropy appear. In fact, with regard to the latter the results of Mann and Seeger show that in some crystalline directions the charge around a defect falls off quite differently than predicted for the perturbed free electron gas. That this should happen for some electrons is not surprising, but is indeed expected. However, that the portions of the electron energy surfaces giving rise to such effects should have sufficient measure to modify the asymptotic radial dependence of the net charge in an essential way is really surprising. Further assessment of these anisotropic effects is in order, both experimentally and theoretically.

However, returning to the strong defect properties, whether it is eventually found that the mathematics is best done by phase shift or by electron Green's function methods, it seems that clear that an extension beyond the linear screening theory is necessary in such cases as vacancies in polyvalent metals, etc. I am indebted to Frank Blatt for his detailed comments on this point and now quote them.

256-724 O-67—10

"The formalism developed by Seeger and Mann and phase-shift calculations are not entirely unrelated; indeed the connection between the two approaches was indicated by Professor Seeger in his talk. The Friedel sum on the phase shifts reappears in the Seeger method as a similar condition imposed on the matrix elements. Although at first glance it may appear that the Seeger method allows for fewer adjustable parameters than the phase-shift calculations, the freedom in the selection of a scattering potential (subject to the Friedel sum) in the latter, corresponds to a freedom in the choice of the relative magnitudes of the matrix elements in the former.

"As regards the calculation of Fukai, it seems to me highly improbable that the relatively large difference between calculated and observed resistivities due to vacancies in aluminum could be ascribed entirely to lattice distortion. In this connection I shall first permit myself a trivial comment concerning the formal expression used in Fukai's calculation. It is only in the free-electron approximation that the Fermi energy appears as indicated by him. What should properly enter is the Fermi velocity, that is, one should use

$$\rho=\left[-\frac{1}{3}V_F^2\int\tau(\epsilon)\frac{\partial f}{\partial\epsilon}\,d\epsilon\right]^{-1}$$

where ϵ is the energy relative to the Fermi energy and V_F the Fermi velocity.

"Second, we must bear in mind that although a scattering potential derived from the pseudopotential method is undoubtedly superior to various crude alternatives that have been employed in the past, the calculation relies on the Born approximation. E. Stern, in a recent paper, showed that a perturbation approach is appropriate only if the screening charge about the imperfection is small compared to the ionic charge, and that when the charges are of equal magnitude, perturbation theory cannot be justified. In the aluminum problem, a perturbation approach may be expected, therefore, to yield reasonably good results for divalent and quadrivalent impurities. In the case of vacancies in aluminum, however, the perturbation method is unreliable. Though past experience indicates that the Born approximation over—rather than underestimates the scattering cross section, it is conceivable that in the present instance the situation might be reversed.

"Finally, in the one case where Fukai as well as Harrison have calculated residual resistivities, namely Zn in Al, the results differ by 60 percent. This clearly points out the sensitivity of the calculated results to the details of the assumed pseudopotentials (Harrison and Fukai used different pseudopotentials). There now exists a variety of data on the influence of impurities on electronic properties of metals, for example, residual resistivity $\Delta\rho$, change in thermopower ΔS, and Knight Shift ΔH. Since the scattering phase shifts appear in linearly independent combinations in the expressions for $\Delta\rho$, ΔS, and it would be interesting to approach the problem of impurity potentials empirically by requiring that the phase shifts conform with the experimental data. One could then construct an impurity potential of reasonable shape which is consistent with these phase shifts and compare this empirical potential to that derived from the pseudopotential method. This is a program in which we are currently engaged."

Similar conclusions are reached by March, on different evidence [see his discussion], so we conclude that the matter of charge distributions and potentials around strong defects is still an open question. Perhaps this was the most quantitatively supported result in Panel III.

5. A Survey of Quantum Formalism for Solids

It may serve a useful purpose to walk through the paths which one follows in applying quantum theory to the problems we have just discussed. We begin with the Hamiltonian

$$H=H_{\text{elec.}}+H_{\text{nucl.}}+H_{\text{interaction electrons-nuclei}}$$

then a series of steps follow:

(1) Nuclear and electronic motions are separated via the Born-Oppenheimer (B.O.) approximation:

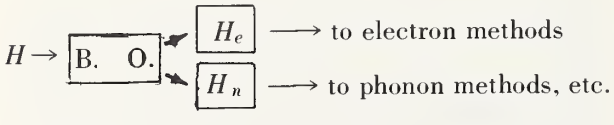

Subsequently H_n may be used to describe phonons, defect vibrational modes, configuration coordinates, etc.; these excitations must eventually be coupled back to the electronic excitations as the B.O. separation is only approximate. Thus vibrionic states at defects and electron-phonon interactions generally are subsequently introduced as corrections to B.O.

(2) Proceeding with H_e, the next filtering is that the optimum reduction to a one-electron language is carried out via the Hartree-Fock method:

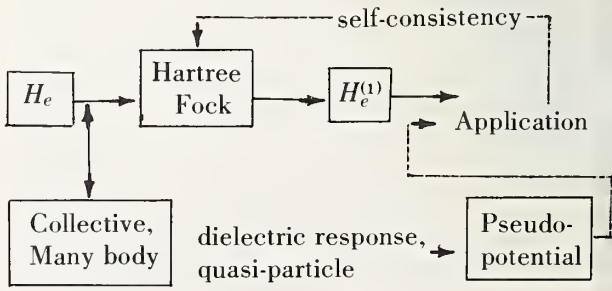

The collective and many body effects may be partly accounted for by dielectric response functions, and through the device of quasi-particle generalization of the Hartree-Fock excitations.

(1) The most direct way for dealing with the electrons in the normal solid seems to be through the OPW method. The inner shells, i.e., core states, are understood to be filled using atomic orbitals. By orthogonalizing plane waves (OPW) to these core states and reintroducing some electron gas polarization, i.e., screening, corrections a pseudo-Hamiltonian $H_e^{(1)}{}_{\text{pseudo}}$ is formed

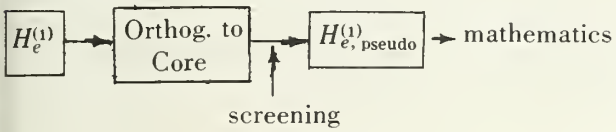

(2) There is now a choice of mathematics: (a) The plane wave approximation; it yields no band structure but can be used as first approximation to energetics, resistivity, etc. for good metals. (b) The linear combination of OPW, i.e., LCOPW, which has been developed extensively by Harrison, Heine, and Cohen; this yields Bloch functions and band structure behavior. Thus the story for the normal solid is usually completed:

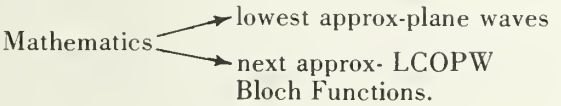

(3) The above is next used as a basis for treating a point defect. In the case of insulators the subsequent steps are somewhat better defined than for metals, and are summarized in Wood's work. In the case of metals the choice of methodology is not so clear, and in fact is just where questions are currently open, so we indicate what might be done for a point defect in a good metal.

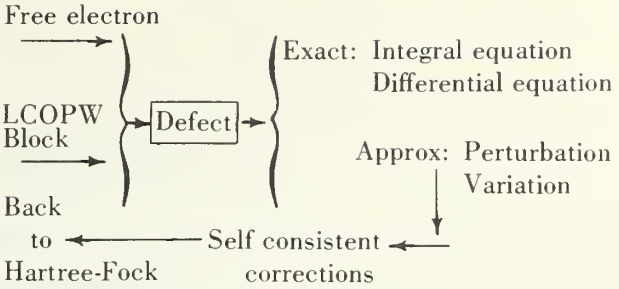

The several approaches possible are:

(a) If the free electron basis is used a partial wave analysis may be used to study the charge around the defect i.e., phase shifts, Friedel sum rule, etc. This approach has been explored much by Friedel and by March and their co-workers.

(b) Perturbation methods may be used in either basis if the defect is not a strong scatterer, i.e., the first Born approximation is valid.

(c) If the defect is a strong scattering center for the conduction electrons, in view of the wide use and development of Green's function methods there seems to be no excuse for not using these as Mozer, and Seeger and Mann have indicated. Not only is this integral equation approach easily capable of dealing with the strong scattering case, it also furnishes a direct way of dealing with the anisotropy of real Bloch states. Of course as yet we do not have nearly as extensive experience in making the always-necessary approximations here, as in the differential form of the Schrödinger representation: no doubt this will develop rapidly as more calculations on real metals are done.

In conclusion, I take pleasure in acknowledging the comments and views of the other panelists, and make the usual apologies for unintended inclusions or omissions. One last detail—I have not referenced this conference report as all of the references are either well known or to be found in the conference papers.

III. Vibrational States

Phase-Shift Analysis of the Scattering of Lattice Vibrations by Localized Perturbation

G. Toulouse and J. Friedel

Laboratoire de Physique des Solides associé au C.N.R.S., Faculté des Sciences, 91-Orsay, France

The scattering of lattice vibrations by localized perturbations is considered here in its similarity with the scattering of electrons in metals. A phase-shift analysis enables one to obtain in a direct way the perturbed energy density of modes, and consequently, the additive thermodynamic functions such as the zero-point energy [1].[1] Further, the vibration amplitudes and phases on the defect are shown to be simply related to the asymptotic phase shifts of formal scattering theory.

The relevance of this analysis to the interpretation of optical properties of defects in ionic solids (vibrational structure, isotope shifts) when one wants to go beyond the simple "one configuration coordinate approximation" is particularly stressed, but these methods might also be of value for the discussion of other physical properties of defects.

The one-component linear chain is first considered, as it permits one to get various general results on a fully tractable model. Considerations concerning the electron-phonon coupling contribution to elastic terms in the vicinity of defects are developed (1).

The extension to three-dimensions is made for simple cubic lattices with nearest neighbor central and noncentral forces, which enables one to separate the polarization complication from the "extended defect" complication. By "extended defect complication," we mean the complication which arises from the fact that one irreducible representation of the point group of the defect may appear several times in the reduction of the perturbation matrix (2).

Application is made of the general concepts to the mass defect and to the vacancy problems in very simple models (3).

1. The One-Component Linear Chain [2]

The model which will be discussed consists of a chain of atoms of identical mass M and force constant λ containing an impurity atom of different mass $M(1+\beta)$ coupled to its two neighbors by different force constants, $\lambda(1+\gamma)$.

$$\underset{M}{\lambda}\quad\underset{M}{\lambda(1+\gamma)}\quad\underset{M(1+\beta)}{\lambda(1+\gamma)}\quad\underset{M}{\lambda}\quad\underset{M}{\lambda}$$

The unperturbed "crystal," with nearest neighbor forces, has the following dispersion relation

$$\omega=\omega_L \sin\frac{qa}{2} \text{ with } \omega_L^2=\frac{4\lambda}{M} \text{ and } 0<qa<\pi;$$

the unperturbed energy density of modes per atom is given by:

$$n_0(\omega)=\frac{2}{\pi\,\omega_L\cos\left(\frac{qa}{2}\right)}.$$

1.1. Eigen Modes

The eigen modes of the perturbed system can be separated by symmetry into even and odd modes, with the following asymptotic expressions for the displacements of the nth atom which are exact in the unperturbed region of the chain:

$$\begin{cases} u_n=A\sin\left(q|n|a+\delta_0\right)=-u_{-n}, & n>0 \\ v_n=A\sin\left(q|n|a-\dfrac{\pi}{2}+\delta_1\right)=v_{-n}. \end{cases}$$

After some algebra, one finds for the phase shifts δ_0 and δ_1

$$\begin{cases} \operatorname{tg}\delta_0=-\dfrac{\gamma\sin(qa)}{1+\gamma\cos(qa)}, \\ \operatorname{tg}\delta_1=\operatorname{tg}\left(\dfrac{qa}{2}\right)\left[\dfrac{(1+\beta)(\gamma\cos(qa)+1)-(1+\gamma)}{\gamma(1+\beta)(1-\cos(qa))+(1+\gamma)}\right]. \end{cases}$$

The energy of a perturbed mode is still given by $\omega=\omega_L\sin\left(\frac{qa}{2}\right)$, with (qa) to be determined by

[1] Figures in brackets indicate the literature references at the end of this paper.

boundary conditions. For instance, with the boundary condition u_N, $v_N = 0$, we get:

$$\begin{cases} N(qa) + \delta_0 = \pi s, \\ N(qa) + \delta_1 = \pi s + \dfrac{\pi}{2}\cdot \end{cases} \qquad (s \text{ is an integer.})$$

The phase-shifts δ_0 and δ_1 are zero for the unperturbed crystal.

The vibration amplitude of the "pulsating mode" on the defect has a simple dependence on δ_0:

$$\overrightarrow{-1}\ \ 0\ \ \overleftarrow{+1}$$

$$u_{-1} - u_1 = 2A \sin(qa + \delta_0) = \frac{2A}{\gamma} \sin \delta_0.$$

The vibration amplitude of the impurity atom depends on δ_1:

$$v_0 = -\frac{A}{1+\beta}\left[\cos \delta_1 + \sin \delta_1 \operatorname{cotg}\left(\frac{qa}{2}\right)\right]$$

$$= -\frac{A}{1+\beta}\frac{\sin\left(\dfrac{qa}{2} + \delta_1\right)}{\sin\left(\dfrac{qa}{2}\right)}.$$

The normalization condition $\sum_n M|u_n|^2 = 1$ determines the value of A [3].

The perturbed energy density of states $\nu(\omega) - \nu_0(\omega)$ is related to the derivative of the phase shift [4]:

$$\nu(\omega) - \nu_0(\omega) = \frac{1}{\pi}\frac{d\delta}{d\omega}, \text{ with } \delta = \delta_0 + \delta_1.$$

1.2. Behavior of the $\delta_0(qa)$ and $\delta_1(qa)$ Phase-Shifts

From the Formula for tg δ_0, it appears that (see fig. 1):

(1) δ_0 is independent of β;

(2) for $\gamma > -1$ or $\lambda' = \lambda(1+\gamma) > 0$, δ_0 has the sign opposite to that of γ, and

$$\begin{cases} \delta_0 = 0 \text{ for } qa = 0, \\ \delta_0 = 0 \text{ or } -\pi \text{ for } qa = \pi \end{cases}$$

according as there is or there is not a localized mode of the same symmetry; the number of localized modes is given by the sum rule $N_0 = \dfrac{1}{\pi}[\delta_0(0) - \delta_0(\pi)]$:

(3) a localized mode appears only for a finite positive value of $\gamma(\gamma > 1)$;

(4) when there is a localized mode i.e., when $\delta_0(0) - \delta_0(\pi) = \pi$, the phase shift necessarily takes the value $\dfrac{\pi}{2}$ for one energy of the band continuum

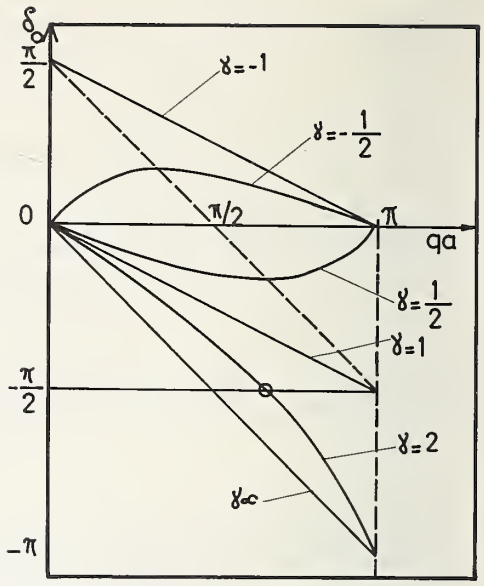

FIGURE 1. *Phase-Shift δ_0 for one-component linear chain.*

and there is a scattering antiresonance for this energy;

(5) for $\gamma = 1$, $\delta_0(\pi) = \dfrac{\pi}{2}$ because a localized mode is just appearing. By continuity, it is counted for half in the band continuum, for half as a localized state, and the sum rule is still valid;

(6) for $\gamma < -1$, $\delta_0(0) = \pi$ and it appears a localized mode of negative energy; the situation is unstable as it is obvious by direct inspection.

The phase-shift δ_1 depends on both β and γ (see figs. 2 and 3):

(1) $\delta_1 = 0$ for $qa = 0$; $\delta_1(\pi) = -\dfrac{\pi}{2}$ or $+\dfrac{\pi}{2}$, according as there is or there is not a localized mode (pushed to $\omega = \infty$ for $\beta = -1$);

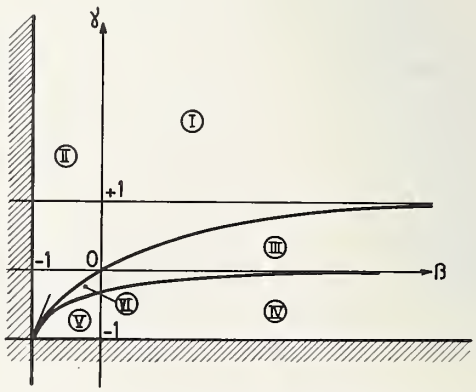

FIGURE 2. *Behavior regions for phase-shift δ_1 for the one-component linear chain.*

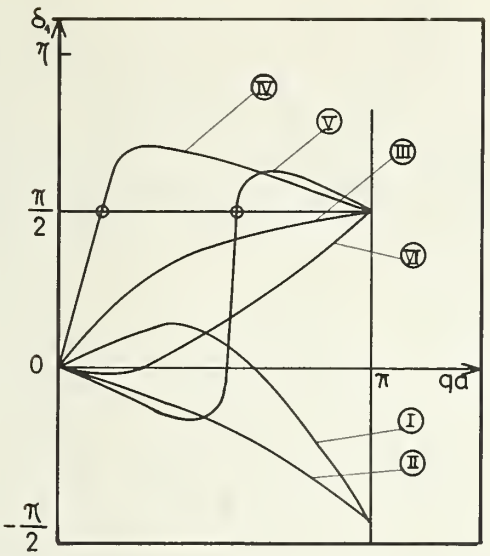

FIGURE 3. *Phase-shift* δ_1 *for one-component linear chain.*

(2) one can define in the plane β, γ (unphysical regions $\beta<-1$ and $\gamma<-1$ excluded) six regions, according to the following criteria (see fig. 2):

$$\begin{cases}\delta_1(\pi)=\pm\dfrac{\pi}{2}\text{ (localized mode),}\\ \delta_1 \text{ can or cannot take the value 0 in the band,}\\ \delta_1 \text{ can or cannot take the value } \dfrac{\pi}{2} \text{ in the band (resonance);}\end{cases}$$

(3) there are scattering resonances which can be very sharp, even in the region $\beta<0$;

(4) for $\gamma=0$ (mass defect), we are in regions (II), (III), there is no resonance and no zero.

The six regions are summarized in the following table:

	$\delta_1(\pi)/\pi/2$ [a]	zero	Resonance
I	−	Yes	No
II	−	No	No
III	+	No	No
IV	+	No	Yes
V	+	Yes	Yes
VI	+	Yes	No

[a] The fact that $\delta_1(\pi)=$ half integer number of π is general for the modes of that symmetry in one dimension. This is due to the fact that modes of even and odd symmetry alternate in such a way that a mode of symmetry 1 constitutes the edge of the band. Hence, the smallest perturbation β can substract this mode from the band and make it localized. In the sum rule language, these modes are counted for one half.

1.3. Scattering

A plane wave is scattered by this localized perturbation:

$$\begin{matrix}Ae^{-iq|n|a} & & Ae^{iq|n|a}.\\ \xrightarrow{\quad -n \quad} & 0 & \xrightarrow{\quad n \quad}\\ Be^{iq|n|a} & & Fe^{iq|n|a}\end{matrix}$$

If we define

$$D_0=\frac{F-B}{2}\text{ and }D_1=\frac{F+B}{2},$$

then we obtain

$$\frac{D_0}{A}=+ie^{i\delta_0}\sin\delta_0,\ \frac{D_1}{A}=ie^{i\delta_1}\sin\delta_1,$$

and we derive:

$$\begin{cases}\dfrac{B}{A}=ie^{i[\delta_0+\delta_1]}\sin(\delta_1-\delta_0),\\ \dfrac{F}{A}=e^{i[\delta+\delta_1]}\cos(\delta_1-\delta_0)-1,\\ \dfrac{G}{A}=\dfrac{A+F}{A}=e^{i[\delta_0+\delta_1]}\cos(\delta_1-\delta_0).\end{cases}$$

The vibration amplitude for the "pulsation" in this stationary scattering wave is

$$u_{-1}-u_1=-\frac{2D_0}{\gamma}=-\frac{2i}{\gamma}Ae^{i\delta_0}\sin\delta_0,$$

whereas the amplitudes of v_0 and u_1+u_{-1} are

$$\begin{cases}v_0=\dfrac{A}{1+\beta}e^{i\delta_1}\left[\cos\delta_1+\sin\delta_1\operatorname{cotg}\left(\dfrac{qa}{2}\right)\right],\\ u_1+u_{-1}=\dfrac{2A}{\gamma}e^{i\delta_1}\left[\left(\dfrac{1+\gamma}{1+\beta}\right)\left(\cos\delta_1\right.\right.\\ \qquad\left.\left.+\operatorname{cotg}\left(\dfrac{qa}{2}\right)\sin\delta_1\right)-\cos\delta_1\right].\end{cases}$$

If $\beta=-1$ (i.e., in the "vacancy case") $u_1+u_{-1}=2A\cos\delta_1$.

One can notice here that the phases of the various vibration amplitudes on the perturbed sites are shifted with respect to the incident wave: these mechanical phase-shifts are the phase-shifts which characterize the asymptotic form of the scattered waves and, thereby, the perturbed density of states. This appears to be valid as well in the 3 dimensional system. Another general fact which should be noticed is the homographic dependence of the phase shift's tangents on the perturbation constants, here β and γ; hence the phase shifts are monotonic functions of these variables.

1.4. Localized Modes (Bound States)

We have seen how the existence of localized modes can be inferred from the knowledge of the phase shift in the band continuum. We shall show now how one can extract quantitative information on localized modes from the phase-shifts.

In the scattering problem, the plane wave Ae^{iqna} gave rise to a scattered wave:

$$Be^{-iqna} \text{ with } \frac{B}{A}=ie^{i[\delta_0+\delta_1]}\sin(\delta_1-\delta_0).$$

A localized mode is a scattered wave without ingoing wave: this implies

$$e^{i\delta}\to\infty \text{ or } \operatorname{tg}\delta=-i.$$

The energy of the localized mode will be solution of

$$\operatorname{tg}\delta=f(qa)=f(\pi+i\theta)=-i, \text{ with } \omega=\omega_L\cosh\frac{\theta}{2}.$$

The phase-shifts δ_0 and δ_1 take the form

$$\begin{cases}\operatorname{tg}\delta_0=-i\dfrac{\gamma\sinh\theta}{1-\gamma\cosh\theta},\\ \operatorname{tg}\delta_1=-\dfrac{i}{\tanh\theta/2}\times\left[\dfrac{(1+\beta)(1-\gamma\cosh\theta)-(1+\gamma)}{\gamma(1+\beta)(1+\cosh\theta)+(1+\gamma)}\right].\end{cases}$$

1.5. Zero Point Energy

The phonon zero-point energy variation due to the defect, which is its self-energy, is given by:

$$\Delta E=-\frac{\hbar}{2\pi}\int_0^{\omega_L}\delta(\omega)d\omega+\sum_i\frac{1}{2}\hbar(\omega_i-\omega_L)$$

where the ω_i are the pulsations of the eventual localized modes. One obtains this formula directly by noticing that—for a localized mode, the pulsation variation is $\omega_i-\omega_L$ since the mode is substracted from the edge ω_L of the band—for the continuum modes, the q variation due to the perturbation is

$$dq=-\frac{\delta(\omega)}{Na}, \tag{1.1}$$

the mode density between q and $q+dq$ is $\frac{1}{\pi}Na\,dq$, and the corresponding energy variation is

$$\int_0^{\omega_2}\frac{1}{2}\hbar\frac{d\omega}{dq}\left(-\frac{\delta(\omega)}{Na}\right)\frac{Na}{\pi}dq=-\frac{\hbar}{2\pi}\int_0^{\omega_L}\delta(\omega)d\omega.$$

The quantity which is measured in an isotope shift optical experiment [5] is related to

$$G\Delta M\Delta\gamma=\frac{d^2\Delta E}{dM\,d\gamma}\times\Delta M\Delta\gamma,$$

where ΔM is the mass variation of impurity (or host) ions and $\Delta\gamma$ is the force constant modification (supposed small) due to the electronic excitation.[2]

We shall take as an example the "F center" defect model, with $M'=M(1+\beta)=0$. The localized level of infinite energy corresponding to the disparition of the u_0 variable will have no influence; taking account of the fact that δ depends only on $\frac{\omega}{\omega_L}$, one finds

$$\frac{d\Delta E}{dM}=-\frac{1}{2M}\Delta E,$$

$$\frac{d^2\Delta E}{dM\,d\gamma}=-\frac{1}{2M}\frac{d\Delta E}{d\gamma}=\frac{\hbar}{4\pi M}\int_0^{\omega_L}\frac{d\delta}{d\gamma}d\omega$$

$\frac{d\delta}{d\gamma}$ is negative, for any γ; if one admits that the force constant must be softer in the excited state, one finds a "red shift" contribution of the self-energy to the isotope shift when the host ions mass is diminished.

Moreover in the "F-center" model,

$$\frac{d\delta_1}{d\gamma}=0,\ \frac{d\delta_0}{d\gamma}=-\frac{1}{\gamma^2\sin qa}\times\sin^2\delta_0.$$

The contribution of the frequency band $(\omega,\ \omega+d\omega)$ to the self-energy shift is

$$G(\omega)\Delta M\Delta\gamma \text{ with } G(\omega)=-\frac{\hbar}{4\pi M}\times\frac{\sin^2\delta_0}{\gamma^2\sin qa}.$$

$G(\omega)$ is simply related to the vibration amplitude of the "pulsating mode" and to the one-phonon structure intensity which is considered now.

1.6. Vibrational Structure

As usually done, we explain the vibrational structure of optical transitions by introducing an electron-phonon interaction term linear in the ions' variables. This term shifts all the coordinates of the normal modes without changing their energy and makes nonorthogonal the n-phonon ground state wave functions and the n'-phonon excited state wave functions.

---

[2] One can notice that

$$\left\langle\sum_\alpha(u_0-u_{1\alpha})^2\right\rangle=\frac{Tr\left[e^{-\beta H}\sum_\alpha(u_0-u_{1\alpha})^2\right]}{Tr[e^{-\beta H}]}=\frac{2}{\lambda}\frac{dF}{d\gamma}$$

where $u_{1\alpha}$ is a first neighbor of the central site, F the free energy, and $\langle A\rangle$ the thermal average of A. In particular, at absolute zero:

$$\left\langle\sum_\alpha(u_0-u_{1\alpha})^2\right\rangle=\frac{2}{\lambda}\frac{d\Delta E}{d\gamma}$$

and the quantity $G\Delta M\Delta\gamma$ may be pictured as:

$$G\Delta M\Delta\gamma=\frac{\lambda}{2}\frac{d}{dM}\left[\left\langle\sum_\alpha(u_0-u_{1\alpha})^2\right\rangle\right]\Delta M\Delta\gamma.$$

We write the adiabatic potential for the mode K, as:

$$V=\frac{\omega_K^2}{2}\,q_K^2+F(x_{-1}-x_1)$$

with the normalization relation $\sum_n M|u_n|^2=1$, which determines $A=\frac{1}{\mathcal{N}}$, and with

$$x_{-1}-x_1=(u_{-1}-u_1)\;q_K=\frac{2A\sin\delta_0}{\gamma}\,q_K=\frac{2}{\mathcal{N}}\,\frac{\sin\delta_0}{\gamma}\,q_K,$$

where

$$q_K=\sqrt{\frac{\hbar}{2\omega_K}}\,(a_K+a_K^+).$$

Then V can be transformed into

$$V=\frac{\omega_K^2}{2}\,[q_K-q_K^0]^2-\frac{\omega_K^2}{2}\,(q_K^0)^2 \text{ with } \omega_K^2\,q_K^0=\frac{2F}{\mathcal{N}}\,\frac{\sin\delta_0}{\gamma}.$$

We shall call $S(\omega)$ the relaxation energy $\frac{\omega_K^2}{2}\,(q_K^0)^2$ expressed in $\hbar\omega_K$ units.

$$S(\omega)=\frac{2}{\hbar\omega^3}\times F^2\times\frac{\sin^2\delta_0}{\gamma^2\mathcal{N}^2}.$$

Then we can rewrite $G(\omega)$ as

$$G(\omega)=-\frac{\hbar^2\omega^2\omega_L^2}{32\,F^2}\times\frac{\mathcal{N}^2}{M}\,n_0(\omega)\,S(\omega).$$

Taking account of the fact that $\mathcal{N}^2\simeq NM$ for a $2N$ atoms chain,

$$G(\omega)\simeq-\left(\frac{\hbar\omega\,\omega_L}{2^3F}\right)^2\times(\nu_0(\omega)\,S(\omega)).$$

The value of F depends on the electronic state of the defect, so one defines

$$S_{eg}(\omega)=\frac{2}{\hbar\omega^3}\,(F_e-F_g)^2\times\frac{\sin^2\delta_0}{\gamma^2\mathcal{N}^2}.$$

The one phonon structure intensity is given by [6]

$$I(\omega)=\nu_0(\omega)\;S_{eg}(\omega),$$

where ω is measured from the zero-phonon line energy, and $I(\omega)$ is relative to the zero-phonon line intensity.

One gets then the relation

$$\frac{d^2\Delta E}{dMd\gamma}\,(\omega)=-\left[\frac{\hbar\omega\omega_L}{2^3(F_e-F_g)}\right]^2\times I(\omega),$$

which relates in a simple way the contribution to the isotope shift from the frequency band $(\omega,\,\omega+d\omega)$ to the observable quantity $I(\omega)$.

In the first Born approximation, valid for γ small, $S_{eg}(\omega)$ and $\frac{d^2\Delta E}{dMd\gamma}$ are found to become independent of the perturbation constant γ:

$$\begin{cases} S_{eg}(\omega)=\dfrac{2}{\hbar\omega^3}\,(F_e-F_g)^2\times\dfrac{\sin^2 qa}{\mathcal{N}^2}, \\ \dfrac{d^2\Delta E}{dMd\gamma}=\dfrac{\hbar\omega_L}{6\pi M} \end{cases}$$

1.7. Electron-Phonon Interaction

The phase-shift analysis allows us to calculate the so-called "linear" and "quadratic" effects. We give here a short discussion of the electron-phonon interaction terms.

Let us call q_g and q_u the even and odd coordinates ("F-center model")

$$q_g=u_{-1}-u_1 \qquad q_u=u_1+u_{-1}$$

and let us develop the electron-phonon interaction up to second order:

$$H_{\text{int}}=A_g q_g+A_u q_u+A_{gg}q_g^2+A_{gu}q_g q_u+A_{uu}q_u^2.$$

We are interested in the diagonal matrix elements $\langle\psi|H_{\text{int}}|\psi\rangle$ where $|\psi\rangle$, an electronic wave function, is by itself even or odd:

$$\langle\psi|A_u|\psi\rangle=0, \qquad \langle\psi|A_g|\psi\rangle\neq 0.$$

(This is why only the δ_0 phase-shift appears in the calculation of $S_{eg}(\omega)$.)

As for the second order terms:

$$\langle\psi|A_{ug}|\psi\rangle=0,$$

which means there is no mixing of even and odd modes up to second order, and

$$\langle\psi|A_{gg}|\psi\rangle\neq 0, \qquad \langle\psi|A_{uu}|\psi\rangle\neq 0.$$

(As we only consider symmetry properties, we may think of A_{gg} and A_{uu} as effective terms including second-order perturbations coming from the first-order terms.)

The A_{gg} term gives an energy contribution in $A_{gg}(u_1-u_{-1})^2$ and the equation of motion of atom 1 becomes

$$M\omega^2u_1=\lambda[u_1-u_2]+A_{gg}[u_1-u_{-1}]$$

instead of, as in our previous model,

$$M\omega^2u_1=\lambda[u_1-u_2]+\lambda(1+\gamma)[u_1-u_0],$$

which, with $u_0=\frac{u_1+u_{-1}}{1}$, becomes

$$M\omega^2 u_1=\lambda[u_1-u_2]+\lambda\frac{(1+\gamma)}{2}[u_1-u_{-1}],$$

so the A_{gg} term was included in $\lambda\left(\frac{1+\gamma}{2}\right)$; however the A_{uu} term, which is symmetry allowed, was not considered. It may be necessary to include these quadratic terms in order to explain the observation of isotope shifts of both sign. If one defines

$$A_{uu}=\lambda\frac{(1+\mu)}{2}[u_1+u_{-1}],$$

the δ_1 phase-shift becomes

$$\text{tg }\delta_1=\frac{\mu\cos(qa)+1}{\mu\sin(qa)},$$

$$\frac{d\delta_1}{d\mu}=-\frac{1}{\mu^2\sin(qa)}\cos^2\delta_1.$$

The sign of the contribution of this term will depend on the sign of the $\Delta\mu$ variation between the excited and ground states.

2. Three-Dimensional Crystal

A. We restrict our study to a one-component, simple cubic lattice with nearest-neighbor forces. In this model, the various polarizations are conveniently independent [9].

The integral equation of scattering is now:

$$|u\rangle=|u^0\rangle+G_0^+P|u\rangle$$

where $|u\rangle$ is a column vector whose components are the x displacements of atoms, $G_0^+=\frac{1}{\omega^2-L_0+i\epsilon}$ is the Green's function, L_0 is the dynamical matrix and P is the perturbation matrix. The unperturbed vectors $|u^0\rangle$ are solutions of

$$(\omega^2-L_0)|u^0\rangle=0.$$

This equation is similar to the Slater-Koster equation, where the displacement of atom l takes the place of the coefficient of the Wannier function centered at l in the electronic wave function. To describe the scattering process, we introduce the usual T^+ matrix by its integral equation [8]:

$$T^+=P+PG_0^+T^+.$$

The stationary scattering wave $|u\rangle$ is obtained from the incident wave $|u^0\rangle$ by application of the X^+-matrix

$$|u\rangle=X^+|u^0\rangle \text{ with } X^+=1+G_0^+PX^+ \text{ and } T^+=PX^+.$$

Finally, the phase-shift matrix will be given by:

$$\text{tg}\eta=-\frac{\pi\delta T^+}{1-i\pi\delta T^+},\qquad \text{where } \delta=\delta(\omega^2-L_0).$$

B. For a point defect interacting with its 6 nearest neighbors, the P matrix is a 7×7 matrix; and so is the T^+ matrix; the 7-component vector $|u_R\rangle$ is a basis for a reducible representation Γ_R of the symmetry point group G (here D_4h); the R index will designate vectors or matrices restricted to the perturbed subspace.

The reduction of the Γ_R representation will give:

$$\Gamma_R=\sum_{\xi,\alpha}\Gamma_{\xi,\alpha},\qquad \sum_\alpha\alpha_\xi=\eta_\xi$$

where η_ξ is the number of times the irreducible representation Γ_ξ appears in the reduction of Γ_R. In our model, the reduction gives [11] $\Gamma_R=A_{1g}+B_{2u}+E_g+3A_{2u}$.

As G_0^+ and P possess the G symmetry, X_R and T^+ have nonzero matrix elements only between basis vectors of the equivalent representations $\Gamma_{\xi,\alpha}$.

C. The case where $\eta_\xi=1$, i.e., the case where Γ_ξ appears just once, is easier to handle and we shall deal with it in this paragraph. Indeed, it is the case for the A_{1g} representation, corresponding to the "pulsating" motion which is most important for electron-phonon interaction.

We define:

$$G_{0\xi}^+=\sum_{\mathbf{K}}\frac{|\langle\mathbf{K}|\xi\rangle|^2}{\omega^2-\omega^2(\mathbf{K})+i\epsilon}=R_\xi(\omega)+i\mathscr{I}_\xi(\omega)$$

where $|\mathbf{K}\rangle$ is an unperturbed plane wave:

$$R_\xi(\omega)=\mathscr{P}\int\frac{\nu_\xi(\omega')}{\omega^2-\omega'^2}d\omega',$$

($\mathscr{P}$ means that the Cauchy principal part must be taken)

$$\mathscr{I}_\xi(\omega)=-\frac{\pi\nu_\xi(\omega)}{2\omega},$$

$$\nu_\xi(\omega)=\sum_{\mathbf{K}}|\langle\mathbf{K}|\xi\rangle|^2\delta(\omega-\omega(\mathbf{K})).$$

Remembering the definition of the phase-shift matrix, we may write

$$\text{tg}\eta_\xi=\frac{P_\xi\mathscr{I}_\xi}{1-P_\xi R_\xi}\text{ or }\eta_\xi=-\arg(1-P_\xi G_{0\xi}^+).$$

The T_ξ^+ and $X_{R\xi}^+$ matrix elements can be conveniently expressed as

$$T_\xi^+ = \frac{e^{i\eta_\xi} \sin \eta_\xi}{\mathscr{J}_\xi} \qquad X_{R\xi}^+ = \frac{e^{i\eta_\xi} \sin \eta_\xi}{P_\xi \mathscr{J}_\xi}.$$

The ξ-type vibration amplitude on the defect is then derived as [10]

$$\langle \xi | u \rangle = \langle \xi | X^+ | \xi \rangle \langle \xi | u^0 \rangle = X_\xi^+ \langle \xi | \mathbf{K} \rangle.$$

So we have extended the linear chain results concerning the mechanical phase shift and the homographic dependence in P of the tangent of the phase shift.

The η_ξ phase-shifts govern also the asymptotic behavior of the scattered wave [11]: writing the stationary wave $|u\rangle$ as

$$|u\rangle = X^+ |\mathbf{K}^0\rangle = |\mathbf{K}_0\rangle + |u^S\rangle = |\mathbf{K}_0\rangle + G_0^+ T^+ |\mathbf{K}_0\rangle,$$

then the amplitude in l of the scattered wave can be written

$$\langle l | u^S \rangle = \sum_\sigma \langle l | G_0^+ | \sigma \rangle \langle \sigma | T^+ | \mathbf{K}_0 \rangle,$$

where the $|\sigma\rangle$ vectors span the perturbed subspace. We can extract the ξ partial amplitude from the sum,

$$\langle l | u^s \rangle_\xi = - \langle l | G_0^+ | \xi \rangle \frac{e^{i\eta_\xi} \sin \eta_\xi}{\pi \nu_\xi(\omega^2)} \langle \xi | \mathbf{K}_0 \rangle$$

Introducing the first Born approximation for the scattered wave

$$|u_B^s\rangle = G_0^+ P |\mathbf{K}_0\rangle,$$

$$\langle l | u_B^s \rangle_\xi = \langle l | G_0^+(\xi) P_\xi \langle \xi | \mathbf{K}_0 \rangle,$$

we derive also:

$$\langle l | u^s \rangle_\xi = - \frac{e^{i\eta_\xi} \sin \eta_\xi}{P_\xi \nu_\xi} \langle l | u_B^s \rangle_\xi.$$

D. In order to obtain the phase-shifts corresponding to the representations $\Gamma_{\xi,\alpha}$, we should like to diagonalize the phase-shift matrix; however a difficulty comes from the fact G_{0R}^+ and P do not have to be diagonal together. The total ξ phase shift is given by

$$\eta_\xi = \sum_\alpha \eta_{\xi,\alpha} = - \operatorname{Arg} \det \, (1 - P G_0^+)_\xi$$

hence $\operatorname{Arg} \det_\xi T^+ = \operatorname{Arg} \det_\xi X^+ = + \eta_\xi.$

E. Finally, in our model, the total phase-shift η_t is the following sum over partial phase-shifts.

$$\eta_t = \eta(A_{1g}) + \eta(B_{2u}) + 2\eta(E_g) + \eta(A_{2u}).$$

F. For the localized modes, the condition $\operatorname{tg}\delta = -i$ implies

$$1 - P(R_e G_0^+) - iP(I_m G_0^+) = 1 - P G_0^+ = 0.$$

3. Results for Simple Models

3.1. Two Examples in the Debye Approximation: the Mass Defect and the Vacancy (*F*-Center)

a. Green's Functions for Small Distances

The Green's function G_{000}^+ has been calculated by various authors [13]:

$$G_{000}^+ = \frac{3}{\omega_L^2} \left(1 - \frac{x}{2} \log_e \left| \frac{1+x}{1-x} \right| \right) + \frac{3i\pi}{2} \cdot \frac{x}{\omega_L^2},$$

where $x = \dfrac{\omega}{\omega_L}$.

The Green's function G_{200}^+ has been estimated in the long wavelength range [12]:

$$G_{200}^+ = G_{000}^+ - \frac{C_1}{\omega_L^2} \left(-\frac{2}{3} - 2x^2 + i\pi x^3 \right),$$

where $C_1 \simeq 1$.

b. Mass Defect

There is only one phase shift given by

$$\operatorname{tg}\eta = \frac{\pi}{2} \frac{x^3}{b - x^2 \left[1 - \dfrac{x}{2} \log_e \left| \dfrac{1+x}{1-x} \right| \right]}$$

with $b = (3\beta)^{-1}$.

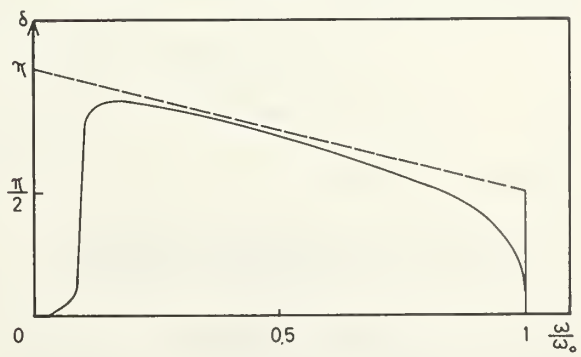

FIGURE 4. *Phase-shift for a mass defect* $\mathrm{b} = 0.01 \dfrac{\Delta m}{m} = 33.$

The curve $\eta(x)$ is plotted in figure 4, for the parameter value $b=0{,}01$ $\left(\frac{\Delta m}{m}=33\right)$ which corresponds to a very heavy defect. We see a very sharp increase of η around the value $x_0=\sqrt{b}=0{,}1$; in this region, we may take the approximate formula:

$$\mathrm{tg}\eta \simeq \frac{\pi}{2}\frac{x^3}{b-x^2}.$$

c. Vacancy (F-Center)

We are mostly interested in the (A_{1g}) phase shift, as far as optical properties are concerned; then we have

$$\langle A_{1g}|1-PG_0^+|A_{1g}\rangle = 1-\frac{\lambda_1\gamma_1}{M}\times(G^+_{000}-G^+_{200}),$$

where $\gamma_1=\frac{\Delta\lambda_1}{\lambda_1}$ is the relative change in central force at the vacancy site. In the long wavelength range [12], the phase-shift $\eta(A_{1g})$ is then given by:

$$\mathrm{tg}\eta(A_{1g})=\frac{\pi}{2}\frac{x^3}{\left(\frac{1}{3}+\frac{1}{2\gamma_1}\right)+x^2}.$$

This formula is very similar to the small x approximation for the mass defect. For the vacancy, we expect $\gamma_1\simeq -1$, so that

$$\frac{1}{3}+\frac{1}{2\gamma_1}\simeq -\frac{1}{6},$$

and we have the relation (keeping in mind all the approximations in its derivation)

$$\eta(A_{1g};\ \gamma_1=-1)=-\eta(\beta=2).$$

The low frequency "resonance" is centered around x_0 with

$$x_0=\sqrt{-\left(\frac{1}{3}+\frac{1}{2\gamma_1}\right)}$$

for $\gamma_1>-1$, $x_0>0{,}4$.

3.2. Simple Cubic Model With Equal Central and Noncentral Forces

a. Green's Functions

Numerical values for the Green's functions have been given by T. Wolfram and J. Callaway [14], in a study of spin-wave impurity states, and we have used their computed values for G^+_{000} and G^+_{200}.

b. Discussion

(a) The phase-shift for the mass defect if given by:

$$\eta=-\arg\left\{1-\frac{\beta\omega^2}{\Omega^2}\,g^+\left(0,0,0,3-\frac{\omega^2}{\Omega^2}\right)\right\}$$

where $\beta=\frac{M'-M}{M}$, $\Omega^2=\frac{2\lambda}{M}$, and $g^+(K,m,n,E)$

$$=i^{(K+m+n+1)}\int_0^\infty dt\,e^{-iEt}J_K(t)J_m(t)J_n(t).$$

A plot of η for the value $\beta=10$ is given in figure 5, showing a marked resonance behavior at low frequency.

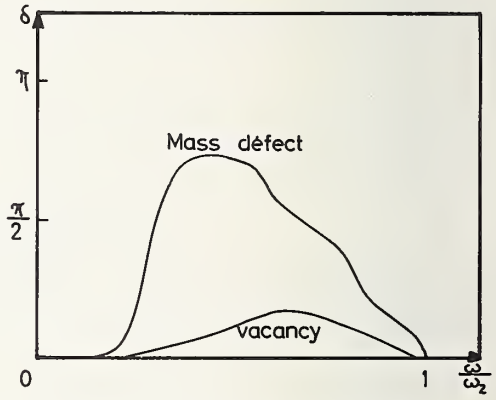

FIGURE 5. *Vacancy: breathing mode; mass defect:* $b=10$.

$$b=\frac{\Delta M}{M}=10.$$

(b) In the vacancy case [15], the phase-shift for the "breathing mode" is given by

$$\eta=-\arg\left\{1-\frac{1}{2}\left[g^+\left(0,0,0,3-\frac{\omega^2}{\Omega^2}\right)-g^+\left(2,0,0,3-\frac{\omega^2}{\Omega^2}\right)\right]\right\}.$$

On figure 5, we see that η has a smooth behavior which seems to indicate that the "resonance" found above is too high in ω for the Debye approximation to be valid.

Appendix: Green's Function Calculation for the Linear Chain

4.1. Green's Function Derivation

We define the Green's function $g_\omega^+(m)$ by the usual equation:

$$(\omega^2 - L_0) g_\omega^+(m) = \delta_{m0}.$$

Then

$$g_\omega^+(m) = \frac{1}{2N} \sum_K \frac{e^{iKma}}{\omega^2 - \omega^2(K) + i\epsilon}$$

$$= -\frac{2i}{\omega_L^2 \sin(qa)} e^{i|m|qa},$$

where $\omega = \omega_L \sin\left(\frac{qa}{2}\right)$ and with $0 < qa < \pi$ for $\omega < \omega_L$, and $qa = \pi + i\theta$ for $\omega > \omega_L$.

4.2. Reduction of Perturbation Matrix

For our general defect, the equations of motion of u_{-1}, u_0, u_1 contain perturbing terms. The perturbation matrix P is a 3×3 matrix:

$$P = \begin{pmatrix} 2\alpha - \beta\omega^2 & -\alpha & -\alpha \\ -\alpha & \alpha & 0 \\ -\alpha & 0 & \alpha \end{pmatrix}, \text{ with } \alpha = \frac{\gamma\lambda}{M} = \frac{\gamma\omega_L^2}{4},$$

which operates on column vectors $\begin{pmatrix} u_0 \\ u_1 \\ u_{-1} \end{pmatrix}$. On symmetry arguments we make the following change of basis:

$$u_0' = u_0; \quad u_1' = \frac{1}{\sqrt{2}}(u_1 + u_{-1}); \quad u_2' = \frac{1}{\sqrt{2}}(u_1 - u_{-1}).$$

Then P becomes P',

$$P' = \begin{pmatrix} 2\alpha - \beta\omega^2 & -\alpha\sqrt{2} & 0 \\ -\alpha\sqrt{2} & \alpha & 0 \\ 0 & 0 & \alpha \end{pmatrix},$$

and g_ω^+ becomes $g_\omega^{+\prime}$,

$$g_\omega^{+\prime} = g_0 \begin{pmatrix} 1 & \sqrt{2}\, e^{i\phi} & 0 \\ \sqrt{2}\, e^{i\phi} & 1 + e^{2i\phi} & 0 \\ 0 & 0 & 1 - e^{2i\phi} \end{pmatrix},$$

$$\text{with } g_0 = \frac{2i}{\omega_L^2 \sin\phi}.$$

4.3. Phase Shifts

The odd or "pulsating" mode phase shift η_0 can be derived from ν_u, given by

$$\nu_u = 1 - P_u G_u^+ = 1 + \alpha \frac{2i}{\omega_L^2 \sin\phi}(1 - e^{2i\phi}) = 1 + \gamma e^{i\phi},$$

and is expressed as

$$\operatorname{tg} \eta_0 = -\frac{\mathcal{I}_m(\nu_u)}{R_e(\nu_u)} = -\frac{\gamma \sin\phi}{1 + \gamma\cos\phi}, \text{ q.e.d.}$$

As for the even mode, we are in the case $n(\xi) = 2$. We then diagonalize the 2×2 matrix, $1 - (PG_0^+)_e$, with the secular equation

$$\begin{vmatrix} g_0[-\beta\omega^2 + 2\alpha(1 - e^{i\phi})] - 1 + \nu & -g_0[\beta\omega^2\sqrt{2}\, e^{i\phi} + \alpha\sqrt{2}\,(e^{i\phi} - 1)^2] \\ -g_0\alpha\sqrt{2}\,(1 - e^{i\phi}) & g_0\alpha(e^{i\phi} - 1)^2 - 1 + \nu \end{vmatrix} = 0,$$

and we get the phase shift η_1 from

$$\operatorname{tg} \eta_1 = \operatorname{tg}(\eta_1^1 + \eta_1^2),$$

with $\operatorname{tg}\eta_1^1 = -\frac{\mathcal{I}_m(\nu_1)}{R_e(\nu_1)}$, $\operatorname{tg}\eta_1^2 = -\frac{\mathcal{I}_m(\nu_2)}{R_e(\nu_2)}$,

$$= \operatorname{tg}\left(\frac{\phi}{2}\right) \frac{(1+\beta)(\gamma\cos\phi + 1) - (1+\gamma)}{\gamma(1+\beta)(1 - \cos\phi) + (1+\gamma)}, \text{ q.e.d.}$$

so that

$$\operatorname{tg} \eta_1 = -\frac{\mathcal{I}_m(\nu_1\nu_2)}{R_e(\nu_1\nu_2)}$$

One sees in this example, where a representation of the point group occurs several times, that there is only one partial phase-shift which governs the asymptotic behavior and the energy density modification.

5. Appendix: Short Derivation of Useful Formulae

The energy density of states functions, $\nu(\omega^2)$ and $\nu_0(\omega^2)$, are given by

$$\nu(\omega^2) = -\frac{1}{\pi} \text{ Im trace } G^+,$$

$$\nu_0(\omega^2) = -\frac{1}{\pi} \text{ Im trace } G_0^+.$$

However, for a resolvant function (and such is a Green's function),

$$\text{Trace } R = -\frac{d}{dE} \log \det R,$$

so that

$$\nu(\omega^2) - \nu_0(\omega^2) = +\frac{1}{\pi} \text{ Im } \left\{ \frac{d}{d\omega^2} \left[\log \frac{\det G^+}{\det G_0^+} \right] \right\}$$

$$= -\frac{1}{\pi} \frac{d}{d\omega^2} \{ \arg \det (1 - PG_0^+) \} = \frac{1}{\pi} \frac{d\eta}{d\omega^2},$$

because $G_0^+ = G^+(1 - PG_0^+)$. Finally, we get

$$\nu(\omega) - \nu_0(\omega) = \frac{1}{\pi} \frac{d\eta}{d\omega},$$

with

$$\eta = -\arg \det (1 - PG_0^+) = \arg \left\{ \frac{\det G^+}{\det G_0^+} \right\}.$$

6. References

[1] For a review of the work done on the influence of defects on lattice vibrations, we refer the reader to: I. M. Lifshitz, Nuovo Cimento Supp., 716 (1956); A. A. Maradudin, E. W. Montroll, and G. H. Weiss, Theory of Lattice Dynamics in the Harmonic Approximation, ch. III (Academic Press, New York, 1963); and A. A. Maradudin, Reports on Progress in Physics, p. 331, (1965).

[2] A. A. Maradudin, Phonons and phonon interactions, p. 424 (Benjamin, New York, 1964); and J. A. Krumhansl and J. A. D. Matthew, Phys. Rev. **140A,** 1812 (1965).

[3] P. G. Dawber and R. J. Elliott, Proc. Roy. Soc. **A273,** 222 (1963).

[4] A. Blandin, Journal de Physique **22,** 507 (1961).

[5] Numerous isotope shifts experiments have been performed. For instance: G. F. Imbusch et al., Phys. Rev. **136A,** 481 (1964); G. Baldini, E. Mulazzi, and N. Terzi, Phys. Rev. **140A,** 2094 (1965); H. R. Fetterman and D. B. Fitchen, International Symposium on color centers in alkali halides, Urbana (1965); P. Durand et G. Toulouse, Comptes-Rendus Acad. Sci. (1966); and A. E. Hughes, submitted to Proc. Phys. Soc.

[6] M. Lax, J. Chem. Phys. **20,** 1752 (1952); and Y. E. Perlin, Soviet Phys. Uspekhi, **6,** 542 (1964).

[7] E. W. Montroll, R. B. Potts, Phys. Rev. **102,** 72, (1956).

[8] T. Y. Wu and T. Ohmura, Quantum Theory of Scattering (Prentice Hall, 1962).

[9] Similar considerations have been developed for the alloy problem. See F. Gautier and P. Lenglart, Phys. Rev. **139A,** 705 (1965).

[10] D. L. Mills, Colloque de Grenoble sur les phonons, Mar. 1966, has previously derived analogous results for the mass defect.

[11] A. Messiah, Mécanique quantique, Dunod.

[12] J. A. Krumhansl, International Conference on Lattice Dynamics at Copenhagen (1963).

[13] R. Brout and W. Visscher, Phys. Rev. Letters **9,** 54 (1962).

[14] T. Wolfram and J. Callaway, Phys. Rev. **130,** 6 (1963).

[15] G. F. Nardelli and N. Terzi, J. Phys. Chem. Solids **25,** 815 (1964).

Influence of Defects on Elastic Constants

W. Ludwig*

Institut für Reaktorwerkstoffe, K F A Jülich, Institut für Theoretische Physik C, Technische Hochschule, Aachen, Germany

If a defect is introduced in a lattice, even in Bravais-crystals, the atoms are no longer centers of inversion. In calculating elastic constants, one has to use the procedure of nonprimitive lattices in a generalized form; since there is no translational invariance now, the region around the defect has to be considered as a large molecule (unit cell). Starting from this, general expressions for the elastic constants in lattices with "small" concentrations of defects can be given. In many cases the expressions can be simplified to a convenient form. The simple case of a vacancy is considered as an example.

When a defect (impurity, vacancy, interstitial) is introduced into a crystal, the force-constants are changed, mainly in the vicinity of the defect. The atoms are displaced from their "ideal" positions. Even in Bravais-lattices, the atoms are no longer centers of inversion. If one wants to calculate the change in the elastic constants due to the defect, then one has to use the procedure of nonprimitive lattices. In the following we give the general procedure for calculating elastic constants in defect lattices, and an application to vacancies in cubic crystals.

We assume a small concentration of defects, in order to neglect the interaction of defects. It will turn out that disregarding the interaction between defects is a good approximation if the mean distance between defects is larger than the range of interatomic forces. But the procedure can be extended immediately to cases with interaction between defects, for example to Frenkel-pairs.

Every defect produces a displacement field (which includes the image-term). We divide the crystal into volumes with radii of half the mean distance of the defects, and calculate the change of elastic constants by a defect from its "own" volume: i.e., we calculate the contribution of a single defect and multiply by the number of defects. We assume further, that there are no defects within a surface layer of depth equal to the range of the interatomic forces, or rather, we assume that we can neglect the contributions of these "surface" defects. This is always possible, if the defects are distributed homogeneously.

We have to distinguish between different displacements:

(i) The displacements produced by the defect (static displacement field) U_i^m, e.g., for a defect with cubic symmetry in an isotropic elastic medium,

$$U_i^m = \frac{M}{4\pi(\lambda+2\mu)} \cdot \frac{X_i^m}{(R^m)^3}.$$

(M: force-moment of defect, λ, μ: Lame constants). The image term has to be added.

(ii) The displacements, which are produced by exerting small external forces (stresses) to the defect crystal, W_i^m. The expansion of the potential energy of the defect crystal with respect to W_i^m defines the force-constants of the defect lattice. The W_i^m can be related to the elastic strains.

(iii) $V_{i|j}$ is the (infinitesimal) elastic strain tensor. But now, because no ion is a center of inversion in a defect crystal, $V_{i|j}$ does not describe all the elastic displacements; each ion may have an individual displacement V_i^m too, therefore

*Present address: Institut für Theoretische Physik, University, Giessen, Germany.

$$W_i^m = \sum_j V_{i|j} X_j^m + V_i^m; \tag{1}$$

m indicates the atoms in an arbitrary way. But we number now the atoms according to their undisplaced positions in the lattice without defect m, because the static displacements are smaller than a lattice constant.[1]

Ψ is the potential energy of the defect lattice, e.g., between impurity and neighbors,

Φ is the potential energy of the ideal lattice, between host lattice atoms.

Positions and force-constants of the defect lattice are

$$X_i^m,\ \Psi_{ij}^{mn}(\ldots \mathbf{R}^h \ldots),\ \Phi_{ij}^{mn}(\ldots \mathbf{R}^h \ldots).$$

Corresponding positions and force constants of the ideal lattice are

$$\tilde{X}_i^m,\ \tilde{\Psi}_{ij}^{mn}(\ldots \tilde{\mathbf{R}}^h \ldots),\ \tilde{\Phi}_{ij}^{mn}(\ldots \tilde{\mathbf{R}}^h \ldots).$$

In the following we drop all those relations which are standard [1–4] and emphasize only the steps, which are characteristic for the defect.

The change in energy with deformation by small external forces f_i^m (stresses) is [2]

$$\Psi - \Psi_0 = \frac{1}{2} \sum_{mn,\ ij} \Psi_{ij}^{mn}(\ldots \mathbf{R}^h \ldots) W_i^m W_j^n + \ldots, \tag{2}$$

where we have assumed that the defect crystal is in equilibrium before the stresses are applied:

$$\Psi_i^m = 0, \qquad \text{all } m, i.$$

With (1) and (2) [1–5]

$$\Psi - \Psi_0 = \frac{1}{2} \sum_{\substack{mn \\ ij}} \Psi_{ij}^{mn} V_i^m V_j^n + \sum_{\substack{mn \\ ijk}} \Psi_{ij}^{mn} X_k^n V_i^m V_{j|k} + \frac{1}{2} \sum_{\substack{mn \\ ijkl}} \Psi_{ij}^{mn} X_k^m X_l^n V_{i|k} V_{j|l} + \ldots. \tag{3}$$

After applying the external forces f_i^m the equilibrium condition is

$$f_i^m = \sum_{nj} \Psi_{ij}^{mn} W_j^n = \sum_{nj} \Psi_{ij}^{mn} V_j^n + \sum_{njk} \Psi_{ij}^{mn} X_k^n V_{j|k} \tag{4}$$

The f_i^m are surface forces (stresses) and are exerted only on surface atoms. In the interior of the crystal (4) simplifies to

$$\sum_{nj} \Psi_{ij}^{mn} V_j^n = -\sum_{njk} \Psi_{ij}^{mn} X_k^n V_{j|k}. \tag{5}$$

As in the theory for ideal crystals, it is sufficient to solve this equation in the interior and to neglect the surface terms, because there are only $N^{2/3}$ surface terms compared to N interior terms.

The elastic constants are defined by [3]

---

[1] We restrict the procedure to Bravais-lattices. The application to other ones is again obvious. If there are interstitials, they must have an extra number, which makes no difficulty.

[2] The sums extend over all the places in a lattice. In case of a vacancy the vacant position has to be included and to be described by missing force constants. If there are N atoms in the lattice, and one vacancy the sum is over $(N+1)$ positions in a volume V. In an ideal lattice the "corresponding" volume contains $N+1$ atoms.

[3] This holds only, if there are no stresses in the initial state before deformation. The generalization to initial stresses can be done according to standard procedure [3–5].

$$\Psi - \Psi_0 = \frac{1}{2} V \sum_{ijkl} S_{ik,jl} V_{i|k} V_{j|l}, \tag{6}$$

where V is the volume of the crystal, here of the defect crystal (footnote 1). With (6) and (5) we have from (3)

$$V \sum_{ijkl} S_{ik,jl} V_{i|k} V_{j|l} = \sum_{\substack{mn \\ ijkl}} \Psi_{ij}^{mn} X_k^m X_l^n V_{i|k} V_{j|l} + \sum_{\substack{mn \\ sjl}} \Psi_{sj}^{mn} X_l^n V_s^m V_{j|l}. \tag{7}$$

Because $\sum_n \Psi_{ij}^{mn} = 0$ (conservation of momentum), $V_j^n = t_j$ is a solution of (5). Therefore the reciprocal of Ψ_{ij}^{mn} does not exist. But (5) allows for a solution with another symmetric matrix R_{ij}^{mn} in the form

$$V_s^m = - \sum_{\substack{m'n \\ rik}} R_{sr}^{mn} \Psi_{ri}^{nm'} X_k^{m'} V_{i|k}. \tag{8}$$

Inserting (8) into (7) we have

$$V S_{ik,jl} = \sum_{mn} \Psi_{ij}^{mn} X_k^m X_l^n - \sum_{\substack{mm' \\ nn' \\ rs}} X_k^{m'} \Psi_{ir}^{m'm} R_{rs}^{mn} \Psi_{sj}^{nn'} X_l^{n'}. \tag{9}$$

This expression has the correct symmetries, because

$$\sum_n \Psi_{ij}^{mn} X_k^n = \sum_n \Psi_{ik}^{mn} X_j^n, \qquad \sum_n \Psi_{ij}^{mn} = 0, \tag{10}$$

which hold for every set of mass-points [1–5].

As in the standard procedure, we form $S_{ik,jl} + S_{il,jk}$ because $S_{ik,jl}$ contains absolute coordinates, whereas the symmetrized expression does not. Defining

$$2V\hat{C}_{ij,kl} = - \sum_{mn} \psi_{ij}^{mn} (X_k^n - X_k^m)(X_l^n - X_l^m), \tag{11}$$

we can resolve the symmetrized expression and obtain

$$V S_{ik,jl} = V\hat{C}_{ij,kl} + V\hat{C}_{kj,il} - V\hat{C}_{ik,jl} - \sum_{\substack{mm' \\ nn' \\ rs}} X_k^{m'} \Psi_{ir}^{m'm} R_{rs}^{mn} \Psi_{sj}^{nn'} X_l^{n'}. \tag{12}$$

We are left with the calculation of (11, 12) and the solution of (5) for the defect crystal. For this, we divide the crystal into an atomistic region around the defect, with radius r_0, and an elastic region. The atomistic region shall be of the order of the range of interatomic forces (or larger). The outer region can be handled according to elastic theory.

Calculation of $\hat{C}_{ij,kl}$. A slight modification of (11) gives

$$2V\hat{C}_{ij,kl} = - \sum_{m<r_0} \sum_h \Psi_{ij}^{mm+h} (X_k^{m+h} - X_k^m)(X_l^{m+h} - X_l^m)$$

$$- \sum_{m>r_0} \sum_h \Phi_{ij}^{mm+h} (X_k^{m+h} - X_k^m)(X_l^{m+h} - X_l^m); \tag{13}$$

256-724 O-67—11

$m < r_0$ indicates the atoms in the atomistic region, $m > r_0$ those in the elastic region. In the elastic region we have the potential function Φ of the host lattice (range of forces smaller than r_0). In the elastic region we have small and slowly varying displacement fields, therefore:

$$X_i^m = \tilde{X}_i^m + U_i^m; \qquad \tilde{X}_i^{m+h} = \tilde{X}_i^m + \tilde{X}_i^h; \tag{14}$$

$$\Phi_i^{mm+h}{}_j = \tilde{\Phi}_i^{mm+h}{}_j + \sum_{g,k} \tilde{\Phi}_i^{mm+h}{}_k^{m+g} U_k^{m+g} + \ldots; \qquad m > r_0$$

$$U_k^{m+g} = U_k^m + \tilde{X}_l^g U_{k|l}^m + \ldots; \qquad m > r_0.$$

Inserting (14) into (13) and neglecting higher terms in $U_{k|l}^m$ we obtain

$$2VC_{ij,kl} = -\sum_{m<r_0} \sum_h \Psi_i^{mm+h}{}_j (X_k^{m+h} - X_k^m)(X_l^{m+h} - X_l^m) - \sum_{m>r_0} \sum_h \tilde{\Phi}_i^{mm+h}{}_j \tilde{X}_k^h \tilde{X}_l^h$$

$$- \sum_{m>r_0} \sum_h \left\{ \sum_{rs}^g \tilde{\Phi}_i^{mm+h}{}_r^{m+g} \tilde{X}_s^g \tilde{X}_k^h \tilde{X}_l^h U_{r|s}^m + \sum_s \tilde{\Phi}_i^{mm+h}{}_j (\tilde{X}_s^h \tilde{X}_l^h U_{k|s}^m + \tilde{X}_k^h \tilde{X}_s^h U_{l|s}^m) \right\}. \tag{15}$$

Now

$$-\sum_h \tilde{\Phi}_{ij}^{mm+h} \tilde{X}_k^h \tilde{X}_l^h = 2V_{z0} \hat{C}_{ij,kl}^0, \tag{16a}$$

independent of m, is the 2d-order-Born-Huang-tensor of the ideal lattice, $V_0 = NV_{z0}$ its volume. Further

$$-\sum_{hg} \tilde{\Phi}_{ijr}^{mm+hm+g} \tilde{X}_s^g \tilde{X}_k^h \tilde{X}_l^h = 2V_{z0} \hat{C}_{ij,rs,kl}^0, \tag{16b}$$

is the 3d-order-Born-Huang-tensor. Adding and subtracting

$$-\sum_{m<r_0} \tilde{\Phi}_{ij}^{mm+h} \tilde{X}_k^h \tilde{X}_l^h$$

we have

$$2\{V\hat{C}_{ij,kl} - V_0 \hat{C}_{ij,kl}^0\} = -\sum_{m<r_0} \sum_h \{\Psi_{ij}^{m,m+h}(X_k^{m+h} - X_k^m)(X_l^{m+h} - X_l^m) - \tilde{\Phi}_{ij}^{mm+h} \tilde{X}_k^h \tilde{X}_l^h\}$$

$$+ 2V_{z0}\{\hat{C}_{ij,rs,kl}^0 + \hat{C}_{ij,sl}^0 \delta_{kr} + \hat{C}_{ij,ks}^0 \delta_{lr}\} \sum_{m>r_0} U_{r|s}^m. \tag{17}$$

If the static displacement field has cubic symmetry, it is

$$\sum_{m>r_0} U_{r|s}^m = \frac{1}{3} \delta_{rs} \sum_{m>r_0} \sum_i U_{i|i}^m;$$

This vanishes in some cases (vacancies). Then contributions of the displacement field arise from higher order terms in $U_{r|s}^m$. In other cases the last term in (17) contributes. Its influence can be estimated. Sometimes it is small and might be neglected; this depends strongly on the kind of defects and on their atomistic structure.

Solution of (5). We make the same assumptions as before, and divide (5) into the equation for the atomistic region

$$m < r_0: \sum_{hj} \Psi_i^{mm_j+h} V^{m_j+h} = -\sum_{hjk} \Psi_i^{mm_j+h} X^{m_k+h} V_{j|k}; \tag{18a}$$

and for the elastic region

$$m > r_0: \sum_{hj} \Phi_i^{mm_j+h} V^{m_j+h} = -\sum_{hjk} \Phi_i^{mm_j+h} X^{m_k+h} V_{j|k}; \tag{18b}$$

where on the right-hand side of (18b) we have used (14). Then ($m > r_0$)

$$\sum_{hj} \Phi_i^{mm_j+h} V^{m_j+h} = -\sum_{jk} \left\{ \sum_h \tilde{\Phi}_i^{mm_j+h} \tilde{X}_k^h + \sum_{rl} \left(\sum_{hg} \tilde{\Phi}_i^{mm_j+hm_r+g} \tilde{X}_k^h \tilde{X}_l^g + \sum_h \tilde{\Phi}_i^{mm_j+h} \tilde{X}_l^h \delta_{kr} \right) U_{r|l}^m \right\} \cdot V_{j|k}, \tag{19}$$

where use has been made of (10) and $\sum_h \tilde{\Phi}_i^{mm_j+hm_k+g} = 0$. In (before introducing defects) Bravais-

lattices all the terms on the right-hand side of (19) vanish, because of the inversion symmetry of Bravais-lattices:

$$\tilde{\Phi}_i^{mm_j+h} = \tilde{\Phi}_{ij}^{0h} = \tilde{\Phi}_i^{0-h}_{j}; \quad \tilde{\Phi}_i^{mm_j+hm_k+g} = \tilde{\Phi}_{ijk}^{0hg} = -\tilde{\Phi}_l^{0-h-g}_{jk}; \quad \tilde{X}_i^h = -\tilde{X}^{-h}_{i}.$$

Up to first order in $U_{r|l}^m$ the right-hand side is zero. Higher orders can be neglected, since they would correspond to 4th-order elastic theory. The solutions of the remaining homogeneous equation for $m > r_0$ are $V_j^{m+h} = t_j$ which solves also the homogeneous equation of (18a). This means a uniform translation of the lattice and does not influence the elastic constants. The V_j^n are different from zero only in the atomistic region; we have to solve (18a) only. The displacement field in the elastic region of a defect contributes to the change in the elastic constants (i) via the last term in (17) and (ii) via the change in volume (difference in V and V_0). The first effect vanishes in some cases.

Example: Vacancy in a fcc-lattice with central-forces. We assume a central-force interaction up to second neighbors. The force constants of the ideal lattice are f and αf. The atomistic region includes the second "neighbors" of the vacancy. We consider an isotropic pressure as the external force, therefore we calculate only the change in the compressibility K.

The calculations can be done in a straightforward manner. It turns out that even the differences between the positions in the defect lattice and those of the ideal lattice can be neglected (contributions smaller than 1%). Also the difference in force-constants in the vicinity of the defect makes a negligible contribution. With $V_{j|k} = \epsilon \delta_{jk}$ for an isotropic pressure we have for the displacements according to (5) or (18a) (a = lattice constant)

$$\mathbf{V}^{110} = \epsilon \cdot \frac{a}{8} \frac{1}{1+3\alpha/4} \cdot \{1, 1, 0\}; \qquad \mathbf{V}^{200} = \epsilon \cdot \frac{a}{4} \frac{\alpha}{1+\alpha/4} \{2, 0, 0\} \cdot \tag{20}$$

That means, the atoms in the vicinity of the vacancy are more displaced than described by the strainfield $V_{j|k}$. This is plausible because of the missing springs. The second term in (7) then is

$$\sum_{\substack{mn \\ sjl}} \Psi_{sj}^{mn} X_l^n V_s^m V_{j|l} = -\frac{3}{2} a^2 \epsilon^2 f \frac{1+\alpha/4+\alpha^2+3\alpha^3/4}{1+\alpha+3\alpha^2/16} \cdot \tag{21}$$

The difference in (17) is

$$\sum_{ij}\{V\hat{C}_{ii,jj}-V_0\hat{C}^0_{ii,jj}\}=-6a^2f(1+\alpha) \tag{22}$$

and therefore

$$\sum_{ij}\{VS_{ii,jj}-V_0S^0_{ii,jj}\}=\left\{\frac{V}{K}-\frac{V_0}{K_0}\right\}\cdot 9\epsilon^2=-6a^2\epsilon^2f(1+\alpha)-\frac{3}{2}a^2\epsilon^2f\frac{1+\alpha/4+\alpha^2+3\alpha^3/4}{1+\alpha+3\alpha^2/16}. \tag{23}$$

This shows, that the second term in (12), the consequence of the fact that the ions are no longer centers of inversion in defect lattices, contributes about 25 percent to the change in the elastic constants!

$$\frac{V}{K}-\frac{V_0}{K_0}=-r\cdot\frac{5}{6}a^2f(1+\alpha)\frac{1+33\alpha/20+23\alpha^2/20+6\alpha^3/20}{1+2\alpha+19\alpha^2/16+3\alpha^3/16}, \tag{24}$$

where r is the number of vacancies. The change in volume is

$$V-V_0=K_0M\cdot r;\qquad 1/K_0=a^2f(1+\alpha)/3V_{z0}. \tag{25}$$

Using Kanzaki's [6] values for M (van der Waals' forces for argon) we finally have for the relative change in the compressibility due to vacancies

$$(1/K-1/K_0)K_0=p\left\{0,\,02-\frac{5}{2}\frac{1+33\alpha/20+23\alpha^2/20+6\alpha^3/20}{1+2\alpha+19\alpha^2/16+3\alpha^3/16}\right\}. \tag{26}$$

The first term arises from the change in volume; it is about 1 percent and can be neglected. Also in other cases this contribution will be small.

$p=r/N$ is the concentration of vacancies. The difference between the elastic constants can be related to Kröner's elastic polarizabilities [7]; in our notation it is e.g., for small p

$$1/K-1/K_0=p\beta_k/V_z, \tag{27}$$

where β_k is the bulk-polarizability. With (26) we have

$$\beta_k=\frac{1}{K_0}V_z\left\{0,\,02-\frac{5}{2}\frac{1+33\alpha/20+23\alpha^2/20+6\alpha^3/20}{1+2\alpha+19\alpha^2/16+3\alpha^3/16}\right\}, \tag{28}$$

$\approx -1,46$ eV for a vacancy in Argon. This value is somewhat small, but it is comparable with the values given by Kröner [7] for the polarizabilities. Equation (26) can be used also to calculate the temperature dependence of the compressibility due to the equilibrium concentration of vacancies. This is given by (E_f = formation energy)

$$p\sim\exp\{-E_f/kT\}, \tag{29}$$

and has to be inserted into (26). More detailed calculations for other defects and better models will be done (see also [8]).

References

[1] G. Leibfried, Hdb. d. Physik 7/I, 104–324 (Springer, Berlin, 1955).
[2] G. Leibfried, W. Ludwig, Solid State Physics **12**, 275 (Academic Press, 1961).
[3] G. Leibfried, W. Ludwig, Z.f. Physik **160**, 80 (1960).
[4] D. C. Wallace, Revs. Mod. Physics **37**, 57 (1965).
[5] W. Ludwig, Springer Tracts in Modern Physics **43** (1967).
[6] H. Kanzaki, J. Phys. Chem. Solids **2**, 24 (1957).
[7] E. Kröner, Phys. kondens, Materie **2**, 262 (1964).
[8] J. Melngailis, Phys. Stat. Solidi **16**, 247 (1966).

A Calculation of Force-Constant Changes for the U Center*

R. F. Wood and R. L. Gilbert**

Solid State Division, Oak Ridge National Laboratory, Oak Ridge, Tenn. 37830

It was established some time ago that a hydride ion can replace a halide ion in alkali halide crystals. This defect, now known as the U center, is responsible for a characteristic absorption in the ultraviolet which has been intensively and extensively investigated [1].[1] Through this work many of the properties of crystals containing U centers have become understood. More recently, attention has shifted to theoretical and experimental research on the infrared absorption of the defect. Shaefer's [2] original experimental work on the subject coincides with an increasing interest in the effects of a defect atom on the vibrational properties of the host crystals, particularly in localized and quasi-localized modes. The U center is an interesting example of the former case, in which a light impurity atom produces a localized mode well above the limit of the band of transverse optical vibrational frequencies of the perfect crystal. The problem of the localized mode connected with the U center and of its interaction with the "in band" modes has been discussed by many people [3]. It was claimed earlier that one could understand the experimental results simply by considering the mass difference between the H^- ion and the negative ion it replaced. It is now generally recognized that it is also necessary to take into account the changes in force constants which must surely occur. In a recent paper, Fieschi et al. [3], go into this question rather thoroughly.

Last summer we carried out extensive calculations on the electronic structure of the U center, and recently these have been taken up again. Our original aim was simply to see how well methods which had been employed for similar calculations on the F center [4] could give the absorption energy of the U center. Since lattice distortions around the defect are allowed in our model, it occurred to us that we could actually calculate the potential energy curve for both the nearest-neighbor relaxation and the movement in a ⟨100⟩ direction of the H^- ion. We were thus in a position to calculate the force constant of the H^- ion from a fairly rigorous quantum mechanical formulation. It is the purpose of this paper to sketch the calculations of both the optical and infrared properties of U centers in KCl, KBr, and KI. Unfortunately, the calculations are not yet finished, and this paper must really be considered as in the nature of a preliminary report.

We follow here very closely the work in reference 4. The wave function of a crystal containing a single U center is written as

$$\Psi(1, 2, \ldots n) = A\psi_U(1, 2)\psi_C(3, 4, \ldots n) \quad (1)$$

in which $\psi_U(1, 2)$ and $\psi_C(3, 4, \ldots n)$ are appropriately antisymmetrized group functions describing the H^- ion embedded in the crystal and the rest of the crystal respectively. A is then an antisymmetrizing operator which interchanges the electrons among the two groups U and C and appropriately normalizes the resulting function. So-called "strong orthogonality" is assumed, e.g., that

$$\int \psi_U(1, 2)\psi_C(3 \ldots k-1, 1, k+1, \ldots n)d\tau_1 = 0, \quad (2)$$

and ψ_U and ψ_C are considered to be separately normalized. The Hamiltonian for the problem can be written as

$$H = H_U + H_{cr} + H_{int}, \quad (3)$$

where

$$H_U(1, 2) = -\frac{1}{2}\nabla_1^2 - \frac{1}{2}\nabla_2^2 - \frac{1}{r_1} - \frac{1}{r_2} + \frac{1}{r_{12}}, \quad (4)$$

$$H_{int}(1, 2, 3, \ldots n) = \sum_{\nu, j}\left\{-\frac{Z_\nu}{|\mathbf{r}_1 - \mathbf{R}_\nu|} + \frac{1}{|\mathbf{r}_1 - \mathbf{r}_{\nu, j}|} - \frac{Z_\nu}{|\mathbf{r}_2 - \mathbf{R}_\nu|} + \frac{1}{|\mathbf{r}_2 - \mathbf{r}_{\nu, j}|}\right\}, \quad (5)$$

$$H_{cr}(3 \ldots n) = \sum_{\mu, i}\sum_{\nu, j}\left\{\frac{1}{2}\nabla_{\mu, i}^2 - \frac{Z_\nu}{|\mathbf{r}_{\mu, i} - \mathbf{R}_\nu|} + \frac{1}{|\mathbf{r}_{\mu, i} - \mathbf{r}_{\nu, j}|}\right\}. \quad (6)$$

$r_{\nu, j}$ is the coordinate of the j electron on the νth ion, etc. The expectation value of H with respect to $\psi_U\psi_C$ is

$$(\psi_U\psi_C|H|\psi_U\psi_C) = (\psi_U|H_U|\psi_U) + (\psi_C|H_{cr}|\psi_C) + (\psi_U\psi_C|H_{int}|\psi_U\psi_C). \quad (7)$$

*Research sponsored by the U.S. Atomic Energy Commission under contract with Union Carbide Corporation.

**Summer participant from Illinois Institute of Technology, Chicago, Illinois.

[1] Figures in brackets indicate the literature references at the end of this paper.

Antisymmetrization merely introduces exchange between the groups U and C. We treat the first and third terms quantum mechanically and the second term by classical ionic crystal theory. The form of $\psi_U(1, 2)$ is taken as

$$\psi_U(1, 2) = N_U[\psi_a(1)\psi_b(2) + \psi_a(2)\psi_b(1)], \tag{8}$$

where

$$\psi_a = N_a\left[\phi_a - \sum_{\nu, j}^{1nn}(a|\nu, j)\phi_{\nu, j}\right] \tag{9}$$

and

$$\phi_a = \sqrt{\frac{a^3}{\pi}}e^{-ar}. \tag{10}$$

An exactly similar form is taken for ψ_b. This type of function, first used for the helium atom, allows for some in-out correlation as well as giving a fairly adequate approximation to the Hartree-Fock doubly-occupied orbital.

From eqs (1) through (8) an expression for the energy can be derived which we shall write, for purposes of discussion, as

$$E_T = T_U + E_{\text{Mad}, U} + \Delta E_{\text{Mad}, U} + E_{\text{pent}} + E_{\text{ex}} + E_{\text{ov}} + E_{\text{cr}}. \tag{11}$$

The first three terms are respectively the kinetic energy, the Madelung energy, and a correction to the Madelung energy due to the fact that some of the charge density may be outside the various rings of neighboring ions; together these three terms give the point ion approximation as discussed by Gourary [5]. E_{pent} is the coulomb energy due to the penetration of the defect electrons into the cores of the neighboring ions, E_{ex} is the exchange energy with these core electrons, and E_{ov} is the energy introduced by the overlap terms $(a|\nu, j)$ in eq (9). E_{cr} is the energy of the rest of the crystal. All of the terms in eq (11), except T_U, depend directly on the positions of the neighboring ions and on the displacement of the H^- ion. All of the terms except E_{cr} depend on the variation parameters a and b appearing in ϕ_a and ϕ_b. The calculation consists in first minimizing E_T as a function of the variation parameters and the positions of the $1nn$ ions in a Γ_1^+ displacement. Thus, we get the distortion of the crystal in the vicinity of the defect. Holding the ions in their new positions, we then displace the H^- ion in a $\langle 100\rangle$ direction in order to map out E_T as a function of this displacement. According to the Born-Oppenheimer theorem, we can obtain in this way the effective potential energy curve for the motion of the H^- ion.

TABLE 1. *Optical absorption energies (in eV)*

The calculated values were obtained with Slater orbitals on the K^+ ions.

Crystal	Calculated	Experiment	Percent error
KCl	5.86	5.79	1.2
KBr	5.68	5.44	4.4
KI	5.32	5.08	4.7

TABLE 2. *Force constants*, K, *in various approximations*

Column 1 shows the equilibrium displacement of the $1nn$ ions in the three crystals in percent of $1nn$ distance of the perfect crystal. The second column contains the results for the force constants in the point-ion approximation, the third the results with the Slater approximation to the $3s$ and $3p$ K^+ Hartree-Fock functions, the fourth the results with accurate Hartree-Fock orbitals for all core functions, and the fifth the experimental values.

Crystal	Cubic distortion	$10^{-3}K$ (in dynes/cm)			
		Point ion	Slater	Hartree-Fock	Experimental
KCl	2	2.78	19.80	26.10	14.43
KBr	2.5	2.31	14.95	18.63	11.44
KI	3.0	1.83	10.10	11.57	8.94

Some of the results of our calculations thus far are given in tables 1 and 2. The optical transition energies in table 1 have been obtained by using very simple approximations to the Hartree-Fock $3s$ and $3p$ K^+ core orbitals constructed according to the Slater prescription. They are

$$\phi_{3s} = N_{3s}r^2e^{-2.583r} \text{ and } \phi_{3p} = N_{3p}r^2e^{-2.583r}\cos\theta$$

where N_{3s} and N_{3p} are normalizing factors. Calculations employing accurate Hartree-Fock orbitals for all core electrons give a ground-state energy level somewhat higher but, since the excited-state energy level should be raised by about the same amount, we do not expect the transition energies to change greatly when the more accurate calculation is completed. Following Gourary's earlier point-ion calculations, we have lowered the ground-state energy by 0.389 eV to include the remaining correlation energy unaccounted for by the form of eq (8). It is assumed that the correlation energy is negligible in the excited state.

The results of the force-constant calculations given in table 2 show, as expected, that the point-ion approximation is totally inadequate to account for the observed local-mode frequency. It is somewhat surprising that the results using the Slater approximation to the $3s$ and $3p$ Hartree-Fock orbitals should be as close as they are to the experimental values. The inclusion of the H^- polarization discussed below would make this agreement even better, but we are forced to assume that it is fortuitous. The results using accurate Hartree-Fock orbitals for all core electrons appear to be very inaccurate, but this calculation is not yet finished. We have still to add the corrections due to orthogonalization to the core electrons in the calculation of the expectation value of $1/r_{12}$, and we have not reminimized the energy for each displacement of the H^- ion. The first of these steps should decrease K significantly;

the second will probably have only a small effect. In all of the calculations of K reported in table 2, the potential curves are very nearly harmonic.

We now wish to include in the calculations the possibility that the H^- ion can be polarized during its vibrations. By far the easiest way of doing this, within the framework of our model, is to assume that the entire electronic shell of the H^- ion can be displaced relative to the proton. We can then calculate the effective force constant between the shell and the proton. In practice, we displace the H^- ion a given distance assuming no polarization, hold the proton at that position and allow the electronic shell to displace until equilibrium is established. Thus, we can calculate an effective potential curve with and without polarization.

Somewhat to our surprise, the polarization of H^- calculated in this way was negligible. The reason for this soon became apparent. The two functions ϕ_a and ϕ_b involved in $\psi(1,2)$ have exponential parameters a and b whose magnitudes are about 1 and 0.5 respectively. ϕ_a is very nearly a free hydrogen 1s function, while ϕ_b gives a fairly adequate representation of the F-center ground state; compared to ϕ_b, ϕ_a is rather compact. Hence, when the H^- ion is polarized, we expect most of the distortion from spherical symmetry to be attributable to the ϕ_b function. In our model this means that ϕ_b is shifted relative to the proton much more than is ϕ_a. In fact, it appears to be a good approximation to assume that ϕ_a is not displaced at all. Even this method of calculating the polarization may not be adequate. A very simple calculation on the free hydrogen atom by the method of rigid shell displacement gives a polarizability too small by a factor of six [6]. Our own calculations give a polarizability of H^- somewhat larger (less than a factor of 2) than the value of 1.9 Å^3 estimated by Calder et al., [7]. The calculations indicate that the effect of the H^- polarization will be to lower the force constants by 10 to 20 percent.

Finally, we would like to mention two problems which have arisen in this calculation. First, there is the one of accuracy. The change in the energy of the H^- ion as it is displaced slightly from equilibrium (say 2% of the nearest neighbor distance) is of the order of 10^{-3} eV. One must calculate all quantities involved to very high accuracy. The second problem really stems from the first. In calculations of this type, accuracy is very expensive in terms of computer time. This problem has been somewhat alleviated for us recently by the installation of an IBM 360–75 at Oak Ridge, and we hope to have these calculations completed sometime in the near future. We are hopeful of eventually obtaining the force constants to within 5 to 10 percent of the experimental values, but this may depend on the importance of the polarization of the K^+ ions.

References

[1] For background information on the U center, see J. H. Schulman and W. Dale Compton, Color Centers in Solids (Pergamon Press, Inc., New York, 1962).
[2] G. Shaefer, Phys. Chem. Solids **12,** 233 (1960).
[3] From a rather lengthy list we mention only the recent work of R. Fieschi, G. F. Nardelli, and N. Terzi, Phys. Rev. **138,** A203 (1965), which seems to be the most closely connected with our work.
[4] R. F. Wood and H. W. Joy, Phys. Rev. **136,** A451 (1964).
[5] B. S. Gourary, Phys. Rev. **112,** 337 (1958).
[6] We wish to thank U. Öpik for pointing this out to us.
[7] R. S. Calder, W. Cochran, D. Griffiths, and R. D. Lowde, Phys. Chem. Solids **23,** 621 (1962).

Local Modes and Resonance Scattering of Lattice Waves Due to Point Defects: Optical and Thermal Properties of Imperfect Crystals*

G. Benedek and G. F. Nardelli

Istituto di Fisica dell'Università, Milan, Italy

The theory of the imperfect lattice dynamics is briefly reviewed and the scattering matrix is introduced. The scattering matrix for a single defect is analyzed according to the irreducible representations of the crystal point group, and defect self-properties, such as entropy, thermal resistance, and optical absorption, are shown to be simply related to the numerator and denominator of the scattering matrix.

A model for substitutional defects accounting for both changes in mass and local interaction is considered in NaCl-lattices as well as in monoatomic f.c.c. lattices. The dynamics of an interstitial atom in a f.c.c. lattice is also presented.

The numerical computations concern mainly substitutional impurities in alkali halides, although some applications are mentioned also for interstitials and vacancies in f.c.c. lattices. For alkali halides the definition and the calculations based on the Hardy DD model of an effective nearest-neighbor force constant are given. Good agreement is found between theoretical predictions and experimental data on optical absorption for several point impurities and also molecular impurities in a KI crystal.

1. Introduction

Since Lifschitz's early papers, the lattice dynamics of imperfect crystals has been extensively developed from the formal point of view and the description of the effect of imperfections on a number of crystal properties has reached a satisfactory state on the basis of well defined models for the perturbation. The simplest of these is the mass defect model. Due to the exact knowledge of the defect mass, this model does not present any difficulty in the physical interpretation of the parameter characterizing the perturbation: so it has been applied exhaustively; see, for example the excellent review by Maradudin [1].[1] However this model has a limited range of validity, because an isolated defect actually interacts with the host lattice through a field of forces which may differ from the field in the host lattice. Sometimes, as one goes far from the defect, the perturbation on the force field vanishes so slowly that it involves a large number of neighbors. In this case the solution of the dynamical problem may represent a formidable task. Fortunately, in many cases of physical interest the model in which only the change in nearest-neighbors (n.n.) interaction is considered (beyond the mass change) represents a good approximation, provided that the parameters which characterize the change in n.n. interaction are suitably defined [2].

Recent calculations on defect properties, such as U-center Raman scattering [3], isotope [4,5], and stress effects [6] on low frequency resonances in alkali halides make use of the change in n.n. effective force constant obtained from fitting theory to the experimental resonance frequencies. Nevertheless, the applicability of such a model to defects in alkali halides, as well as metals or solid rare gases, presupposes the definition of an effective n.n. force constant (which is affected by the presence of defects) on the basis of the model employed for the host lattice dynamics.

On this line of thought we have based a recent discussion of doped alkali halides [7]. In this paper we summarize the general method of the scattering matrix, in terms of which we express thermal and optical properties of an imperfect lattice. Then we report the resonance conditions for:

(a) Mass and n.n. force constant changes in NaCl-type lattices;

(b) mass and n.n. force constant changes in monoatomic f.c.c. lattices. The vacancy case, already studied [8], is here mentioned;

*This research has been sponsored by EOAR under Grant N. 65-05 with the European Office of Aerospace Research—U.S. Air Force.

[1] Figures in brackets indicate the literature references at the end of this paper.

(c) interstitial atoms coupled with n.n. in monoatomic f.c.c. lattices as a limiting case of the point (a).

We report the models (b) and (c) with the aim of applying them to the solid rare gases and simple metals (Na-type): however we restrict ourselves to a discussion of a simplified model for calculating the interstitial resonances. As regards point (a) an effort is made to define an effective n.n. force constant. The numerical section of this paper is devoted to the point (a), namely to the KI crystal with positive or negative impurities. Indeed many experimental results on doped KI resonant modes [9–12] as well as a very good calculation for KI:Cl^- based on the mass-defect model [12] are available to permit a detailed comparison with our theoretical predictions. The effective n.n. force constant here used is defined according to Hardy's DD model [13].

2. Scattering Matrix Formalism

In this section we summarize the main results of the imperfect lattice dynamics on the basis of the scattering matrix formalism. For sake of simplicity we consider the case of low defect concentration. Hereafter we refer to the vibrational spectrum of the perfect lattice as the vibrational continuum. Let $\Lambda(\omega^2)$ be the frequency-dependent perturbation; then, the normal mode equation reads:

$$[L_0+\Lambda(\omega^2)]\psi=\omega^2\psi, \tag{1}$$

with the orthonormality condition

$$(\psi_\lambda, M_0^{-1}M\psi_{\lambda'})=\delta_{\lambda,\lambda'}.$$

L_0 and M_0 denote the dynamical matrix and the mass matrix, respectively, of the perfect lattice, M, the mass matrix and ψ the normal mode of the imperfect lattice, $\delta_{\lambda,\lambda'}$ the Kronecker symbol. Index λ labels the normal modes and ω is the circular frequency. A normal mode of the imperfect lattice can be written as

$$\psi=\alpha\varphi_g+\sigma; \tag{2}$$

α is an arbitrary a priori constant (eventually $\alpha=0$), φ_g a lattice wave, i.e., a normal mode of the perfect lattice, and σ the diffused wave. By putting

$$R_0(z)=(L_0-z)^{-1} \tag{3}$$

where z is the complex squared frequency, i.e., $z=\omega^2+i0^+$, eq (1) is seen to be equivalent to

$$\psi=\alpha\varphi_g-R_0(z)\Lambda(\omega^2)\psi. \tag{4}$$

For $\alpha\neq 0$, (4) is a linear equation of inhomogeneous type; it accounts for the wavelike modes of the imperfect lattice. Indeed, eq (4) admits solutions only for $\alpha\neq 0$ when ω is one of the frequencies of the vibrational continuum and these solutions are recognized to be the wavelike modes. For $\alpha=0$, the homogeneous case, eq (4) may admit solution only when ω is not a frequency of the vibrational continuum; then we consider the equation

$$\sigma=R(\omega^2+i0^+)\Lambda(\omega^2)\varphi_g, \tag{5}$$

which follows from eq (4) when eq (2) is taken into account. By $R(z)$ we have denoted the inverse matrix

$$[L_0+\Lambda(\omega^2)-z]^{-1},$$

which is seen to play in eq (5) the role of the resolvent matrix. At a frequency ω of the vibrational continuum $R(\omega^2+i0^+)$ exhibits resonance denominators with real and imaginary parts: the imaginary part never vanishes, while the real may have one or more zeros. Resonance scattering is said to occur when the real part of this denominator vanishes. Moreover, $R(z)$ may have singularities on the real axis at frequencies above the maximum, ω_L, of the vibrational continuum or inside the forbidden gap. The inspection of the homogeneous case of eq (4) shows that these singularities correspond to local modes. We look for resonance denominators and singularities of the resolvent matrix. $R(z)$ can be split as follows:

$$R(z)=R_0(z)-R_0(z)T(z)R_0(z), \tag{6}$$

where

$$T(z)=\sum_{n=0}^{\infty}(-1)^n\Lambda(\omega^2)[R_0(z)\Lambda(\omega^2)]^n \tag{7}$$

is the scattering matrix. Thus, the scattering matrix is seen to be the solution of the equation

$$T(z)=\Lambda(\omega^2)-T(z)R_0(z)\Lambda(\omega^2)=\Lambda(\omega^2)-\Lambda(\omega^2)R_0(z)T(z) \tag{7'}$$

and the diffuse wave turns out to be

$$\sigma=R_0(\omega^2+i0^+)T(\omega^2+i0^+)\varphi_g. \tag{5'}$$

The first term on the right side of (7') corresponds to the first Born approximation of the diffuse wave. (5') is seen to be in the form of the first Born approximation, provided that we use the scattering matrix instead of the physical perturbation $\Lambda(\omega^2)$. It appears from eq (7) that the scattering matrix has the same dimension and the same symmetry as the perturbation matrix. The inspection of (6) tells us that the defect-induced resonance denominators as well as the singularities of the resolvent matrix are all contained in the scattering matrix.

The scattering matrix can be analyzed in terms of the irreducible representations (i.r.) Γ of the point group pertaining to the perturbation $\Lambda(\omega^2)$. One obtains:

$$T_\Gamma(z)=\mathcal{N}_\Gamma(z)/\mathrm{D}_\Gamma(z), \tag{8}$$

where $\mathcal{N}_\Gamma(z)$ is a matrix of rank equal to the number of times the i.r. Γ is contained in $\Lambda(\omega^2)$, and $D_\Gamma(z)$ is the resonance denominator. The inspection of the solution of eq (7') tells us that $D_\Gamma(z)$ is given by the following expression

$$D_\Gamma(z)=\det\,[I+R_0(z)\Lambda(\omega^2)]_\Gamma. \tag{9}$$

The subscript Γ on the right side of eq (9) means that we have considered the projection on the oriented symmetry coordinates which transform according to the i.r. Γ. In the limit $z=\omega^2+i0^+$ eq (9) can be written as

$$D_\Gamma(z)=|D_\Gamma(z)|e^{i\theta_\Gamma(\omega^2)},$$

where $\theta_\Gamma(\omega^2)$ is the argument of the resonance denominator pertaining to the i.r. Γ. The resonance condition is

$$\mathrm{Re}\;D_\Gamma(z)=0. \tag{10}$$

In the same limit considered above, $R_0(z)$ splits into real and imaginary parts as

$$R_0(\omega^2 + i0^+) = \tilde{\mathscr{P}}(\omega^2) + i\pi\mathscr{P}(\omega^2), \tag{11}$$

where $\mathscr{P}(\omega^2)$ is the projection operator

$$\Sigma_g{}^{(\omega_g^2=\omega^2)} |\varphi_g)(\varphi_g| \tag{12}$$

and $\tilde{\mathscr{P}}(\omega^2)$ its Hilbert transform.
Remembering that the secular equation for the squared frequency fractional shift $\xi(\omega^2)$ reads [8]

$$\det \{I + \tilde{\mathscr{P}}(\omega^2)\Lambda(\omega^2) - \pi \operatorname{cotg}(\pi\xi)\mathscr{P}(\omega^2)\Lambda(\omega^2)\} = 0, \tag{13}$$

except for a trivial numerical factor, the argument of the resonance denominator for a given i.r. is recognized to be nothing else than the sum of the squared frequency fractional shifts which pertains to the same i.r., i.e.,

$$\vartheta_\Gamma(\omega^2) = \pi \sum_{j=1}^{n(\Gamma)} \xi_{\Gamma,j}(\omega^2). \tag{14}$$

In other words, $\pi\xi_{\Gamma,j}(\omega^2)$ is recognized to be the phase shift in the scattering problem. It is an easy matter to analyze, in terms of $\mathscr{N}_\Gamma(z)$ and $D_\Gamma(z)$ the effects due to resonance and local modes on crystal properties.

2.1. Thermodynamic Properties

Let F denote a thermodynamical potential of the crystal phonon gas. In a harmonic lattice F can be written as

$$F = \Sigma_\lambda f(\omega_\lambda^2). \tag{15}$$

We regard eq (15) as the definition of the function $f(\omega^2)$. The Lifschitz trace formula [14] for the thermodynamic self-potential reads

$$\Delta F = \Sigma_{\Gamma,j} d_\Gamma \int d\omega^2 f'(\omega^2)\xi_{\Gamma,j}(\omega^2) = \Sigma_\Gamma d_\Gamma \frac{1}{\pi} \int d\omega^2 f'(\omega^2)\vartheta_\Gamma(\omega^2). \tag{16}$$

A prime on $f(\omega^2)$ denotes the first order derivative with respect to ω^2; index j labels the number of times an i.r. appears in $\Lambda(\omega^2)$, and d_Γ is the dimension of Λ. If a local modes occurs, we have to add the term

$$d_\Gamma\{f(\omega_{\text{loc}}^2) - f(\omega_\Gamma^2)\}$$

and a similar term for a gap mode.

2.2. Transport Properties

Let us consider a phonon gas interacting with a random distribution of defects of the same kind at low concentration, and let the system be subjected to a constant thermal gradient. It can be shown easily [15] that the inverse phonon life time, as limited by defect scattering, can be written as

$$\tau_g^{-1} = -(\pi p/\omega_g) \operatorname{Im} (\varphi_g|T(\omega_g^2 + i0^+)|\varphi_g), \tag{17}$$

where p denotes the fractional concentration of defects. The long wave approximation of (17) in cubic crystals involves only the Γ_{15} i.r. and exhibits Lorentian-shaped peaks at the resonance frequencies like the optical absorption coefficient.

2.3. Optical Properties

As a last example, we consider the linear response of an imperfect polar crystal to the electromagnetic field at infrared frequencies. It can be shown [7, 16] that in cubic crystals the dielectric susceptibility can be written as

$$\chi(\omega)=(e_T^{*2}/\mu v)(\varphi_{\mathbf{0},TO}\ |[L_0+pT(\omega^2+i0^+)-\omega^2-i0^+]^{-1}|\varphi_{\mathbf{0},TO}\ ), \tag{18}$$

where the subscript $\mathbf{0}, TO$ on φ stands for $\mathbf{g}\sim 0$, transverse optic branch. The quantity e_T^* is the macroscopic effective charge associated with transverse optic mode, μ the reduced mass of the primitive cell and v its volume. Thus, the absorption coefficient reads

$$\alpha(\omega)=-(4\pi\omega/\eta c)\ \mathrm{Im}\ \chi(\omega), \tag{19}$$

in which η denotes refractive index and c velocity of light. Keeping in mind eq (8) and putting

$$N_{\Gamma_{15}}(z)=(\varphi_{\mathbf{0},TO}|\mathcal{N}_{\Gamma_{15}}(z)|\varphi_{\mathbf{0},TO}) \tag{20}$$

the absorption coefficient is seen to be given by

$$\alpha(\omega)=\frac{4\pi e_T^{*2}}{\mu v\eta c}\frac{\omega}{(\omega_T^2-\omega^2)^2}\frac{p[D^{(2)}N^{(1)}-N^{(2)}D^{(1)}]}{[D^{(1)}+p(\omega_T^2-\omega^2)^{-1}N^{(1)}]^2+[D^{(2)}+p(\omega_T^2-\omega^2)^{-1}N^{(2)}]^2}. \tag{21}$$

By the indices (1) or (2) we have denoted real or imaginary parts and we have dropped out the subscript Γ_{15} as well as the argument ω^2 of both D and N.

3. Resonance Conditions

We consider now the frequency-dependent perturbation

$$\Lambda(\omega^2)=-M_0^{-1/2}\{\Delta\Phi-\omega^2\Delta M\}M_0^{-1/2} \tag{22}$$

where the change in force constants of both central and noncentral types are assumed to extend only to the nearest neighbors of the defect. $\Delta\Phi$ is the variation of the force constant matrix Φ. As usual Φ is defined by the tensor $\Phi=\nabla\nabla\varphi(r)$, i.e.,

$$\Phi_{\alpha\beta}(\mathbf{x})=\left\{\frac{x_\alpha x_\beta}{r^2}\frac{\partial^2}{\partial r^2}+\left(\delta_{\alpha\beta}-\frac{x_\alpha x_\beta}{r^2}\right)\frac{\partial}{r\partial r}\right\}\varphi(r). \tag{23}$$

where $\varphi(r)$ is the interionic potential, function of the distance r, $r^2=\Sigma_\alpha \mathbf{x}_\alpha^2$, $\mathbf{x}\equiv\mathbf{x}(l\kappa)-\mathbf{x}(l'\kappa')$ and l and κ denote Bravais and cell indexes respectively. $\Delta\Phi$ must satisfy the translational invariance condition:

$$\Sigma_{l\kappa\alpha}\Delta\Phi_{\alpha\beta}(l\kappa,\ l'\kappa')=0. \tag{24}$$

3.1. Substitutional Defects in NaCl-Type Lattices

Consider first a substitutional defect in a NaCl-type lattice; let $M_{\pm}$ and $M_{\mp}$ be the masses of the substituted and n.n. ions, respectively, r_0 the lattice constant, $\omega_{\mathbf{g}\cdot j}$, and $\mathbf{e}\,(\pm|\mathbf{g}j)$ the frequency and eigenvector of the host lattice for wave vector $\mathbf{g}$ and branch index j. The change of mass involves only the lattice site of the defect (assumed as the origin of coordinate axes) and enters $\Lambda(\omega^2)$ through the parameter $\epsilon = -\Delta M_{\pm}/M_{\pm}$.

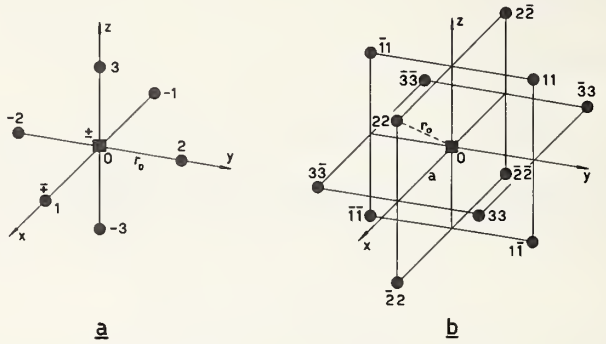

FIGURE 1. *Representations of the impurity atom (0) and its nearest neighbors for a* NaCl*-lattice (a) and a f.c.c. lattice (b).*

The geometry of the perturbation on the central and noncentral n.n. force constants is described by figure 1a. The symmetric tensor matrix $\Delta\Phi$ is given by:

$$\Delta\phi(\pm 1, 0) = -\Delta\phi(1, 1) = -\Delta\phi(-1, -1) = \begin{vmatrix} \lambda/2 & 0 & 0 \\ 0 & \lambda'/2 & 0 \\ 0 & 0 & \lambda'/2 \end{vmatrix} \text{ and cyclic permutations,}$$

$$\Delta\phi(0, 0) = \begin{vmatrix} -(\lambda+2\lambda') & 0 & 0 \\ 0 & -(\lambda+2\lambda') & 0 \\ 0 & 0 & -(\lambda+2\lambda') \end{vmatrix}, \tag{25}$$

$$\Delta\phi(\mathbf{x}) = 0 \text{ otherwise,}$$

where

$$\lambda/2 = \Delta\left\{\frac{\partial^2}{\partial r^2}\varphi(r)\right\}, \qquad \lambda'/2 = \Delta\left\{\frac{\partial}{r\partial r}\varphi(r)\right\} \tag{26}$$

account for the changes of central and noncentral force constants, respectively. On the whole $\Delta\phi$ is, in the lattice displacement representation, a 21×21 matrix and so is the scattering matrix T. The point group which pertains to the perturbation is 0_h: the irreducible representation (i.r.) Γ of the 0_h-group is contained in Λ $n(\Gamma)$ times, as follows:

$$n(\Gamma_1) = 1 \qquad n(\Gamma_{25'}) = 1 \qquad n(\Gamma_{15'}) = 1$$

$$n(\Gamma_{12}) = 1 \qquad n(\Gamma_{25}) = 1 \qquad n(\Gamma_{15}) = 3. \tag{27}$$

The symmetry coordinates in the wave vector representation are

$$(\Gamma_1|\mathbf{gj}) = (2i/\sqrt{6})\{e_x(\mp|\mathbf{gj}) \sin r_0 g_x + e_y(\mp|\mathbf{gj}) \sin r_0 g_y + e_z(\mp|\mathbf{gj}) \sin r_0 g_z\}$$

$$(\Gamma_{12}, t|\mathbf{gj}) = (i/\sqrt{3})\{2e_x(\mp|\mathbf{gj}) \sin r_0 g_x - e_y(\mp|\mathbf{gj}) \sin r_0 g_y - e_z(\mp|\mathbf{gj}) \sin r_0 g_z\}$$

$$(\Gamma_{12}, r|\mathbf{gj}) = i\{e_x(\mp|\mathbf{gj}) \sin r_0 g_x - e_y(\mp|\mathbf{gj}) \sin r_0 g_y\}$$

$$(\Gamma'_{15}, z|\mathbf{gj}) = i\{e_y(\mp|\mathbf{gj}) \sin r_0 g_x - e_x(\mp|\mathbf{gj}) \sin r_0 g_y\}$$

$$(\Gamma'_{25}, z|\mathbf{gj}) = i\{e_y(\mp|\mathbf{gj}) \sin r_0 g_x + e_x(\mp|\mathbf{gj}) \sin r_0 g_y\} \tag{28}$$

$$(\Gamma_{15,1}, z|\mathbf{gj}) = e_z(\pm|\mathbf{gj})$$

$$(\Gamma_{15,2}, z|\mathbf{gj}) = \sqrt{2}e_z(\mp|\mathbf{gj}) \cos r_0 g_z$$

$$(\Gamma_{15,3}, z|\mathbf{gj}) = e_z(\mp|\mathbf{gj})\{\cos r_0 g_x + \cos r_0 g_y\}$$

$$(\Gamma_{25}, z|\mathbf{gj}) = e_z(\mp|\mathbf{gj})\{\cos r_0 g_x - \cos r_0 g_y\}$$

(t = tetragonal; r = rhombic)

In the symmetry coordinate representation the perturbation matrix is diagonalized in blocks of dimension at most 3×3 (for Γ_{15}) i.e.:

$$(\Gamma_1|\Lambda|\Gamma_1) = (\Gamma_{12}|\Lambda|\Gamma_{12}) = \lambda/2M_\mp$$

$$(\Gamma_{25'}|\Lambda|\Gamma_{25'}) = (\Gamma_{25}|\Lambda|\Gamma_{25}) = (\Gamma_{15'}|\Lambda|\Gamma_{15'}) = \lambda'/2M_\mp, \tag{29}$$

$$(\Gamma_{15}|\Lambda|\Gamma_{15}) = \begin{vmatrix} \epsilon\omega^2 + (\lambda + 2\lambda')/M_\pm & -\lambda/\sqrt{2M_\pm M_\mp} & -\lambda'/\sqrt{M_\pm M_\mp} \\ -\lambda/\sqrt{2M_\pm M_\mp} & \lambda/2M_\mp & 0 \\ -\lambda'/\sqrt{M_\pm M_\mp} & 0 & \lambda'/2M_\mp \end{vmatrix}.$$

Hereafter we drop the argument ω^2 from $\Lambda(\omega^2)$. For each i.r. the scattering matrix can be written down straightforwardly; the matrix elements of $(L_0 - z)^{-1}$ are easily obtained by using the symmetry coordinates and are expressed by means of complex-valued integrals on the Brillouin zone (BZ). Usually λ' is an order of magnitude smaller than λ and a central force constant model in which λ' is neglected is a good approximation. In what follows we put $\lambda' = 0$ in our perturbation; in this case we have only Γ_1, Γ_{12} (Raman active) and Γ_{15} (optic active) resonance modes, whose frequencies are roots of the secular equations (10).

$$\text{Re}\ \{1 + (\lambda/M_\pm)[\mathcal{G}_4^\mp(z) + \alpha\mathcal{G}_5^\mp(z)]\} = 0 \tag{30.a}$$

with $\alpha = 2$ for Γ_1 and $\alpha = -1$ for Γ_{12}, and

$$\text{Re}\ \{1 + \epsilon\omega^2\mathcal{G}_1^\mp(z) + (\lambda/M_\pm)[\mathcal{G}_1^\mp(z) + (M_\pm/M_\mp)\mathcal{G}_3^\mp(z) - 2\sqrt{M_\pm/M_\mp}\,\mathcal{G}_2^\mp(z)] + \epsilon\omega^2(\lambda/M_\mp)[\mathcal{G}_1^\mp(z)\mathcal{G}_3^\mp(z) - \mathcal{G}_2^\mp(z)^2]\} = 0 \tag{30.b}$$

for Γ_{15} i.r. The complex valued integrals $\mathcal{G}^{\pm}_{\mu}(z)$ are given by:

$$\mathcal{G}^{\pm}_{1}(z) = (r_0^3/4\pi^3)\Sigma_j \int d\mathbf{g} e_x^2(\pm|\mathbf{g}j)/(\omega^2_{\mathbf{g}j} - z)$$

$$\mathcal{G}^{\pm}_{2}(z) = (r_0^3/4\pi^3)\Sigma_j \int d\mathbf{g} e_x(\pm|\mathbf{g}j) e_x(\mp|\mathbf{g}j) \cos r_0 g_x/(\omega^2_{\mathbf{g}j} - z)$$

$$\mathcal{G}^{\pm}_{3}(z) = (r_0^3/4\pi^3)\Sigma_j \int d\mathbf{g} e_x^2(\mp|\mathbf{g}j) \cos^2 r_0 g_x/(\omega^2_{\mathbf{g}j} - z)$$

$$\mathcal{G}^{\pm}_{4}(z) = (r_0^3/4\pi^3)\Sigma_j \int d\mathbf{g} e_x^2(\mp|\mathbf{g}j) \sin^2 r_0 g_x/(\omega^2_{\mathbf{g}j} - z)$$

$$\mathcal{G}^{\pm}_{5}(z) = (r_0^3/4\pi^3)\Sigma_j \int d\mathbf{g} e_y(\mp|\mathbf{g}j) e_z(\mp|\mathbf{g}j) \sin r_0 g_y \sin r_0 g_z/(\omega^2_{\mathbf{g}j} - z). \tag{31}$$

The evaluation of the integrals $\mathcal{G}^{\pm}_{\mu}(z)$ needs the knowledge of the eigenvectors and eigenfrequencies of the crystal. In our numerical application to KI, given below, these dynamical data are calculated according to the Hardy DD model: in this framework a definition of λ is given there.

3.2. Substitutional Defects in a Monoatomic F.C.C. Lattice

The geometry of the lattice is shown in figure 1b.

We consider the perturbation on the mass and n.n. force constant of both central and non-central type. By using the same notation as before we have

$$\Delta\phi(0,0) = \begin{vmatrix} -8\lambda_1 & 0 & 0 \\ 0 & -8\lambda_1 & 0 \\ 0 & 0 & -8\lambda_1 \end{vmatrix},$$

$$\Delta\phi(11,0) = \Delta\phi(\bar{1}\bar{1},0) = -\Delta\phi(11,11) = -\Delta\phi(\bar{1}\bar{1},\bar{1}\bar{1}) = \begin{vmatrix} 0 & 0 & 0 \\ 0 & \lambda_1 & \lambda_2 \\ 0 & \lambda_2 & \lambda_1 \end{vmatrix} \text{ and cyclic permutations,}$$

$$\Delta\phi(\bar{1}\bar{1},0) = \Delta\phi(\bar{1}1,0) = -\Delta\phi(1\bar{1},1\bar{1}) = -\Delta\phi(\bar{1}1,\bar{1}1) = \begin{vmatrix} 0 & 0 & 0 \\ 0 & \lambda_1 & -\lambda_2 \\ 0 & -\lambda_2 & \lambda_1 \end{vmatrix} \text{ and cyclic permutations,}$$

$$\Delta\phi(\mathbf{x}) = 0 \text{ otherwise,} \tag{32}$$

where

$$\lambda_1 = (1/2)\Delta\{\varphi''(r) + \varphi'(r)/r\}$$

$$\lambda_2 = (1/2)\Delta\{\varphi''(r) - \varphi'(r)/r\}. \tag{33}$$

Here the first derivative term $\varphi'(r)/r$ accounts for the change in noncentral force constant. On the whole $\Delta\phi$ is a 39×39 matrix in the lattice displacement representation. The group analysis in this case was already performed [8]; one has

$$\begin{aligned} &n(\Gamma_1) = 1 \quad n(\Gamma_{12}) = 2 \quad n(\Gamma_{15'}) = 2 \quad n(\Gamma_{12'}) = 1 \\ &n(\Gamma_2) = 1 \quad n(\Gamma_{25'}) = 2 \quad n(\Gamma_{2'}) = 1 \quad n(\Gamma_{25}) = 2 \end{aligned} \qquad n(\Gamma_{15}) = 4. \tag{34}$$

For sake of simplicity we refer to the case in which noncentral terms are neglected, i.e., $\lambda_1 = \lambda_2$. In this case the symmetry coordinates which are involved in the perturbation are

$$(\Gamma_1|\mathbf{g}j) = (2i/\sqrt{6})\{e_x(\mathbf{g}j) \sin ag_x (\cos ag_y + \cos ag_z) + \text{cycl. perm.}\}$$

$$(\Gamma_{12,1};\, t|\mathbf{g}j) = (i/\sqrt{3})\{2(e_y(\mathbf{g}j)\,\sin ag_y - e_x(\mathbf{g}j)\,\sin ag_x)\cos ag_z$$
$$-(e_z(\mathbf{g}j)\,\sin ag_z - e_y(\mathbf{g}j)\,\sin ag_y)\cos ag_x$$
$$-(e_x(\mathbf{g}j)\,\sin ag_x - e_z(\mathbf{g}j)\,\sin ag_z)\cos ag_y\}$$

$$(\Gamma'_{25,1};\, x|\mathbf{g}j) = i\sqrt{2}\{e_y(\mathbf{g}j)\,\sin ag_y\cos ag_z + e_z(\mathbf{g}j)\,\sin ag_z\cos ag_y\}$$

$$(\Gamma_{15,1};\, x|\mathbf{g}j) = e_x(\mathbf{g}j)$$

$$(\Gamma_{15,2};\, x|\mathbf{g}j) = \sqrt{2}\, e_x(\mathbf{g}j)\,\cos ag_x\,(\cos ag_y + \cos ag_z) \tag{35}$$

$$(\Gamma_{15,3};\, x|\mathbf{g}j) = \sqrt{2}\,\{e_y(\mathbf{g}j)\,\sin ag_y + e_z(\mathbf{g}j)\,\sin ag_z\}\,\sin ag_x$$

$$(\Gamma_{25,1};\, x|\mathbf{g}j) = \sqrt{2}\,\{e_y(\mathbf{g}j)\,\sin ag_y - e_z(\mathbf{g}j)\,\sin ag_z\}\,\sin ag_x$$

$$(\Gamma_{25,2};\, x|\mathbf{g}j) = \sqrt{2}\, e_x(\mathbf{g}j)\,\cos ag_x\,(\cos ag_z - \cos ag_y)$$

In symmetry coordinates the perturbation is diagonalized in the following blocks:

$$(\Gamma_1|\Lambda|\Gamma_1) = -\lambda_1/(2M)$$

$$(\Gamma_{12}|\Lambda|\Gamma_{12}) = (\Gamma_{25'}|\Lambda|\Gamma_{25'}) = \begin{vmatrix} -\lambda_1/(2M) & 0 \\ 0 & 0 \end{vmatrix}$$

$$(\Gamma_{25}|\Lambda|\Gamma_{25}) = \begin{vmatrix} -\lambda_1/4M & -\lambda_1/4M \\ -\lambda_1/4M & -\lambda_1/4M \end{vmatrix} \tag{36}$$

$$(\Gamma_{15}|\Lambda|\Gamma_{15}) = \begin{vmatrix} \epsilon\omega^2 & \lambda_1/\sqrt{2}M & \lambda_1/\sqrt{2}M & 0 \\ \lambda_1/\sqrt{2}M & -\lambda_1/4M & -\lambda_1/4M & 0 \\ \lambda_1/\sqrt{2}M & -\lambda_1/4M & -\lambda_1/4M & 0 \\ 0 & 0 & 0 & 0 \end{vmatrix}$$

The resonance condition for each i.r. can be easily obtained in terms of complex valued integrals on the BZ, in analogy to the preceding case.

In a previous work on the vibrational properties of a vacancy in a f.c.c. lattice [8], these integrals have been evaluated in an approximate way and expressed in term of the zero-order spherical Bessel function. As a general remark we note that the perturbation due to a vacancy should contain, beyond the force constant perturbation in a rigid lattice, the anharmonic contribution due to the nonnegligible elastic relaxation around the defect. An example of the evaluation of the self-entropy of a vacancy in solid Ar in such a framework is given in that paper, where a reasonable agreement was found with experimental data.

3.3. Interstitial Atom in a Monoatomic F.C.C. Lattice

Consider now a diatomic f.c.c. lattice (NaCl-type) containing a substitutional defect. Let the

256-724 O-67—12

mass $M_\pm$ be replaced by $\tilde{M}$ i.e., $\epsilon = 1 - \tilde{M}/M_\pm$ and let the 1st neighbor central and noncentral force constants be changed by the amounts $\lambda/2$, $\lambda'/2$, as well as the 2d neighbor force constants by the amounts λ_1 and λ_2 respectively. Take now the limit in which either $M_\mp$ or $M_\pm$, as well as the n.n. force constants in the whole host lattice, vanish: the first case yields the case of section 3.2, namely the substitutional defect in a monoatomic f.c.c. lattice, with parameters $\epsilon = 1 - \tilde{M}/M$, λ_1 and λ_2, being $M \equiv M_\pm$ and $\lambda = \lambda' = 0$. The second case is more interesting, leading to the configuration of an interstitial with mass $\tilde{M}$ coupled by central and noncentral force constants $\tilde{f} = \lambda$ and $\tilde{f}' = \lambda'$ to its six nearest neighbors, in a monoatomic f.c.c. lattice, with atomic mass $M = M_\mp$; of course we put $\lambda_1 = \lambda_2 = 0$.

The above considerations are meaningful only from a geometrical point of view, because the dynamics of a f.c.c. lattice, such as a rare-gas crystal, cannot of course be considered as the limiting case of a NaCl-type polar lattice, due to the substantial difference between the fields of force existing in these two types of lattice. Nevertheless the analytical form of our secular equations depends exclusively on the geometry of the perturbation, while the host lattice dynamics enters only through the explicit values of the frequencies and eigenvectors in the BZ integrals. Thus the only care we must take in performing these limits on the eqs (30) and (31) is to consider the three optic branches of the original diatomic lattice as branches of Einstein type whose frequency tends to infinity, and the three acoustic branches as the branches of the monoatomic f.c.c. lattice. By neglecting $\tilde{f}'$ the secular equations which are so obtained for the interstitial read:

$$1 + (\tilde{f}/M)(a^3/4\pi^3) \sum_{j=1}^{3} \int d\mathbf{g} (\omega_{gj}^2 - \omega_{\mathbf{g}j}^2)^{-1} \times (e_x^2(\mathbf{g}j) \sin^2 ag_x + \alpha e_y(gj) e_z(gj) \sin ag_y \sin ag_z) = 0, \quad (37.a)$$

$$\tilde{M}\omega^2 - \tilde{f} + \tilde{M}\omega^2(\tilde{f}/M)(a^3/4\pi^3) \sum_{j=1}^{3} \int d\mathbf{g} (\omega_{\mathbf{g}j}^2 - \omega^2)^{-1} \times e_x^2(\mathbf{g}j) \cos^2 ag_x = 0, \quad (37.b)$$

where $\mathbf{g}$, j, ω_{gj}, $\mathbf{e}(\mathbf{g}j)$, and a refer now to the f.c.c. lattice. Notice that the present results on the interstitial dynamics can be directly obtained starting from the equations of motion for a free atom and a perfect monoatomic f.c.c. lattice [17]. The first step is to introduce an additional lattice site I for the interstitial so that the new coordinate space has $3(N+1)$ dimensions, N being the number of atoms of the perfect lattice. Consider now the interstitial atom and the lattice as uncoupled systems, i.e.,

$$L_{\alpha\beta}(l, \mathrm{I}) = L_{\alpha\beta}(\mathrm{I}, l) = L_{\alpha\beta}(\mathrm{I}, \mathrm{I}) = 0,$$

where L denotes the dynamical matrix in the $3(N+1)$ dimensional space; one realizes immediately that

$$\psi_{\mathbf{g}j}(l) = \mathcal{N}^{-1/2} \times \begin{cases} \mathbf{e}(\mathbf{g}j) e^{i\mathbf{g}\cdot\mathbf{x}_l} & \text{for } l \neq \mathrm{I} \\ A^{1/2} \delta_{\mathbf{g},\mathbf{o}} \mathbf{e}(\mathbf{o}j) & \text{for } l = \mathrm{I} \end{cases} \quad (38)$$

are the $3(N+1)$ dimensional eigenvectors of the uncoupled-system. Indeed, they are solutions of the eigenvector equation

$$\Sigma_{l'\alpha'} L_{\alpha\alpha'}(l, l') \psi_{\alpha', \mathbf{g}j}(l') = \omega_{\mathbf{g}j}^2 \psi_{\alpha, \mathbf{g}j}(l),$$

A being a suitable real constant and $\mathcal{N}$ the normalization factor. The orthonormality condition for the eigenvectors (38) yields:

$$\mathcal{N} = N + \delta_{\mathbf{g},\mathbf{o}} A;$$

now we need the orthonormalized set (38) to be complete in the $3(N+1)$ dimensional space; one finds

$$\Sigma_{gj}\psi^{*}_{\alpha,\,g_j}(l)\psi_{\alpha',\,g_j}(l') \begin{cases} \delta_{\alpha\alpha'}(\delta_{ll'}-A/(AN+N^2)) & \text{for } l,\ l' \neq \mathrm{I} \\ \delta_{\alpha\alpha'}A/(A+N) & \text{for } l=l'=\mathrm{I} \\ \delta_{\alpha\alpha'}A^{1/2}/(A+N) & \text{for } l \neq l'=1, \end{cases} \tag{39}$$

so that, by choosing $A=N^2$ the completeness relations (39) are satisfied within terms of the order of N^{-1}.

We suppose now the interstitial atom to be in equilibrium at the center of the cage formed by the six n.n. atoms $l=\pm 1, \pm 2, \pm 3$ and to be coupled only with them through central force constants. The coupling force-constant tensor matrix reads:

$$\Lambda(\mathrm{I},\mathrm{I})=\begin{vmatrix} \tilde{f}/\tilde{M} & 0 & 0 \\ 0 & \tilde{f}/\tilde{M} & 0 \\ 0 & 0 & \tilde{f}/\tilde{M} \end{vmatrix};\ \Lambda(\pm 1,\mathrm{I})=\Lambda(\mathrm{I},\pm 1)$$

$$=\begin{vmatrix} -\tilde{f}/\sqrt{M\tilde{M}} & 0 & 0 \\ 0 & 0 & 0 \\ 0 & 0 & 0 \end{vmatrix} \text{ and cyclic permutations; } \Lambda(\pm 1,\pm 1)=\begin{vmatrix} \tilde{f}/M & 0 & 0 \\ 0 & 0 & 0 \\ 0 & 0 & 0 \end{vmatrix}$$

and cyclic permutations: $\Lambda(l,l')=0$ otherwise.

We are now able to express the scattering matrix by using the same group analysis as in sec. 3.3, except that the set of eigenvectors (38) must be used. By taking into account that

$$(\mathrm{I}|(L-z)^{-1}|\mathrm{I})=-1/\omega^2,\ (\mathrm{I}|(L-z)^{-1}|\pm 1)=-1/N\omega^2\to 0,$$

the resonance conditions as expressed by eqs (37) are easily obtained. In this framework the interstitial atom presents some analogy with the substitutional defect: when $\tilde{M}$ is very small, a Γ_{15}-localized frequency appears, while a very small coupling ($\tilde{f}\to 0$) gives rise to a low Γ_{15}-resonance frequency. As regards breathing resonance modes (Γ_1 or Γ_{12} symmetry) only a large enough value of $\tilde{f}$ can produce resonances; beyond this, since $\tilde{f}>0$, resonance frequencies will occur when the BZ integral in eq (37.a) is negative, i.e., near the maximum frequency of the host lattice or in the upper region. To give a qualitative idea about these considerations, we calculate the BZ integrals in eqs (37) for a monoatomic chain, for which

$$M\omega_g^2=4f\sin^2(ag/2),$$

where f is the host lattice n.n. force constant. Using the nondimensional notations

$$\beta\equiv\tilde{M}/M,\qquad \gamma\equiv\tilde{f}/4f \text{ and } x\equiv\omega^2M/4f$$

the odd-mode and even-mode resonance conditions, corresponding to Γ_{15} and Γ_1 (or Γ_{12} undifferently) modes, respectively, are

$$\beta x-\gamma-\gamma\beta x(1-\mathrm{Re}\sqrt{1-1/x})=0, \tag{40.a}$$

$$1+\gamma(1-\mathrm{Re}\sqrt{x/(x-1)})=0, \tag{40.b}$$

where Re denotes real part. The hyperbolas in the (β,γ)-plane which eq (40.a) represent are plotted in figure 2 for some values of the interstitial resonance frequency x. The cases $x<1$

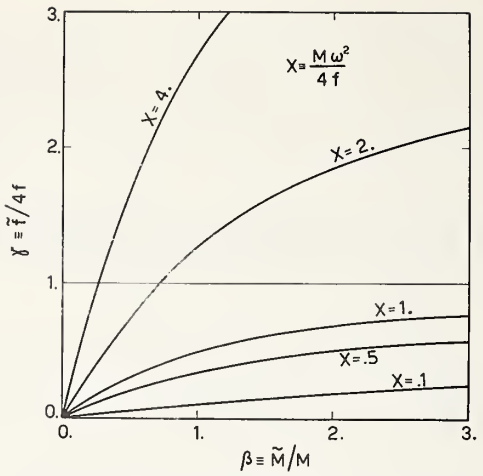

FIGURE 2. *Interstitial atom in a linear chain: odd-mode resonance frequency mapped as a function of the interstitial mass and coupling constant.*

and $x > 1$ correspond to resonance and localized modes, respectively. Equation (40.b) for $\gamma > 0$ gives only the localized frequency

$$x_{\text{even}} = (1+\gamma)^2/(2\gamma+1).$$

Do models 3.2 and 3.3 give a good picture of substitutional or interstitial defects in rare gas crystals or metals? For a neutral impurity in a solid rare gas (say another rare gas or a hydrogen atom) they surely do because the impurity-lattice interaction can be well described in terms of short range potentials (like the 6–12) usually employed for the host lattice dynamics [18] which,

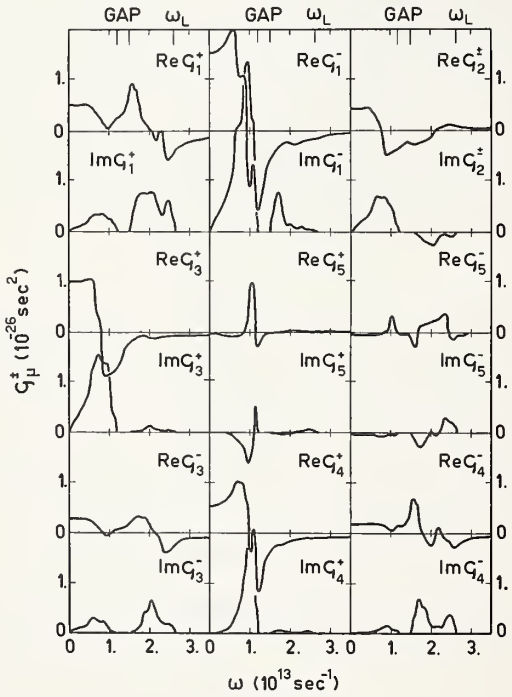

FIGURE 3. *The complex valued BZ integrals involved in the scattering matrix for defects in a KI crystal.*
Numerical values correspond to; $T = 0$ °K. Only seven of these ten integrals are linearly independent.

in first approximation, may be cut at the nearest neighbors. Furthermore these models probably hold also in metals. In spite of the fact that in several metals, like metallic sodium, the ion-ion interaction is long range in character ($\varphi(r)$ behaving like r^{-3}), the screening capability of the electrons seems, indeed, to be large enough to prevent the perturbation on the force constants to extend beyond the first neighbors [19].

4. The n.n. Effective Force Constant in Alkali Halides and Numerical Results for KI

Let us now apply eqs (30) and (31) to a doped alkali halide crystal. To evaluate the BZ integrals a *good* knowledge of the host lattice dynamics is required, particularly for values of the frequency belonging to the vibrational continuum: here we have used for KI the Hardy DD model [13], with zero temperature input data and a grid of 4409 **g**-values in the BZ.

In figure 3 the ten complex-valued integrals involved in the scattering matrix and secular equations (30) are reported.

In figure 4 the fractional change in n.n. force constant is plotted versus both Γ_1 and Γ_{12} resonance frequencies for either positive or negative defects, according to eq (30.a). The resonance conditions for Γ_{15}-modes are shown in figure 5 and figure 6 for positive and negative defects, respectively: here the resonance frequency ω_r is mapped as a function of the fractional changes of both mass and n.n. force constants. For a fixed value of ω_r the relation (30.b) between ϵ and $\lambda=\tilde{f}_{\text{eff}}-f_{\text{eff}}$ is represented by a hyperbola. We have used here the concept of the n.n. effective force constant f_{eff}. For a defect of given ϵ the value of λ can be obtained by fitting an experimental resonance frequency to these plots. To obtain theoretical support for the interpretation of such a fitted value of λ we try now to define a n.n. effective force constant according to the DD model. In the DD model the force-constant tensor matrix is

$$\phi^{(DD)}=\phi^{(R)}+(1+Se^{-1})\phi^{(c)}(1-e^{-1}\alpha e^{-1}\phi^{(c)})^{-1}(1+e^{-1}\tilde{S}) \tag{41}$$

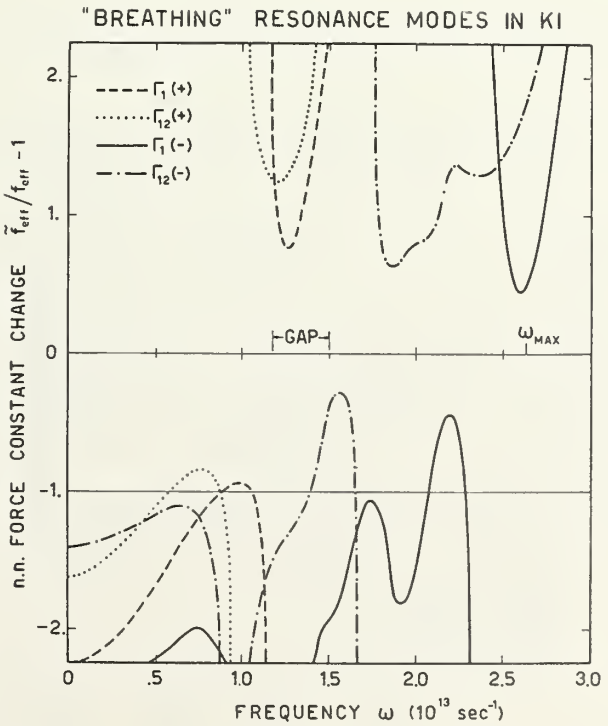

FIGURE 4. *The change in n.n. effective force constant plotted versus Γ_1 or Γ_{12} resonance frequency for positive or negative defects in* KI *at* T = 0 °K, *with* $f_{\text{eff}}=2.210\times10^{4}$ *gr sec*$^{-2}$.

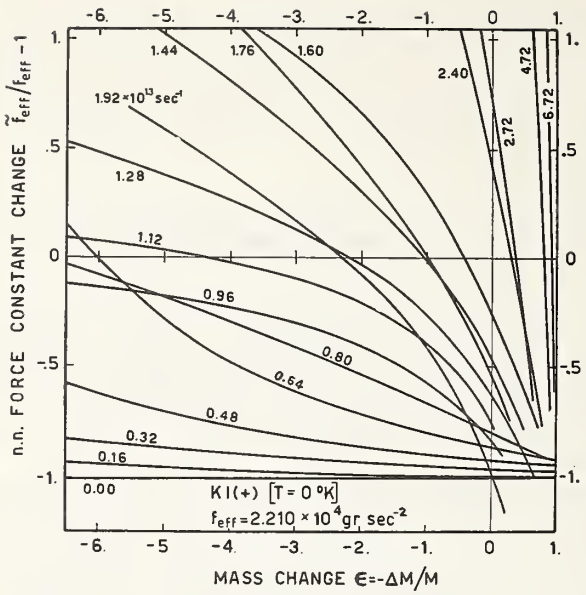

FIGURE 5. *Γ_{15}-resonance frequency is mapped as a function of the changes in mass and n.n. effective force constant for positive defects in* KI.

where $\phi^{(R)}$ is the n.n.-repulsive term, $\phi^{(c)}$ the coulomb term, e the ionic charge matrix, α the polarizability, S the deformation dipole matrices (see ref. 13), and $\tilde{S}$ the transpose of S. Near $\mathbf{g}=0$, $\phi^{(DD)}$ admits the decomposition

$$\phi^{(DD)}=\phi^{(R)}_{\text{eff}}+\phi^{(c)}_{\text{eff}} \tag{42}$$

where $\phi^{(c)}_{\text{eff}}$ is a coulomb-type force constant matrix with effective charge equal to e_s^* (Szigeti effective charge) and is considered unaffected by the presence of the defect. $\phi^{(R)}_{\text{eff}}$ is a overlap type

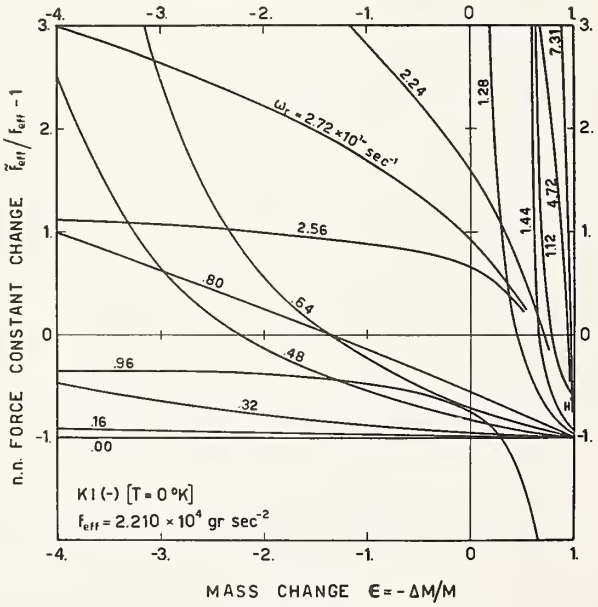

[1]FIGURE 6. *Same caption as figure 5 for negative defects in* KI.
The hyperbola for $\omega_r=7.31\times10^{13}$ sec^{-1} corresponds to the experimental localized frequency for *U*-center (H).

force-constant matrix with the n.n. effective force constant given by

$$f_{\text{eff}}=\frac{e^2}{v}\left\{A+2B-\frac{8\pi}{3}\left(\frac{e_s^*}{e}\right)^2\frac{\alpha_+ +\alpha_-}{\alpha_+ +\alpha_- +3v/8\pi}\right\}. \tag{43}$$

$v=2r_0^3$ is the cell volume, $\alpha_\pm$ the ion polarizabilities, e the electronic charge, while

$$A=(2v/e^2)\left[\partial^2\varphi^{(R)}(r)/\partial r^2\right]_{r_0}$$

and (44)

$$B=(2v/e^2)\left[\partial\varphi^{(R)}(r)/r\partial r\right]_{r_0}$$

are the central and noncentral force constants, respectively, due to n.n. core repulsive potential $\varphi^{(R)}(r)$.

By assuming that our decomposition (42) holds to a good approximation for all $\mathbf{g}$'s, we can write

$$\lambda=\tilde{f}_{\text{eff}}-f_{\text{eff}}; \tag{45}$$

$\tilde{f}_{\text{eff}}$ is given by the same eq (43), where now all parameters refer to defect-n.n. interaction and r_0 is replaced by the defect-n.n. equilibrium distance in the host lattice. Due to the effects of polarizability it appears from eq (43) that $\tilde{f}_{\text{eff}}$ may be negative when $A+2B$ is sufficiently small. It follows that small impurity ions may be unstable, at the center of the cage formed by the n.n. ions [20, 21]. This means that for $\tilde{f}_{\text{eff}}=0$, i.e., $\lambda=-f_{\text{eff}}$, the Γ_{15}-resonance frequency must vanish. From eq (30.b) we see that this occurs for:

$$-\lambda_{(\omega=0)}=\{v/8\pi^3\Sigma_j\int d\mathbf{g}\omega_{gj}^{-2}[M_\pm^{-1/2}e_x(\pm|\mathbf{g}j)-M_\mp^{-1/2}e_x(\mp|\mathbf{g}j)\cos r_0g_x]^2\}^{-1}. \tag{46}$$

The quantity $-\lambda_{(\omega=0)}$ evaluated from eq (46) is found equal to f_{eff} as given by eq (43) within 2 percent. This fact well supports the present definition of f_{eff}. In table 1 the values of the change in force constant calculated by this method are compared with the fitted values. The agreement can be said to be satisfactory if we consider that $\tilde{f}_{\text{eff}}$ depends strongly on the n.n. elastic relaxation ξ around the defect and that the Brauer method [21] we have used for evaluating ξ gives only a rough estimation of the n.n. elastic relaxation (see table 1). In these calculations the Born-Mayer form was used for $\varphi^{(R)}(r)$; for Ag^+ and Tl^+ van der Waals terms were included also. In the last column of table 1 the resonance frequency used in the fitting is reported. Any other experimental resonance which may be activated by a given defect should be consistent with the fitted value of λ. Indeed for KI:Cl^- we see in figure 7 that some other resonances are predicted in the low frequency region which agree with the experimental absorption peaks better than those predicted by the

TABLE 1. *Fitted and calculated defect-nearest neighbor effective force constants*

Crystal	Fitted $\tilde{f}_{\text{eff}}/f_{\text{eff}}$	Calculated $\tilde{f}_{\text{eff}}/f_{\text{eff}}$	Calculated n.n. elastic relax. (%)	Mass change ϵ	Explt. res. frequency used in fitting (10^{13} sec^{-1})
KI:Na^+	~0.18	0.25	−2.0	0.411	~1.2
KI:Tl^+	1.27	1.33	0.6	−4.22	1.23
KI:Ag^+	0.072	0.045	−7.0	−1.77	0.33
KI:Cl^-	.50	.58	−4.2	0.719	1.45
KI:H^-	.38	.....	−5.0	.992	7.31

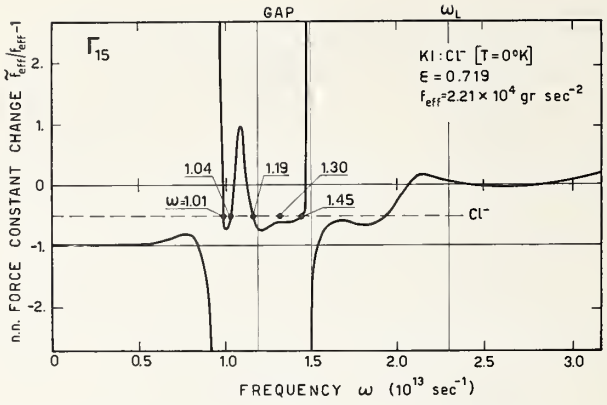

FIGURE 7. *The charge in n.n. effective force constant versus* Γ_{15}*-resonance frequency for* KI : Cl^- ($\epsilon = 0.719$).
The intersections of this curve with the abscissa give the resonance frequencies for mass-defect models (compared with ref. 12). Excellent fitting to the experimental IR spectrum is found by assuming the $Cl^- - K^+$ interaction to be *softer* than the $I^- - K^+$ interaction: the broken line indicates the fitted f_{eff}.

simple mass defect model. However, the present model is unable to predict the weak absorption peak which has been observed [12] at 72 cm^{-1} ($\omega_r = 1.36 \times 10^{13}$ sec^{-1}). Note that both fitting and theory show that for Cl^- in KI a softening in n.n. force constant occurs, in contrast with what was argued in reference 12. For KI:H^-, on the basis of the fitted value of λ (which is found to be equal to -0.51 in units of $A+2B$, in perfect agreement with the value calculated previously by the shell model [23]) two other resonances, $\omega_r = 1.15 \times 10^{13}$ sec^{-1} and $\omega_r = 1.56 \times 10^{13}$ sec^{-1}, are expected to occur: the first, localized in the gap, agrees very well with that observed by Sievers [9]; the second has not been observed till now.

On the contrary the broad absorption peak observed in KI:Tl^+ near the acoustic edge is not expected from the value of λ fitted to the sharp peak frequency. However, as we have demonstrated extensively elsewhere [7], the infrared absorption spectrum depends on the phonon spectrum of the host lattice in such a way that structure may appear even if the resonance condition is not satisfied, or, vice versa, no absorption peak may be observed at a resonance frequency when it falls in a region of high density of host lattice frequencies; thus some care must be paid in interpreting experimental data.

As a final remark it is interesting to note that the plots in figures 5 and 6 give the possibility of assigning the experimental resonance frequencies due to "external" modes of a molecular impurity. These external modes, which can be of vibrational or librational kind, were recently observed as "sidebands" of internal high frequency modes [11]. The symmetry of such defects is usually lower than O_h-symmetry but the departure from the O_h-symmetry is often small (e.g., small splitting of the degeneracy) so that the Γ-type irreducible representations can be used in first approximation. Consider for example the linear molecule NCO^- as a substitutional defect in KI ($\epsilon = 0.669$): two sharp doublets $\omega_{a1} = 1.47$, $\omega_{a2} = 1.55$ and $\omega_{b1} = 2.87$, $\omega_{b2} = 3.24$, a broad doublet $\omega_{c1} = 2.24$, $\omega_{c2} = 2.51$ and two other broad structures $\omega_d = 1.11$ and $\omega_e = 0.59 \times 10^{13}$ sec^{-1} are observed at $T = 100$ °K. From a more detailed plot than that reported in figure 6 one finds that ω_{a1}, ω_{b1}, ω_d are well consistent with the value $\tilde{f}_{eff,1}/f_{eff} = 0.80$, while ω_{a2}, ω_{b2}, $\sim \omega_d$ with the value $\tilde{f}_{eff,2}/\tilde{f}_{eff} = 2.0$. Thus it seems possible to assign these frequencies to translational modes of transverse type ($\tilde{f}_{eff} = \tilde{f}_{eff,2}$) and longitudinal type ($\tilde{f}_{eff} = \tilde{f}_{eff,1}$) with respect to the molecular axis.

The encouraging results we have obtained for doped KI and several other alkali halides [7] enable us to believe that a close comparison between experimental results and the theoretical calculations based on refined dynamical models constitutes a valid instrument for the investigation of the interatomic forces in crystals.

5. References

[1] A. A. Maradudin, in Theoretical and experimental aspects of the effects of point defects and disorder on the vibrations of crystals—Scient. Paper 65-9FS-442-PS-May 6, 1965—Westinghouse Research Labs. 35, Pa.

[2] We may have more than one parameter, if force constants of central and noncentral type are separately considered.

[3] C. T. Sennett, J. Phys. Chem. Solids **26**, 1097 (1965).

[4] A. J. Sievers and S. Takeno, Phys. Rev. **140**, A1030 (1965).

[5] L. Genzel, K. F. Renk and R. Weber, Phys. Stat. Sol. **12**, 639 (1965).

[6] G. Benedek and G. F. Nardelli, Phys. Rev. Letters **16**, 517 (1965).

[7] G. Benedek and G. F. Nardelli, to be submitted to Phys. Rev.

[8] G. F. Nardelli and N. Terzi, J. Phys. Chem. Solids **25**, 815 (1964).

[9] A. J. Sievers, Bull. Am. Phys. Soc. **9**, 228 (1964); Phys. Rev. Letters **13**, 310 (1964) and **15**, 1020 (1965) and Phys. Letters **14**, 271 (1965).

[10] K. F. Renk, Phys. Letters **20**, 137 (1966).

[11] M. A. Cundill and W. F. Shermann, Phys. Rev. Letters **16**, 570 (1966).

[12] A. J. Sievers, A. A. Maradudin, S. S. Jasval, Phys. Rev. **138**, A272 (1965).

[13] J. R. Hardy, Phil. Mag. **7**, 315 (1961).

[14] M. Lifshitz, Nuovo Cimento Suppl. **4**, 7716 (1956).

[15] M. Klein, Phys. Rev. **141**, A716 (1966).

[16] A. A. Maradudin, in Astroph. & Many-Body Probl. (Benjamin Inc., 1963).

[17] We are indebted to Dr. R. J. Elliott for having suggested this alternative way to investigate the interstitial dynamics.

[18] J. Grindlay and R. Howard in Proc. Int. Conf. on lattice dynamics, Copenhagen 1963 (Pergamon Press 1965).

[19] J. S. Langer and J. H. Vosko, J. Phys. Chem. Sol. **12**, 196 (1960).

[20] G. J. Dienes, R. D. Hatcher, R. Smoluchowsky, and W. Wilson, Phys. Rev. Letters **16**, 25 (1966).

[21] J. A. D. Matthew, Sol. St. Comm. **3**, 365 (1965).

[22] Y. Fukai, J. Phys. Soc. Japan **18**, 1413 (1963).

[23] R. Fieschi, G. F. Nardelli, N. Terzi, Phys. Rev. **138**, A203 (1965).

Comment on the Paper of G. Benedek and G. F. Nardelli

Wm. M. Hartmann

Argonne National Laboratory, Argonne, Ill. 60439

Professor Nardelli has pointed out that an "in-band" resonance may not be seen in the infrared absorption spectrum if the density of unperturbed vibrational states is high at the frequency of the resonance. In other words, when a resonance occurs at a frequency where there is a large number of modes of the perfect system the resonant mode will decay rapidly and its line will be so broad that it will not appear as a separate peak in the absorption.

There is another possible explanation for a resonance which does not appear in the absorption spectrum. Wolfram and Callaway[1] have considered the imperfect crystal density of states in the region of a resonance for magnetic systems. They find that at some resonances called "anti-resonances" the density of perturbed states is less that that of the unperturbed states; a dip, instead of a peak, should appear in the spectrum. Application of Wolfram and Callaway's idea to the phonon problem would suggest that the occurrence of a resonance or an antiresonance is determined by the sign of the derivative of a resonance curve, such as Professor Nardelli's figure 7, at the resonance frequency. The general rule still applies that both the peak and the dip in the absorption spectrum should be less pronounced at frequencies where the unperturbed density of states is high. A more detailed discussion of this idea for vibrating systems with mass and force constant changes is presently being written for publication.

[1] T. Wolfram and J. Callaway, Phys. Rev. **130**, 2207 (1963).

One-Phonon Infrared Absorption in a Rare Gas Crystal Induced by Rare Gas Defects

Wm. M. Hartmann*

Argonne National Laboratory, Argonne, Ill. 60439

The far infrared absorption of argon crystals with 1 percent krypton and ½ percent xenon impurities has been measured at 80 and 55 °K respectively [1] [1] (fig. 1). It is the purpose of this paper to begin a theoretical discussion of the experimental results by solving a very simple model, approximating the actual physical system only crudely, but of some interest in itself.

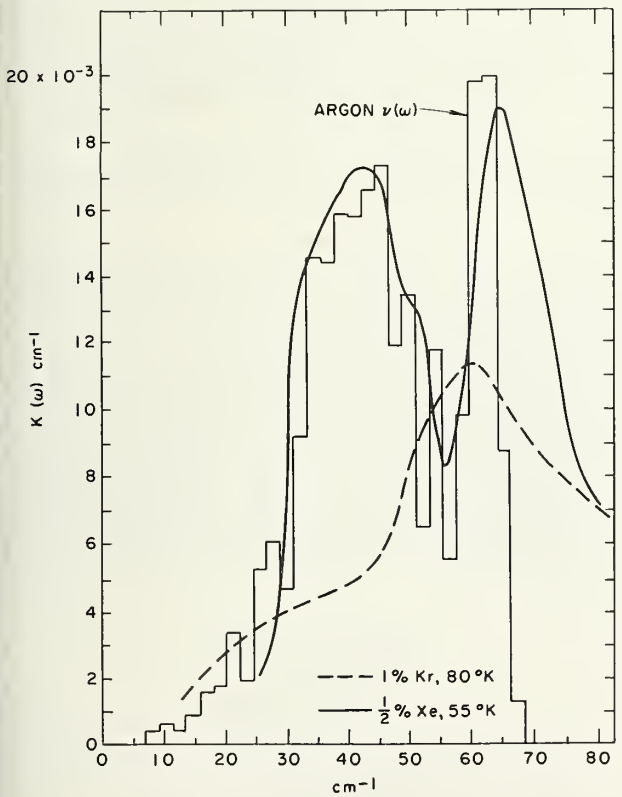

FIGURE 1. *Experimental infrared absorption; calculated one-phonon density of states, nearest-neighbor interaction model.*

The harmonic vibrations of an argon crystal can be made optically active to first order in the dipole moment operator if two conditions are met. The inversion symmetry of the f.c.c. structure must be destroyed, accomplished by the introduction of defects, and the uncharged atoms must be made polarizable. The atomic polarizability is introduced theoretically by an approximate shell model [2,3] with harmonic dynamical equations

$$\begin{aligned} m\omega^2 u_{\alpha l} + \sum_{l'\beta} (A+\kappa)_{ll'\alpha\beta} u_{l'\beta} + (B-\kappa)_{ll'\alpha\beta} v_{l'\beta} = 0 \\ M\omega^2 v_{\alpha l} + \sum_{l'\beta} (\tilde{B}-\kappa)_{ll'\alpha\beta} u_{l'\beta} + (D+\kappa)_{ll'\alpha\beta} v_{l'\beta} = 0. \end{aligned} \tag{1}$$

The symbols m, M and $u_{l\alpha}$, $v_{l\alpha}$ stand for the masses and the displacements in the αth direction for core and shell of the lth atom. A, B, and D are nearest-neighbor force constants, and since cores and shells have a charge $+ze$ and $-ze$, κ represents the long range Coulomb interaction. A single defect atom of mass m' and an internal force constant equal to $B_{ll\alpha\alpha} + c$ may be introduced by adding

$$\left.\begin{aligned} &[-(c+\omega^2(m-m'))u_{l'\beta} + cv_{l'\beta}]\,(\delta_{ll'}\delta_{\alpha\beta} \equiv \delta_l) \\ &\text{and} \\ &[cu_{l'\beta} - cv_{l'\beta}]\delta_l \end{aligned}\right\} \tag{2}$$

to the right-hand sides of eqs (1). Notice that with force constants so changed a uniform translation of the crystal results in no force on any atom. In addition, the charges on the shell and core of the defect atom may be changed equally and oppositely by an amount

$$e\left(\frac{z'-z}{z} \equiv dz\right) z.$$

It is useful to transform to coordinates

$$\xi = \frac{mu+Mv}{m+M}$$

and $\mu = u - v$, the center of mass and relative internal displacements. Assuming $M \ll m$, we find from (1) in matrix notation

*Present address: Solid State Science Division, Argonne National Laboratory, Argonne, Ill. 60439.

[1] Figures in brackets indicate the literature references at the end of this paper.

$$m\omega^2\xi = [R + \delta_{ll'}\omega^2(m - m')]\xi + S\mu$$

$$M\omega^2\mu = \tilde{S}\xi + [T + \delta_{ll'}(c + (M - M')\omega^2) + \Delta\kappa]\mu, \quad (3)$$

where

$$\begin{aligned} R &= A + 2B + D \\ S &= -B - D \\ T &= D + \kappa \end{aligned} \quad (4)$$

and where $\Delta\kappa$ results from the change dz. The equations for the perfect crystal are obtained by setting $(m - m') = c = (M - M') = \Delta\kappa = 0$. These perfect equations have solutions of acoustic and optic forms. At acoustic frequencies the shell is considered to feel no force due to core displacements and

$$S\xi = -T\mu. \quad (5)$$

Then substituting we find an acoustic equation for the center of mass

$$m\omega^2\xi = (R - \tilde{S}T^{-1}S)\xi \equiv R'\xi. \quad (6)$$

The optic solution represents the motion of atomic electrons as influenced by other atoms in the cyrstal. If the core is too heavy to follow the electronic motion, $\xi = 0$ and

$$M\omega_e^2\mu = T\mu. \quad (7)$$

We approximate the electronic motion by an isotropic Einstein oscillator. Since the Fourier transform $T(\bar{k}) = \sum_{l'} e^{i\bar{k}\cdot(\bar{r}_l - \bar{r}_{l'})} T_{ll'}$ is then independent of $\bar{k}$, $T_{ll'}$ is diagonal on ll' and we take $T_{ll'\alpha\beta} = M\omega_e^2\delta_{ll'}\delta_{\alpha\beta}$, where $\omega_e = 12.2$ eV, an exciton frequency. This approximation results in a great simplification of the equations. For the imperfect crystal c and $\Delta\kappa$ are considered to be only a lumped change c in the diagonal elements of T.

The properties of the imperfect crystal expressed in terms of Green functions G for the type introduced by Elliott and Taylor [4] may be calculated from perfect crystal Green functions

$$P^{\eta\eta'}_{ll'\alpha\beta}(\omega) = \sum_{j\bar{k}} \frac{\sigma^{\eta, j}_{\alpha}(\bar{k})\sigma^{\eta', j}_{\beta}(\bar{k})}{\omega^2 - \omega_j^2(\bar{k})} e^{i\bar{k}\cdot(\bar{R}_l - \bar{R}_{l'})} \quad (8)$$

where $\eta = 1$ or 2 for core or shell; σ's represent appropriate eigenvectors of the dynamical matrix equations.

In matrix form

$$G = P - PVG, \quad (9)$$

where V is a perturbation due to the defect. For a defect isolated in the $l = 0$ unit cell the solution to this equation is

$$G_{ll'} = P_{ll'} - P_{l0}C_{00}P_{0l'}, \quad (10)$$

where C is the 6×6 matrix, which for a cubic crystal is diagonal on $\alpha\beta$:

$$C^{\eta\eta'} = \frac{\begin{bmatrix} \omega^2 m\epsilon(cP^{22}_{00} - 1) & -\omega^2 m\epsilon cP^{12}_{00} \\ -\omega^2 m\epsilon cP^{21}_{00} & c(\omega^2 m\epsilon P^{11}_{00} - 1) \end{bmatrix} \delta_{\alpha\beta}}{\{1 - \omega^2 m\epsilon P^{11}_{00} - cP^{22}_{00} + c\omega^2 m\epsilon(P^{11}_{00}P^{22}_{00} - P^{12}_{00}P^{21}_{00})\}}, \quad (11)$$

ϵ is the mass change parameter $(m - m')/m$.

The correction $ST^{-1}S$ to R (eq (6)) is small and may be assumed to leave the form of R' the same as that of R, hence of S. But then using eq (5) we find from eq (8) in terms of $\lambda = -S/R'M\omega_e^2$

$$P^{12} = \lambda(m\omega^2 P^{11} - 1), \quad (12)$$

$$P^{22} = \lambda^2 m(m\omega^4 P^{11} - \omega^2 - \overline{\omega^2}) + \frac{1}{M(\omega^2 - \omega_e^2)}, \quad (13)$$

where $\overline{\omega^2} = \frac{1}{3N}\sum_{j\bar{k}} \omega_j^2(\bar{k}) = \int_0^{\omega_m} \nu(\omega)\omega^2 d\omega$, and $\nu(\omega)$ is a normalized density of one-phonon states with maximum frequency $\omega_m = 68$ cm^{-1}. According to the adiabatic approximation only P^{22} includes a contribution from the optic modes.

A specific calculation will involve the density of one-phonon states, here calculated from a simple nearest-neighbor interaction model (fig. 1) [5]. The additional parameters z or $M = 2.73$ electrons and $\lambda = 2.34 \times 10^{-6}$ g^{-1}(r/s)$^{-2}$ may be found from the polarizabilities of the free argon atom and the atom in the crystal [6], the density [7], and ω_e [8] together with the rules

$$\begin{aligned} B(k = 0) &= -A(0) \\ B(0) &= -D(0). \end{aligned} \quad (14)$$

A rough guide for choosing defect parameters c and dz may be drawn from the exciton frequencies in the imperfect crystals [9, 10].

Finally we may write an expression for the optical absorption coefficient K in terms of the imperfect crystal Green function for relative core-shell displacement, G^{22}. The Green function (1) to first order in the defect concentration ζ is easily found from the zeroth order Green function (0) by multiplying the defect part of $G^{(0)}$ by ζ. To first order in the concentration, valid for this experimental system,

$$K(\omega)=\left(\frac{4\pi e^2\Lambda}{\eta v_c V}\equiv U\,\frac{2}{\pi}\right)\omega^2 z^2\ \mathrm{Im}\left\{\sum_{ll'} G^{(1)22}_{ll'}\right.$$

$$\left.+2\zeta(dz)\sum_{l'} G^{(0)22}_{0l'}+\zeta(dz)^2 G^{(0)22}_{00}\right\}, \qquad (15)$$

where η is the refractive index of argon, v_c the velocity of light, and V the unit cell volume. There is a local field correction factor $\Lambda=\left(\frac{\epsilon_A+2}{3}\right)^2$. The absorption coefficient may be found by substituting (11) with (12) and (13) into (10) and then (10) into (15).

If the defect is regarded as only an atom of different mass and shell-core charge ($c=0$) only the C^{11} element of C is nonzero and $K(\omega)$ results from only the defect atom itself.

$$K(\omega)=-(U=4.2\times10^{-6})z_{\mathrm{eff}}^2\zeta$$

$$\frac{\nu(\omega)/m}{\left(1-\epsilon\omega^2\int\frac{\nu(\omega')d\omega'}{\omega^2-\omega'^2}\right)^2+(\omega\epsilon\pi\nu(\omega)/2)^2}, \qquad (16)$$

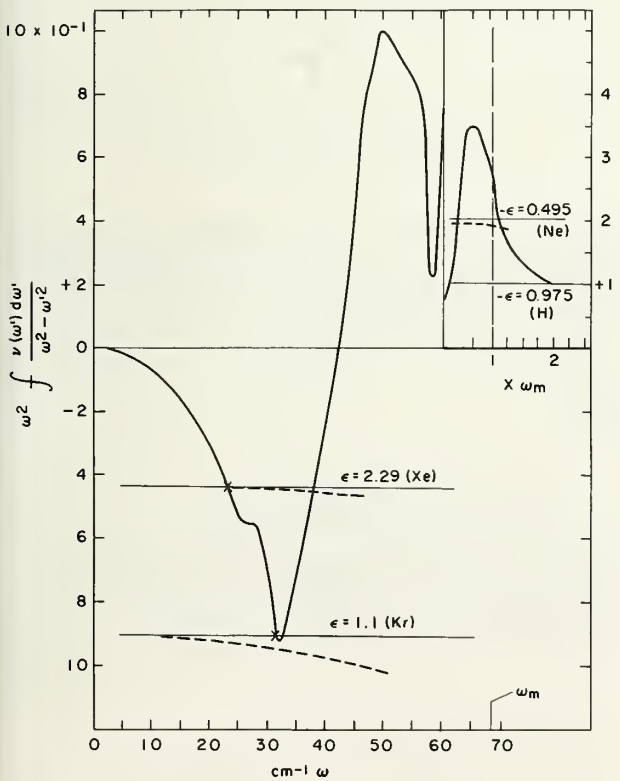

FIGURE 2. *Mass defect resonance condition,*

$$1/\epsilon=\omega^2\int\frac{\nu(\omega')d\omega'}{\omega^2-\omega'^2}.$$

where the effective charge

$$z_{\mathrm{eff}}=z\,dz\,m'\omega^2\lambda. \qquad (17)$$

For a light defect such as neon the local mode results in an absorption

$$K(\omega_l)=-Uz_{\mathrm{eff}}^2\zeta\left[m\epsilon^2\omega_l^4\int\frac{\nu(\omega')d\omega'}{(\omega_l^2-\omega'^2)^2}-m\epsilon\right]^{-1} \qquad (18)$$

The resonant condition for band modes is plotted in figure 2. It may be shown that the resonance occurs at that intersection where the slope is negative. The infrared absorption, which may be compared with experiment, is shown in figure 3.

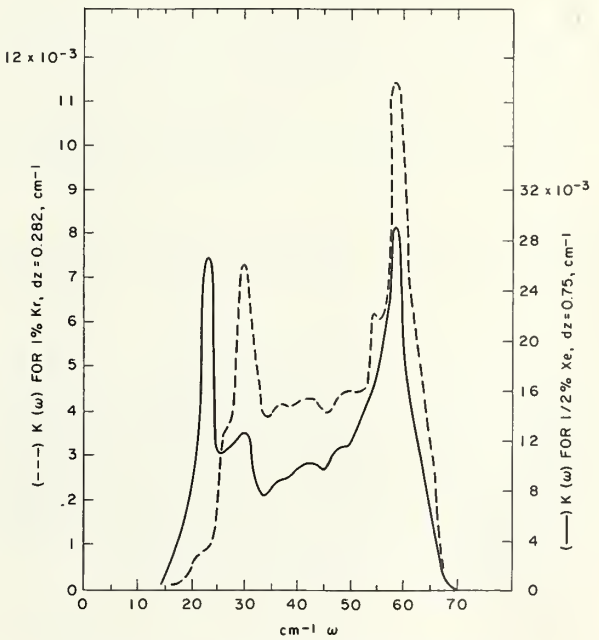

FIGURE 3. *Mass defect absorption coefficient.*

A calculation for $c\neq0$ is best done for a given value of ϵ. In figure 4 is plotted that value of c which will lead to a band resonance at ω_r. $c(\omega_r=0)$ is that value which effectively decouples the defect from the rest of the crystal; the asymptotic value for large ω_r is that value of c which ionizes the defect. The singularities in c occur at frequencies given by the dashed line in figure 2, close to the mass defect resonant frequencies; the conclusion drawn is that for physically reasonable values of the polarizability change c the resonant frequency cannot be shifted appreciably from the mass defect value.

The strength of the absorption, which now includes all of the atoms in the crystal, however, will vary with c. See figure 5, which may be compared with experimental results. The principal cause for the discrepancy would seem to be the anharmonic lattice vibrations certainly present within 5°

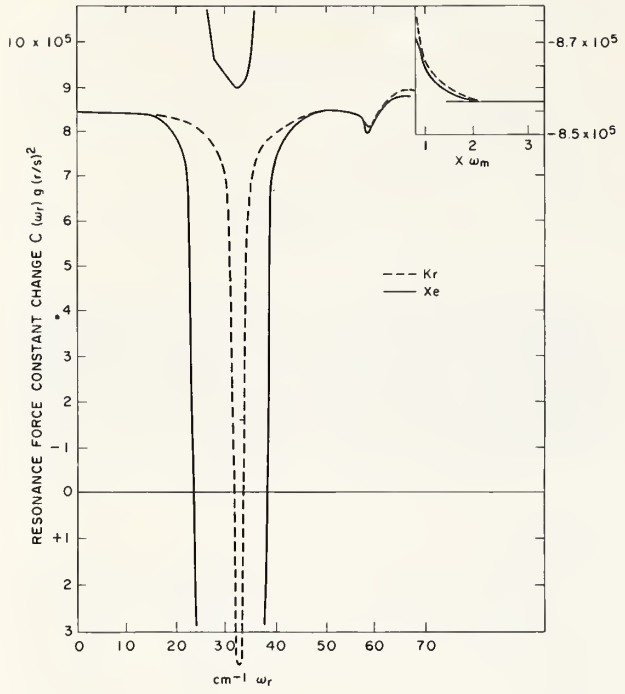

FIGURE 4. *Force constant resonance condition for* Kr *and* Xe *mass defects.*

of the melting point 85 °K. Whereas the experimental absorption for krypton defects is still appreciable at 120 cm^{-1}, no theory within the harmonic approximation will result in finite absorption beyond the one-phonon cutoff at 68 cm^{-1}. The most promising direction for further work on this problem would seem to be towards experiments at lower temperatures or an anharmonic theory.

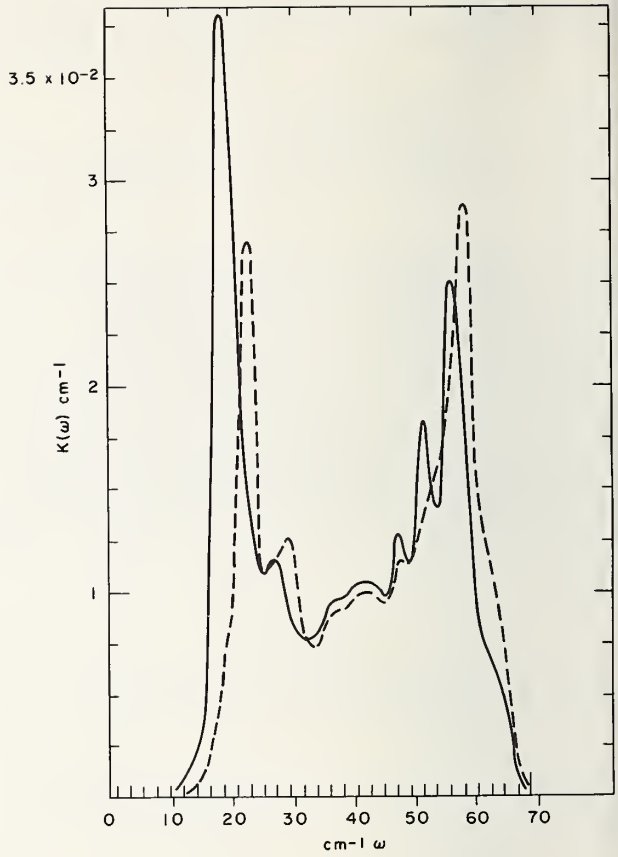

FIGURE 5. *Absorption coefficient for reasonable and unreasonable force constant changes with 1/2 percent xenon defect.*
---: $c = -1.88 \times 10^5\ g(r/s)^2$, $dz = 0.366$
——: $c = -8 \times 10^5\ g(r/s)^2$, $dz = -0.88$.

The author thanks Dr. R. J. Elliott for innumerable helpful discussions. The problem was suggested by Prof. G. O. Jones and the work supported by the Rhodes Scholarship Trust.

References

[1] G. Jones and M. Woodfine, Proc. Phys. Soc. (London) **86,** 101–103 (1965).
[2] B. J. Dick and A. W. Overhauser, Phys. Rev. **112,** 90–103 (1958).
[3] W. Cochran, Proc. Roy. Soc. (London) **253,** 260–276 (1959).
[4] R. J. Elliott and D. W. Taylor, Proc. Phys. Soc. (London) **83,** 189–197 (1964).
[5] Our formalism actually allows any computed density of states to be used; for example, J. Grindlay and R. Howard, Proc. Int. Conf. Lattice Dynamics, pp. 129–134 (ed. R. F. Wallis, Pergamon Press, 1965).
[6] R. H. Orcott and R. H. Cole, Physica **31,** 1779–1791 (1966).
[7] G. L. Pollack, Revs. Modern Phys. **36,** 748–791 (1964).
[8] G. Baldini, Phys. Rev. **128,** 1562–1567 (1962).
[9] G. Baldini, Phys. Rev. **136,** A248–251 (1964).
[10] G. Baldini, Phys. Rev. **137,** A508–513 (1965).

Vibrations in Molecular Lattices

K. Dettmann and W. Ludwig

Institut für Theoretische Physik, C, der T. H. Aachen, Institut für Reaktorwerkstoffe der KFA Jülich, Germany

In molecular lattices there can be translational and librational modes, which in general are coupled. If there is a molecular defect, incoming waves of given polarization can be scattered into another kind of polarization. Under certain conditions there might be resonance scattering. This scattering is investigated with the simple example of a linear molecular lattice, making the simplest assumptions on the structure and the intermolecular forces.

In a preceding paper (referred to as [1]) [1] we have investigated the possible localized states in a simple linear model of a molecular lattice. In this report we want to extend the discussion to the scattering states in such molecular lattices. We use the same model as in [1]: A linear arrangement of dumbbell-molecules, having an impurity-molecule at the origin. There are translational and librational modes. The stationary equation of motion for the ideal lattice can be written as

$$\lambda S_\mu^m = \sum_{n\nu} D_{\mu\nu}^{mn} S_\nu^n; \qquad S_\mu^m \sim e^{-i\omega t};$$

$$\lambda = \omega^2; \; D_{\mu\nu}^{mn} = (M_\mu M_\nu)^{-1/2} \phi_{\mu\nu}^{mn}. \tag{1}$$

The lower index μ, $\nu = 1$ refers to translational motion, μ, $\nu = 2$ to librational motion. M_1 is the total mass of the molecules, $M_2 = I$ is the moment of inertia. m is the number of the molecule. $\phi_{\mu\nu}^{mn}$ are the force-constants. The solution of the ideal lattice equation is

$$S_\mu^m(q\sigma) = \frac{1}{\sqrt{N}} e_\mu(q\sigma) e^{iqm}; \tag{2}$$

q is the wave number, σ the polarization (e.g., mainly translational or mainly librational). In the simplest model there are four independent force-constants [1], which we denote by

$$a = -4D_{11}^{10}; \qquad s = -4D_{22}^{10};$$

$$p = 2D_{22}^{10} + D_{22}^{00}; \qquad b = 2D_{12}^{10}; \tag{3}$$

b describes the coupling between translational and librational motion. We assume in the following $b < p < p+s < a$: such an assumption can be justified by a central-force-model. The secular equation is

$$\begin{Bmatrix} a \sin^2 q/2 - \lambda(\sigma) & -ib \sin q \\ ib \sin q & p + s \sin^2 q/2 - \lambda(\sigma) \end{Bmatrix} \begin{Bmatrix} e_1(\sigma) \\ e_2(\sigma) \end{Bmatrix} = 0. \tag{4}$$

The squared frequency spectrum is given in figure 1 (qualitatively).

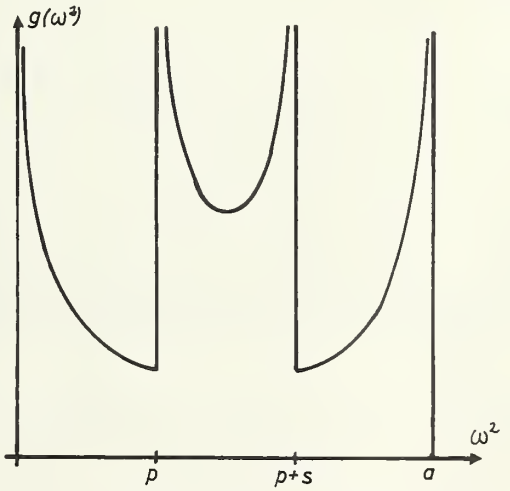

FIGURE 1. *Squared frequency distribution for a one-dimensional molecular lattice of dumbbell-molecules for a certain choice of parameters.*
The wings contain mainly translational modes, the width is a mixture of translational and librational motion.

If there is an impurity molecule in the lattice, the equation of motion can be written as [1]

$$\sum_{n\nu} D_{\mu\nu}^{mm} S_\nu^n - \lambda S_\mu^m = \sum_{n\nu} \mathcal{F}_{\mu\nu}^{mn} S_\nu^n \tag{5}$$

$\mathcal{F}_{\mu\nu}^{mn}$ describes the impurity molecule. If there is a change in mass and moment of inertia only (at the origin, e.g.,), then

$$\mathcal{F}_{\mu\nu}^{mn} = \lambda \epsilon_\mu \delta_{\mu\nu} \delta^{0m} \delta^{0n};$$

$$\epsilon_1 = \frac{M' - M}{M}; \qquad \epsilon_2 = \frac{I' - I}{I}. \tag{6}$$

[1] K. Dettmann and W. Ludwig, physica status solidi. **10**, 689 (1965).

256-724 O-67—13

The solution of (5) can be given as [1]

$$S=\mathring{S}+\mathcal{G}\mathcal{F}S, \tag{7}$$

$\mathcal{G}$ is the Green's function which satisfies the boundary conditions. For the scattering states, where $\mathring{s}$ is an incoming plane wave, $\mathcal{G}\,\mathcal{F}\,S$ has to represent outgoing scattered waves. With

$$\tau=(1-\mathcal{G}\mathcal{F})^{-1}, \tag{8}$$

we have

$$S=\mathring{S}+\mathcal{G}\mathcal{F}\tau\mathring{S}. \tag{7a}$$

In the case described by (6) a simple calculation gives

$$S_\mu^m=\mathring{S}_\mu^m+\sum_\nu \mathcal{G}_{\mu\nu}^{m0}\frac{\lambda\epsilon_\nu}{1-\lambda\epsilon_\nu\mathcal{G}_{\nu\nu}^{00}}\mathring{S}_\nu^0. \tag{9}$$

The Green's function is given in [1]:

$$\mathcal{G}_{\mu\nu}^{m0}(\lambda)=\frac{16}{as+4b^2}$$

$$\sum_{|z_i|\leq 1}\lim_{z\to z_i}\frac{(z-z_i)z^{m+1}K_{\mu\nu}(z;\,\lambda)}{(z-z_1)(z-1/z_1)(z-z_2)(z-1/z_2)}, \tag{10}$$

$$m>0$$

$$\mathcal{G}_{\nu\nu}^{-m0}=\mathcal{G}_{\nu\nu}^{m0}; \qquad \mathcal{G}_{\mu\nu}^{-m0}=-\mathcal{G}_{\mu\nu}^{m0}; \qquad \mu\neq\nu. \tag{10a}$$

The sum over z_i extends over all the roots z_1, $1/z_1$, z_2, $1/z_2$ inside the contour of integration. This is determined by the boundary condition. Figure 2

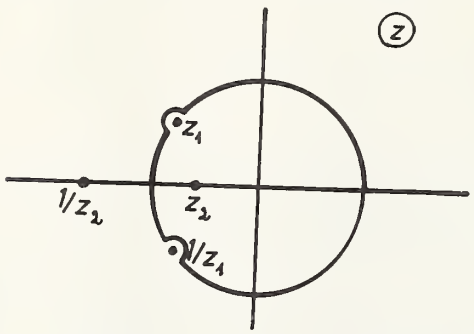

FIGURE 2. *Choice of the path of integration in the Green-function for* $p+s<\omega^2<a$.

shows the situation for $p+s<\lambda<a$. It is

$$(z_1)^{\pm 1}=M+\sqrt{M^2-N}\pm\sqrt{2M^2-N-1+2M\sqrt{M^2-N}}$$

$$(z_2)^{\pm 1}=M-\sqrt{M^2-N}\pm\sqrt{2M^2-N-1-2M\sqrt{M^2-N}}$$

$$M(as+4b^2)=a(p+s)-\lambda(a+s) \tag{11}$$

$$N(as+4b^2)=2ap+as-4b^2-2\lambda(2p+a+s)+4\lambda^2$$

$$K_{\mu\nu}(z;\,\lambda)=\begin{Bmatrix} p-\frac{s}{4z}(1-z)^2-\lambda & \frac{b}{2z}(1-z^2) \\ -\frac{b}{2z}(1-z^2) & -\frac{a}{4z}(1-z)^2-\lambda \end{Bmatrix}$$

From figure 2 it can be seen, that (for $p+s<\lambda<a$)

$$\mathcal{G}_{\mu\nu}^{m0}(\lambda)=\frac{4}{(as+4b^2)\sqrt{M^2-N}}$$

$$\left\{z_1^m\frac{K_{\mu\nu}(z_1;\,\lambda)}{z_1-1/z_1}-z_2^m\frac{K_{\mu\nu}(z_2;\,\lambda)}{z_2-1/z_2}\right\}. \tag{12}$$

Because $z_1=e^{iq}$; $|z_1|=1$, $z_2=e^{-\kappa}<1$ this means, that the first part in $\mathcal{G}$ represents a wave-like behavior, whereas the second part shows a localized behavior, decreasing exponentially with increasing m. For $p+s<\lambda<a$ the solutions of (5) for scattering states represent the following situation: There is an incoming plane wave of mostly translational character; this wave is scattered by the molecular impurity. In the scattering process a localized state is excited, which has mainly librational character. For the mainly translational scattered part of the wave one can define a backward and forward scattering amplitude by the asymptotic behavior of the waves. The second part of (12) can be dropped asymptotically. It can be proved simply, with the use of (10, 11), that (9) can be rewritten as

$$S_\mu^m=\frac{1}{\sqrt{N}}\left\{e_\mu e^{iqm}+F(-1)e_\mu e^{-iqm}\right\}$$

$$\text{for } m\to-\infty \tag{13}$$

with

$$F(-1)=\frac{4\lambda}{(as+4b^2)\sqrt{M^2-N}\,(z_1-1/z_1)}\cdot$$

$$\cdot\left\{\frac{\epsilon_1K_{11}(z_1;\,\lambda)}{1-\epsilon_1\lambda\mathcal{G}_{11}^{00}}-\frac{\epsilon_2K_{22}(z_1;\,\lambda)}{1-\epsilon_2\lambda\mathcal{G}_{22}^{00}}\right\}. \tag{13a}$$

$F(-1)$ is the backward scattering amplitude which can be related to the reflection coefficient

$$\mathcal{R}=|F(-1)|^2.$$

A similar expression holds for the forward scattering (transmission coefficient $\mathcal{T}$), but because

$$\mathcal{R}+\mathcal{T}=1$$

we will not give it here.

From (11) and figure 2 it can be seen, that $\mathcal{G}_{\nu\nu}^{00}$ contains a real (first) and an imaginary part (second part of (12)). Therefore the scattering amplitude shows a resonance behavior. The resonance "frequencies" λ_R are defined by

$$1=\frac{-4\lambda\epsilon_1}{(as+4b^2)\sqrt{M^2-N}}\cdot\frac{K_{11}(z_2;\,\lambda)}{z_2-1/z_2};\quad \text{if } \epsilon_2=0 \qquad (14a)$$

and

$$1=\frac{-4\lambda\epsilon_2}{(as+4b^2)\sqrt{M^2-N}}\cdot\frac{K_{22}(z_2;\,\lambda)}{z_2-1/z_2};\quad \text{if } \epsilon_1=0. \qquad (14b)$$

We discuss the cases $\epsilon_1\neq 0$, $\epsilon_2=0$ and $\epsilon_1=0$, $\epsilon_2\neq 0$ separately. By using the first (imaginary) part of (12) for $\mathcal{G}_{\nu\nu}^{00}$ it can be seen immediately from (13a) that $\mathcal{R}=1$ at the resonance frequencies in these simple cases. Figures 3 show the resonance frequencies ω_R and the widths γ of the resonances as a function of ϵ_1 or ϵ_2, resp. It is assumed $a=12$; $p=s=4$; $b=2$ here.

$$\epsilon_1=\frac{8}{\sqrt{\lambda(\lambda-8)}};\qquad \gamma=\frac{\lambda\sqrt{\lambda-8}}{2\sqrt{16-(8-\lambda)^2}};$$

$$\epsilon_2=-\frac{8\sqrt{\lambda-8}}{\lambda^{3/2}};\qquad \gamma=\frac{(\lambda-8)^{3/2}}{2\sqrt{16-(8-\lambda)^2}}. \qquad (15)$$

Figure 3 shows the position of the resonance frequencies relative to the frequency band of the ideal molecular lattice as well as the widths. For a change in total mass only, there are resonances if $\epsilon_1>2/\sqrt{3}$. This means a heavy mass, therefore we have nearly total reflection and the resonances are not very pronounced (width large). The reflection coefficient is shown in figure 4a. For smaller values of ϵ_1 or for negative ones, the reflection is smaller, but there are no resonances.

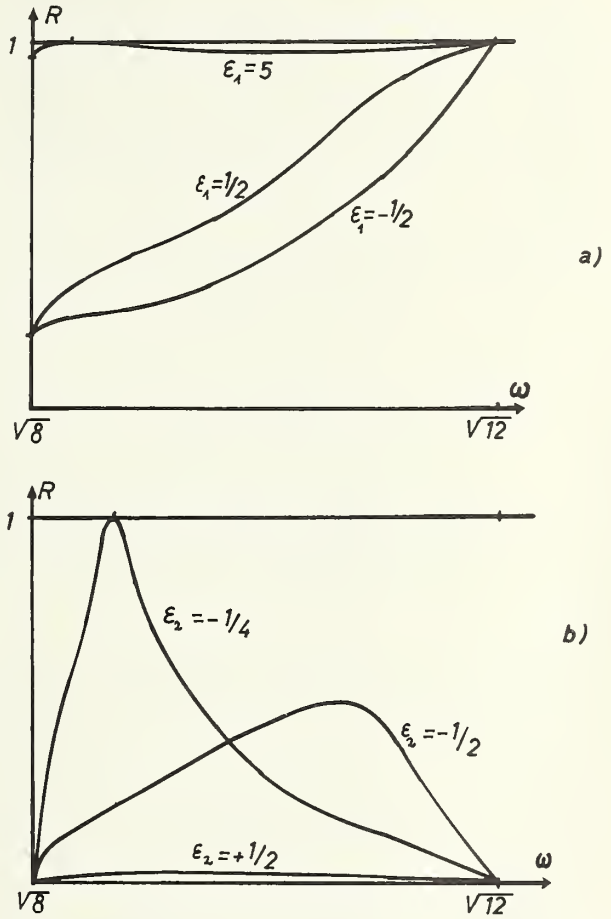

FIGURE 4. *Reflection coefficient in the band with* $p+s<\omega^2<a$ *as a function of* ω *for (a)* $\epsilon_1=5$, $\epsilon_1=\pm 1/2$, $\epsilon_2=0$ *and (b)* $\epsilon_2=-1/4$, $\epsilon_2=\pm 1/2$, $\epsilon_1=0$.

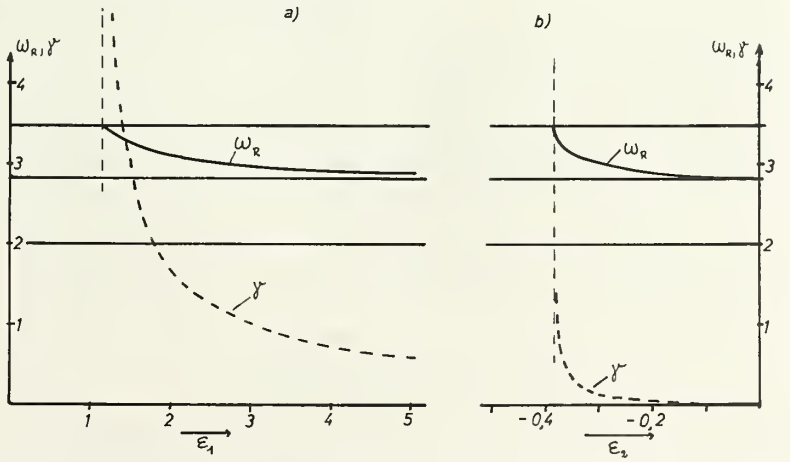

FIGURE 3. *Resonance frequencies in the band* $p+s<\omega^2<a$ *and widths as a function of (a)* ϵ_1 *with* $\epsilon_2=0$ *and (b)* ϵ_2 *with* $\epsilon_1=0$.

In the case of a change in the moment of inertia of the impurity molecule, there is a pronounced resonance, if $0 > \epsilon_2 > -0{,}385$; this resonance has a small width.

In the scattering process of the "translational" waves the molecule is excited to a "localized" librational motion. In the resonance this librational motion is especially pronounced. If $\epsilon_2 < -0{,}385$, we have localized librational states with frequencies above the maximal band frequency. The reflection coefficient (fig. 4b) shows the resonance phenomena for $\epsilon_2 = -1/4$, e.g., but not for $\epsilon_2 = +1/2$ or $-1/2$, e.g.

In general the reflection coefficient in the upper region of the spectrum (fig. 1) can be written as

$$2r_{1,2} = z_{1,2} + 1/z_{1,2}.$$

$\epsilon_2 = 0$:

$$\mathscr{R} = \frac{\epsilon_1^2 f_1^2(\lambda)}{[1-\epsilon_1 g_1(\lambda)]^2 + \epsilon_1^2 f_1^2(\lambda)},$$

$$f_1^2(\lambda) = \frac{4\lambda^2\left[p-\lambda-\frac{s}{2}(r_1-1)\right]^2}{(as+4b^2)^2(M^2-N)(1-r_1^2)},$$

$$g_1(\lambda) = \frac{2\lambda\left[\lambda+\frac{s}{2}(r_2-1)-p\right]}{(as+4b^2)\sqrt{M^2-N}\sqrt{r_2^2-1}}.$$

$\epsilon_1 = 0$:

$$\mathscr{R} = \frac{\epsilon_2^2 f_2^2(\lambda)}{[1-\epsilon_2 g_2(\lambda)]^2 + \epsilon_2^2 f_2^2(\lambda)},$$

$$f_2^2(\lambda) = \frac{4\lambda^2\left[\lambda+\frac{a}{2}(r_1-1)\right]^2}{(as+4b^2)^2(M^2-N)(1-r_1^2)},$$

$$g_2(\lambda) = \frac{2\lambda\left[\lambda+\frac{a}{2}(r_2-1)\right]}{(as+4b^2)\sqrt{M^2-N}\sqrt{r_2^2-1}}. \qquad (16)$$

The following general features can be seen from these relations. In the first case, the resonance frequency varies from $\omega_R^2 = p+s = \lambda_R$ for $\epsilon_1 = \infty$ to $\omega_R^2 = a$ (upper limit of band) for

$$\epsilon_1 = \frac{a[a-p-s-4b^2/a]^{3/2}}{4b^2\sqrt{a-p}} > 0 \qquad (18)$$

i.e., resonance does occur only if there is a coupling between librational and translational modes ($b \neq 0$). The width γ is zero for $\omega_R^2 = p+s$ and infinite for $\omega_R^2 = a$. If resonance occurs, the reflection coefficient has a certain finite value for $\omega^2 = p+s$, increases to one at ω_R, then decreases (slightly) and reaches again $R=1$ for $\omega^2 = a$. If there is no resonance, then R increases over the whole region from a finite value to one at $\omega^2 = a$.

In the second case, there is a resonance for

$$0 > \epsilon_2 > -\frac{1}{a}\sqrt{(a-p)[a-p-s-4b^2/a]} \qquad (19)$$

which does not vanish for $b=0$. Then it becomes truly "localized". γ shows the same behavior as in the first case, but it is smaller. The reflection coefficient is zero at $\omega^2 = p+s$, passes a maximum between these limits and is again zero for $\omega^2 = a$. The maximum value is $R=1$ at ω_R, if resonance occurs.

If both ϵ_1 and ϵ_2 are different from zero, the situation is more difficult, but qualitatively similar phenomena are possible.

This holds also, if the frequency of the incoming "translational" wave lies between $\omega = 0$ and $\omega^2 = p$. Quantitative differences occur. So resonances of the second kind are present if $0 < \epsilon_2 < \infty$.

If $p < \omega^2 < p+s$, no resonance scattering is possible (for single molecular defects). But because of the interaction it happens that an incoming wave of given polarization is scattered into outgoing waves, one of the original polarization and one of the other kind of polarization. Thus one has two reflection coefficients $\mathscr{R}_{\sigma\sigma'}$ and two transmission coefficients $\mathscr{T}_{\sigma\sigma'}$ with

$$\sum_{\sigma'} (\mathscr{R}_{\sigma\sigma'} + \mathscr{T}_{\sigma\sigma'}) = 1.$$

But these states are less interesting.

The Use of Morphic Effects for the Study of Vibrational and Optical Properties of Impurity Atoms in Crystals

A. A. Maradudin* and S. Ganesan*

Department of Physics, University of California, Irvine, Calif. 92664

and

E. Burstein**

Laboratory for Research on the Structure of Matter,

Department of Physics, University of Pennsylvania, Philadelphia, Pa. 19104

Morphic effects are effects induced in a crystal by the lowering of its symmetry through the application of a generalized external force. In this paper we study the effects of static electric fields and of strains on the frequencies of localized vibration modes associated with substitutional impurity atoms in ionic and homopolar crystals. It is shown that the splitting of the triple degeneracy of such modes when the impurity is at a site of cubic symmetry by the application of these generalized forces can yield valuable information about the anharmonic forces, electric dipole moment, and electronic polarizability associated with the impurity atom.

A crystal subjected to a generalized external force, such as a static electric or magnetic field, or a stress, shows several interesting effects, called *morphic effects*, which are the results of a general lowering of the symmetry of the crystal on the application of the force. They manifest themselves, among other ways, by lifting the degeneracies and shifting the frequencies of the normal modes of vibration, by altering the selection rules for various physical processes, making it possible for certain otherwise forbidden processes to occur, and by modifying the strengths of various optical transitions.

The effects of static electric fields and of a strain or stress are particularly interesting, and recently have been observed experimentally. Hayes, MacDonald, and Elliott [1] observed a splitting of the triply degenerate localized modes associated with U-centers at the F^- sites in CaF_2 (which have T_d symmetry) produced by either a static electric field or a uniaxial stress, and gave a phenomenological theory of these splittings.

We present in this paper a microscopic theory of these morphic effects. Until now a theory which relates the magnitudes of such splittings to the harmonic and anharmonic force constants with which the impurity is coupled to the atoms of the host crystal, and to the elements of the dipole moment and static electronic polarizability operators associated with the impurity and with its neighbors has not been available. We deal here with substitutional impurity atoms occupying sites having either T_d or O_h symmetry in nonionic dielectric crystals. The results become complicated in ionic crystals owing to the long range coulomb interactions.

First we consider the morphic effects induced by static electric fields. When an electric field E is present the interaction term in the crystal Hamiltonian is of the form [2]

$$-\sum_{\mu} M_{\mu}E_{\mu} - \frac{1}{2}\sum_{\mu\nu} P_{\mu\nu}E_{\mu}E_{\nu},$$

*Research supported by the Air Force Office of Scientific Research, Office of Aerospace Research, United States Air Force, under AFOSR Grant Number 1080–66.

**Research supported in part by the U.S. Office of Naval Research.

[1] W. Hayes, H. F. MacDonald, and R. J. Elliott, Phys. Rev. Letters **15**, 961 (1965).

[2] M. Born and K. Huang, Dynamical Theory of Crystal Lattices, p. 310 (Clarendon Press, Oxford, 1954).

where M_μ and $P_{\mu\nu}$ are the operators representing the electric dipole moment and static electronic polarizability of the crystal. Since they are functions of the atomic positions, we can expand these operators in powers of the displacements of the atoms from their equilibrium positions in the field-free crystal. The equations of motion for a dielectric crystal containing impurities in the presence of a static field, in the adiabatic approximation, can be written in terms of the displacements of the atoms as

$$-M_{lk}\ddot{\xi}(lk) = \bar{\Phi}_\alpha(lk) + \sum_{l'k'\beta} \bar{\Phi}_{\alpha\beta}(lk;\, l'k')\xi_\beta(l'k') + \frac{1}{2}\sum_{l'k'\beta}\sum_{l''k''\gamma} \bar{\Phi}_{\alpha\beta\gamma}(lk;\, l'k';\, l''k'')\xi_\beta(l'k')\xi_\gamma(l''k'') + \ldots . \tag{2}$$

Here $\xi_\alpha(lk)$ is the α-Cartesian component of the displacement of the kth atom in the lth unit cell, and the various $\bar{\Phi}$ coefficients are the sums of contributions from the unperturbed atomic force constants, dipole moments, and static electronic polarizabilities. The first term, which is independent of the displacements $\xi_\alpha(lk)$, shows that there is a force acting on the atoms in the presence of the field. We can write

$$\xi_\alpha(lk) = d_\alpha(lk) + u_\alpha(lk), \tag{3}$$

where $d_\alpha(lk)$ is the static displacement of the atom (lk) from its field free equilibrium position and $u_\alpha(lk)$ is the dynamic displacement from its new equilibrium position. In eq (3) we have omitted terms which arise from electrostriction, as they are of higher order than the ones we consider here.

The static displacement $d_\alpha(lk)$ can be determined from the condition that when all of the atoms are situated at the new equilibrium positions there is no force acting on any atom. This means that when we substitute eq (3) for $\xi_\alpha(lk)$ in the equations of motion and reexpand them in powers of the dynamic displacements $\{u_\alpha(lk)\}$, the term independent of $u_\alpha(lk)$ must be zero. Using this condition we get an expression for the effective harmonic force constants of a crystal in the presence of a static external electric field, which, to first order in the field components, is given by

$$\hat{\Phi}_{\alpha\beta}(lk;\, l'k') = \Phi_{\alpha\beta}(lk;\, l'k') + \sum_\mu E_\mu \Phi_{\mu,\,\alpha\beta}(lk;\, l'k'), \tag{4}$$

where the $\{\Phi_{\alpha\beta}(lk;\, l'k')\}$ are the unperturbed harmonic force constants and

$$\Phi_{\mu,\,\alpha\beta}(lk;\, l'k') = -M_{\mu,\,\alpha\beta}(lk;\, l'k') + \sum_{l''k''\gamma}\sum_{l'''k'''\delta} \Phi_{\alpha\beta\gamma}(lk;\, l'k';\, l''k'') \times \Gamma_{\gamma\delta}(l''k'';\, l'''k''')M_{\mu,\,\delta}(l'''k'''). \tag{5}$$

Here $\Phi_{\alpha\beta\gamma}(lk;\, l'k';\, l''k'')$ is the unperturbed cubic anharmonic force constant; $\Gamma_{\gamma\delta}(l''k'';\, l'''k''')$ is an effective inverse matrix of the matrix $\Phi_{\alpha\beta}(lk;\, l'k')$; $M_{\mu,\,\delta}(l'''k''')$ is the coefficient of the term in the expansion of the crystal dipole moment which is linear in the atomic displacement; and $M_{\mu,\,\alpha\beta}(lk;\, l'k')$ is the coefficient of the term in the expansion of the crystal dipole moment which is quadratic in the atomic displacements. Now the equations of motion in the harmonic approximation for a crystal subjected to a static external electric field can be written as

$$M_{lk}\ddot{u}_\alpha(lk) = -\sum_{l'k'\beta} \hat{\Phi}_{\alpha\beta}(lk;\, l'k')\, u_\beta(l'k'). \tag{6}$$

We can solve for the eigenvectors and eigenfrequencies of the crystal in the standard manner. The dynamical matrix of the secular equation is then expanded in powers of the applied field E

$$\hat{D}_{\alpha\beta}(lk;\ l'k') = D^{(0)}_{\alpha\beta}(lk;\ l'k') + D^{(1)}_{\alpha\beta}(lk;\ l'k') + \ldots \tag{7}$$

where $D^{(0)}_{\alpha\beta}(lk;\ l'k')$ is the unperturbed dynamical matrix and $D^{(1)}_{\alpha\beta}(lk;\ l'k')$ is the perturbation due to the field. Using degenerate perturbation theory we can calculate the splittings of the triply degenerate localized modes associated with a substitutional impurity having O_h or T_d site symmetry, and we obtain the following results.

(1) For an impurity at a site possessing O_h symmetry, there is, of course, no splitting to first order in the field, and we have to go to second order in the field to get any splitting.

(2) For an impurity site possessing T_d symmetry the degeneracy is lifted to first order in the field, when the field is applied along the [100], [110], and [111] directions.

(a) For the static electric field in the XY-plane, the triple degeneracy is completely lifted. The expressions for the three frequencies are

$$\begin{aligned} \Omega_1 &= \omega_0 + mE/2\omega_0 \\ \Omega_2 &= \omega_0 \\ \Omega_3 &= \omega_0 - mE/2\omega_0 \end{aligned} \tag{8}$$

where E is the magnitude of the electric field, ω_0 is the frequency of the unperturbed localized mode, and the coefficient m is given in terms of atomic force constants and eigenvectors.

(b) For the field along the [111] direction, the triply degenerate mode splits into a doublet and a singlet. The expressions for the frequencies are

$$\begin{aligned} \Omega_1 &= \omega_0 - mE/(2\sqrt{3}\omega_0) \\ \Omega_2 &= \omega_0 - mE/(2\sqrt{3}\omega_0) \\ \Omega_3 &= \omega_0 + mE/(\sqrt{3}\omega_0). \end{aligned} \tag{9}$$

We find that in a plot of Ω versus E, the line corresponding to the singlet Ω_3 will have twice the slope of the doublet Ω_1, and Ω_2.

In the case of an impurity atom occupying a T_d site in a crystal of the diamond structure, the inversion symmetry of the two T_d sites in a primitive unit cell, the result that the splitting of the degeneracy of the localized mode is linear in the field, and the assumption that both sublattices of the crystal contain impurity atoms, lead to the conclusion that in addition to the localized mode frequencies given by eqs (8) and (9), there exist localized modes whose frequencies are obtained on replacing E by $-E$ in eq (9).

No new frequencies result for the field applied in the XY-plane. However for the field in the [111] direction, the shift in the localized mode frequencies is opposite in sign for the two T_d sites and, consequently, there will be two doublet frequencies and two singlet frequencies. In their phenomenological theory of the splitting of the triply degenerate localized modes associated with U-centers at the F^- sites in CaF_2, Hayes, MacDonald, and Elliott did not take into account the existence of the two T_d sites in the primitive cell of the CaF_2 structure. They accordingly obtained an expression for the frequencies of the localized mode at a single T_d site in an externally applied electric field, similar to that of eq (9), which only produces a splitting into a doublet and a singlet. Experimentally, they observed a splitting of the localized mode absorption line into two lines, rather than into four lines which is predicted on the basis of the two T_d sites. The reason for the discrepancy between experiment and theory is as yet unclear.

We now turn to the morphic effects induced by a strain. We again start with the equations of motion of the crystal and write the displacements $\xi_\alpha(lk)$ as

$$\xi_\alpha(lk) = \sum_\beta \epsilon_{\alpha\beta} x_\beta(lk) + d_\alpha(lk) + u_\alpha(lk). \tag{10}$$

Here the first term describes a homogeneous deformation, the second term gives the rigid body displacement due to alteration of the force constants by the introduction of the impurity, and the third term gives the displacement from the new equilibrium position. Now the equations of motion can be written as

$$-M_{lk}\ddot{u}_\alpha(lk) = \overline{\Phi}_\alpha(lk) + \sum_{l'k'\beta} \overline{\Phi}_{\alpha\beta}(lk;\, l'k')\, u_\beta(l'k') \tag{11}$$

where

$$\overline{\Phi}_\alpha(lk) = \sum_{l'k'\beta} \Phi_{\alpha\beta}(lk;\, l'k') V_\beta(l'k') + \frac{1}{2} \sum_{l'k'\beta} \sum_{l''k''\gamma} \Phi_{\alpha\beta\gamma}(lk;\, l'k';\, l''k'') V_\beta(l'k') V_\gamma(l''k'') \tag{12a}$$

$$\overline{\Phi}_{\alpha\beta}(lk;\, l'k') = \Phi_{\alpha\beta}(lk;\, l'k') + \sum_{l''k''\gamma} \Phi_{\alpha\beta\gamma}(lk;\, l'k';\, l''k'')\, V_\gamma(l''k'') \tag{12b}$$

and we have used the displacement

$$V_\alpha(lk) = \sum_\beta \epsilon_{\alpha\beta} x_\beta(lk) + d_\alpha(lk). \tag{13}$$

The first term on the right hand side of eq (11), which is independent of $u_\alpha(lk)$, must be zero as there is no force on an atom in the new equilibrium position. This enables us to express $d_\alpha(lk)$ in terms of $\epsilon_{\alpha\beta}$. Using the Lagrangian finite strain parameter $\eta_{\alpha\beta}$ $\left(=\frac{1}{2}(\epsilon_{\alpha\beta} + \epsilon_{\beta\alpha} + \sum_\gamma \epsilon_{\gamma\alpha}\epsilon_{\gamma\beta})\right)$ and rotational invariance conditions on the atomic force constants we get an expression for the effective harmonic force constants. As before, we can express the effective dynamical matrix in ascending powers of the strain parameter. Since we are interested in first order effects, we treat the term linear in strain as a perturbation on the original unperturbed dynamical matrix, and obtain the following results for *both* T_d and O_h symmetries.

(a) A hydrostatic pressure does not split the degeneracy of the localized mode but merely shifts the frequencies. The expressions for the frequencies are

$$\Omega_1 = \Omega_2 = \Omega_3 = \omega_0 + (a + 2b)\Delta/(6\omega_0) \tag{14}$$

where a, b, c are constants given in terms of atomic force constants and eigenvectors and Δ is the dilation.

(b) A uniaxial strain $\eta_{\alpha\beta} = \eta\delta_{\alpha 1}\delta_{\beta 1}$ splits the triple degeneracy into a doublet and a singlet whose frequencies are

$$\begin{aligned} \Omega_1 &= \omega_0 + a\eta/(2\omega_0) \\ \Omega_2 &= \omega_0 + b\eta/(2\omega_0) \\ \Omega_3 &= \omega_0 + b\eta/(2\omega_0) \end{aligned} \tag{15}$$

(c) A shear strain $\eta_{\alpha\beta}=\eta\delta_{\alpha 1}\delta_{\beta 2}+\delta_{\beta 1}\delta_{\alpha 2}$ completely lifts the degeneracy. The perturbed frequencies are

$$\begin{aligned}\Omega_1&=\omega_0+c\eta/\omega_0\\ \Omega_2&=\omega_0\\ \Omega_3&=\omega_0-c\eta/\omega_0\end{aligned}\tag{16}$$

We next consider the experimental conditions for the observation of these effects and discuss the orientations of the electric field vector of the incident light with respect to the static electric field and the crystal axes which are necessary for the observation of the perturbed localized modes in infrared lattice absorption experiments.

The localized mode contribution to the imaginary part of the dielectric tensor in the harmonic approximation is

$$\epsilon^{(2)}_{\mu\nu}(\omega)=\frac{\pi\Lambda^2}{V}\,\omega\ \mathrm{sgn}\ \omega\sum_{s=1}^{3}\mathscr{M}^{\mu}_{s}\mathscr{M}^{\nu}_{s}\delta(\omega^2-\Omega_s^2)\tag{17}$$

where

$$\mathscr{M}^{\mu}_{s}=\sum_{lk\alpha}M_{\mu,\alpha}(lk)V^{(s)}_{\alpha}(lk)/(M_{lk})^{1/2}.\tag{18}$$

In these expressions ω is the frequency of the incident electromagnetic field, the light; V is the crystal volume; $V^{(s)}_{\alpha}(lk)$ is the eigenvector of the perturbed dynamical matrix, given, for example, by eq (7), associated with the eigenvalue Ω_s^2; and Λ is a factor which takes account of the fact that the macroscopic electromagnetic field inside the crystal is not necessarily equal to the externally applied field, due to the depolarization field. To observe the perturbed localized mode labeled by the index s, $\mathscr{M}^{\mu}_{s}$ must be nonzero for at least one value of μ, and the external electromagnetic field $\mathscr{E}^0(t)$ must have such nonzero components that the scalar product $\mathscr{M}_s\cdot\mathscr{E}^0(t)$ is nonzero. On the assumption that the localized mode is so spatially localized that only the impurity atom is vibrating, we obtain the following results.

(a) For the static electric field in the XY-plane we find that the two perturbed localized modes will be observed regardless of the direction of the static field in the XY-plane, provided the electromagnetic field has a nonzero Z component. Also all three modes can be observed for $\mathscr{E}^0(t)$ in the XY-plane if $E_y\mathscr{E}^0_x\neq -E_x\mathscr{E}^0_y$ and $E_x\mathscr{E}^0_x\neq E_y\mathscr{E}^0_y$.

(b) For the static electric field along the [111] direction we can observe all the three modes, for the electromagnetic field along the [100] direction.

(c) In the case of a hydrostatic pressure, for the observation of the triply degenerate perturbed mode $\mathscr{E}^0(t)$ can be parallel to any one of the coordinate axes.

(d) In the case of a uniaxial strain, we can observe the singlet if $\mathscr{E}^0_x\neq 0$ and the doublet if $\mathscr{E}^0(t)$ is in the YZ-plane.

(e) In the case of a shear strain we can observe one localized mode if the electromagnetic field has a Z component, the second mode if the field is along the [110] direction, and the third mode if the field is anywhere in the XY-plane and not along the [$1\bar{1}0$] direction.

The above theory gives us an understanding of the mechanisms responsible for the morphic effects induced by static electric fields or strains in a crystal containing substitutional impurity atoms. These results apply to gap modes also. We find that the frequency shift of the localized mode induced by a static electric field can be given in terms of contributions from charge deformations and static displacements of the atoms in the crystal. The frequency shifts in this case are expressed in terms of only one parameter m. For the strain induced frequency shifts, we have shown that they can be expressed in terms of three parameters, a, b, and c. These parameters

are very difficult to evaluate for a crystal containing impurities. With more experimental data and a much simplified theoretical model, one can evaluate the strengths of the electric field or strains necessary to produce appreciable frequency shifts. A more detailed account of the electric field and strain induced morphic effects in crystals containing impurities will be published elsewhere.

The Vibrational Properties of Point Defects in Solids

Report of Panel III Discussion

C. W. McCombie

Physics Laboratory, Whiteknights Park, Reading, Berks, England

(Panel Members: R. J. Elliott, J. A. Krumhansl, W. Ludwig, A. A. Maradudin, C. W. McCombie, and G. F. Nardelli)

1. Introduction

Panel III was concerned with the vibrational properties of defects. Some of those who contributed to the discussion have provided short accounts of what they said and these accounts will form the main part (Part 3) of this report. They are prefaced (Part 2) by an outline of the overall picture of the present state of the subject which emerged from the Panel Session and from those of the contributed papers which were on related topics.

2. Overall Picture

2.1. Processes at Isolated Defects in a Harmonic Lattice

The first topic considered by the Panel was the determination of the effect of lattice vibrations on processes (such as the absorption of radiation) at an isolated imperfection. From the point of view of lattice dynamics the crux of these problems lies in taking account of the fact that the presence of the imperfection will modify the normal modes of vibration of the lattice. The general features of these modifications are now well known. A few modes may appear which are localized at the imperfection and which have frequencies outside the ranges of perfect lattice mode frequencies. Most modes, on the other hand, will still extend through the crystal and have frequencies in the ranges of perfect lattice frequencies, but their forms, and so their coupling to processes at the imperfection, will be changed. It may happen that modes of this latter type in a particular fairly narrow range of frequencies are modified in such a way as to have their coupling to the process at the defect greatly enhanced. In this case one talks of having an "in-band resonance" or a "quasi-localized mode," and conspicuous features in the experimental data on the effect being considered may be directly correlated with these resonances in the coupling. It is, however, important to be able to take account of modifications of the coupling even when the resonances have no such direct effect or when there are no marked resonances at all.

It was emphasized (3.1) that if one can take the changes in force constants at the imperfection to be known (and if anharmonic effects are unimportant) the coupling to the lattice vibrations, allowing for the modification of the modes, can be reduced to machine computation. This is because the required results can be expressed in terms of certain response functions (or Green's functions) for the perfect lattice which are easily determined if the forms and frequencies of a sufficiently large sample of perfect lattice modes are known. The case of infrared absorption by a charged defect was used as an illustration (3.1) but the method can also be applied to determining the absorption structure associated with an electronic transition, the strength of the zero-phonon line in the Mossbauer Effect, the scattering of phonons by the imperfection, and so on. The essential point is that in each case a function of frequency which determines the result we require can be related directly to a response function (or Green's function) for the imperfect lattice. The method depends on the simple relation which exists between the imperfect-lattice response functions and the corresponding perfect-lattice response functions.

The relation between perfect and imperfect lattice response functions has been derived in many ways by many authors. It seemed clear that the main objective now should be to apply the methods based on this relation to realistic models of centers in realistic crystals, the problem becoming one of straightforward machine computation when the changes in force constants at the imperfection have been decided upon (see 2.3). There seems no reason why quite complicated centers should not be analyzed. The difficulty is greater the more extended the imperfection and the lower its symmetry but there should be no insurmountable ob-

stacles in the way of such calculations.

The calculation of the perfect-lattice response functions depends on determining the forms and frequencies of the modes associated with a large number of points in k-space. To get satisfactory response functions (particularly at low frequencies) a sample of something like 10^5 points may be desirable. It was suggested that whenever eigenfrequencies and eigenvectors for a sample of this order are determined some of the simpler response functions (including cross response functions) should be determined as this requires very little extra time on the computer. Some doubts were expressed as to whether this was a practical suggestion but at all events it seems worth emphasizing to those concerned for any reason with large machine computations on perfect lattice dynamics that some cooperation with people primarily interested in the dynamics of imperfect lattices may be very fruitful.

While considerable progress in the directions indicated has been made, as is seen in the paper by Benedek and Nardelli presented at the Conference, much remains to be done. Alternative ways of considering the modifications of the modes may be important in that they may show how to get rapidly to useful results. They may, moreover, in some cases give better insight into what is going on. The paper presented by Toulouse on a phase shift analysis of the scattering of lattice vibrations is an example of an approach which may be useful in this way.

2.2. Finite Concentrations of Defects in a Harmonic Lattice

Elliott pointed out (3.2) that there were problems associated with finite concentrations of randomly distributed defects which had not been completely solved. One might be interested in investigating, for example, the neutron scattering or the vibrational contributions to the thermodynamic functions for a random alloy. The problem is essentially one of multiple scattering. Taylor (3.3) contributed a brief account of an approximate approach to such problems.

2.3. Modified Force Constants at Defects

Ludwig (3.5) and Maradudin (3.6) contributed to a discussion of the treatment of the modification of force constants in the vicinity of a defect which, as already indicated, is a necessary preliminary to the sort of calculations discussed in 2.1. Wood and Gilbert also contributed to this topic at the Conference with their paper on calculations for the U-center. The difficulties of such calculations are formidable and there is no doubt that much work in the immediate future will evade these difficulties by introducing a number of adjustable parameters which describe the force constant changes, full use being made of symmetry considerations to keep the number of parameters as small as possible. Where one is accounting for experimental results which are rich in detail (as where one has sharp-line electronic absorption accompanied by complicated vibrational structure) one may allow oneself one or two such parameters and still be able to regard agreement with experiment as significant. This will hold even more strongly if one has, for the center considered, data on a variety of different effects involving lattice vibrations. One might, for example, have information on both optical absorption and the Raman effect associated with an electronic transition at the center, on infrared absorption associated with motion of the charged ions at the center and on the scattering of phonons by the center. A small set of force constants which fitted such a range of data for a particular center would be of great interest.

The quantum mechanical calculation of the changes in force constants can, however, be expected to be a field of investigation of growing importance. Maradudin (3.6) outlines how such a calculation might be carried through. One point which came up in a number of places during the Conference (cf. Ludwig's contribution 3.5) was that whenever forces such as van der Waals forces are important (as they appear to be in ionic crystals) one will have to go beyond a Hartree-Fock calculation, since these forces depend on correlations which are ignored in the Hartree-Fock treatment.

2.4. Anharmonic Effects

Treatments which ignore anharmonic effects entirely are adequate for many purposes but there are other effects which depend essentially on cubic and higher terms in the interaction between ions. For example, the infrared absorption associated with a localized vibration is frequently not a single sharp line but is accompanied by an attendant structure lying predominantly on the high frequency side of the main sharp line. This is associated with transitions in which other modes of lattice vibration are excited at the same time as the localized mode. Such multiple transitions are possible only because of anharmonic effects (among which one must include nonlinear terms in the expression for the dipole moment). Anharmonic terms are responsible also for the shift in frequency of localized mode absorption under the action of applied fields or stresses. Such effects (termed by them "morphic effects") are discussed in the paper by Maradudin, Ganesan, and Burstein. As discussed in that paper and as emphasized by Elliott (3.4), study of these effects can form a very interesting source of information about anharmonic forces at the defect.

2.5. Entropy of Formation

The calculation of the entropy of formation of, say, a vacancy and an interstitial is clearly one of

the aspects of the dynamics of imperfect lattices which is most relevant to the central theme of the Conference. It was discussed in the paper by Benedek and Nardelli and some time was devoted to it by the Panel. The calculation involves investigating the changes in frequency of the modes of vibration of the lattice consequent upon forming the defects, since in the harmonic approximation the entropy can be expressed as a sum over modes of a function of frequency. These changes in frequency arise in two ways. In the first place there is a "local" effect due to the modified masses and force constants at the imperfections. This short range effect can be handled by an application of response function techniques. In addition there is a long range effect. This arises because a defect causes a change in the bulk lattice spacing which, because of the anharmonic terms in the interaction potentials, changes the restoring forces on all the atoms of the crystal. In order to calculate this long range effect one would first have to calculate the change in lattice parameter: the change in entropy consequent upon a change in lattice parameter may then be calculated from thermodynamic data. The calculation of both effects reduces therefore to an investigation of the way in which the potential energy of the system depends on the position of atoms in the immediate vicinity of the defect, so that one can calculate both the relaxed positions of the atoms and the restoring forces returning the atoms to these relaxed positions. Such calculations are, of course, extremely delicate and it is here that the whole difficulty of the problem lies. There are additional difficulties when the vacancy and interstitial are effectively charged as in the alkali halides. In that case the first effect, which we termed "short range," contains a long range part and dielectric effects have to be considered.

2.6. Diffusion

There was some discussion of the calculation of jump rates in diffusion (the rate, for example, at which interstitial atoms jump from one site to another, or the rate at which neighboring atoms jump into a vacancy). According to Rate Theory one has to calculate the energy and entropy of the system when, roughly speaking, the atom is midway between its two equilibrium positions. Thus one encounters again all the difficulties of the entropy of formation calculation which has just been discussed. Some doubt was expressed about the inclusion in the saddle point entropy of the long range part (which corresponds to dilatation of the lattice) since, it was argued, the extent of the disturbance of the lattice produced by the atom during its brief presence near the saddle point would be very limited. Against this it was argued that the jump process is a cooperative effect of the diffusing atom and its surroundings and it is just as valid to think of a fluctuation in density of the lattice over an appreciable region around the defect as encouraging the jump as it is to think of the jumping atom tending to cause the lattice to dilate: on the first of these views the time of response argument appears to lose its force.

The question of the status of Rate Theory in this problem was raised and considered briefly. There was strong support from a number of people for the validity of Rate Theory with a transmission factor of order unity, but it was also argued that this theory might be inappropriate if the damping on an atom was so large that it had to be thought of as diffusing over the barrier rather than jumping over it. (See the paper by H. A. Kramers, Physica Vol. **7**, p. 284 (1940).)

2.7. Displaceable Ions. Jahn-Teller Effects

Krumhansl contributed a brief discussion of cases such as Li^+ in KCl where the substitutional ion is in a potential field which has its minima, which are shallow, at points other than the normal lattice position. This situation (which was described as "extreme anharmonic") clearly introduces new features not considered in the usual lattice dynamics.

Krumhansl's survey followed a paper by Bowen, Gomez, Krumhansl, and Matthew in Phys. Rev. Letters Vol. **16**, p. 1105, to which reference should be made. Most of the discussion in that paper takes the form of a quantum mechanical treatment of the states of the Lithium ion moving in a rigid potential field. Many features of the experimental results can be understood in terms of this model. However, as pointed out by the authors, the surrounding ions may tend to exhibit a distortion which follows to a greater or less extent the motion of the Lithium ion, so that one has, strictly speaking, a Jahn-Teller type of problem to consider. One will also have to consider the way in which a center of the type under discussion scatters phonons. Both these topics present interesting problems for lattice dynamics. It may be remarked in conclusion that Jahn-Teller type problems for electronic states also raise many interesting questions but these were not discussed by the Panel.

3. Individual Discussions

3.1. Response Function Methods. C. W. McCombie (Reading)

The Green's function (or response function) approach can be applied to the treatment of the effect of defects on lattice vibrations in two rather different ways, one mathematical and the other more physical. In the first approach the matrix equations involved in determining the normal modes of the whole system are formally written down and

the matrix problem is then reduced by the introduction of Green's functions in the usual way. In the second approach we start with a physical argument, thinking of the system as a perfect lattice with extra masses (possibly negative) rigidly attached to some atoms and extra springs (possibly with negative spring constants) connecting certain pairs of atoms. The extra masses will correspond, of course, to the changes in masses of any substitutional foreign atoms involved in the imperfections and the extra springs to the changes in force constants between the atoms in the vicinity of the defect. To deal with an interstitial atom one will have to consider an extra mass, not rigidly attached to any lattice atom, but connected to several (the neighbors of the interstitial) by springs. To deal with a vacancy one can simply add springs which cancel out the interaction forces between the atom to be removed and its neighbors while at the same time adding springs between other atoms of the perfect lattice to take account of the changes of force between them. In some problems one will have to take care to eliminate contributions from the atom which is still present although uncoupled to the lattice, but this is unlikely to present serious difficulties.

To illustrate the procedure in this second approach we shall consider the infrared absorption by a charged substitutional atom in a monatomic cubic lattice. The mass of the atom is supposed to exceed the mass of a normal lattice atom by an amount ΔM, but the atom is supposed to interact with surrounding atoms in exactly the same way as a normal atom. According to the approach we are adopting, we shall consider a perfect lattice in which one atom carries an (extra) charge e and also has a mass ΔM rigidly attached to it. Because of our assumption about the interaction of the foreign atom with its neighbors it is not necessary to introduce attached springs. The system of perfect lattice with attached mass and added charge which we have described will clearly respond in the same way as the actual crystal (with its substitutional impurity) to the electric field $Ee^{i\omega t}$ which a beam of infrared radiation causes to act at the impurity: in particular the absorption of energy from the beams will be the same in the two cases.

To calculate the absorption we need a response function for the imperfect lattice which is defined as follows. A force $Fe^{i\omega t}$ is applied to the impurity atom and the resulting displacement of the impurity atom after transients have died away (so that the disturbance in the lattice will be an outgoing wave) is denoted by $De^{i\omega t}$. (The force and displacement will be in the same direction because the crystal is cubic.) The response function $P_{\text{imp}}(\omega) - iQ_{\text{imp}}(\omega)$ is defined by

$$D = \frac{1}{M}\{P_{\text{imp}}(\omega) - iQ_{\text{imp}}(\omega)\}F$$

where M, the mass of a normal atom of the lattice, is introduced into the definition merely for convenience. The rate of absorption of energy by the lattice, which will be equal to the rate at which work is done by the force $Fe^{i\omega t}$ acting on a particle with displacement $De^{i\omega t}$, is easily seen to be $\frac{1}{2}(\omega/M)Q_{\text{imp}}|F|^2$: replacing F by eE gives the rate of absorption of energy from the infrared beam.

A direct calculation of P_{imp} and Q_{imp} is possible if one is prepared to investigate directly the normal modes of the imperfect lattice: where the forms and frequencies of the modes are known it is easy to determine the response of each mode to a force applied to the lattice and so to get the resulting contribution of the mode to the displacement of the atom of interest; the total response, which determines the response functions, is then obtained by summing over the modes. Unfortunately the forms of the modes of the imperfect lattice are difficult to determine and so the direct approach we have just outlined is very messy and difficult to carry through with any accuracy.

On the other hand the corresponding response function for a force applied to an atom of the perfect lattice is easily obtained since it is easy for an electronic computer to determine the forms and frequencies of a very large sample of perfect lattice modes. If $Fe^{i\omega t}$ and $De^{i\omega t}$ are the applied force and resulting displacement (after transients) of an atom of the perfect lattice, the perfect lattice response function is defined by

$$D = \frac{1}{M}(P_{\text{perf}}(\omega) - iQ_{\text{perf}}(\omega))F.$$

As already asserted there is a simple relation between the response functions for the imperfect and perfect lattices, so that a direct calculation of the imperfect lattice response function by the method outlined above becomes quite unnecessary. To establish the relation we suppose the force $Fe^{i\omega t}$ applied to the atom with the attached mass ΔM and consider explicitly the force exerted by the extra mass on the lattice: by Newton's Laws this is easily seen to be $\Delta M\omega^2 De^{i\omega t}$ where D is the displacement of the atom (and so, of course, of the rigidly attached mass ΔM). The total force acting on the atom of the perfect lattice is, therefore, $\{F + \Delta M\omega^2 D\}e^{i\omega t}$ and we may use the perfect lattice response function to write

$$D = \frac{1}{M}\{P_{\text{perf}}(\omega) - iQ_{\text{perf}}(\omega)\}\{F + \Delta M\omega^2 D\}$$

which gives

$$D = \frac{\frac{1}{M}\{P_{\text{perf}}(\omega) - iQ_{\text{perf}}(\omega)\}}{\left\{1 - \frac{\Delta M}{M}\omega^2 P_{\text{perf}}(\omega)\right\} + i\frac{\Delta M}{M}\omega^2 Q_{\text{perf}}(\omega)}F.$$

But here $De^{i\omega t}$ is the displacement of the isotope when the force $Fe^{i\omega t}$ is applied to it and so D and F are related by

$$D=\frac{1}{M}\{P_{\text{imp}}(\omega)-iQ_{\text{imp}}(\omega)\}F.$$

Comparing the last two equations gives $P_{\text{imp}}(\omega)$ and $Q_{\text{imp}}(\omega)$ in terms of the perfect lattice response functions. One has in particular

$$Q_{\text{imp}}(\omega)=\frac{Q_{\text{perf}}(\omega)}{\left\{1-\frac{\Delta M}{M}\omega^2 P_{\text{perf}}(\omega)\right\}^2+\left(\frac{\Delta M}{M}\right)^2\omega^4 Q^2_{\text{perf}}(\omega)}.$$

This at once allows us to express the rate of absorption of energy from the radiation field, which will be $\frac{1}{2}(\omega/M)Q_{\text{imp}}e^2|E|^2$, in terms of the perfect lattice response function. We have, therefore, given an example of how the relation between the response functions for the perfect and imperfect lattices is established and how this relation is applied.

If one wishes to consider changes in the interaction between the foreign atom and its neighbors (which, as already explained, one does by introducing attached springs as well as an attached mass) one needs more elaborate response functions (and cross response functions) for the perfect lattice, and one gets in general a small number of simultaneous equations which determine the relation between the required imperfect lattice response functions and the perfect lattice response functions. The procedure, however, still goes through in a straightforward way and it is easy to arrange to make full use of symmetry to reduce the complexity of the computations.

It may be worth remarking that the relation between the quantity of interest and an imperfect lattice response function is not always quite as obvious as it is in the case of infrared absorption. Suppose, for example, that we wished to determine as a function of temperature the mean square displacement of the isotope from its equilibrium position. One finds that this is easily obtained provided one knows for all the modes in each small frequency range the sum of the squares of their contributions to a component of displacement of the isotope, the magnitude of the displacement in each mode being adjusted to make the potential energy in the mode unity. But the same information also enables us to determine the simple response function considered previously, and, conversely, we can extract this information if the response function is known. Thus expressing the imperfect lattice response function in terms of the perfect lattice response function again solves the problem.

3.2. Finite Concentration of Defects. R. J. Elliott (Oxford)

I agree with McCombie that the single defect problem is now well understood and that future interest will center on the solutions of models of more complex defects using one or other of the established methods. One problem which is of great interest which is still far from solution is that of vibrations in random alloys. At small concentrations of defects the properties may be discussed in terms of the single isolated defects. The density of states, for example, will be modified with peaks near resonances and impurity bands near local mode frequencies. As the concentration of defects is increased interference between scattering by several defects becomes important. It is essential to include pair effects even at low concentrations to obtain a satisfactory treatment of impurity bands. The methods which expand in clusters of increasing size look unlikely to be convergent for sizeable concentrations and some self-consistent approximation must be sought.

Some important references in this field are

J. S. Langer, J. Math. Phys. **2**, 584 (1961); Phys. Rev. **131**, 163 (1963).

S. Takeno, Prog. Theor. Phys. **28**, 33 (1962); **29**, 191 (1963); **30**, 144 (1963); Supp. **23**, 94 (1962).

S. Edwards and J. Beeby, Proc. Roy. Soc. **A269**, 518; **A274**, 395 (1962); **A279**, 82 (1964); Phys. Rev. **135**, A130 (1964).

J. des Cloizeaux, Phys. Rev. **139**, A1531 (1965).

R. J. Elliott and D. W. Taylor, Proc. Roy. Soc. (to be published).

3.3. Finite Concentration of Defects. D. W. Taylor (Bell Telephone Laboratories)

The multiple scattering theory of Lax has been used to obtain equations for the displacement-displacement Green's functions for a crystal containing substitutional defect atoms. A simple approximation for a random array of defects yields previous results that are correct to first order in the concentration. A self-consistent procedure using a coherent self-energy to describe the configuration-averaged system and suitable for large concentrations of mass defects is described. It is evaluated in a simple approximation in both one and three dimensions to give the spectral function and the density of states for various concentrations. The method is symmetric in both defect and host atoms and can be considered to give a good description of the coherent behavior of the imperfect crystal. In particular it predicts that in the three dimensional example the maximum frequency of the host crystal phonon band is reduced as light defects are added, a somewhat surprising result but in qualitative agreement with recent machine calculations. The nature of the approximation precludes the appearance of the detailed structure found in the machine calculations.

3.4. Anharmonic Effects. R. J. Elliott (Oxford)

Another aspect of crystal dynamics which can be conveniently studied through the spectroscopy of defect vibrations is anharmonic effects. In the perfect lattice some information may be obtained from third order elastic constants. These reflect

sums over anharmonic interatomic force constants with a weighting in favor of those at long range. A study of very localized modes, such as those of H ions in alkali halides and alkaline earth fluorides, yields information about short range, anharmonic interactions and the shape of the local potential well. The most detailed results come from harmonics and side bands of the localized vibration absorption.

Some important references in this field are

W. Hayes et al., Proc. Roy. Soc. **A289**, 1, (1965); Phys. Rev. Letters **15**, 961 (1965).

M. V. Klein and T. Timusk, Phys. Rev. **141**, 664 (1966).

3.5. Force-Constants and Distortions Near Defects. W. Ludwig (Jülich)

Straightforward quantum mechanical calculations of force constants and distortions near defects are difficult and have scarcely been done. R. F. Wood and R. L. Gilbert [1][1] presented calculations for the U-center in alkali halides, which look rather promising. For alkali halides this seems to be the first attempt at calculating force-constants for defects. The main problem is to find reasonable eigenfunctions and then, using the Hamiltonian or a suitably chosen model Hamiltonian, to calculate the energy for different positions of the atoms. This enables one to find the equilibrium positions and the force constants. There are various steps which must involve approximations if the calculations are to be practicable and these approximations limit the accuracy of the results. However, this procedure seems a good starting point for further calculations.

Often Born-Mayer [$\exp(-\alpha r)$] and Verwey [$(A+B/r)\exp(-\alpha r)$] potentials have been used in alkali halides and also to other types of crystal. In a certain sense the Born-Mayer potential can be derived from first principles (statistical models), whereas there seems to be no justification for the Verwey potential. It looks rather sophisticated, and the agreement of some calculated data with experiment cannot be looked upon as a justification. Instead of this, there is a certain hint from statistical models that an $\exp(-\beta r)/r$ potential might be more realistic for small distances. It behaves similarly to the Verwey potential for $r \to 0$.

It seems that a statistical calculation of interactions using Thomas-Fermi-Dirac-type methods provides reasonable results, at least for closed-shell interactions (Gombas, Abrahamson et al.). The difficulty here is that most investigations can be done only numerically, at least if exchange and correlation-effects are taken into account. So one is forced to find analytic expressions for the potential, which are not always unique.

This method has been used also for the calculation of the mutual interaction of three atoms, resulting in three-body-forces [2]. It should be possible to continue with more general models. Near defects the contribution of many-body forces (e.g., polarization effects lead to many-body forces) should be even more essential than in ideal lattices. These many-body forces are neglected in most calculations of force constants (perhaps apart from the electronic volume forces) and it might turn out that the neglect affects the results for force-constants near defects appreciably.

In metals it should be possible to calculate the force-constants near defects, if the electronic density distribution is known. Then one might be able to calculate the potential using some self-consistent method. So the task is to find some reasonable starting point for the electronic density. For ideal lattices the procedures of Toya [3] and Vosko [4] are promising; it should be possible to extend these methods to lattices with defects.

The situation seems to be worst for covalent crystals. Even in ideal lattices there is little information on the true potentials between such atoms.

Another possibility of studying the interatomic forces near defects consists in the use of general force constants. When making a model with general constants, symmetry and invariance relations should be used to limit the number of independent constants. The invariance relations (rotational invariance) are not satisfied in a number of models. Having made such a model, one has to compare with experimental results to fit the constants. So information about the constants, especially the harmonic constants, can be found. But in general this is a difficult procedure, because, for example, the range of the forces is not known. It is also difficult to use the constants and to construct a potential, though this is facilitated by using also anharmonic data, for example those which can be obtained by "morphic" effects on the localized modes or perhaps by life-time measurements of modes.

In any case, it seems to me very important to improve our knowledge of the interatomic forces, not only between atoms near defects, but even for atoms in ideal lattices. We know a lot of general relations and statements, but in comparing with experiments the knowledge of forces enters. By fitting we can explain every experiment, but if experiment and theory do not agree, the origin of disagreement can often not be found, because we do not know the forces.

References

[1] R. F. Wood, R. L. Gilbert, this conference.

[2] A. A. Abrahamson, R. D. Hatcher, G. H. Vineyard, Phys. Rev. **121**, 159 (1961).

[3] T. Toya, Lattice Dynamics, J. Phys. Chem. Solids Suppl. I. **91** (1965) and papers cited there.

[4] S. H. Vosko, R. Taylor, G. H. Keech, Canad. J. of Physics **43**, 1187 (1965) and further papers.

3.6. Force Constants and Distortions Near Defects. A. A. Maradudin (Irvine)

I should like to outline here a method for computing various properties associated with impurity

[1] Figures in brackets indicate the literature references on this page.

atoms in non-metallic crystals. These properties, for example, can be the static distortion of the crystal about the impurity atom, the force constants of the impurity atom-host crystal interaction, and the effective charges on the impurity and on its neighbors in the crystal.

The basic assumption underlying this method is the validity of the adiabatic approximation in which the potential energy for nuclear motion is the sum of the ground state energy of the electronic system with the nuclei displaced arbitrarily from their equilibrium positions and the potential energy of interaction of the ion cores. By "ion core" we mean the atomic nucleus together with the core electrons, i.e., all of the atomic electrons not including the valence electrons. If there is no overlap between the charge distributions of the core electrons on neighboring atoms, the calculation of the potential energy of interaction of the ion cores can be carried out by Ewald's method. If there is appreciable overlap of the ion cores, the interaction energy arising from core-core exchange must be included in this part of the potential energy as well, This energy can be computed in various approximations [1],[2] and we will regard the problem of computing the core-core interaction energy as solved. It is the electronic contribution to the potential energy for nuclear motion on which we focus our attention.

The starting point for our discussion is the expression for the ground state energy of a system of electons moving in a potential set up by ion cores displaced arbitrarily from the lattice sites of a perfectly periodic lattice. One of the ion cores is that of the impurity atom, which can be taken to be at the origin of our coordinate system. The ground state energy in the Hartree-Fock approximation is given by

$$E=\sum_k n_k \int dx_1 \psi_k^*(1)\left[-\frac{\hbar\nabla^2}{2m}\Delta_1^2+v(1)\right]\psi_k(1) + \int dx_1 \int dx_2 \rho(1)\rho(2)\frac{e^2}{2r_{12}} - \frac{3}{2}\left(\frac{3}{8\pi}\right)^{1/3} e^2 \int dx_1 (\rho(1))^{4/3}. \quad (1)$$

In this equation, $v(r)$ is the electron-ion interaction. It is the sum of the coulomb interactions between a valence electron and the atomic nuclei, the interaction of a valence electron with the charge distribution of the core electrons, and the exchange and correlation interactions between the valence and core electrons. Because the atoms are displaced from their equilibrium positions, the index k merely labels the one-electron states, and is not to be interpreted as a wave vector and band index. n_k equals unity if k is an occupied state and is zero otherwise. The electron number density $\rho(1)$ is given by

$$\rho(1)=\sum_k n_k \psi_k^*(1)\psi_k(1). \quad (2)$$

Finally, we note that in writing the exchange energy term in eq (1), we have approximated it by the free electron expression as derived by Kohn and Sham [2].

The stationarity of the ground state energy E with respect to variations of the $\{\psi_k\}$ yields the following set of equations for the one-electron wave functions

$$\left[-\frac{\hbar^2}{2m}\nabla_1^2+v(1)+\int dx_2 e^2\frac{\rho(2)}{r_{12}} - 2\left(\frac{3}{8\pi}\right)^{1/3} e^2\rho^{1/3}(1)\right]\psi_k(1)=E_k\psi_k(1). \quad (3)$$

with the aid of which we rewrite eq (1) as

$$E=\sum_k n_k E_k - \int dx_1 \int dx_2 e^2 \frac{\rho(1)\rho(2)}{2r_{12}} + \frac{1}{2}\left(\frac{3}{8\pi}\right)^{1/3} e^2 \int dx_1 (\rho(1))^{4/3} \quad (4)$$

We now expand the electron-ion interaction in powers of the displacements of the atoms from the lattice sites of a perfectly periodic lattice:

$$v(\mathbf{r})=\sum_{l\kappa} U_{l\kappa}(\mathbf{r}-\mathbf{x}(l\kappa)-\mathbf{u}(l\kappa))=\sum_{l\kappa} U_{l\kappa}(r-x(l\kappa)) - \sum_{l\kappa\alpha} u_\alpha(l\kappa)\frac{\partial}{\partial x_\alpha}U_{l\kappa}(\mathbf{r}-\mathbf{x}(l\kappa)) + \frac{1}{2}\sum_{l\kappa}\sum_{\alpha\beta} u_\alpha(l\kappa)u_\beta(l\kappa)\frac{\partial^2}{\partial x_\alpha \partial x_\beta}U_{l\kappa}(\mathbf{r}-\mathbf{x}(l\kappa))+\ldots = v^{(0)}(r)+v^{(1)}(r)+v^{(2)}(r)+\ldots \quad (5)$$

In eq (5) $U_{l\kappa}(\mathbf{r}-\mathbf{x}(l\kappa))$ is the potential energy of interaction between a valence electron at $\mathbf{r}$ and an ion at the lattice site $\mathbf{x}(l\kappa)$, where l labels the unit cells of the crystal and κ labels the atoms within a unit cell.

We also expand the wave function $\psi_k(\mathbf{r})$, the single particle energy E_k, and the density $\rho(\mathbf{r})$ in powers of the atomic displacements:

$$\psi_k(\mathbf{r})=\psi_k^{(0)}+\psi_k^{(1)}+\psi_k^{(2)}+\ldots \quad (6a)$$

$$E_k=E_k^{(0)}+E_k^{(1)}+E_k^{(2)}+\ldots \quad (6b)$$

$$\rho(\mathbf{r})=\rho^{(0)}+\rho^{(1)}+\rho^{(2)}+\ldots \quad (6c)$$

[2] Figures in brackets indicate the literature references on page 202.

Substituting eqs (5) and (6) into eqs (3) and (4), we solve for the ground state energy of the electronic system to second order in the atomic displacements. The result is

$$E = E^{(0)} + E^{(1)} + E^{(2)} + \ldots \tag{7a}$$

where

$$E^{(1)} = \int dx_1 v^{(1)}(1)\rho^{(0)}(1) \tag{7b}$$

$$E^{(2)} = \int dx_1 v^{(2)}(1)\rho^{(0)}(1) + \frac{1}{2}\sum_{kl} \frac{n_k - n_l}{E_k^{(0)} - E_l^{(0)}} \langle \psi_k^{(0)}|H^{(1)}|\psi_l^{(0)}\rangle \times \langle \psi_l^{(0)}|v^{(1)}|\psi_k^{(0)}\rangle. \tag{7c}$$

In the expression (7c) for $E^{(2)}$, the matrix element $\langle \psi_k^{(0)}|H^{(1)}|\psi_l^{(0)}\rangle$ is the solution of the integral equation

$$\langle \psi_m^{(0)}|H^{(1)}|\psi_n^{(0)}\rangle = \langle \psi_m^{(0)}|v^{(1)}|\psi_n^{(0)}\rangle + \sum_{kl} [A_{mnkl} - B_{mnkl}] \frac{n_k - n_l}{E_k^{(0)} - E_l^{(0)}} \times \langle \psi_k^{(0)}|H^{(1)}|\psi_l^{(0)}\rangle \tag{8}$$

with

$$A_{mnkl} = e^2 \times \int dx_1 \int dx_2 \frac{\psi_m^{(0)*}(1)\psi_n^{(0)}(1)\psi_k^{(0)}(2)\psi_l^{(0)*}(2)}{r_{12}} \tag{9a}$$

$$B_{mnkl} = \frac{2}{3}\left(\frac{3}{8}\right)^{1/3} \times e^2 \int dx_1 \frac{\psi_m^{(0)*}(1)\psi_n^{(0)}(1)\psi_k^{(0)}(1)\psi_l^{(0)*}(1)}{(\rho^{(0)}(1))^{2/3}}. \tag{9b}$$

The first order change in the electronic charge density $\rho^{(1)}$, which is required for the calculation of the effective charge on the impurity atom, is given by

$$\rho^{(1)}(1) = \sum_{kl} \frac{n_k - n_l}{E_k^{(0)} - E_l^{(0)}} \langle \psi_l^{(0)}|H^{(1)}|\psi_k^{(0)}\rangle \times \psi_k^{(0)*}(1)\psi_l^{(0)}(1). \tag{10}$$

When the ground state energy of the electronic system given by eq (7) is added to the potential energy of interaction of the ion cores, the effective potential energy for nuclear motion takes the form

$$\Phi = \Phi_0 + \sum_{l\kappa\alpha} \Phi_\alpha(l\kappa)u_\alpha(l\kappa) + \frac{1}{2}\sum_{l\kappa\alpha}\sum_{l'\kappa'\beta} \Phi_{\alpha\beta}(l\kappa;\, l'\kappa') \times u_\alpha(l\kappa)u_\beta(l'\kappa') + \ldots \tag{11}$$

to second order in the nuclear displacements. To this order of approximation the static distortion of the crystal about the impurity site is described by the displacements

$$d_\alpha(l\kappa) = -\sum_{l'\kappa'\beta} \Phi^{-1}_{\alpha\beta}(l\kappa;\, l'\kappa')\Phi_\beta(l'\kappa'), \tag{12}$$

while the atomic force constants are just the coefficients $\{\Phi_{\alpha\beta}(l\kappa;\, l'\kappa')\}$. The μ-cartesian component of the first order dipole moment can be written as

$$M_\mu^{(1)} = \sum_{l\kappa\alpha} M_{\mu,\alpha}(l\kappa)u_\alpha(l\kappa), \tag{13a}$$

where

$$M_{\mu,\alpha}(l\kappa) = \delta_{\mu\alpha}Z_{l\kappa} + \int dx_1 r_{1\mu}\rho^{(1)}(1), \tag{13b}$$

and $Z_{l\kappa}$ is the charge on the ion core $(l\kappa)$.

The evaluation of the first and second order contributions to the ground state energy of the electronic system $E^{(1)}$ and $E^{(2)}$, clearly presents formidable computational difficulties. However, Green's function methods for computing $\rho^{(0)}(1)$ have been described at this Conference by Professor Seeger, and they should be useful for evaluating $E^{(1)}$ and the first term in the expression for $E^{(2)}$. The second term on the right hand side of eq (7c) can be evaluated without much difficulty for perfectly periodic crystals [3]. It is hoped that this fact provides a starting point for the evaluation of this term for a perturbed crystal.

The application of the method outlined here to the study of some simple impurity atom-host crystal systems is now being investigated.

References

[1] S. H. Vosko, Physics Letters **13**, 97 (1964).
[2] W. Kohn and L. J. Sham, Phys. Rev. **140**, A1133 (1965).
[3] L. J. Sham, Proc. Roy. Soc. (London) **283**, 33 (1965).

THE NATIONAL BUREAU OF STANDARDS

The National Bureau of Standards[1] provides measurement and technical information services essential to the efficiency and effectiveness of the work of the Nation's scientists and engineers. The Bureau serves also as a focal point in the Federal Government for assuring maximum application of the physical and engineering sciences to the advancement of technology in industry and commerce. To accomplish this mission, the Bureau is organized into three institutes covering broad program areas of research and services:

THE INSTITUTE FOR BASIC STANDARDS . . . provides the central basis within the United States for a complete and consistent system of physical measurements, coordinates that system with the measurement systems of other nations, and furnishes essential services leading to accurate and uniform physical measurements throughout the Nation's scientific community, industry, and commerce. This Institute comprises a series of divisions, each serving a classical subject matter area:

—Applied Mathematics—Electricity—Metrology—Mechanics—Heat—Atomic Physics—Physical Chemistry—Radiation Physics—Laboratory Astrophysics[2]—Radio Standards Laboratory,[2] which includes Radio Standards Physics and Radio Standards Engineering—Office of Standard Reference Data.

THE INSTITUTE FOR MATERIALS RESEARCH . . . conducts materials research and provides associated materials services including mainly reference materials and data on the properties of materials. Beyond its direct interest to the Nation's scientists and engineers, this Institute yields services which are essential to the advancement of technology in industry and commerce. This Institute is organized primarily by technical fields:

—Analytical Chemistry—Metallurgy—Reactor Radiations—Polymers—Inorganic Materials—Cryogenics[2]—Office of Standard Reference Materials.

THE INSTITUTE FOR APPLIED TECHNOLOGY . . . provides technical services to promote the use of available technology and to facilitate technological innovation in industry and government. The principal elements of this Institute are:

—Building Research—Electronic Instrumentation—Technical Analysis—Center for Computer Sciences and Technology—Textile and Apparel Technology Center—Office of Weights and Measures —Office of Engineering Standards Services—Office of Invention and Innovation—Office of Vehicle Systems Research—Clearinghouse for Federal Scientific and Technical Information[3]—Materials Evaluation Laboratory—NBS/GSA Testing Laboratory.

---

[1] Headquarters and Laboratories at Gaithersburg, Maryland, unless otherwise noted; mailing address Washington, D.C., 20234.

[2] Located at Boulder, Colora o 80302.

[3] Located at 5285 Port Royal Road, Springfield, Virginia 22151.

U.S. GOVERNMENT PRINTING OFFICE : 1967 OL—256-724